The AE-8 Trapped Electron Model Environment

James I. Vette

November 1991

Contents

List of Tables

v

List of Figures

Chapter 1
Introduction

The machine-sensible version of the AE-8 electron model environment was completed in December 1983. It has been sent to users on the model environment distribution list and is made available to new users by the National Space Science Data Center (NSSDC). AE-8 is the last in a series of terrestrial trapped radiation models that includes eight proton and eight electron versions. With the exception of AE-8, all of these models were documented in formal reports as well as being available in a machine-sensible form. The purpose of this report is to complete the documentation, finally, for AE-8 so that users can understand its construction and see the comparison of the model with the new data used, as well as with the AE-4 model.

Chapter 2
Overview of the Model

The model is comprised of three parts: (1) an inner zone that covers the L (McIlwain parameter) range 1.2 - 2.4, (2) an outer zone that covers the L range 3 - 11, and (3) a transition region for 2.4 < L < 3.0. For each part there are two versions: One depicts solar maximum (SOLMAX) conditions, and the other is for solar minimum (SOLMIN). An overview of each part follows.

Inner Zone

The inner zone parts were produced and documented earlier as models in the overall series: AE-5 Projected (AE-5P) for SOLMIN (Teague and Vette, 1974) and AE-6 for SOLMAX (Teague et al., 1976). Both of these were based on AE-5 (Teague and Vette, 1972) and the revision of the OV3-3 flux levels used in AE-5. AE-5, with an epoch of October 1967, was developed in a unidirectional differential energy flux form and converted to omnidirectional integral energy flux for its final output form. Analytical functions for the pitch angle dependence, including an atmospheric cutoff, and the energy spectrum were chosen based on the data. Three time effects were studied and modeled: magnetic substorms, Starfish decay, and solar cycle. For electrons below 0.7 MeV, the main temporal effect was a result of the solar cycle. Above this energy and at the L values above 2, substorm injections were large but infrequent. At epoch the Starfish residue was important for L < 1.7 mainly at intermediate energies. AE-5P was obtained from AE-5 by using the Starfish decay model of Teague and Stassinopoulos (1972) to remove the Starfish residue and by adjusting the solar cycle dependent fluxes of AE-5 to SOLMIN. The AE-6 model consisted of the removal of the Starfish residue from AE-5; no solar cycle changes were needed, since the epoch of AE-5 was one of SOLMAX. A later study of a number of new inner zone electron data sets indicated that no changes to these models were needed (Teague et al., 1979).

Transition Region

This region is the most difficult to model since it is affected by infrequent but large substorm injections that result in greatly varying energy spectra. Long-term (~ yearly) averages do not provide the quasi-steady picture found in the outer zone. Since the analysis of data to produce models differs between the inner zone and outer zone, the decision was made to use a transition region as an interpolation region between the two models. In practice this means prescribing the flux at specified energies on the five L shells 2.5, 2.6, 2.7, 2.8, and 2.9. This was done as part of the original AE-5P and AE-6 models to stitch them together with the AE-4 outer zone model. Naturally, the values for AE-8 in this region are different from these earlier models. These differences are mainly for energies above 1 MeV, as shown in Chapter 4. Both SOLMIN and SOLMAX transition region versions exist, since the solar cycle effect is seen from $L = 1.4$ out to $L = 5.5$.

Outer Zone

AE-8 in this region was formulated by

- Studying the data from Hovestadt's Proton-Electron Detector experiment flown on the German Research Satellite A (GRS-A); Vampola's Energy Spectra, Fluxes, and Pitch Angle Distribution of Electrons experiment flown on OV1-19; and Vampola's Magnetic Electron Spectrometer experiment flown on OV3-3.

- Using the analyzed results of Paulikas and Blake (1979) of the energetic electron data from their experiment on ATS 6 and McIlwain's experiment on ATS 5.

- Using the outer zone AE-4 model (Singley and Vette, 1972a and 1972b) to make modifications dictated by the data above to arrive at the outer zone portion of AE-8.

The GRS-A satellite is commonly called Azur; this latter name will be used in this report. Using the Azur data, an empirical atmospheric cutoff was determined for AE-8 to replace the conservatively (pessimistically) chosen $h_{max} = 200$ km for AE-4. The local time variation was extended down from $L = 5$ to $L = 3$, also using the Azur data. Based on the ATS 6 local time variation obtained from Paulikas (1981), no solar cycle effect for this variation exists in AE-8, as opposed to AE-4. The energy spectrum above 2.5 MeV was enhanced at $L = 6.6$, using the geostationary data and then using Azur and OV1-19 data, the spectra above 2.5 MeV were altered from AE-4 throughout the outer zone. The flux variation along the field line has the same dependence as AE-4, and the statistical variation given by the standard deviation of the logarithm of the flux is also unchanged, except for the extension to higher energies.

Chapter 3
Data Processing/Analysis

The framework for the outer zone portion of AE-8 will be discussed now so that the processing and analysis of the new data can be understood. The details of the inner zone formalism will be reviewed in Chapter 5 (page 5-3 through 5-5). The formalism for AE-8 outer zone (OZ) is the same as that used for AE-4, where the omnidirectional flux above an energy (E) is given as a function of the position along a field line (b), the L shell (L), the local time (ϕ), and the epoch (T). The variable b is

$$b = B/B_o \tag{3.1}$$

where B_o is the magnetic field strength at the geomagnetic equator based on an internal field only. B is the magnetic field strength of the internal field at the position in question; thus b is a coordinate along the field line that has the value 1 at the equator and ∞ at the dipole. The local time variation is mainly the effect of the magnetic field generated by current sources external to the Earth's surface. Although this choice of variables for the model is not the best for studying the details of particle dynamics in the outer zone, it is much more convenient for the user to apply the model to satellite orbits.

The AE-8OZ omnidirectional flux is written as

$$J(>E,b,L,\phi,T) = N_T(>E,L)\,\Phi(>E,L,\phi)\,G(b,L) \tag{3.2}$$

where N_T gives the equatorial integral spectrum, Φ gives the local time variation, and G provides the variation of flux along the field line. This simplification of three product functions is justified by the outer zone data. Specifically, the local time function has the form

$$\Phi(>E,L,\phi) = K(>E,L)\,10^{\left[C(>E,L)\cos\frac{\pi(\phi-11)}{12}\right]} \tag{3.3}$$

The peak in this function at $\phi = 11$ hours is an approximation that is good down to 0.2 MeV, and it was felt, as in AE-4, that more detail was not necessary. The function K is merely one of normalization so that

$$\int_0^{2\pi} \frac{\Phi d\phi}{24} = 1 \tag{3.4}$$

The function C represents the amplitude of the local time variation as seen in the log of the flux. In AE-4 Φ was dependent on epoch; this is no longer true for AE-8OZ as noted earlier and discussed further in the next section.

The G function has the value of unity at the geomagnetic equator and is

$$G(b,L) = \begin{cases} b^{-m(L)}\left\{\dfrac{b_c-b}{b_c-1}\right\}^{m(L)+0.5} & ; \ b < b_c \\[2ex] 0 & ; \ b \geq b_c \end{cases} \tag{3.5}$$

The value for the exponent m is the same as AE-4, since this quantity can best be determined by data covering the low and mid latitudes, not high latitudes. The cutoff given by b_c can only be obtained from high latitude satellites such as Azur. It is useful to note that the form of the b dependence given by G for an omnidirectional flux has an analytical counterpart for the unidirectional flux perpendicular to the magnetic field line given by (Roberts, 1965)

$$g_p(b,L) = \begin{cases} \dfrac{b^{-m}}{2\pi\beta(0.5,m+1)}\left\{\dfrac{b_c-b}{b_c-1}\right\}^m\sqrt{\dfrac{b_c}{b_c-1}} & ; \ b < b_c \\[2ex] 0 & ; \ b \geq b_c \end{cases} \tag{3.6}$$

where $\beta(0.5,m+1)$ is the well known β function. Equation (3.6) was used in OV1-19 data analysis.

The processing of the Azur data will be described next. This will be followed by the OV1-19 processing, then that for OV3-3. Finally, the ATS 5 and 6 analyzed data will be discussed.

Azur Proton-Electron Detector

Azur was launched on November 10, 1969, into a 103° inclination orbit with perigee and apogee altitudes of 387 km and 3150 km. The Proton-Electron Detector experiment consisted of two cubical silicon (lithium-drifted) detectors, each covered by hemispherical shielding. There were two pulse height discriminators associated with each detector. This instrument provided four channels of information: (1) electrons greater than 1.5 MeV and protons greater than 20 MeV, (2) protons 20-45 MeV, (3) electrons greater than ~ 4 MeV and protons greater than 40 MeV, and (4) protons greater than 72 MeV. This experiment provided data over the lifetime of the mission and covered the time period November 25, 1969 - March 15, 1970. The original data set supplied to NSSDC (ID# 69-097A-04A) contains count rates (CR) from the four channels described above along with all the position, time, and correlative data needed to analyze the data. More details on the instrument can be found in Achtermann et al. (1970). Ebel (1972) has given the details of the data processing of the raw data by the experimenters.

For $L > 3$, channels (1) and (3) above were measuring only electron fluxes. The conversion from CR to flux was provided by the experimenter. The calibration curves were not provided, so the usual threshold energy/average efficiency studies outlined by Singley and Vette (1972a) could not be done. However, comparison with other data showed that the threshold of 1.5 MeV was good while the higher energy threshold was better suited to 4.5 MeV for analysis purposes.

The data were binned into selected L shells of ± 0.05 width and tagged by the geographic local time ϕ and the value of b. Plots were made of the flux versus b and, using equation (3.5) with m values from AE-4, a value for b_c was determined. Having this, each CR at $b = b_i$ and $L = L_j$ was projected to the equator by using the G function. This procedure is given by

$$A = CR(b_i, L_j) / G(b_i, L_j, m_j, b_{cj}) \tag{3.7}$$

and since G is unity at the equator $(b = 1)$, one has

$$A = CR(b = 1, L_j) \tag{3.8}$$

Then these data projected to the equator were binned in one-hour ϕ cells to determine the local time distribution. The empirical distribution is given in Table 1 with a normalization the same as that given in equation (3.4). Any bins with no data were ignored, and the integral (or sum in this case) was divided by the number of occupied bins. The least squares fit to the log of the flux provides values of C, which are also given in Table 1. The 95% confidence interval half width for C, which is quite small, is also given there. The value of K was also determined in the fitting process, and, as expected, its value given in Table 1 is close to unity. In any satellite orbit except geostationary (or near geostationary), it requires a long time to sample all the local time bins. The coverage for Azur, which lived for about four months, can be seen in Table 1. A highly elliptical satellite such as OGO 1, 3, or 5 takes one year to sample all local times; geostationary satellites require only 24 hours. Consequently, there is "noise" introduced in the local time "signal" by enhancements (substorm injections) in the outer zone. One expects that the local time variation should cease around $L = 3$. The values of C at energies above 1.5 MeV for various L values are plotted in Figure 1 for AE-4MAX and MIN, for Azur, and for ATS 6. The interval for ATS 6 data corresponds to SOLMIN conditions. The curve for AE-8 is shown; this applies to all solar cycle conditions. The AE-4MIN points are now believed to be elevated because of "noise" in the elliptical satellite data. AE-4MAX had the benefit of having the ATS 1 data of Paulikas and Blake incorporated. Below $L = 6$ the AE-8 curve differs from the AE-4MAX model so as to conform to the Azur results. The fall of the curve at high L values reflects the fact that as the flux goes to zero (literally to $J = 1$, which is about the value of the cosmic-ray proton background), there is no local time variation.

After the AE-8 Φ function was determined, it was used to convert the Azur data base to the local time of $\phi_{m(L)}$, which is defined by the equation

$$\Phi(\phi_m) = 1 \tag{3.9}$$

and explicitly is

$$\phi_m = 11 + \frac{12}{\pi} \cos^{-1}\left(-\frac{K}{C}\right) \tag{3.10}$$

If a measurement was made at b_i, L_j, ϕ_i, then to convert this to ϕ_{mj} the following procedure was used.

$$CR(b_i, L_j, \phi_{mj}) = CR(b_i, L_j, \phi_i) / \Phi(L_j, \phi_i) \tag{3.11}$$

For each L value this converts the measurement to that which would be observed for the local time average at b_i. The CRs were then converted to flux using the geometrical conversion factor provided by the experimenter. Then the data were plotted with J versus b at various L values. The results for L = 3.0, 4.0, 5.0, and 6.0 are shown in Figures 2 through 5. In this region the data provide good coverage where the cutoff effects occur. The curves that are drawn require some explanation. These have the form of equation (3.5) with a multiplicative factor inserted such that equatorial value of J is the time average of the Azur fluxes projected there, as discussed earlier. The two curves in each figure differ only in the value of b_c that was chosen. The larger value was chosen so that practically all the points have a b < b_{c2}. The smaller value was chosen to represent a boundary for "undisturbed" conditions. This is best seen in Figure 2 where there seems to be a boundary of some small width with a relatively small number of points with larger b values. This curve was selected to pass through the center of the boundary, not its outer edge. As one looks at the higher L values, one sees a much higher percentage of points with b values above b_{c1}. A vertical dotted line at b_{c1} is included to help the reader see the points beyond this undisturbed boundary. The figures also illustrate why the Azur data are not good for determining the m value of equation (3.5). Satellites with 30° - 50° inclinations provide good coverage of the b region where cutoff effects are not present; all the available data of this type were analyzed in the construction of AE-4.

The b_{c2} cutoffs are the ones used in AE-8. The reason for this choice was to ensure that one is very unlikely to experience fluxes beyond the AE-8 cutoff. Feedback from the users have indicated this is preferable to them. The b_{c1} cutoff is more useful in studying the particle population. This is illustrated in Figure 6 where the cutoff values are plotted versus L. The inner zone values are taken from the AE-5 document (Teague and Vette, 1972). Notice that the outer zone b_{c1} is virtually an extension of this inner zone boundary with nearly the same L power law dependence. In the outer zone b_{c2} is about a factor of 1.4 greater than b_{c1}. After passing through the transition region, there is no distinction between these two boundaries in the inner zone.

The greater than 4.5 MeV channel was processed in the same manner as described earlier in this section for the greater than 1.5 MeV data. The data from this channel showed the same atmospheric cutoff (b_{c2}) as the greater than 1.5 MeV data. The dynamic range for the greater than 4.5 MeV channel was not as large as that for the greater than 1.5 MeV, being about a factor of 50, and the intensity threshold corresponded to a flux of about 20 electrons/cm^2-s. Because of these limitations the data did not reveal a consistent local time distribution. So the C (> 1.5 MeV) was scaled using the AE-4 model energy dependence to obtain the local time distribution.

Returning to Figures 2 through 5, if one imagines moving the curve associated with b_{c2} so that it passes through each plotted point in chronological order, then the projected equatorial flux value as a function of time is obtained. The daily averages of these projected equatorial fluxes from the two Azur channels are shown in Figures 7 and 8 for the L values corresponding to the outer zone peak. The daily sample size varied from 5 to 18 and averaged about 10. The standard deviations of the logarithm of the flux (σ) for these plots are 0.51 and 0.12, respectively. The statistical function for AE-8, which uses σ is discussed in Chapter 5 (pages 5-5 through 5-7). It was felt that the new data used in AE-8 could not add much to this statistical function over that provided by the data used in AE-4. Both σ values above from Azur are low compared to AE-4. Data sets that have a duration of less than six months often show lower (or higher) σs than longer lived ones. The use of daily averages also reduces the σ value. It is concluded that Azur statistical behavior is similar to other outer zone data sets.

Thus, the Azur data have supplied the omnidirectional flux for E > 1.5 and > 4.5 MeV for L values from 3.0 to 6.6. It is believed that the greater than 4.5 MeV data suffer from a bremsstrahlung background that becomes important for L above 5.5. Another contributing factor might be the intensity threshold for this channel; when flux levels fall more often below this threshold, the average value is distorted upwards. This effect would also reduce the value of the σ just discussed.

OV1-19 Electron Spectrometers

OV1-19 was launched on March 18, 1969, into a 105° inclination orbit with perigee and apogee altitudes of 466 km and 5764 km. Thus, it was in a similar but higher orbit than that of Azur. Vampola had an experiment on board that was comprised of two magnetic electron spectrometers. These instruments provided data from March 18, 1969, to the end of spacecraft life in March 1970. The data set deposited in NSSDC (ID# 69-025C-05A) terminates on January 25, 1970; consequently, there is a data overlap period with Azur of about 61 days, neglecting data gaps.

The initial results from this experiment were used to claim that the AE-4 model was in gross error for electrons whose energies are above 1.5 MeV. Unfortunately, it was many years after these distorted (but not completely false) claims before the resolution of this matter was obtained. This came about through the analysis described here, the result of which was the utilization of much of the data from this experiment in AE-8. However, the channels above 2 MeV are rather useless in the outer zone as independent data, since a background correction is absolutely necessary.

The description of the instrument was given by Vampola (1971) and will be summarized here since an understanding of it is necessary to follow some of the analysis. The spacecraft was spin stabilized at a rate of 8.4 rpm. Both spectrometers had their look direction perpendicular to the spin axis. A three-axis magnetometer was also on board. The low energy spectrometer (LES) had eight detectors for measuring electrons and one detector for background, all in an analyzing field of 470 gauss. The background detector had two channels, one for measuring protons greater than 55 MeV and one for measuring electron bremsstrahlung (BREM). The BREM discriminator was set to the nominal energy loss level used by the eight detectors. The high energy spectrometer (HES) contained 16 detectors plus a background detector with two channels, one for protons greater than 130 MeV and one for electron BREM; this latter discriminator was set in the same manner as that for the LES. All detectors were lithium-drifted silicon 1 mm thick with an unshielded sensitive area of 0.95 cm × 1.37 cm. The energy levels and other information about this instrument are given in Table 2. Both spectrometers were the 180° focusing type with internal baffling around the edges of the uniform field and on the pole plates to provide a disk-loaded collimator. A tungsten collimator was used at the entrance of the magnet. Magnet pole pieces were made of Indox V, and an iron yoke enclosed the whole assembly. From the threshold energy of protons arriving at the background detectors, one can infer that the HES had about five times as much shielding as the LES.

Data on magnetic tape (NSSDC ID# 69-025C-05A) contained the CRs for each detector along with all the ancillary data needed for analysis. A subset of these data was selected for AE-8 analysis; only data with local pitch angles within 3° of the perpendicular to the measured magnetic field as determined by the on-board magnetometer were studied. Thus, one is dealing with the unidirectional flux perpendicular to the field line, denoted here by j_p. The CR meters were sampled every second; however, only eight detectors plus two background channels were read out at one time. LES was read and then two reads were required for the HES.

The big mystery for this experiment was the background. The proton channels had such small counting rates that they could be ignored in the outer zone. However, the HES BREM channel counted much too high to be background for the HES detectors. In Table 3 the ratio (CR - BREM)/CR, averaged over the whole interval March 18, 1969, to January 25, 1970, is given. Negative ratios mean that the background exceeded the raw electron CRs, and from these numbers one can rule out the use of all channels above 1.7 MeV and the 53 keV channel over the range of L values shown, unless appropriate backgrounds can be obtained for subtraction. The ratio of the two BREM channels has also been studied without shedding any light on the problem. Ignoring the BREM channel, as Vampola did, one arrives at flux values that are much too high (factor of 10-100) compared to other data, as shown in Chapter 4.

The ATS 6 data of Paulikas and Blake (1979) showed clearly in the geostationary region for energies above 2.5 MeV that AE-4 was too low and therefore needed revision in the high energy range. Since the OV1-19 data was the only data set that covered the energy range between 2 and 5 MeV at other outer zone L values, it was imperative to try to use these data to revise the outer zone .

The following technique was developed. In Figures 9 through 11 the OV1-19 data are shown projected to the equator using the same techniques applied to Azur data except that equation (3.6) was used instead of (3.5) . The open solid squares, labeled *uncorrected*, are the raw CRs converted to flux using the conversion factors of Table 2. Notice that the spectrum is flat above about 3 MeV for all the L values. This raw directional flux, j_r, consists of the true electron flux, j_p, plus a background flux, j_b, resulting from BREM; i.e.,

$$j_r = j_p + j_b \tag{3.12}$$

By taking the last three channels of the HES with the background (supposedly) removed and performing the following operation

$$S = j_p(5091 \text{ keV}) [5243-4942] + j_p(4783 \text{ keV}) [4942-4633] +$$

$$j_p(4476 \text{ keV}) [4633-4500] \tag{3.13}$$

the total electrons/cm^2-ster-s in the energy interval 4500 to 5243 keV results. Now this can be converted to an omnidirectional flux at the equator in electrons/cm^2-s by multiplying by the ratio of equation (3.5) to (3.6)

$$f = G/g_p = 2\pi\beta(0.5, \text{ } m+1) (1-1/b_c)^{0.5} \tag{3.14}$$

The product fS obtained from equations (3.13) and (3.14) is denoted here by J_{e3}. Then

$$J_{e3} \cong J(> 4500 \text{ keV}) \cong J_A(> 4500 \text{ keV}) \tag{3.15}$$

where J_A is the Azur data. This is approximately true since J (> 5243 keV) in the outer zone is small relative to J (> 4500 keV). If j_r is substituted for j_p in equation (3.13), then J_{r3} replaces J_{e3} in equation (3.15). J_{r3} is larger than J_A, the amount depending on the background contamination. Taking the ratio

$$d = \frac{J_A}{J_{r3}} \tag{3.16}$$

the fraction of the uncorrected flux representing the real electron flux results. The empirical results for d are shown in Table 4. The data from both the Azur and OV1-19 experiments were averaged over the data overlap period November 25,1969 - January 25, 1970, to obtain this ratio. It is quite clear that in this energy range the OV1-19 experiment was highly contaminated with BREM from lower energy electrons. This quantity d has the same meaning as the ratio given in Table 3 except that the background is determined by using the Azur > 4500 keV data. The BREM channels had some 25 to 90 times more counts than expected. The most likely cause of this was that the HES BREM discriminator level in orbit was much lower than those for the HE1-16 detectors. In the case of the LES, the problem may have been that the LE1 and LE2 discriminator levels were set high relative to the LES BREM discriminator. The considerably lower conversion factor in Table 2 suggests this was the case and is so noted in the remarks column. This would mean that the background for these two channels would be less than that indicated by the LES BREM channel. Noting that

- The six highest channels of the HES showed nearly the same uncorrected flux for the L interval 3.0 to 6.6,

- Most of the uncorrected flux was produced by BREM,

- The HES BREM channel had much higher CRs than many of the HES detectors and could not be used to properly subtract the background,

the following procedure was used to determine the average HES background. This is expressed as a directional background flux, j_b. This was obtained by averaging the six highest HES channels and applying the factor $(1-d)$

$$j_b = \frac{(1-d)}{6} \sum_{i=HE11}^{HE16} j_r(i) \qquad (3.17)$$

Since Figures 9 through 11 show that these j_rs are essentially independent of energy, it is believed that j_b applies to all of the HES detectors. Then using equation (3.12) the value of j_p can be obtained from the uncorrected flux. In the few instances where this procedure resulted in a negative j_p, then the equation

$$j_p(k) = dj_r(k) \qquad (3.18)$$

was used. These results are plotted as the open squares, labeled *corrected*, in Figures 9 through 11. It is apparent that the corrected and uncorrected data above 3 MeV differ by more than a factor of 10. The results also indicate that no correction is required for the LES detectors.

The first corrected integral spectrum for OV1-19 was then constructed by

$$J_V(> E_i) = f \sum_{k=i}^{17} j_p(k) W(k) + J_A(> 4500 \text{ keV})$$
$$+ 175 df j_r(4476 \text{ keV}) \qquad (3.19)$$

where $W(k)$ is the energy channel width for the kth useful channel, and the factor 175 (keV) is the width from 4325 to 4500 keV. The useful channel index and the Ws are identified in Table 5. In the final results for OV1-19, J_{AE-8} (> 4500 keV) was used in equation (3.19) in place of J_A (> 4500 keV).

The numerical results of all these procedures of this section are given in Tables 6A through 6D. The comparisons of the final corrected data with other data are presented in Chapter 4.

OV3-3 Electron Spectrometer

The OV3-3 satellite was launched into a 81.4° inclination orbit with perigee and apogee altitudes of 360 km and 4492 km. Vampola had a magnetic electron spectrometer on board very similar to those on OV1-19. This one used nine detectors for measuring electrons, and one of them had a discriminator channel for measuring penetrating protons greater than 105 MeV. Since BREM was found not to be a problem in calibration, no BREM background channel was provided. The detectors, collimation, and baffling were nearly identical to those used later in OV1-19. Each detector had an independent set of electronics consisting of an amplifier, two-level pulse height analyzer and log(CR) to analog converters covering the CR ranges $1-10^3$ and

$300\text{-}2 \times 10^5$. More details have been given by Vampola (1969). The channel energy widths and geometric factors are given in Table 7; also included are the threshold energies for integral spectrum calculations that are employed in the data processing done for AE-8. The geometric factors are four times greater than those published by Vampola and are based on his revision (Vampola, 1972, as given in Teague and Vette, 1974).

The data were supplied as flux values versus time and included the pitch angle as inferred from a model geomagnetic field along with other parameters needed for analysis. The subset of this data used in the AE-8 analysis consisted of the data for pitch angles close to 90° for L < 10. The NSSDC data set (ID# 66-070A-05C) covers the time period August 4, 1966, to September 9, 1967.

The main purpose in processing the OV3-3 data in the outer zone was to provide a comparison with the OV1-19 data in the energy ranges that overlapped. The OV3-3 data had been used in producing AE-5, and when Vampola changed the geometric factors of the instrument, it was necessary to produce AE-6 to replace AE-5. The processing for OV3-3 in the outer zone was done in an identical manner to that used for OV1-19 with one exception. The integral spectrum J (> 2.445 MeV) was estimated by extrapolating the OV3-3 differential spectrum to higher energies. This procedure was not possible for OV1-19 because of the background problem. The results are shown and discussed in Chapter 4. The agreement between the OV3-3 and the corrected OV1-19 data is good at certain L values. Time variations can explain the disagreements at other L values.

ATS 5 and 6 Omnidirectional Spectrometers

On ATS 5 McIlwain flew an Omnidirectional High-Energy Particle Detector experiment comprised of three plastic scintillator detectors with a 2π field of view and hemispherical shielding. The instrument measured electrons in the range 0.5 to 5 MeV in 12 channels and protons greater than 12, 16, and 24 MeV. Paulikas flew an Omnidirectional Spectrometer experiment on ATS 6 that consisted of four solid state instruments. One was a two-element telescope with a 30° full cone angle, and the other three were omnidirectional instruments similar to the Azur detectors described earlier. Particles and energy ranges (in MeV) measured were

Electrons:	0.14-0.60, > 0.7, > 1.55, and > 3.9
Protons:	2.3-5.3, 3.4-5.3, 12-26, 20-52, and 40-90
Alphas:	9.4-21.2, 13.4-21.2, and 46-100

The lowest energy electron channel and the two lowest proton and alpha channels were directional (from the telescope); all the rest were omnidirectional. Only the electron channels of these two experiments are of interest here.

Paulikas and Blake (1979) presented the data from McIlwain's ATS 5 experiment and their ATS 6 data in the following manner, as shown in Figure 12. They produced from McIlwain's data the omnidirectional fluxes to match their four channels on ATS 6. The ATS 5 data cover the approximate period 1969.7-1972.3 while the ATS 6 data cover 1974.5-1978.3. The ATS 5 data were normalized to the ATS 6 data during some simultaneous coverage in mid-1974. The Zurich monthly sunspot number is also plotted in Figure 12 and shows that the combined data cover both SOLMIN and SOLMAX conditions. The ATS 1 data of Paulikas used in AE-4 also appear in Figure 12. All of the electron data are plotted as 27-day running averages, and yearly averages are shown by the horizontal bars extending across each year or partial year. These yearly or partial year averages provide the pertinent parameters for AE-8. It can be seen in Figure 12 that there are no trends in these averages associated with the solar cycle. The variations are less than a factor of two except for the highest energy channel where variations as large as a factor of 5 are seen; these are more stochastic in nature and possibly related to

high speed solar wind streams according to Paulikas and Blake (1979). The three satellites were at slightly different coordinates, since they were operating at different longitudes. ATS 1 was right on the geomagnetic equator at $L = 6.6$ while ATS 5 and ATS 6 were slightly off the equator at $L \sim 6.7$ and 6.8, respectively. Paulikas and Blake ignored these differences since they were unimportant to their study.

Chapter 4
Comparison of the AE-8 Model with Data

This comparison is limited to the data discussed in Chapter 3 and to the AE-4 model. The documentation for AE-4 and AE-5 gives the comparison of many data sets to the models, and the work of Teague et al. (1979) shows comparison of other data sets with inner zone models. Therefore, this section is confined to outer zone electrons, whose phenomenology has been discussed for modeling purposes by Singley and Vette (1972b) and by Chan et al. (1979). These comparisons are shown in Figures 13 through 39. In all of these AE-8MAX (MIN) is represented by the large open squares (circles) and the other entries (except for Figure 33) by smaller symbols so that the reader can clearly see the data to which the new model conforms.

Figures 13 through 17 cover the transition region. Each is broken into two graphs: (a) SOLMAX and (b) SOLMIN. For SOLMAX, AE-8 and AE-6 agree up to energies of 0.75 MeV. Above this energy AE-8 becomes larger and extends to higher energies. For SOLMIN the agreement between AE-8 and AE-5P is good up to 3.5 MeV at which point AE-8 grows larger and extends to higher energies. In Figures 17a and 17b AE-4MAX and MIN replace AE-6 and AE-5P, respectively. Here for SOLMAX the agreement extends up to energies of 3 MeV, then AE-4 falls rapidly below AE-8. For SOLMIN the departure of AE-4 from AE-8 begins at 0.75 MeV, with AE-4 falling rapidly below AE-8; again AE-8 extends to higher energies.

The next set of figures that will be discussed involves Figures 18 through 32. In these the comparisons of AE-8MAX with AE-4MAX and data from Azur, OV1-19 uncorrected (19U), OV1-19 corrected (19C), and OV3-3 are presented. OV3-3 is presented only for L values of 3.0, 3.5, 4.0, 4.5, 5.5, and 6.0; thus, these data are only found in Figures 19, 20, 22, 23, 25, 26, 28, and 29.

Some remarks relative to this set of plots are appropriate. First, the focus will be on Figures 18 through 21, which cover the L region 3.0 through 3.5. The electron fluxes above 0.5 MeV in this region are very volatile, even when one considers yearly averages. This is the same volatility as that demonstrated in Figure 12 for the greater than 3.9 MeV fluxes. If one concentrates on the energy region 0.75 through 2 MeV, one finds at L = 3.0 that 19C is low, Azur is in the middle, and OV3-3 is high with the ratio OV3-3/19C ~ 20. At L = 3.5 Azur is low, OV3-3 is middle, and 19C is high with the ratio 19C/Azur ~ 6. The reason for this behavior has been

discussed previously (Chan et al., 1979) and is related to injection events that penetrate deeply into the radiation belts. During the lifetimes of OV3-3 and OV1-19, there were two major injection events that penetrated to L = 3.5, but only one of those four events penetrated to L = 3.0. This latter event occurred during the OV3-3 lifetime. During the Azur lifetime only one of the OV1-19 events was present. Consequently, the observed behavior seen in Figures 18 through 21 is understood. The position of AE-8MAX is consistent with AE-4MAX and lies near the geometric mean of OV3-3 and 19C at L = 3.0. The high energy extension above 2.5 MeV for AE-8MAX follows the Azur and 19C results. It is noted that there is forced agreement between 19C and AE-8MAX at 4.5 MeV, as explained in Chapter 3 (page 3-5 and subsequent pages). Below 0.5 MeV there is relatively good agreement. The extreme of the 19U data above 2 MeV is obvious throughout this L region.

A few remarks relative to errors are appropriate at this time. The general error assigned to the models in this series has been stated as about a factor of 2. For AE-5 a more detailed statement was made. What is meant by the factor of 2 error is that for a flux of J_m the reasonable upper limit is J_u and the reasonable lower limit is J_l where

$$\frac{J_u}{J_m} = \frac{J_m}{J_l} = 2 \tag{4.1}$$

Thus, the ratio $\frac{J_u}{J_l}$ = 4. Now the symbol for AE-8 in Figures 18 and 19 would have to have a vertical extent about three times longer (linear not the log scale) to represent this error. The actual dimension represents a factor of 1.25. Consequently, the symbol can be used to roughly gauge how well the data and the model *agree*. Therefore, in the worst situation at L = 3 the error is a factor of 4.5. Elsewhere in this region the factor of 2 is appropriate and, in some cases, is pessimistic. Only data lying outside the factor of 2 error will be noted for the remainder of the discussion of these figures.

In Figures 22 through 32 all is good save for a few spurious points until the Azur greater than 4.5 MeV data gets too high by L = 4.6 and continues this trend at the higher L values. The disparity of the 19U data is obvious throughout this region. It should be noted in Figure 32 that AE-8MAX and AE-4MAX are replaced by AE-8 and AE-4 since the solar cycle effect is no longer evident and the MAX and MIN models are the same at higher L values.

For L = 6.6, the nominal geostationary L shell, instead of plotting AE-4, all of the satellite data used in constructing both AE-4 and AE-8 are shown. This requires two figures because of the large number of satellites involved. In Figure 33a the ATS 5/6 data are plotted for both the highest (U) and lowest (L) averages shown in Figure 12. It should be noted that the 4 MeV model value conforms to ATS 5/6 U value and so is a pessimistic value. At least the neighboring 19C points are in accordance. The Azur point at 4.5 MeV is clearly too high, as discussed in Chapter 3 (page 3-2 and subsequent pages). The OGO 1 point around 2 MeV is high, and the ATS 5/6 point at 0.7 MeV is at the factor of 2 limit. The 19C points between 0.8, and 3 MeV are also errant. In Figure 33b the high energy points for Explorers 6 and 12 are low, but as ATS 5/6 data at high energies have shown, fluctuations in long-term averages can be expected in this energy-L region. The high energy 19U points reach their ultimate departure from reality. For the latest ideas on time variations of high energy electrons in this region, consult Baker et al. (1986, 1989, and 1990) and Nagai (1988).

For the higher L values 7 through 11 there are no new data to compare with AE-8. Consequently, in Figures 34 through 39, the comparison of AE-8 and AE-4 is given. It is apparent that AE-8 possesses a high energy tail except for L = 11.

Chapter 5
Presentation of the Model

This model has several different forms of presentation. The most important for use is the machine-sensible or numerical form, which will be given first. Based on the analyses conducted to construct the model, there were certain analytical descriptions not incorporated in the numerical model that might be useful to some recipients; these are summarized next. Graphics provide a good way of conveying the model. However, some of the standard forms used in previous model documents do not appear, such as the b-L and R-Λ flux contour plots and the J versus b. The radial profile equatorial flux plots are included to illustrate the solar cycle effect. Finally, the results of fluences obtained in the standard set of circular orbits are given in tabular form.

Numerical

The function

$$Z = \log_{10} \mathcal{J} \tag{5.1}$$

where

$$\mathcal{J}(>E, b, L, T) = \int_{0}^{2\pi} J(>E, b, L, \phi, T) \, d\phi \tag{5.2}$$

is given at a fixed set of instances of the variables. This presentation consists of both the logical and physical organization, since the physical format may vary depending on the storage medium on which the model is conveyed.

Logical Organization

The logical organization for the numerical AE-8 was dictated by the desire to store the essential data in a minimum amount of storage space. This goes back to the early 1970s when the memory size of most computers was well under a megabyte. AE-4 and -5 were just coming out and were larger than earlier models. Consequently, a BLOCK DATA statement approach was taken using binary coded decimal (BCD) representation with six characters per storage cell. Also, the integer format made for easier interchange; this required the scaling of the data by differing scale factors.

The logical record chosen has been explained in Teague et al. (1972), but it will be described in detail here, since some updating is necessary. This logical record is variable in length with the first field giving the number of fields in the record. The second field is the scaled energy value. The rest of the fields are organized first by L value and then by a variable related to b. In addition, the variable Z of equation (5.1) is given at the equator and denoted z_1 here. The first field in the L substructure is the number of cells in the substructure, followed by the scaled L value and then the field for scaled z_1. The remainder of the cells in this substructure contain scaled values of

$$\delta(b-1) = \delta(x) = \delta b = \delta x \tag{5.3}$$

where the change is defined by a fixed Z decrement, ZDEL, which for AE-8 has the value of 0.25. Therefore, on the L shell to reach

$$z_2 = z_1 - \text{ZDEL}$$

the b value must change from 1 to

$$b_1 = 1 + db_1$$

Thus, the value of δb_i is variable, but given z_1 the value of z_{i+1} is known from the cell index of δb_i. This pattern continues for each of the L values in the AE-8 grid, which can total up to 45 depending on the energy. (The variable x is convenient for the method of interpolation described in Appendix A.) This logical record then repeats for the other 17 energies (18 total) of the AE-8 grid. As shown in Table 8 this scheme utilizes 13,548 cells for AE-8MAX and 13,168 for AE-8MIN. What are not contained in the basic model map are the scale factors for E, L, Z, and db as well as the total number of cells, ZDEL, name, and epoch, the latter being redundant to the name. These are given in a header record and are included in Table 8. The parameter ZDEL does not appear in the BLOCK DATA statement.

Physical Representation

Magnetic Tape. The data set NSSDC ID# MT- 2AB contains AE-8MAX with a BCD representation and a physical record size of 80 bytes. The physical record is a card image; the header record and first part of the model map are given in Table 9. There are 1692 physical records in this data set. The first 28 physical records are header records, and there is one trailer record containing the END statement. The format of the BLOCK DATA is given in Table 9. The model is broken into 84 (sub) maps with the first 83 being of dimension 163 and the last 19. By decoding MAP1, one can see that the first two L values are 0 and 1.1 with $z_1 = 0$. These are guard values at the inner edge of the map. At certain energies the L value of 1.1 is replaced by one of the grid values in Table 9 that is just prior to the L grid value for which Z has a non-zero value. The same two "empty" L sets occur at L values of 12.0 and 15.6 at the outer boundary, with the L value of 12 being replaced by a lower value for certain energies. The details of the L grid can be seen more clearly in Chapter 5 (page 5 - 7) where Table 13 is

discussed. AE-8MIN differs only in its total length being 1646 physical records, containing 79 (sub) maps of dimension 163, one of 159, and the last of 132. The data set ID# is MT-2AA. As noted above, the value of ZDEL is missing from the BLOCK DATA statement. This parameter is contained in the software program MODEL sent with this data set and used to decode the map to produce flux values.

Microfiche. These two data sets (AE-8MAX—#MT-52A and AE-8MIN—#MT-52B) provide integral flux values from L = 1.2 to 11.0 at 0.1 intervals for B values (magnetic field intensities) from the equator to the flux cutoff limit of 1 electron/cm^2-s in 100 gamma steps starting at the first multiple of 100 gammas. The energy levels covered are slightly different than the MAP energies being in MeV: 0.04, 0.10, then the range 0.25-4.00 in 0.25 steps, and finally 4.00-7.00 in 0.50 steps.

Floppy Disk. In 1988 Bilitza completed the revision of Program MODEL (MODEL87) and wrote an interactive driver program RADBELT to handle the models in the BLOCK DATA format (Bilitza, 1990). Included as part of this package is AE-8. The whole package has a data set ID number of PT-11B and is available on two PC floppy disks. The parameter ZDEL is included in the BLOCK DATA statement in this form.

Since the main element of decoding the BLOCK DATA format is contained in the FORTRAN function TRARA2, this is described in Appendix A with some additional comments added to the source listing to make it easier to follow the logic.

Analytical Forms

There are several analytical expressions that have been used in constructing the model, some of which are not incorporated in the numerical model. An example is the local time function given by equation (3.3); this function also contains tabular functions. These analytical/tabular forms will be summarized in this section.

Magnetic Cutoffs Resulting from the Atmosphere

For AE-8 this takes the form

$$b_{c2} = \begin{cases} 0.6572L^{3.452} & ; \quad 1.2 \le L < 2.4 \\ 0.196L^{4.878} & ; \quad 2.4 \le L \le 3.0 \\ 1.4567L^{3.050} & ; \quad 3.0 < L \end{cases} \tag{5.4}$$

Results from equation (5.4) were incorporated into the numerical model. A more physical cutoff was also obtained but not incorporated. This was given by

$$b_{c1} = \begin{cases} 0.6572L^{3.452} & ; \quad 1.2 \le L \le 3.23 \\ 1.0523L^{3.050} & ; \quad 3.23 < L \end{cases} \tag{5.5}$$

5-3

Local Time Function

The function $C(> E, L)$ is needed to use equation (3.3); the function $K(> E, L)$ can be derived once C is known. C is given as a tabular function in Table 10. As noted in Chapter 3 (page 3-3), C has no dependence on epoch.

Flux Variation Along the Field Line

In the inner zone this was given as an equatorial pitch angle distribution, differential in energy, in the form

$$j(E, \alpha_o, L, T) = a(\alpha_o, L, T) E \exp(-E/X(\alpha_o, L, T)) \qquad (5.6)$$

where

$$a(\alpha_o, L, T) = \begin{cases} a_r(L, T)\dfrac{\sin^P(\alpha_o-\alpha_c)}{\sin^P(\alpha_e-\alpha_c)} & ; \quad \alpha_c \leq \alpha_o < \alpha_e \\[2em] a_r(L, T) & ; \quad \alpha_e \leq \alpha_o \leq 90° \end{cases} \qquad (5.7)$$

Here the cutoff is expressed by

$$\alpha_c = \sin^{-1}\left(\sqrt{\frac{1}{b_{cl}}}\right) \qquad (5.8)$$

The function X of equation (5.7) is given by

$$X(\alpha_o, L, T) = \begin{cases} X_r(L, T)\dfrac{\sin^n\alpha_o}{\sin^n\alpha_e} & ; \quad \alpha_c \leq \alpha_o < \alpha_e \\[2em] X_r(L, T) & ; \quad \alpha_e \leq \alpha_o \leq 90° \end{cases} \qquad (5.9)$$

Now the functions a_r, p, α_e, X_r, and n were given as tabular functions for AE-5. However, in constructing AE-5P and AE-6 these functions were not tabulated. The only tabular function remaining for magnetic field line variation is in the outer zone and is the exponent m of equation (3.5); this is given as a tabular function in Table 11.

It may be instructive to compare in more detail the differences between equations (3.5) and (5.6). Since there is no local time dependence in the inner zone, the Φ function does not appear in equation (5.6). To show the comparison better, integrate equation (5.6) over energy to obtain the integral spectrum

$$j_{iz}(> E, \alpha_o, L, T) = aX^2\left(\frac{E}{X} + 1\right)\exp\left(-\frac{E}{X}\right) \qquad (5.10)$$

Then by substituting

$$b = \sin^{-2}\alpha_o \qquad (5.11)$$

the perpendicular flux

$$j_{piz} = a_r X_r^2 \left(\frac{b}{b_e}\right)^{-p/2} \left(\frac{1-\sqrt{\dfrac{b-1}{b_c-1}}}{1-\sqrt{\dfrac{b_e-1}{b_c-1}}}\right)^p \left(\frac{E\left(\dfrac{b}{b_e}\right)^{n/2}}{X_r} + 1\right) \exp\left(\frac{-E\left(\dfrac{b}{b_e}\right)^{n/2}}{X_r}\right) \qquad (5.12)$$

results. It is not possible to convert this analytically into an omnidirectional flux. Consequently, the best that can be done is to convert equation (3.2) into its j_p form using equation (3.6) to obtain

$$j_{poz} = \frac{b^{-m}}{2\pi\beta(0.5,m+1)}\left(\frac{b_c-b}{b_c-1}\right)^m \sqrt{\frac{b_c}{b_c-1}}\ N_T(>E,L) \qquad (5.13)$$

In the case where $X_r \ll E$ and keeping only terms that convey functional dependence

$$j_{piz} \sim b^{-(p-n)/2}\left(1-\sqrt{\frac{b-1}{b_c-1}}\right)^p E\exp\left(\frac{-E\left(\dfrac{b}{b_e}\right)^{n/2}}{X_r}\right) \qquad (5.14)$$

$$j_{poz} \sim b^{-m}(b_c-b)^m\ N_T(>E,L) \qquad (5.15)$$

A comparison of these two equations shows that the inner zone spectral function depends on b as well as E; both spectral functions also depend on L and T. All exponents depend on L and T. The main field line variation near the equator expressed by the first factor in each equation is the same; however, the behavior near cutoff is of a different form. In addition, the exponential in equation (5.14) has a profound effect on the b variation. It is possible to use the form of the b variation given in equation (5.13) or (5.15) to fit the one given in equation (5.12) or (5.14) at a given energy by adjusting the value of m, but then m is strongly E dependent. Since AE-4 and AE-5 were developed somewhat independently, a common form for the b variation was not enforced.

This discussion shows where the character of the inner and outer zone portions of the model are different and why a transition region is necessary.

Statistical Function

The statistical model associated with AE-8 is the same as that for AE-4 but extended to higher energies. The time variations in the outer zone make the flux a random variable. All random variables in this section will be denoted with bold face symbols. The empirical cumulative distribution function is obtained by

$$P(\mathbf{J} > J_s) = \frac{\text{Time that } J > J_s}{\text{Total time of sample}} \tag{5.16}$$

where $\mathbf{J}$ is the random variable representing the local time averaged flux, which is still subject to large excursions resulting from injections. To a reasonable approximation this function P can be represented by

$$P(\mathbf{Z} > Z_s) = \frac{1}{\sigma\sqrt{2\pi}} \int_{Z_s}^{\infty} \exp\left(-\frac{(\mathbf{Z}-\mu)^2}{2\sigma^2}d\mathbf{Z}\right) \tag{5.17}$$

which is the well known normal distribution, and $\mathbf{Z}$ is defined by equation (5.1). When $Z_s = \mu$, then $P = 0.5$. For AE-8, σ ($> E, L$) is a tabular function given in Table 12. This function follows the AE-4 function and is extended in energy. As the flux tends to zero, σ also tends to zero. The value of μ is obtained using σ and the long-term average value of the flux, as will now be shown. The probability density function q is

$$q(\mathbf{Z}) = \frac{1}{\sigma\sqrt{2\pi}} \exp\left(-\frac{(\mathbf{Z}-\mu)^2}{2\sigma^2}\right) \tag{5.18}$$

It is convenient to change variables from $\mathbf{Z}$ to $\mathbf{Y}$ to obtain a random variable with mean of zero and standard deviation of 1. With

$$\mathbf{Y} = \frac{(\mathbf{Z}-\mu)}{\sigma} \tag{5.19}$$

and $\qquad \mathbf{J} = 10^{\mu}\exp(k\sigma\mathbf{Y}) \tag{5.20}$

where $k = \ln(10) = 2.30259 \tag{5.21}$

one can compute the average value of $\mathbf{J}$

$$\mathbf{J}^{\star} = \int_{-\infty}^{\infty} \frac{1}{\sqrt{2\pi}} \mathbf{J}\exp\left(-\frac{\mathbf{Y}^2}{2}d\mathbf{Y}\right)$$

$$= 10^{\mu}\exp\left(\frac{k^2\sigma^2}{2}\right) \int_{-\infty}^{\infty} \frac{1}{\sqrt{2\pi}} \exp\left(-\frac{(\mathbf{Y}+k\sigma)^2}{2}d\mathbf{Y}\right) \tag{5.22}$$

Since the integral is unity and the exponential can be written as a power of 10, the result is

$$logJ^* = \mu + \frac{k\sigma^2}{2}$$ (5.23)

With AE-4 it was noticed that some users considered the relationship to be

$$logJ^* = \mu$$

which would result from treating the 50% probability of occurrence as being the average flux value. Since σ is typically equal to 0.5, this produces an error of about a factor of 2.

Although the statistical model for AE-8 is not directly incorporated into the machine-sensible model, it can be done using Table 12 along with some suitable coding. This has been done at the European Space Agency (ESA) European Space Technology Center (ESTEC), for example.

Graphical Presentation

In Figures 13 through 39 the integral spectral plots of equatorial omnidirectional flux versus energy were used to demonstrate the comparison among AE-8, AE-4, and various data. The equatorial omnidirectional flux versus the L value is now used to convey some features of the model and to illustrate the solar cycle effect in some detail. The data base for these plots was extracted from the BLOCK DATA statement and is printed as Table 13A (for AE-8MAX) and Table 13B (for AE-8MIN). An examination of these tables shows the position of the L values where z_1 is equal to zero. Besides the special values of L (0, 1.1, 12, and 15.6) discussed earlier (page 5 - 2), the values 2.69, 2.79, and 2.89 also appear to handle the region near where the flux minima occur in the slot region.

In Figure 40 the equatorial flux profile for all of the grid energies are shown for AE-8MAX. No electrons greater than about 4.5 MeV appear in the inner zone, while the outer zone contains electrons up to 7 MeV. When the energies are above about 0.75 MeV, the inner zone peak occurs at an L value of 1.50, while at lower energies this peak is at 1.80. For energies above 2.0 MeV the slot is very deep. In the outer zone the flux peak moves inward from about an L of 4.8 as the energy increases to about an L of 3.1 for the highest energies.

Figures 41 through 45 show the equatorial profiles for AE-8MAX and AE-8MIN for the same energies, so that the solar cycle effect is clearly demonstrated. Large open symbols have been chosen for AE-8MAX, while small solid symbols have been used for AE-8MIN. With this choice it is easy to see when the fluxes are essentially the same value. From these figures it can be ascertained

- For energies below 0.75 MeV the inner zone fluxes are higher at SOLMAX.

- For energies above 1.0 MeV the inner zone fluxes are independent of the solar cycle.

- For energies above 6.0 MeV the outer zone fluxes are independent of the solar cycle.

- For energies below 6.0 MeV there is a region starting at the outer edge of the slot and ending in the L range between 3.0 and 6.0 depending on energy where the SOLMIN fluxes are less than SOLMAX fluxes. The ratio of these fluxes ranges up to 4 at the lowest energies.

Orbital Integration Results

There is a standard set of circular orbits that are run with the models to demonstrate the amount of fluence in electrons/cm^2-day accumulated in various energy windows and above certain threshold energies. The results are shown in Table 14 for AE-8MAX. The sampling interval and the accumulation time vary with orbit altitude to take into account certain factors and provide a reasonable average value. Thus, at low altitudes the sampling time is 30 seconds because the satellite moves rapidly through the regions where flux gradients are large. The accumulation length is 36 hours to average out the South Atlantic Anomaly effects. These parameters are shown at the top of each page of the table. For orbits that traverse the inner zone the standard sampling interval is one minute and the accumulation time is 24 hours. Then the accumulation rises in discrete steps up to 4608 hours and the sampling interval increases up to 48 minutes. The table is organized with four orbits per page with the altitude constant and fixed inclination orbits of 0°, 30°, 60°, and 90°. The first column under each inclination gives the daily fluence above the energy given in the first column of the page. The second column under each inclination gives the daily fluence in the energy band defined by the first two columns of the page.

Appendix A
Function TRARA2

Within Program MODEL and now MODEL87 the subroutine TRARA1 handles the interpolation of Z in E, L, and b, and so serves as the gateway to the numerical AE-8 models. A FORTRAN function, TRARA2, which is in TRARA1, handles the Z, L, and b interpolation linearly, but the paths are not along constants of the variables. TRARA2 has been discussed briefly in Teague et al. (1972), but this and the source listing for the function leave some points unclear about how TRARA2 really works. Because of this additional comments have been added to the source listing, and the names of some variables have been changed to make it easier to follow the logic. The original code was written in the days when the GOTO command was in vogue rather than structured programming. This has not been changed so that the function operates in exactly the same manner as before. This makes the code harder to follow, but the description of the method and the newly commented listing presented in this appendix should make everything clear to the user.

Method

The method can best be illustrated by using Figure A1. Here two Z versus x curves are shown for adjacent L values, L1 and L2 (L2 > L1) at one of the model grid energies. Each grid point in Z-x space for L1 and L2 is shown in Figure A1. The grid energy is fed to TRARA2 in the form of the starting address in the BLOCK DATA for that energy by the argument of MAP, which itself is an argument of TRARA2. Based on the input L value, TRARA2 determines L1 and L2. The general idea is to find the two radial lines passing from the Z-x origin through any grid point that most closely brackets the input point. Since the Z coordinate of the input is what is desired, then an iterative approach is needed. The coordinates of the grid points are known; the equations of the two curves are known (these are straight lines connecting the grid points); the equations of the radial lines are known. Except for OCB3 these radial lines are shown as line segments in Figure A1. The intersection of a radial line with the other curve can readily be computed iteratively. On these two radial lines the L interpolation is done to find the x values. Using this and the equation of the radial lines, the Z coordinates are obtained. Then the interpolation along the line defined by these two interpolated points provides the output Z value.

The specifics will be given by considering three input points shown in Figure A1 as P1, P2, and P3. On the basis of the equatorial values, Z1(L1) and Z1(L2), TRARA2 sets up the larger one as the top (T) set of δx points and the other as the bottom (B) set. These sets are shown converted to x values in Figure A1 and are referred to as the T and B curves. Thus, initially the L1 curve is the T curve. The procedure to find the bracketing radial lines starts by stepping on the T curve from the equator to grid points until the grid point with an x value greater than the input value FNx is reached.

Consider the P1 case first. One can see that no grid point on L1 satisfies this condition. Then the code reverses the role of L1 and L2 so that L2 becomes the T curve. When the stepping reaches the grid point near P1 labeled BT1, then the following procedure is employed. The line OAT1 is constructed (shown as AB1:AT1). Then the B curve (now L1) is stepped from the equator until the grid point labeled CB1 is found. The criterion used is to compute the intersection point AB1 between OAT1 and the B curve until

$$x(AB1) \leq x(B_i) \tag{A.1}$$

where i is the index of the grid point. The formula for x(AB1) is given by

$$x(AB1) \;=\; \left[\frac{Z(B_i) \ast (x(B_i)-x(B_{i-1}))}{ZDEL} + x(B_i) \right] \Big/$$

$$\left[\frac{Z(AT1) \ast (x(B_i)-x(B_{i-1}))}{ZDEL \ast x(AT1)} + 1 \right] \tag{A.2}$$

Thus, the straight line that represents the B curve changes with the value of i. For the example being discussed, B_{21} = CB1 and the equation of the line representing curve B are considerably different than for the segment AT3:BT3. One can see by inspection that any grid point on L1 closer to the equator would not satisfy the condition. The assumption is now made that the x values vary linearly in L along OAT1, so a linear interpolation in L is done to obtain x(AT1). The Z(AT1) value is given by

$$Z(AI1) \;=\; \frac{Z(AT1) \, x(AB1)}{x(AT1)} \tag{A.3}$$

These coordinates are then stored in the XPCM and ZPCM registers, which are used to hold the trial coordinates for the nearest point with XPCM less than FNx. Next the slopes of OBT1 and OCB1 are compared, and the larger one (OCB1) is used first to produce the point labeled CI1, whose coordinates are placed in the XPCP and ZPCP registers. Then the check is made if x(CI1) is greater than or equal to x(P1). Since it is not true in this case, the PCP registers are dumped into the PCM registers (OCT1 replaces OAT1), and the B curve is stepped and tested until the test slope is less than the OBT slope. In this case the next grid point tested would be that of BT1. Since x(BI1) is greater than FNx, the final interpolation in x can be done. This final interpolation assumes that Z is linear in x. Knowing the coordinates of BI1 and CI1, the value of Z(P1) is computed.

If one now considers P2, which has the same x value as P1, things would proceed in the same fashion as for P1 up to the test x(BI1) is greater than x(P1). However, the position of P2 implies L(P2) is less than L(P1), so all the interpolated points AI1, BI1, and CI1 would be closer to the origin than shown in Figure A1. Thus, the new BI1 would fail the test x(BI1) is greater than x(P2). This would result in testing the next grid point radial line that had the larger slope, and the ping-ponging between the L1 and L2 curve would continue until the lines
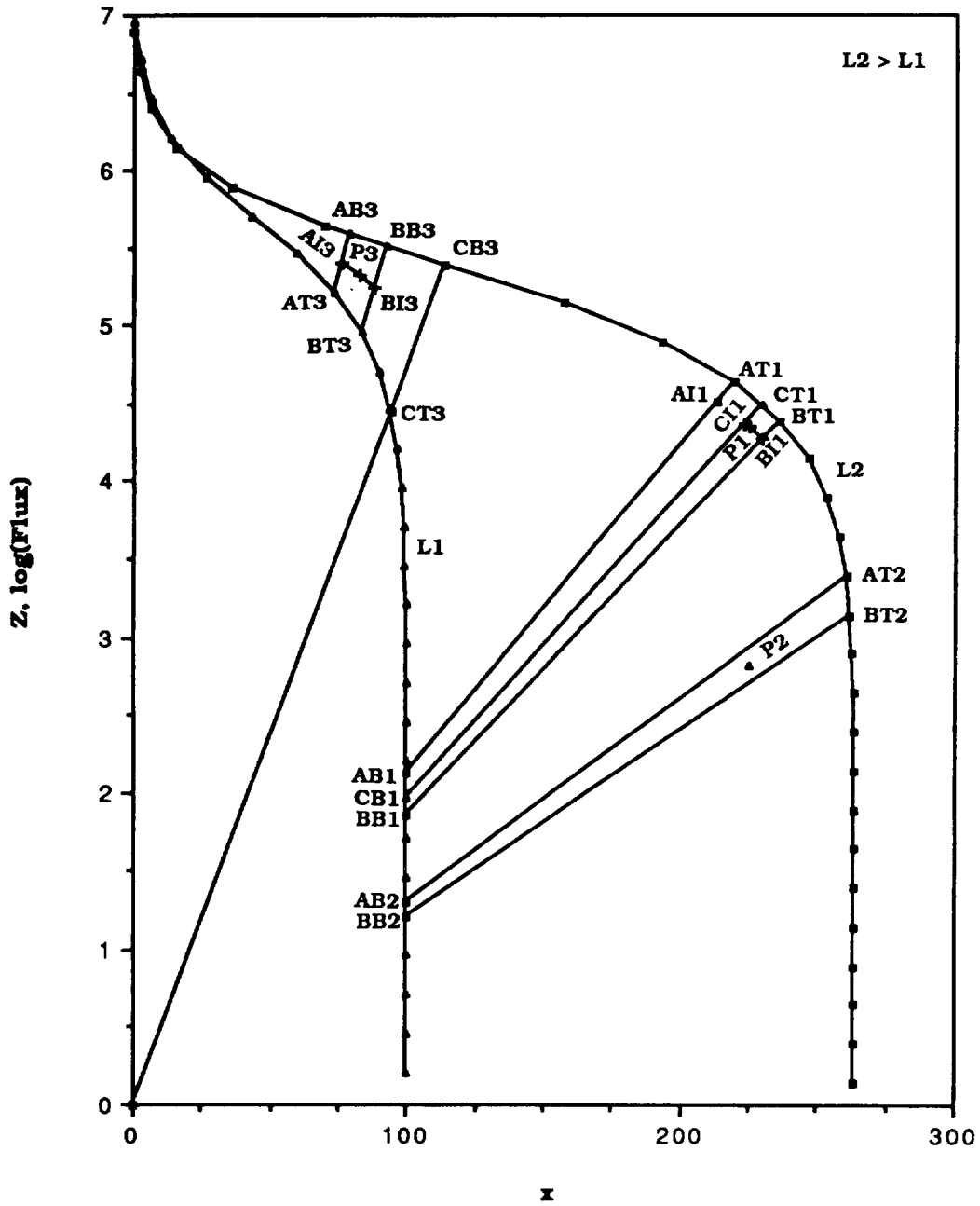
Figure A1. Illustration of TRARA2 Method of Calculation

OAT2 and OBT2 would be reached. The final solution would be done in the same manner as described above.

What has been described above is the most straightforward way for the program to proceed. However, there is a conservative approach in the logic that produces a path that leads to the correct answer but apparently is not the most direct path. Things actually proceed as described above up to the place where AT1 and BT1 are identified. Because there has been a reversal of the curves, the logic now forces a path through the code that has been devised to handle the case where FNx is near the equator. This procedure makes OAT (the numeric suffix is dropped at this point) the Z axis so that the determination of AI does not involve any interpolation using x. Then BT is the first step on the T curve and CB is the first step on the B curve. The larger slope point is tested for the solution as described above, and the ping-pong procedure is started. In the case of FNx near 0, either this first step BT or CB provides the XPCP. In the P1 example the failure of the first step to provide an XPCP starts the ping-pong procedure that results in the same solution as described previously.

Now consider P3 because it illustrates another aspect of the logic employed in the code. No reversal is needed because the point BT3 satisfies the condition. In this case the L1 curve remains the T curve. Thus, AT3 and BT3 are identified as shown in Figure A1. However, the fact that now x(AB3) is greater than x(AT3) causes the logic to force the computation to pass through the FNx near 0 procedure described above. Here again the ping-pong procedure produces the proper answer, which in this case uses the lines OAB3 and OBB3 shown near P3. If in Figure A1 Z1(L2) is greater than Z1(L1), then for all cases considered above the procedure would progress as initially described above, except no reversal would be needed for any of the cases considered.

There are several other cases handled in the code, but these are quite transparent. It is believed the code is now commented well enough that users can understand in detail exactly what is being done.

Source Code Listing

```
        FUNCTION TRARA2(MAP,IL,IX)
C***********************************************************************
C***    TRARA2 INTERPOLATES LINEARLY IN L-B/B0-MAP TO OBTAIN      ***
C***    THE LOGARITHM OF INTEGRAL FLUX AT GIVEN L AND B/B0.       ***
C***     INPUTS: MAP(..)   IS SUB-MAP FOR SPECIFIC GRID ENERGY    ***
C***                       OF TRAPPED RADIATION MODEL MAP         ***
C***             IL        SCALED-L VALUE                         ***
C***             IX        SCALED-(B/B0 - 1)=X VALUE              ***
C***     OUTPUTS: TRARA2   SCALED-LOGARITHM OF PARTICLE FLUX=Z    ***
C***    MOST WORKING VARIABLES, I.E., THOSE THAT CHANGE MEANING   ***
C***    IN COURSE OF THE PROGRAM ARE DENOTED WITH THE SUFFIX      ***
C***    LETTER, W.  THIS DOES NOT APPLY TO INDEXES.               ***
C***********************************************************************
C***    SEE MAIN PROGRAM 'MODEL' OR 'RADBELT' FOR EXPLANATION     ***
C***    OF MAP FORMAT SCALING FACTORS                            ***
C***    THE PARAMETER THAT DEFINES THE FIXED CHANGE OF Z BE-      ***
C***    TWEEN X GRID POINTS IS OBTAINED FROM 'COMMON/TRA2/'       ***
C***********************************************************************
```

```
          DIMENSION MAP(1)
          COMMON/TRA2/FISTEP
C
C CHANGE INTEGER INPUTS TO FLOATING POINT, RENAME FISTEP, AND
C INITIALIZE.
C
          FNL=IL
          FNX=IX
          ZDEL=FISTEP
          ITIME=0
          IT=0
C
C FIND CONSECUTIVE SUB-SUB MAPS FOR SCALED-L VALUES, LSB & LST,
C WITH LSB.LT.IL AND IL.LE.LST . LB & LT ARE LENGTHS OF THE
C SUB-SUB MAPS.  IB+1 & IT+1 ARE THE INDEX VALUES IN MAP
C WHERE THE VALUES OF LB & LT ARE STORED.  IB+2 & IT+2 ARE
C THE INDEX VALUES WHERE LSB AND LST ARE STORED.  IB+3 & IT+3
C ARE THE INDEX VALUES WHERE THE EQUATORIAL Z VALUES, Z1B AND
C Z1T ARE STORED.
        1 LT=MAP(IT+1)
          IF(MAP(IT+2).GT.IL) GOTO 2 !PROPER LST HAS BEEN FOUND
             IB=IT
             LB=LT
             IT=IT+LT                    !CHECKING ON NEXT L VALUE
             GOTO 1
        2    CONTINUE
C
C IF A SUB-SUB MAP IS EMPTY, I.E., LENGTH LESS THAN 4, THEN
C TRARA2=0; DOUBLE EMPTY SETS OCCUR AT THE INNER AND OUTER
C BOUNDARIES OF THE MODELS.
C
          IF((LB.LT.4).AND.(LT.LT.4)) GOTO 50 !THIS SETS TRARA2=0.
C
C IF Z1T IS LESS THAN Z1B INTERCHANGE VARIABLES AND INDEXES SO
C THAT THE SUFFIX LETTER T IS ASSOCIATED WITH THE L VALUE THAT
C HAS THE LARGER Z1. THIS MAKES IT EASIER TO FOLLOW THE LOGIC OF
C THE CODE.
C
          IF(MAP(IT+3).GT.MAP(IB+3))  GOTO 10 !NO INTERCHANGE NEEDED
        5    KT=IB
             IB=IT
             IT=KT
             KT=LB
             LB=LT
             LT=KT
C
C DETERMINE THE INTERPOLATION FACTOR IN SCALED-L VALUE
C
       10 FLLB=MAP(IB+2)
          FLLT=MAP(IT+2)
          DFL=(FNL-FLLB/(FLLT-FLLB)
          Z1B=MAP(IB+3)
          Z1T=MAP(IT+3)
          XBW=0.                    !SET WORKING VARIABLES
          XTW=0.
          ZBW=Z1B
          ZTW=Z1T
          IF(LB.LT.4) GOTO 32  !CASE WHERE Z1B=0.
```

A-5

```
C
C THE X LOOPING IS BASED ON FINDING, FOR A GRID ENERGY AND THE
C TWO SELECTED SCALED-L VALUES, IN X-Z SPACE TWO POINTS, PCM AND
C PCP, WHERE X(PCM) AND X(PCP) BRACKET THE INPUT X VALUE, FNX.
C EACH SUB-SUB MAP CONTAINS THE INFORMATION TO CONSTRUCT A PLOT
C OF POINTS GIVING Z VERSUS X SO WILL BE REFERRED TO AS A CURVE.
C FOR THE LINEAR INTERPOLATION USED THESE GRID POINTS ARE CONNECTED
C BY STRAIGHT LINES. THERE ARE SEVERAL SPECIAL CASES BUT THE GENERAL
C APPROACH IS TO START AT THE EQUATOR (X=0) FOR THE TOP CURVE AND
C STEP FROM GRID POINT TO GRID POINT UNTIL FNX IS
C BRACKETED.  TAKING THE SMALLER XT GRID POINT, AT, ONE DRAWS A
C RADIAL LINE,OAT, TO THE X-Z ORIGIN.  THE INTERSECTION OF OAT
C AND THE LOWER CURVE IS POINT AB. IT CAN BE DETERMINED DIRECTLY
C SINCE THE EQUATIONS OF BOTH LINES ARE KNOWN. THE SECOND XT GRID
C POINT IS BT AND THE INTERSECTION OF LINE OBT WITH B CURVE IS BB.
C A GRID POINT ON THE B CURVE IS CB AND THE INTERSCTION OF LINE OCB
C WITH THE CURVE IS CT.  USING COMPUTED X(AB) AND X(CT)
C AN L-INTERPOLATED X(PCM) IS FOUND.  THEN ONE ITERATES BY STEPPING
C IN X FIRST ON THE B CURVE AND THEN IF NEEDED ON THE T CURVE IN A
C PING PONG FASHION TO GET THE BRACKETING.  THEN AN X, Z
C INTERPOLATION USING PCM AND PCP IS MADE. FINALLY THE INTERPOLATED
C Z VALUE IS RETURNED.
C

        DO 17 J2=4,LT
          XTINCR=MAP(IT+J2)
          IF(XTW+XTINCR.GT.FNX) GOTO 23 !USUAL CASE,SELECTED POINT,AT
          XTW=XTW+XTINCR
     17 ZTW=ZTW-ZDEL
          ITIME=ITIME+1   !SETS FLAG THAT NO SUCH POINT FOUND ON CURVE.
C
C IN THIS CASE FNX LIES IN THE RANGE BETWEEN CUTOFFS OF THE TWO
C L VALUES AND REVERSAL OF CURVES IS REQUIRED.
C
        IF(ITIME.EQ.1) GOTO 5 !LEADS TO REVERSAL OF T AND B CURVES
        GOTO 50   !SET TRARA2=0. REVERSAL FAILED.
     23 IF(ITIME.EQ.1) GOTO 30
C
C THE GOTO 30 OCCURS FOR THE CASE WHERE THERE IS A REVERSAL AND THE
C POINT, AT, HAS BEEN FOUND. IT IS NOT CLEAR WHY THE CODE IS WRITTEN
C THE WAY IT IS. PROCEEDING AT 30 RESETS THE LINE OAT TO BE THE Z
C AXIS(X=0) AND THINGS PROCEED LIKE FNX IS NEAR THE EQUATOR.  THE
C TEST IN 15 THROWS THIS OUT AS A SOLUTION AND THE PING PONG BETWEEN
C 15 AND 20 EXPLAINED BELOW RESULT IN STEPPING OUT ON BOTH CURVES
C UNTIL THE PROPER TWO BRACKETING LINES ARE FOUND. THUS THE RIGHT
C ANSWER IS OBTAINED BUT THE LOGIC IS CONFUSING.
C
        IF(J2.EQ.4) GOTO 28   !THIS IS CASE WHERE FNX  IS NEAR 0.
        SLTW=ZTW/XTW !SLOPE OF RADIAL LINE, OAT
C
C THE GRID POINT, AT, HAS BEEN FOUND. NOW THE B CURVE IS STEPPED
C AND THE X(AB)=XABW BELOW IS COMPUTED UNTIL ITS VALUE IS LESS THAN
C THE VALUE OF X(CB)=XBW BELOW.
C
        DO 27 J1=4,LB
          XBINCR=MAP(IB+J1)
          XBW=XBW+XBINCR
          ZBW=ZBW-ZDEL
```

```
         XABW=((ZBW/ZDEL)*XBINCR+XBW)/((XBINCR/ZDEL)*SLTW+1.)
         IF(XABW.LE.XBW) GOTO 31
      27 CONTINUE
         IF(XABW.LE.XTW) GOTO 50 !TRARA2=0.
      31 IF(XABW.LE.XTW) GOTO 29 !USUAL CASE.ONLY FALSE FOR REVERSAL
C
C 31 WILL NOT BE REACHED IF THERE IS A REVERSAL OR FNX IS NEAR 0.
C FAILURE OF TEST IN 31 OCCURS ONLY WHEN T CURVE LIES BELOW B CURVE
C IN THE REGION OF THE INPUT VALUE FNX. IT IS NOT CLEAR
C WHY SUCH CASES ARE ROUTED THIS WAY. HOWEVER, THE
C CORRECT ANSWER IS OBTAINED. CODE BELOW TREATS PROPERLY THE CASE
C WHERE FNX IS NEAR 0. THUS OAT = Z AXIS AND ZPCM IS COMPUTED USING
C ONLY L INTERPOLATION. THE SLOPES OF OBT AND OCB ARE EXAMINED TO
C SELECT THE LARGER ONE AT 15. THEN XPCP AND ZPCP ARE COMPUTED IN 15
C OR 20. IF THIS IS A SOLUTION, I.E. XPCP.GE.FNX, THE FINAL ANSWER
C IS COMPUTED. IF NOT IT STEPS THE CURVE AND TESTS UNTIL THE TEST
C SLOPE IS LESS THAN THE OTHER CURVE'S SLOPE.
C
         XBW=0.                   !SETTING TO EQUATOR
      30 XTW=0.                   !AT FOUND AFTER A REVERSAL
      32 J2=4                     !CASE FOR Z1B=0
         XTINCR=MAP(IT+J2)
         ZBW=Z1B
         ZTW=Z1T
      28 ZPCM=Z1B+(ZTW-ZBW)*DFL !Z VALUE AT X=0;CASE FOR FNX NEAR 0
         XPCM=0.                  !X VALUE FOR ZPCM
         XTW=XTW+XTINCR           !1ST STEP ON T CURVE, BUT IS BT NOW
         ZTW=ZTW-ZDEL
         SLTW=ZTW/XTW             !OBT SLOPE
         IF(LB.LT.4) GOTO 35 !LB IS AN EMPTY L SET SO XBINCR=0.
         J1=4
         XBINCR=MAP(IB+J1)
         XBW=XBW+XBINCR                !1ST STEP ON B CURVE, CB
         ZBW=ZBW-ZDEL
         SLBW=ZBW/XBW
         GOTO 15
C
C THIS GENERATES PARAMETERS FOR THE NON-NEAR EQUATORIAL CASES
C
      29 XPCM=XABW+(XTW-XABW)*DFL !L INTERPOLATION BETWEEN AT & AB
         ZPCM=XPCM*SLTW
         ZTW=ZTW-ZDEL !NOW THE T CURVE IS STEPPED.
         XTW=XTW+XTINCR
         SLTW=ZTW/XTW   !SLOPE OF OBT
         SLBW=ZBW/XBW   !SLOPE OF OCB
C
C THE CODE IN 20 COMPUTES INTERSECTION POINTS ON THE B CURVE AND
C STEPS ALONG THE T CURVE UNTIL THE SLOPE OF THE RADIAL LINE TO THE
C GRID POINT IS LESS THAN THE SLOPE OF THE RADIAL LINE THROUGH THE
C LAST SELECTED POINT ON THE B CURVE.  THE CODE IN 15 HANDLES THE
C SAME FUNCTIONS WITH THE B AND T CURVES REVERSED. IF THE PATH TO
C 60 IS FROM 15 CODE THEN XPCP COMES FROM A T GRID RADIAL LINE.  A
C B GRID RADIAL LINE COMES FROM 20 CODE. THE SELECTION AT 15 ALWAYS
C MAKES THE LARGER SLOPE RADIAL LINE THE FIRST TO BE TESTED.  IF
C THAT FAILS THAT CURVE IS STEPPED AND TESTED UNTIL THE PCP POINT
C IS FOUND OR THE TEST SLOPE BECOMES SMALLER THAN THE SLOPE OF THE
C LINE THROUGH THE GRID POINT WAITING TO BE TESTED ON THE OTHER
C CURVE.  THIS IS THE PING PONG.
```

```
C
   15 IF(SLBW.LT.SLTW) GOTO 20
      XCTW=((ZTW/ZDEL)*XTINCR+XTW)/((XTINCR/ZDEL)*SLBW+1.)
      XPCP=XBW+(XCTW-XBW)*DFL   !L INTERPOLATION
      ZPCP=XPCP*SLBW
      IF(XPCP.GE.FNX) GOTO 60 !READY FOR FINAL X INTERPOLATION
C
C MUST BEGIN ITERATION TO GET  POINTS PCM AND PCP BRACKETING INPUT
C SO PCP REPLACES PCM AND NEXT POINT ON B CURVE IS EXAMINED TO FIND
C A PCP.
C
      XPCM=XPCP
      ZPCM=ZPCP
      IF(J1.GE.LB) GOTO 50 !LB GRID IS EXHAUSTED, SET TRARA2=0.
      J1=J1+1
      XBINCR=MAP(LB+J1)
      ZBW=ZBW-ZDEL
      XBW=XBW+XBINCR
      SLBW=ZBW/XBW
      GOTO 15  !NOW RETURN TO SEE IF 20 OR 60 EXIT IS OPEN
C
C THE BB OR SUBSEQUENT INTERSECTION POINTS ARE COMPUTED AND TESTED
C
   20 XBBW=((ZBW/ZDEL)*XBINCR*+XBW)/((XBINCR/ZDEL)*SLTW+1.)
      XPCP=XBBW+(XTW-XBBW)*DFL
      ZPCP=XPCP*SLTW
      IF(XPCP.GE.FNX) GOTO 60 !USUAL CASE
C
C NOW THE TOP CURVE MUST BE STEPPED TO THE NEXT POINT AND THE
C PCP VALUES MUST BE TRANSFERRED TO THE PCM CELLS
C
      XPCM=XPCP
      ZPCM=ZPCP
      IF(J2.GE.LT) GOTO 50  !END OF TOP CURVE, SET TRARA2=0.
      J2=J2+1
      XTINCR=MAP(I2+J2)
      ZTW=ZTW-ZDEL
      XTW=XTW-XTINCR
      SLTW=ZTW/XTW
      GOTO 15
   35 XBINCR=0.
      SLBW=-900000. !T CURVE WILL ALWAYS BE TESTED AT 15 BRANCH
      GOTO 20        !ENTERS 20 WITH XBW=0.
   60 IF(XPCP.LT.XPCM+1.E-20) GOTO 50
      TRATRA2=ZPCM+(ZPCP-ZPCM)*((FNX-XPCM)/(XPCP-XPCM))
      TRARA2=AMAX1(TRARA2,0.)
      RETURN
   50 TRARA2=0.
      RETURN
      END
```

References

Achtermann, E., B. Hausler, D. Hovestadt, G. Paschmann, and P. Laeverenz, *Experiments EI 88 and EI 93 for the Measurement of High-Energy Electrons, Protons, and Alpha Particles in the Azur Satellite—Physical Properties and Test Measurements*, Max-Planck-Institute for Extraterrestrial Physics, BMBW-FB 70-67, December 1970.

Baker, D. N., J. B. Blake, R. W. Klebesadel, and P. R. Higbie, "Highly Relativistic Electrons in the Earth's Outer Magnetosphere I, Lifetimes and Temporal History 1979-1984," *J. Geophys. Res.* 91, 4265, 1986.

Baker, D. N., J. B. Blake, L. B. Callis, R. D. Belian, and T. E. Cayton, "Relativistic Electrons Near Geostationary Orbit: Evidence for Internal Magnetospheric Acceleration," *Geophys. Res. Lett.* 16, 559, 1989.

Baker, D. N., R. L. McPherron, T. E. Cayton, and R. W. Klebesadel, "Linear Prediction Filter Analysis of Relativistic Electron Properties at 6.6 R_E," *J. Geophys. Res.* 95, 15133, 1990.

Bilitza, D., *Solar-Terrestrial Models and Applications Software*, National Space Science Data Center, NSSDC/WDC-A-R&S 90-19, July 1990.

Chan, K. W., M. J. Teague, N. J. Schofield, and J. I. Vette, "Modeling of Electron Time Variations in the Radiation Belts," *Quantitative Modeling of Magnetospheric Processes*, ed. W. P. Olson, Amer. Geophys. Union, Washington, D.C., 121, 1979.

Ebel, B., *Processing Raw Data from Experiments EI 88 and EI 93 on the Satellite Azur*, Max-Planck-Institute for Extraterrestrial Physics, MPI-PAE/Extraterrestrial 76, March 1972.

Nagai, T., " 'Space Weather Forecast:' Prediction of Relativistic Electron Intensity of Synchronous Orbit," *Geophys. Res. Lett.* 15, 425, 1988.

Paulikas, G. A., and J. B. Blake, "Effects of the Solar Wind on Magnetospheric Dynamics: Energetic Electrons at the Synchronous Orbit," *Quantitative Modeling of Magnetospheric Processes*, ed. W. P. Olson, Amer. Geophys. Union, Washington, D.C., 180, 1979.

Paulikas, G. A., private communication, 1981.

Roberts, C. S., "On the Relationship Between the Unidirectional and Omnidirectional Flux of Trapped Particles on a Magnetic Line of Force," *J. Geophys. Res.* 70, 2517, 1965.

Singley, G. W., and J. I. Vette, *The AE-4 Model of the Outer Radiation Zone Electron Environment*, C72-06, August 1972a.

Singley, G. W., and J. I. Vette, *A Model Environment for Outer Zone Electrons*, National Space Science Data Center, NSSDC 72-13, December 1972b.

Teague, M. J., and J. I. Vette, *The Inner Zone Electron Model AE-5*, National Space Science Data Center, NSSDC 72-10, November 1972.

Teague, M. J., J. Stein, and J. I. Vette, *The Use of the Inner Zone Electron Model AE-5 and Associated Computer Programs*, National Space Science Data Center, NSSDC 72-11, November 1972.

Teague, M. J., and E. G. Stassinopoulos, *A Model of the Starfish Flux in the Inner Radiation Zone*, Goddard Space Flight Center, X-601-72-487, December 1972.

Teague, M. J., and J. I. Vette, *A Model of the Trapped Electron Population for Solar Minimum*, National Space Science Data Center, NSSDC 74-03, April 1974.

Teague, M. J., K. W. Chan, and J. I. Vette, *AE-6: A Model Environment for Trapped Electrons for Solar Maximum*, National Space Science Data Center, NSSDC/WDC-A-R&S 76-04, May 1976.

Teague, M. J., N. J. Schofield, K. W. Chan, and J. I. Vette, *A Study of Inner Zone Electron Data and Their Comparison with Trapped Radiation Models*, National Space Science Data Center, NSSDC/WDC-A-R&S 79-06, August 1979.

Vampola, A. L., "Energetic Electrons at Latitudes Above the Outer-Zone Cutoff," *J. Geophys. Res.* 74, 1254, 1969.

Vampola, A. L., "Access of Solar Electrons to Closed Field Lines," *J. Geophys. Res.* 76, 36, 1971.

Vampola, A. L., private communication, 1972.

Tables

Table 1. Azur Greater Than 1.5 MeV Normalized Local Time Distribution

Local Time (Hrs.)	L = 3 Φ/K	L = 4 Φ/K	L = 5 Φ/K	L = 5.5 Φ/K	L = 6 Φ/K
1	–	–	–	–	–
2	–	–	0.767	0.672	0.698
3	–	0.700	0.894	0.810	0.594
4	1.038	0.795	0.853	0.992	1.081
5	1.122	0.849	1.024	0.960	0.861
6	0.968	0.973	0.951	0.885	0.796
7	0.953	0.996	1.026	1.034	0.951
8	0.820	1.039	1.087	1.064	1.257
9	–	1.130	1.127	1.254	1.203
10	–	–	–	1.151	1.385
11	–	–	–	–	–
12	–	–	–	–	–
13	–	–	–	1.024	1.434
14	–	–	1.099	1.160	1.170
15	–	1.055	1.057	1.065	1.199
16	0.952	1.033	1.096	1.231	1.048
17	0.929	0.992	1.051	1.045	1.040
18	1.079	1.057	1.047	0.987	0.961
19	1.014	1.063	1.075	1.071	1.031
20	0.968	0.997	1.008	0.940	1.002
21	–	0.889	0.811	0.904	0.916
22	–	–	–	0.629	0.859
23	–	–	–	–	–
24	–	–	–	–	–
C	-0.049	0.053	0.063	0.090	0.106
95% Confidence Interval Half Width	0.003	0.004	0.003	0.005	0.007
K	0.981	0.962	0.992	0.970	0.991

Table 2. Characteristics of the OV1-19 Low and High Energy Electron Spectrometers

| Detector ID | Electron Energy (keV) | | | | Count Rate to Flux Conversion Factor (sq cm-ster-keV) | Remarks |
	Upper Limit	Effective Midpoint	Lower Limit	Channel Width		
LE1	68	53	39	29	2.05E-03	Efficiency of detection lower than rest of LE channels.
LE2	111	92	74	37	8.33E-02	Efficiency of detection lower than rest of LE channels.
LE3	161	139	118	43	1.36	Not used in AE-8; fluxes are much too high.
LE4	216	192	168	48	2.53	OK
LE5	276	250	224	52	2.34	Channel is suspect; all fluxes are a bit high.
LE6	339	312	285	54	2.16	OK
LE7	404	376	348	56	2.01	OK
LE8	473	444	415	58	1.86	OK
LE9	–	N/A	–	–	–	2 bkg channels; protons greater than 55 MeV and bremsstrahlung (B). BCRs are much too high to use as bkg subtraction in outer zone.
HE1	656	537	423	233	45.70	OK
HE2	946	822	698	248	36.50	OK
HE3	1241	1112	988	253	30.10	Not used in AE-8. No data after day 282; data OK before this.
HE4	1542	1409	1283	259	25.50	Not used in AE-8. Went bad after day 282; × 100 increase.
HE5	1844	1711	1585	259	22.10	OK
HE6	2152	2018	1888	264	19.40	OK
HE7	2457	2321	2192	265	17.30	OK
HE8	2766	2632	2498	268	15.70	OK
HE9	3071	2932	2803	268	14.30	OK
HE10	3381	3245	3111	270	13.10	Bad channel; all fluxes are much too high.
HE11	3690	3557	3423	267	12.10	OK
HE12	3999	3863	3725	274	11.30	OK
HE13	4310	4169	4033	277	10.50	OK
HE14	4623	4476	4339	284	9.87	OK
HE15	4930	4783	4643	287	9.29	OK
HE16	5243	5091	4955	288	8.64	OK
HE17	–	N/A	–	–	–	2 bkg channels; protons greater than 55 MeV and bremsstrahlung (B). BCRs are much too high to use as bkg subtraction in outer zone.

Table 3. Ratio of (CR-BREM)/CR for OV1-19 Spectrometers

Detector ID	Energy (keV)	L 3	3.5	4	4.5	5	5.5	6	6.6
LE1	53	-0.83	-3.56	-4.42	-1.86	-1.30	-0.63	-0.39	-0.75
LE2	52	0.92	-0.55	-0.51	0.63	0.69	0.83	0.88	0.80
LE4	192	0.99	0.87	0.92	0.98	0.99	1.00	1.00	0.99
LE5	250	0.99	0.90	0.91	0.97	0.99	0.99	0.99	0.99
LE6	312	0.97	0.79	0.77	0.93	0.96	0.98	0.98	0.97
LE7	376	0.95	0.71	0.67	0.89	0.95	0.97	0.97	0.95
LE8	444	0.92	0.56	0.53	0.85	0.92	0.95	0.95	0.90
HE1	537	0.97	0.96	0.98	0.98	0.98	0.99	0.97	0.98
HE2	822	0.51	0.57	0.76	0.83	0.86	0.90	0.85	0.41
HE5	1711	-2.12	0.79	0.80	0.61	0.34	0.06	-1.09	-0.53
HE6	2018	-0.86	0.73	0.70	0.48	0.14	-0.06	-1.54	-0.24
HE7	2321	-6.62	0.27	0.10	-1.29	-3.75	-6.24	-14.03	-3.69
HE8	2632	-2.69	0.50	0.24	-1.03	-2.80	-4.53	-7.72	-1.90
HE9	2932	-7.55	0.16	-0.70	-3.55	-7.49	-9.49	-7.50	-3.06
HE11	3557	-8.09	-1.76	-4.40	-11.40	-14.79	-12.77	-6.22	-2.20
HE12	3863	-9.82	-1.12	-3.56	-9.15	-14.67	-16.70	-9.35	-3.76
HE13	4169	-13.97	-3.08	-8.00	-17.57	-22.13	-20.16	-6.87	-3.53
HE14	4476	-9.13	-2.04	-5.15	-10.62	-13.60	-12.51	-5.68	2.46
HE15	4783	-11.46	-3.61	-8.63	-16.49	-19.33	-16.22	-6.42	-3.16
HE16	5091	-12.36	-3.33	-8.80	-16.30	-18.61	-18.77	-7.41	-3.18

Table 4. Flux Fraction d for OV1-19 HES Channels

L	d	Remarks
3.0	0.1450	Determined using AZUR > 4500 keV data.
3.2	0.1040	Determined using AZUR > 4500 keV data.
3.4	0.0744	Determined using AZUR > 4500 keV data.
3.5	0.0720	Determined using AZUR > 4500 keV data.
3.6	0.0549	Determined using AZUR > 4500 keV data.
3.8	0.0444	Determined using AZUR > 4500 keV data.
4.0	0.0486	Determined using AZUR > 4500 keV data.
4.2	0.0496	Determined using AZUR > 4500 keV data.
4.4	0.0503	Determined using AZUR > 4500 keV data.
4.5	0.0440	Determined using AZUR > 4500 keV data.
4.6	0.0541	Determined using AZUR > 4500 keV data.
4.8	0.0551	Determined using AZUR > 4500 keV data.
5.0	0.0547	Determined using AZUR > 4500 keV data.
5.5	0.0478	Determined using AZUR > 4500 keV data.
6.0	0.0322	Determined by interpolation between L = 5.5 and 6.6; d AZUR = .0527.
6.6	0.0145	Determined using ATS 6 > 3900 keV data; d AZUR = .0592.

Table 5. Parameters for Conversion of OV1-19 Flux to Integral Energy Spectrum

Useful Channel Index-k	Detector ID	Upper Limit	Electron Energy (keV)		
			Effective Midpoint	Lower Limit	Channel Width W(k)
1	LE1	71	55	39	32
2	LE2	140	106	71	69
3	LE4	220	180	140	80
4	LE5	281	251	220	61
5	LE6	344	313	281	63
6	LE7	409	377	344	65
7	LE8	448	429	409	39
8	HE1	677	563	448	229
9	HE2	1266	972	677	589
10	HE5	1866	1566	1266	600
11	HE6	2172	2019	1866	306
12	HE7	2478	2325	2172	306
13	HE8	2785	2632	2478	307
14	HE9	3237	3011	2785	452
15	HE11	3708	3473	3237	471
16	HE12	4016	3862	3708	308
17	HE13	4325	4171	4016	309

Table 6A. OV1-19 Equatorial Unidirectional Flux Uncorrected for Background (electrons/sq cm-ster-keV-s)

Energy (keV)	L=3.0	L=3.2	L=3.4	L=3.5	L=3.6	L=3.8	L=4.0	L=4.2	L=4.4	L=4.5	L=4.6	L=4.8	L=5.0	L=5.5	L=6.0	L=6.6
53	1.55E+05	7.36E+04	1.48E+05	1.85E+05	2.20E+05	1.73E+05	1.97E+05	2.02E+05	1.69E+05	1.84E+05	1.67E+05	1.46E+05	1.37E+05	1.09E+05	8.38E+04	4.71E+04
92	9.12E+04	1.51E+04	1.33E+04	1.34E+04	1.58E+04	3.64E+04	1.74E+04	1.84E+04	2.08E+04	3.53E+04	2.22E+04	1.97E+04	2.47E+04	2.62E+04	2.33E+04	1.02E+04
192	2.50E+04	4.54E+03	5.01E+03	5.33E+03	7.64E+03	1.51E+04	1.08E+04	1.33E+04	1.71E+04	2.14E+04	2.22E+04	1.67E+04	3.23E+04	3.61E+04	2.14E+04	7.43E+03
250	2.36E+04	5.43E+03	6.41E+03	7.51E+03	7.74E+03	8.55E+03	9.86E+03	1.24E+04	1.34E+04	1.55E+04	1.50E+04	1.67E+04	1.87E+04	1.92E+04	1.54E+04	9.12E+03
312	9.06E+03	2.80E+03	2.93E+03	3.70E+03	3.56E+03	3.75E+03	4.41E+03	5.27E+03	5.12E+03	6.79E+03	6.77E+03	7.50E+03	8.08E+03	8.64E+03	5.99E+03	2.80E+03
376	5.29E+03	1.91E+03	2.24E+03	2.92E+03	2.93E+03	3.05E+03	3.33E+03	4.23E+03	4.31E+03	4.90E+03	5.06E+03	5.62E+03	5.82E+03	5.61E+03	3.62E+03	1.71E+03
444	3.70E+03	1.43E+03	1.60E+03	2.11E+03	2.03E+03	2.27E+03	2.49E+03	3.13E+03	3.28E+03	3.79E+03	3.90E+03	4.39E+03	4.41E+03	3.68E+03	2.40E+03	9.22E+02
537	9.46E+02	3.83E+02	5.62E+02	7.01E+02	8.48E+02	1.03E+03	1.36E+03	1.58E+03	2.01E+03	2.11E+03	2.22E+03	2.33E+03	2.31E+03	1.86E+03	9.90E+02	3.78E+02
822	8.11E+01	3.88E+01	6.83E+01	7.94E+01	9.29E+01	1.21E+02	1.64E+02	2.20E+02	2.48E+02	2.83E+02	2.78E+02	3.11E+02	3.28E+02	3.24E+02	2.43E+02	1.40E+01
1711	2.10E-01	5.02E-01	1.80E+02	2.67E+02	3.08E+02	3.84E+02	3.20E+02	2.77E+02	2.39E+02	2.10E+02	1.86E+02	1.53E+02	1.16E+02	5.70E+01	2.82E+01	8.90E+00
2018	4.02E-01	5.74E+01	1.67E+02	2.34E+02	2.78E+02	3.01E+02	2.52E+02	2.18E+02	1.85E+02	1.78E+02	1.62E+02	1.31E+02	1.02E+02	5.78E+01	2.64E+01	1.25E+01
2321	1.10E+01	1.97E+01	6.96E+01	9.95E+01	1.19E+02	1.21E+02	9.28E+01	7.00E+01	5.37E+01	4.54E+01	3.95E+01	2.91E+01	2.07E+01	9.50E+00	5.00E+00	3.70E+00
2632	2.50E+01	3.63E+01	1.19E+02	1.58E+02	1.85E+02	1.77E+02	1.22E+02	8.80E+01	6.78E+01	5.64E+01	4.85E+01	3.63E+01	2.85E+01	1.37E+01	9.50E+00	6.60E+00
2932	1.80E+01	2.69E+01	7.74E+01	1.00E+02	1.12E+02	9.94E+01	7.00E+01	4.82E+01	3.56E+01	3.00E+01	2.73E+01	1.97E+01	1.40E+01	8.00E+00	5.10E+00	5.00E+00
3557	2.00E+01	1.34E+01	2.86E+01	3.59E+01	3.86E+01	3.42E+01	2.60E+01	1.82E+01	1.47E+01	1.30E+01	1.31E+01	1.38E+01	8.90E+00	7.20E+00	7.10E+00	7.50E+00
3863	1.80E+01	1.72E+01	4.28E+01	5.02E+01	5.53E+01	4.82E+01	3.30E+01	2.35E+01	1.84E+01	1.70E+01	1.46E+01	1.21E+01	9.60E+00	6.00E+00	5.30E+00	5.40E+00
4169	1.40E+01	8.60E+00	2.95E+01	2.69E+01	2.69E+01	2.52E+01	1.80E+01	1.40E+01	1.19E+01	1.00E+01	8.80E+00	8.10E+00	7.00E+00	5.40E+00	7.50E+00	6.10E+00
4476	2.20E+01	1.35E+01	2.03E+01	4.00E+01	4.00E+01	3.91E+01	2.80E+01	2.32E+01	1.97E+01	1.70E+01	1.49E+01	1.28E+01	1.18E+01	9.00E+00	9.40E+00	8.50E+00
4783	1.90E+01	9.30E+00	2.80E+01	2.89E+01	2.89E+01	2.68E+01	1.90E+01	1.65E+01	1.36E+01	1.20E+01	1.05E+01	1.04E+01	9.00E+00	7.50E+00	9.00E+00	7.50E+00
5091	1.90E+01	1.01E+01	2.30E+01	3.20E+01	3.21E+01	3.00E+01	2.00E+01	1.90E+01	1.62E+01	1.30E+01	1.24E+01	1.16E+01	1.00E+01	7.00E+00	8.50E+00	8.00E+00

Table 6B. OV1-19 Equatorial Unidirectional Flux Corrected for Background and Using AE-8 (electrons/sq cm-ster-keV-s)

Energy (keV)	L=3.0	L=3.2	L=3.4	L=3.5	L=3.6	L=3.8	L=4.0	L=4.2	L=4.4	L=4.5	L=4.6	L=4.8	L=5.0	L=5.5	L=6.0	L=6.6
53	1.55E+05	7.36E+04	1.48E+05	1.85E+05	2.20E+05	1.73E+05	1.97E+05	2.02E+05	1.69E+05	1.84E+05	1.67E+05	1.46E+05	1.37E+05	1.09E+05	8.38E+04	4.71E+04
92	9.12E+04	1.51E+04	1.33E+04	1.34E+04	1.58E+04	3.64E+04	1.74E+04	1.84E+04	2.08E+04	3.53E+04	2.22E+04	1.97E+04	2.47E+04	2.62E+04	2.33E+04	1.02E+04
192	2.50E+04	4.53E+03	4.99E+03	5.33E+03	7.60E+03	1.51E+04	1.08E+04	1.33E+04	1.71E+04	2.14E+04	1.72E+04	1.24E+04	3.23E+04	3.61E+04	2.14E+04	7.42E+03
250	2.36E+04	5.43E+03	6.41E+03	7.51E+03	7.70E+03	8.52E+03	9.84E+03	5.25E+03	1.34E+04	6.78E+03	6.76E+03	7.49E+03	8.07E+03	8.63E+03	5.98E+03	9.11E+03
312	9.04E+03	2.79E+03	2.93E+03	3.70E+03	3.52E+03	3.72E+03	4.39E+03	4.21E+03	4.30E+03	4.89E+03	5.05E+03	5.61E+03	5.81E+03	5.60E+03	3.61E+03	2.79E+03
376	5.27E+03	1.89E+03	2.21E+03	2.89E+03	2.90E+03	3.02E+03	3.31E+03	3.11E+03	3.27E+03	3.78E+03	3.89E+03	4.38E+03	4.40E+03	3.67E+03	2.39E+03	1.70E+03
444	3.68E+03	1.42E+03	1.57E+03	2.08E+03	2.24E+03	2.24E+03	2.47E+03	1.56E+03	1.99E+03	2.10E+03	2.21E+03	2.32E+03	2.30E+03	1.85E+03	9.82E+02	9.15E+02
537	9.30E+02	3.72E+02	5.37E+02	6.68E+02	8.13E+02	1.00E+03	1.34E+03	2.02E+02	2.33E+02	2.70E+02	2.66E+02	3.00E+02	3.19E+02	3.17E+02	2.35E+02	3.71E+02
822	6.51E+01	2.80E+01	4.31E+01	4.63E+01	5.80E+01	8.86E+01	1.41E+02	2.59E+02	1.97E+02	1.74E+02	1.50E+02	1.20E+02	1.07E+02	2.07E+01	6.94E+00	
1711	5.04E+00	3.94E+01	1.55E+02	2.34E+02	2.73E+02	3.51E+02	2.97E+02	2.00E+02	2.33E+02	1.65E+02	1.42E+02	1.07E+02	9.31E+01	5.03E+01	1.89E+01	1.84E+00
2018	2.42E+01	4.66E+00	1.42E+02	2.01E+02	2.43E+02	2.69E+02	2.29E+02	5.19E+01	1.70E+02	3.23E+01	2.78E+01	1.83E+01	1.18E+01	5.11E+01	1.61E+00	5.44E+00
2321	1.60E+00	8.93E+00	4.44E+01	6.64E+01	8.42E+01	8.90E+01	7.00E+01	6.99E+01	3.87E+01	4.33E+01	3.68E+01	2.55E+01	1.96E+01	2.82E+00	1.95E+00	5.37E-02
2632	9.04E+00	2.55E+01	9.36E+01	1.25E+02	1.50E+02	1.45E+02	9.92E+01	3.01E+01	5.28E+01	1.69E+01	1.56E+01	8.87E+00	5.13E+00	7.02E+01	1.64E-01	9.57E-02
2932	2.04E+00	1.61E+01	3.44E+01	2.79E+01	3.66E+00	1.79E+00	4.72E+00	7.90E-02	2.06E-01	1.69E-01	1.39E+00	2.97E+00	2.99E-02	1.32E+00	1.29E-01	7.25E-02
3557	4.04E+00	2.63E+00	1.76E+00	1.71E+00	2.04E+00	1.58E+00	3.17E+00	7.39E-01	7.39E-01	5.72E-01	2.89E+00	1.27E+00	7.30E-01	5.19E-01	1.71E-01	4.37E-01
3863	2.04E+00	6.43E+00	1.41E+00	2.02E+00	1.48E+00	1.12E+00	1.02E+00	5.38E+00	3.44E+00	3.93E+00	2.89E-01	4.46E-01	3.83E-01	2.58E-01	2.42E-01	7.83E-02
4169	2.03E+00	8.94E-01	4.34E+00	6.89E+00	5.06E+00	6.69E+00	8.75E-01	6.94E-01	5.99E-01	4.40E+00	4.76E-01	1.97E+00	2.93E+00	2.32E+00	1.85E+00	8.85E-02
4476	6.04E+00	2.73E+00	1.51E+00	2.02E+00	1.59E+00	1.19E+00	5.17E-01	5.08E+00	4.74E+00	3.93E-01	3.19E+00	5.73E-01	1.30E-01	8.19E-01	1.45E+00	1.44E+00
4783	3.04E+00	9.67E-01	1.51E+00	2.02E+00	1.19E+00	6.69E+00	9.23E-01	8.18E-01	6.84E-01	5.28E-01	5.68E-01	5.73E-01	1.30E-01	8.19E-01	1.45E+00	4.37E-01
5091	3.04E+00	1.05E+00	1.71E+00	2.30E+00	1.76E+00	1.33E+00	9.72E-01	8.79E-01	1.24E+00	5.72E-01	6.87E-01	7.65E-01	1.13E+00	3.19E-01	9.51E-01	9.37E-01

Table 6C. OV1-19 Equatorial Omnidirectional Integral Energy Spectrum Corrected for Background and Using AE-8 (electrons/sq cm-s)

Threshold Energy (keV)	L=3.0	L=3.2	L=3.4	L=3.5	L=3.6	L=3.8	L=4.0	L=4.2	L=4.4	L=4.5	L=4.6	L=4.8	L=5.0	L=5.5	L=6.0	L=6.6
39	1.53E+08	4.40E+07	6.87E+07	8.31E+07	9.81E+07	1.05E+08	9.81E+07	1.05E+08	1.01E+08	1.21E+08	1.04E+08	9.45E+07	1.12E+08	1.06E+08	7.67E+07	3.60E+07
71	1.06E+08	2.15E+07	2.35E+07	2.66E+07	3.09E+07	5.19E+07	3.79E+07	4.35E+07	4.93E+07	6.52E+07	5.32E+07	4.99E+07	6.98E+07	7.24E+07	5.10E+07	2.17E+07
140	4.55E+07	1.15E+07	1.47E+07	1.78E+07	2.04E+07	2.79E+07	2.64E+07	3.14E+07	3.56E+07	4.19E+07	3.85E+07	3.69E+07	5.35E+07	5.51E+07	3.57E+07	1.49E+07
220	2.64E+07	8.09E+06	1.09E+07	1.37E+07	1.46E+07	1.64E+07	1.25E+07	1.82E+07	2.13E+07	2.56E+07	1.67E+07	2.74E+07	2.88E+07	2.75E+07	1.94E+07	9.27E+06
281	1.27E+07	4.93E+06	7.15E+06	9.37E+06	1.02E+07	1.15E+07	1.25E+07	1.41E+07	1.48E+07	1.65E+07	1.67E+07	1.77E+07	1.79E+07	1.64E+07	1.04E+07	3.96E+06
344	7.22E+06	3.25E+06	5.39E+06	7.14E+06	8.03E+06	9.23E+06	9.81E+06	1.09E+07	1.17E+07	1.25E+07	1.26E+07	1.32E+07	1.31E+07	1.12E+07	6.79E+06	2.28E+06
409	3.95E+06	2.08E+06	4.01E+06	5.35E+06	6.23E+06	7.36E+06	7.76E+06	8.29E+06	9.04E+06	9.43E+06	9.48E+06	9.74E+06	9.47E+06	7.68E+06	4.55E+06	1.22E+06
448	2.58E+06	1.55E+06	3.43E+06	4.58E+06	5.49E+06	6.52E+06	6.84E+06	7.13E+06	7.82E+06	8.03E+06	8.03E+06	8.11E+06	7.83E+06	6.32E+06	3.65E+06	8.80E+05
677	5.45E+05	7.32E+05	2.25E+06	3.12E+06	3.71E+06	4.33E+06	3.92E+06	3.71E+06	3.47E+06	3.44E+06	3.21E+06	3.04E+06	2.80E+06	2.26E+06	1.51E+06	6.90E+05
1266	1.79E+05	5.75E+05	2.01E+06	2.85E+06	3.38E+06	3.83E+06	3.12E+06	2.58E+06	2.16E+06	1.92E+06	1.71E+06	1.35E+06	1.01E+06	4.77E+05	1.83E+05	3.00E+04
1866	1.50E+05	3.49E+05	1.12E+06	1.51E+06	1.82E+06	1.82E+06	1.42E+06	1.09E+06	8.73E+05	7.95E+05	7.13E+05	5.39E+05	3.92E+05	1.89E+05	6.50E+04	1.94E+04
2172	7.88E+04	2.13E+05	7.11E+05	9.28E+05	1.11E+06	1.04E+06	7.51E+05	5.09E+05	3.76E+05	3.13E+05	2.75E+05	1.87E+05	1.20E+05	3.97E+04	9.90E+03	3.55E+03
2478	7.42E+04	1.86E+05	5.81E+05	7.34E+05	8.63E+05	7.78E+05	5.46E+05	3.57E+05	2.63E+05	2.18E+05	1.94E+05	1.34E+05	8.51E+04	3.14E+04	9.43E+03	3.39E+03
2785	4.77E+04	1.12E+05	3.06E+05	3.67E+05	4.22E+05	3.54E+05	2.56E+05	2.25E+05	1.08E+05	1.08E+05	5.90E+04	2.75E+04	5.40E+04	1.08E+04	9.43E+03	3.11E+03
3237	3.88E+04	4.19E+04	8.07E+04	7.86E+04	8.89E+04	6.44E+04	5.20E+04	3.78E+04	1.88E+04	1.54E+04	1.90E+04	2.07E+04	5.27E+03	2.82E+03	3.00E+03	2.80E+03
3708	2.07E+04	3.01E+04	6.52E+04	6.61E+04	7.25E+04	5.64E+04	3.78E+04	2.22E+04	1.54E+04	1.58E+04	1.27E+04	7.40E+03	3.12E+03	1.98E+03	1.97E+03	6.00E+02
4016	1.47E+04	1.11E+04	1.33E+04	1.59E+04	1.26E+04	9.95E+03	7.86E+03	6.37E+03	5.32E+03	4.20E+03	4.23E+03	3.68E+03	3.12E+03	1.21E+03	1.47E+03	6.00E+02
4325	8.68E+03	8.50E+03	9.17E+03	9.91E+03	8.22E+03	6.65E+03	5.27E+03	4.32E+03	3.56E+03	2.90E+03	2.83E+03	2.36E+03	1.99E+03	7.59E+02	3.39E+02	3.39E+02
4500	3.35E+03	6.15E+03	5.50E+03	5.10E+03	4.55E+03	3.75E+03	3.00E+03	2.40E+03	1.90E+03	1.65E+03	1.48E+03	1.18E+03	9.10E+02	4.95E+02	2.53E+02	1.33E+02

Table 6D. OV1-19 Equatorial Omnidirectional Integral Energy Spectrum Uncorrected for Background and Using AE-8 (electrons/sq cm-s)

Threshold Energy (keV)	L=3.0	L=3.2	L=3.4	L=3.5	L=3.6	L=3.8	L=4.0	L=4.2	L=4.4	L=4.5	L=4.6	L=4.8	L=5.0	L=5.5	L=6.0	L=6.6
39	1.54E+08	4.44E+07	6.97E+07	8.45E+07	9.95E+07	1.06E+08	9.90E+07	1.06E+08	1.02E+08	1.22E+08	1.05E+08	9.50E+07	1.12E+08	1.06E+08	7.69E+07	3.63E+07
71	1.06E+08	2.19E+07	2.45E+07	2.80E+07	3.23E+07	5.33E+07	3.88E+07	4.43E+07	4.99E+07	6.57E+07	5.37E+07	5.03E+07	7.01E+07	7.27E+07	5.13E+07	2.19E+07
140	4.61E+07	1.20E+07	1.57E+07	1.92E+07	2.19E+07	2.93E+07	2.74E+07	3.22E+07	3.62E+07	4.24E+07	3.90E+07	3.74E+07	5.39E+07	5.54E+07	3.60E+07	1.52E+07
220	2.70E+07	8.52E+06	1.19E+07	1.51E+07	1.60E+07	1.77E+07	1.34E+07	1.91E+07	2.20E+07	2.61E+07	1.71E+07	2.79E+07	2.92E+07	2.78E+07	1.96E+07	9.53E+06
281	1.33E+07	5.35E+06	8.14E+06	1.07E+07	1.15E+07	1.28E+07	1.34E+07	1.48E+07	1.54E+07	1.71E+07	1.71E+07	1.82E+07	1.83E+07	1.66E+07	1.07E+07	4.22E+06
344	7.83E+06	3.67E+06	6.37E+06	8.44E+06	9.40E+06	1.05E+07	1.07E+07	1.16E+07	1.23E+07	1.30E+07	1.31E+07	1.36E+07	1.34E+07	1.14E+07	7.06E+06	2.53E+06
409	4.55E+06	2.49E+06	4.98E+06	6.63E+06	7.57E+06	8.61E+06	8.64E+06	8.99E+06	9.61E+06	9.94E+06	9.93E+06	1.02E+07	9.82E+06	7.94E+06	4.81E+06	1.47E+06
448	3.17E+06	1.96E+06	4.38E+06	5.84E+06	6.82E+06	7.76E+06	7.71E+06	7.82E+06	8.39E+06	8.53E+06	8.48E+06	8.52E+06	8.17E+06	6.57E+06	3.92E+06	1.13E+06
677	1.10E+06	1.12E+06	3.15E+06	4.31E+06	4.96E+06	5.50E+06	4.74E+06	4.37E+06	4.01E+06	3.91E+06	3.63E+06	3.43E+06	3.12E+06	2.50E+06	1.75E+06	3.00E+05
1266	6.45E+05	9.00E+05	2.77E+06	3.86E+06	4.44E+06	4.82E+06	3.82E+06	3.13E+06	2.61E+06	2.32E+06	2.07E+06	1.68E+06	1.28E+06	6.79E+05	3.89E+05	2.21E+05
1866	5.25E+05	6.13E+05	1.74E+06	2.33E+06	2.68E+06	2.62E+06	1.98E+06	1.54E+06	1.24E+06	1.12E+06	1.00E+06	8.04E+05	6.12E+05	3.53E+05	2.27E+05	1.70E+05
2172	4.07E+05	4.45E+05	1.25E+06	1.65E+06	1.86E+06	1.74E+06	1.25E+06	9.04E+05	7.00E+05	5.96E+05	5.30E+05	4.21E+05	3.14E+05	1.84E+05	1.50E+05	1.34E+05
2478	3.75E+05	3.87E+05	1.05E+06	1.36E+06	1.51E+06	1.39E+06	9.77E+05	7.00E+05	5.43E+05	4.63E+05	4.14E+05	3.36E+05	2.54E+05	1.56E+05	1.35E+05	1.23E+05
2785	3.02E+05	2.81E+05	6.99E+05	8.95E+05	9.71E+05	8.68E+05	6.19E+05	4.42E+05	3.44E+05	2.98E+05	2.72E+05	2.29E+05	1.70E+05	1.16E+05	1.08E+05	1.04E+05
3237	2.24E+05	1.65E+05	3.65E+05	4.64E+05	4.87E+05	4.39E+05	3.17E+05	2.33E+05	1.90E+05	1.68E+05	1.54E+05	1.44E+05	1.10E+05	8.15E+04	8.56E+04	8.20E+04
3708	1.34E+05	1.05E+05	2.96E+05	3.02E+05	3.13E+05	2.85E+05	2.03E+05	1.52E+05	1.24E+05	1.10E+05	9.53E+04	8.21E+04	6.95E+04	4.91E+04	5.37E+04	4.82E+04
4016	8.14E+04	5.41E+04	1.11E+05	1.55E+05	1.43E+05	1.03E+05	8.25E+04	5.96E+04	4.12E+04	4.13E+04	4.65E+04	4.13E+04	4.13E+04	1.55E+04	3.81E+04	3.23E+04
4325	4.01E+04	2.87E+04	5.48E+04	7.20E+04	7.14E+04	6.91E+04	4.98E+04	4.12E+04	3.48E+04	3.01E+04	2.64E+04	2.26E+04	2.06E+04	1.55E+04	1.60E+04	1.43E+04
4500	3.35E+04	6.15E+03	5.50E+03	5.10E+03	4.55E+03	3.75E+03	3.00E+03	2.40E+03	1.90E+03	1.65E+03	1.48E+03	1.18E+03	9.10E+02	4.95E+02	2.53E+02	1.33E+02

Table 7. Characteristics of the OV3-3 Magnetic Spectrometer

Detector ID	Electron Energy (MeV)			Channel Width	Count Rate to Flux Conversion Factor (sq cm-ster-MeV)	Remarks
	Upper Limit	Effective Midpoint	Lower Limit			
1	2.473	2.310	2.148	0.325	0.0908	
2	2.200	2.040	1.880	0.320	0.0992	Became noisy after 18 months in orbit.
3	1.925	1.770	1.615	0.310	0.1108	
4	1.651	1.490	1.329	0.322	0.1240	
5	1.375	1.225	1.075	0.300	0.1668	
6	1.100	0.957	0.815	0.285	0.1869	
7	0.850	0.712	0.575	0.275	0.2184	
8	0.600	0.475	0.350	0.250	0.2920	
9	0.375	0.300	0.225	0.150	0.1852	2 channels; upper one for protons > 105 MeV.

For Integral Spectrum Computations

Detector ID	Upper Limit	Lower Limit	Channel Width
1	2.445	2.155	0.290
2	2.155	1.878	0.277
3	1.878	1.640	0.238
4	1.640	1.354	0.286
5	1.354	1.092	0.262
6	1.092	0.827	0.265
7	0.827	0.594	0.233
8	0.594	0.372	0.222
9	0.372	0.213	0.159

Table 8. Grid Points and Other Parameters for AE-8 Numerical Representation

Energy Value (MeV)	L Value	L Value	Other Parameters	Values of Other Parameters	Notes/Remarks
0.04	0.00	3.20	Model Names	AE-8MIN	
0.10	1.10	3.40		AE-8MAX	
0.25	1.20	3.50	Total Storage	13168	Cells for AE-8MIN.
0.50	1.25	3.60		13548	Cells for AE-8MAX.
0.75	1.30	3.80	Scale Factors		Stored Value/Scale Factor = True Value.
1.00	1.35	4.00	Energy	6400	
1.50	1.40	4.20	L	2100	
2.00	1.45	4.40	b Increments	1024	Occurs when Z has dropped by 0.25.
2.50	1.50	4.50	Z1	1024	This parameter ZDEL = 0.25 does not
3.00	1.60	4.60			appear in BLOCK DATA statement but
3.50	1.70	4.80			is in Program MODEL87 that handles
4.00	1.80	5.00			BLOCK DATA statement.
4.50	1.90	5.50			
5.00	2.00	6.00			
5.50	2.20	6.60			
6.00	2.40	7.00			
6.50	2.50	7.50			
7.00	2.60	8.00			
	2.69	–			
–	2.70	9.00			
	2.79	–			
–	2.80	10.00			
	2.89	–			
–	2.90	11.00			
–	3.00	12.00			
–	–	15.60			

Table 9. AE-8MAX Header and Logical Data Record (partial)

```
C*******                AE8MAX                                          00000010
      BLOCK DATA                                                        00000020
      DOUBLE PRECISION        NAME                                      00000030
      COMMON/AE8MAX   /NAME,EPOCH,SCAE,SCAL,SCAB,SCAF,LENGTH            00000040
     X,MAP   1(163),MAP   2(163),MAP   3(163),MAP   4(163),MAP   5(163) 00000050
     X,MAP   6(163),MAP   7(163),MAP   8(163),MAP   9(163),MAP  10(163) 00000060
     X,MAP  11(163),MAP  12(163),MAP  13(163),MAP  14(163),MAP  15(163) 00000070
     X,MAP  16(163),MAP  17(163),MAP  18(163),MAP  19(163),MAP  20(163) 00000080
     X,MAP  21(163),MAP  22(163),MAP  23(163),MAP  24(163),MAP  25(163) 00000090
     X,MAP  26(163),MAP  27(163),MAP  28(163),MAP  29(163),MAP  30(163) 00000100
     X,MAP  31(163),MAP  32(163),MAP  33(163),MAP  34(163),MAP  35(163) 00000110
     X,MAP  36(163),MAP  37(163),MAP  38(163),MAP  39(163),MAP  40(163) 00000120
     X,MAP  41(163),MAP  42(163),MAP  43(163),MAP  44(163),MAP  45(163) 00000130
     X,MAP  46(163),MAP  47(163),MAP  48(163),MAP  49(163),MAP  50(163) 00000140
     X,MAP  51(163),MAP  52(163),MAP  53(163),MAP  54(163),MAP  55(163) 00000150
     X,MAP  56(163),MAP  57(163),MAP  58(163),MAP  59(163),MAP  60(163) 00000160
     X,MAP  61(163),MAP  62(163),MAP  63(163),MAP  64(163),MAP  65(163) 00000170
     X,MAP  66(163),MAP  67(163),MAP  68(163),MAP  69(163),MAP  70(163) 00000180
     X,MAP  71(163),MAP  72(163),MAP  73(163),MAP  74(163),MAP  75(163) 00000190
     X,MAP  76(163),MAP  77(163),MAP  78(163),MAP  79(163),MAP  80(163) 00000200
     X,MAP  81(163),MAP  82(163),MAP  83(163),MAP  84( 19)             00000210
      DATA NAME   /8HAE8-MAX /                                          00000220
      DATA EPOCH  /    1990.000/                                        00000230
      DATA SCAE   /    6400.000/                                        00000240
      DATA SCAL   /    2100.000/                                        00000250
      DATA SCAB   /    1024.000/                                        00000260
      DATA SCAF   /    1024.000/                                        00000270
      DATA LENGTH/     13548/                                           00000280
      DATA MAP   1/                                                     00000290
     X 1442,   256,     3,     0,     0,     3,  2310,     0,    27,     00000300
     X 2520,  5907,    37,    19,    19,    19,    18,    17,    16,     00000310
     X   15,    13,    12,    11,    10,     9,     8,     7,     6,     00000320
     X    6,     5,     4,     4,     3,     3,     3,     2,    32,     00000330
     X 2625,  7393,    72,    33,    33,    32,    30,    28,    26,     00000340
     X   24,    22,    19,    17,    16,    14,    12,    11,     9,     00000350
     X    8,     7,     6,     6,     5,     4,     4,     3,     2,     00000360
     X    3,     2,     2,     2,    34,  2730,  7926,   171,    55,     00000370
     X   49,    46,    42,    38,    34,    30,    27,    23,    20,     00000380
     X   18,    15,    13,    11,    10,     8,     7,     6,     5,     00000390
     X    4,     4,     2,     3,     2,     1,     2,     2,     1,     00000400
     X    1,     0,    35,  2835,  8153,   279,    85,    72,    65,     00000410
     X   58,    51,    44,    37,    32,    26,    22,    18,    15,     00000420
     X   12,    10,     8,     6,     6,     4,     4,     2,     3,     00000430
     X    3,     2,     1,     0,     0,     0,     0,     0,     0,     00000440
     X    0,    36,  2940,  8339,   389,   123,   105,    93,    80,     00000450
     X   67,    55,    45,    36,    29,    23,    18,    14,    11,     00000460
     X    9,     7,     5,     4,     4,     2,     1,     1,     0,     00000470
     Y    0/                                                            00000480
```

T-9

Table 10. AE-8 Local Time Amplitude Function

Energy (MeV)	L 3.0 C(>E,L)	3.2 C(>E,L)	3.4 C(>E,L)	3.5 C(>E,L)	3.6 C(>E,L)	3.8 C(>E,L)	4.0 C(>E,L)	4.2 C(>E,L)	4.4 C(>E,L)	4.5 C(>E,L)	4.6 C(>E,L)	4.8 C(>E,L)	5.0 C(>E,L)	5.5 C(>E,L)	6.0 C(>E,L)	6.5 C(>E,L)	7.0 C(>E,L)	7.5 C(>E,L)	8.0 C(>E,L)	9.0 C(>E,L)	10.0 C(>E,L)	11.0 C(>E,L)
0.04	0.000	0.004	0.008	0.010	0.012	0.016	0.020	0.025	0.030	0.033	0.036	0.043	0.049	0.070	0.100	0.140	0.181	0.225	0.266	0.321	0.298	0.198
0.10	0.000	0.001	0.001	0.002	0.002	0.002	0.003	0.005	0.007	0.008	0.010	0.013	0.016	0.029	0.050	0.086	0.124	0.160	0.197	0.266	0.286	0.189
0.25	0.000	0.002	0.003	0.004	0.005	0.006	0.008	0.011	0.014	0.016	0.018	0.022	0.026	0.042	0.064	0.098	0.134	0.169	0.204	0.259	0.210	0.160
0.50	0.000	0.003	0.006	0.008	0.010	0.013	0.016	0.020	0.025	0.027	0.030	0.035	0.041	0.060	0.086	0.120	0.161	0.193	0.220	0.254	0.220	0.000
0.75	0.000	0.004	0.008	0.011	0.013	0.017	0.021	0.026	0.032	0.034	0.038	0.044	0.051	0.073	0.102	0.138	0.177	0.202	0.221	0.226	0.181	0.000
1.00	0.000	0.005	0.010	0.013	0.016	0.021	0.026	0.032	0.038	0.042	0.045	0.053	0.060	0.085	0.117	0.157	0.193	0.211	0.220	0.198	0.142	0.000
1.50	0.000	0.006	0.013	0.016	0.019	0.026	0.032	0.039	0.047	0.051	0.055	0.064	0.073	0.100	0.136	0.182	0.220	0.220	0.203	0.147	0.000	0.000
2.00	0.000	0.007	0.014	0.017	0.020	0.027	0.034	0.042	0.050	0.054	0.058	0.068	0.077	0.106	0.144	0.200	0.235	0.225	0.175	0.036	0.000	0.000
2.50	0.000	0.008	0.015	0.019	0.023	0.030	0.038	0.047	0.056	0.060	0.065	0.075	0.086	0.117	0.158	0.213	0.248	0.227	0.148	0.026	0.000	0.000
3.00	0.000	0.008	0.017	0.021	0.025	0.034	0.042	0.052	0.061	0.066	0.072	0.083	0.094	0.127	0.171	0.225	0.260	0.225	0.120	0.015	0.000	0.000
3.50	0.000	0.009	0.018	0.022	0.026	0.035	0.044	0.053	0.063	0.068	0.074	0.085	0.096	0.129	0.174	0.231	0.263	0.210	0.080	0.009	0.000	0.000
4.00	0.000	0.009	0.018	0.023	0.027	0.036	0.045	0.055	0.065	0.071	0.076	0.086	0.097	0.131	0.177	0.236	0.265	0.195	0.050	0.003	0.000	0.000
4.50	0.000	0.009	0.019	0.023	0.028	0.037	0.047	0.057	0.068	0.073	0.078	0.088	0.099	0.133	0.179	0.235	0.240	0.140	0.033	0.000	0.000	0.000
5.00	0.000	0.010	0.019	0.024	0.029	0.038	0.048	0.059	0.070	0.075	0.080	0.090	0.100	0.135	0.128	0.043	0.000	0.000	0.000	0.000	0.000	0.000
5.50	0.000	0.010	0.020	0.025	0.030	0.040	0.050	0.061	0.072	0.077	0.082	0.092	0.102	0.000	0.000	0.000	0.000	0.000	0.000	0.000	0.000	0.000
6.00	0.000	0.010	0.020	0.026	0.031	0.041	0.051	0.062	0.074	0.000	0.000	0.000	0.000	0.000	0.000	0.000	0.000	0.000	0.000	0.000	0.000	0.000
6.50	0.000	0.011	0.021	0.026	0.032	0.042	0.000	0.000	0.000	0.000	0.000	0.000	0.000	0.000	0.000	0.000	0.000	0.000	0.000	0.000	0.000	0.000
7.00	0.000	0.011	0.022	0.018	0.000	0.000	0.000	0.000	0.000	0.000	0.000	0.000	0.000	0.000	0.000	0.000	0.000	0.000	0.000	0.000	0.000	0.000

Table 11. AE-8 Outer Zone Magnetic Field Line Parameter m(L)

L	m	L	m
3.00	1.12	4.80	0.60
3.20	0.71	5.00	0.60
3.40	0.66	5.50	0.60
3.50	0.65	6.00	0.60
3.60	0.63	6.50	0.60
3.80	0.62	7.00	0.60
4.00	0.60	7.50	0.60
4.20	0.60	8.00	0.60
4.40	0.60	9.00	0.57
4.50	0.60	10.00	0.44
4.60	0.60	11.00	0.24

Table 12. AE-8 Standard Deviation of the Z Function, σ ($>$ E, L)

Energy (MeV)	L 3.0	3.2	3.4	3.5	3.6	3.8	4.0	4.2	4.4	4.5	4.6	4.8	5.0	5.5	6.0	6.5	7.0	7.5	8.0	9.0	10.0	11.0
	σ	σ	σ	σ	σ	σ	σ	σ	σ	σ	σ	σ	σ	σ	σ	σ	σ	σ	σ	σ	σ	σ
0.04	0.310	0.366	0.407	0.418	0.428	0.439	0.448	0.455	0.462	0.466	0.464	0.459	0.454	0.451	0.488	0.583	0.600	0.612	0.623	0.840	0.810	0.750
0.10	0.330	0.384	0.425	0.435	0.445	0.455	0.465	0.471	0.476	0.479	0.475	0.468	0.461	0.430	0.375	0.345	0.350	0.394	0.438	0.750	0.650	0.475
0.25	0.360	0.425	0.471	0.480	0.489	0.494	0.499	0.503	0.506	0.508	0.503	0.493	0.483	0.430	0.350	0.310	0.330	0.374	0.415	0.550	0.235	0.012
0.50	0.410	0.490	0.526	0.535	0.543	0.544	0.545	0.547	0.549	0.550	0.547	0.541	0.535	0.495	0.460	0.413	0.405	0.409	0.405	0.333	0.050	0.000
0.75	0.438	0.523	0.560	0.569	0.577	0.576	0.575	0.576	0.577	0.577	0.576	0.575	0.574	0.553	0.547	0.513	0.495	0.452	0.401	0.230	0.037	0.000
1.00	0.460	0.543	0.583	0.592	0.600	0.599	0.598	0.599	0.600	0.601	0.600	0.599	0.598	0.600	0.603	0.580	0.556	0.482	0.398	0.180	0.022	0.000
1.50	0.487	0.566	0.608	0.617	0.625	0.625	0.625	0.627	0.628	0.629	0.629	0.629	0.629	0.647	0.656	0.638	0.594	0.475	0.390	0.131	0.000	0.000
2.00	0.497	0.572	0.623	0.632	0.640	0.640	0.640	0.640	0.640	0.640	0.641	0.643	0.645	0.660	0.662	0.640	0.602	0.465	0.378	0.099	0.000	0.000
2.50	0.498	0.575	0.626	0.635	0.644	0.645	0.645	0.645	0.645	0.645	0.646	0.647	0.648	0.651	0.652	0.632	0.595	0.450	0.363	0.072	0.000	0.000
3.00	0.500	0.577	0.630	0.639	0.648	0.649	0.650	0.650	0.650	0.650	0.650	0.650	0.650	0.655	0.652	0.615	0.578	0.430	0.342	0.050	0.000	0.000
3.50	0.500	0.577	0.631	0.640	0.649	0.650	0.653	0.653	0.653	0.653	0.651	0.648	0.645	0.631	0.628	0.578	0.542	0.392	0.313	0.030	0.000	0.000
4.00	0.500	0.577	0.631	0.640	0.649	0.650	0.650	0.650	0.650	0.650	0.648	0.644	0.640	0.470	0.583	0.519	0.485	0.335	0.265	0.012	0.000	0.000
4.50	0.500	0.577	0.631	0.640	0.649	0.650	0.650	0.650	0.650	0.650	0.631	0.618	0.605	0.528	0.510	0.412	0.382	0.231	0.166	0.000	0.000	0.000
5.00	0.500	0.577	0.628	0.631	0.634	0.638	0.638	0.638	0.638	0.638	0.586	0.559	0.532	0.407	0.340	0.100	0.000	0.000	0.000	0.000	0.000	0.000
5.50	0.500	0.577	0.620	0.610	0.600	0.600	0.600	0.600	0.600	0.600	0.474	0.405	0.335	0.000	0.000	0.000	0.000	0.000	0.000	0.000	0.000	0.000
6.00	0.490	0.534	0.602	0.575	0.547	0.545	0.532	0.523	0.514	0.509	0.000	0.000	0.000	0.000	0.000	0.000	0.000	0.000	0.000	0.000	0.000	0.000
6.50	0.461	0.475	0.570	0.512	0.453	0.448	0.412	0.279	0.146	0.080	0.000	0.000	0.000	0.000	0.000	0.000	0.000	0.000	0.000	0.000	0.000	0.000
7.00	0.318	0.328	0.475	0.420	0.195	0.238	0.000	0.000	0.000	0.000	0.000	0.000	0.000	0.000	0.000	0.000	0.000	0.000	0.000	0.000	0.000	0.000

Table 13A. AE-8MAX Equatorial Omnidirectional Fluxes Above Energy E

E,L	0.04 MeV	0.10 MeV	0.25 MeV	0.50 MeV	0.75 MeV	1.00 MeV	1.50 MeV	2.00 MeV	2.50 MeV	3.00 MeV	3.50 MeV	4.00 MeV	4.50 MeV	5.00 MeV	5.50 MeV	6.00 MeV	6.50 MeV	7.00 MeV
0.00	1.00E+00	1.00E+00	1.00E+00	1.00E+00	1.00E+00	1.00E+00	1.00E+00	1.00E+00	1.00E+00	1.00E+00	1.00E+00	1.00E+00	1.00E+00	1.00E+00				
1.10	1.70E+00	1.00E+00	1.00E+00	1.00E+00	1.00E+00	1.00E+00	1.00E+00	1.00E+00	1.00E+00	1.00E+00	1.00E+00							
1.20	5.87E+05	4.62E+05	2.34E+05	1.60E+04	3.45E+03	1.19E+03	3.25E+02	1.50E+02	5.30E+01	1.59E+01	3.99E+00	3.99E+00						
1.25	1.66E+07	1.30E+07	6.10E+06	3.50E+05	6.41E+04	2.30E+04	6.00E+03	2.80E+03	9.39E+02	3.00E+02	3.68E+01	4.50E+00	1.00E+00					
1.30	5.50E+07	4.31E+07	1.60E+07	1.10E+06	2.50E+05	1.00E+05	3.15E+04	1.35E+04	6.00E+03	1.70E+03	1.65E+02	1.60E+01	1.00E+00					
1.35	9.16E+07	6.92E+07	2.55E+07	2.20E+06	6.41E+05	2.85E+05	9.54E+04	4.25E+04	2.00E+04	4.25E+03	3.80E+02	3.40E+01	2.40E+00					
1.40	1.39E+08	1.03E+08	3.59E+07	3.38E+06	1.25E+06	6.00E+05	2.20E+05	9.50E+04	4.42E+04	7.50E+03	6.60E+02	5.80E+01	4.40E+00					
1.45	1.84E+08	1.37E+08	4.39E+07	4.39E+06	1.68E+06	8.39E+05	3.40E+05	1.53E+05	1.53E+05	1.53E+05	8.96E+02	7.30E+01	6.00E+00					
1.50	2.33E+08	1.70E+08	5.92E+07	5.50E+06	1.85E+06	8.60E+05	3.60E+05	1.70E+05	7.99E+04	1.10E+04	9.02E+02	7.40E+01	6.29E+00					
1.60	3.28E+08	2.35E+08	7.99E+07	7.58E+06	1.70E+06	6.99E+05	2.60E+05	1.12E+05	4.55E+04	6.00E+03	6.15E+02	6.29E+01	5.45E+00					
1.70	4.03E+08	2.91E+08	9.93E+07	9.18E+06	1.40E+06	4.65E+05	1.62E+05	5.86E+04	2.10E+04	2.70E+03	3.49E+02	4.50E+01	3.51E+00					
1.80	4.31E+08	3.10E+08	1.08E+08	1.06E+07	1.10E+06	2.68E+05	8.39E+04	2.10E+04	6.60E+03	1.02E+03	1.60E+02	2.50E+01	1.40E+00					
1.90	4.05E+08	2.84E+08	9.22E+07	1.01E+07	8.00E+05	1.35E+05	3.25E+04	6.90E+03	1.85E+03	3.10E+02	5.84E+01	1.10E+01	1.00E+00					
2.00	3.64E+08	2.55E+08	7.53E+07	7.70E+06	5.40E+05	7.81E+04	1.35E+04	3.20E+03	7.76E+02	1.09E+02	2.09E+01	4.00E+00	1.00E+00					
2.20	2.92E+08	2.03E+08	4.78E+07	4.35E+06	2.85E+05	4.00E+04	5.70E+03	1.25E+03	2.72E+02	2.35E+01	2.04E+00	1.00E+00	1.00E+00					
2.40	2.38E+08	1.58E+08	3.20E+07	3.90E+06	3.79E+05	5.50E+04	1.00E+04	1.25E+03	1.70E+02	1.00E+01	1.00E+00	1.00E+00	1.00E+00					
2.50	1.90E+08	1.28E+08	2.34E+07	3.35E+06	4.99E+05	1.00E+05	4.00E+04	1.07E+04	2.15E+03	3.15E+02	3.25E+01	2.79E+00	1.00E+00					
2.60	1.55E+08	1.01E+08	1.65E+07	2.96E+06	6.49E+05	1.90E+05	9.00E+04	3.44E+04	1.05E+04	2.50E+03	4.10E+02	3.25E+01	1.90E+00					
2.69														1.00E+00	1.00E+00			
2.70	1.02E+08	7.50E+07	1.10E+07	2.63E+06	8.49E+05	3.25E+05	1.52E+05	6.49E+04	2.45E+04	8.00E+03	2.20E+03	5.50E+02	1.15E+02	2.05E+01	3.40E+01			
2.79															1.00E+00			
2.80	8.40E+07	4.29E+07	7.50E+06	2.50E+06	1.10E+06	5.70E+05	2.34E+05	9.98E+04	4.00E+04	1.55E+04	5.99E+03	1.95E+03	5.50E+02	1.35E+02	2.90E+01	5.70E+00		
2.89																1.00E+00		
2.90	4.70E+07	2.10E+07	6.79E+06	2.65E+06	1.35E+06	8.50E+05	3.74E+05	1.70E+05	7.50E+04	3.30E+04	1.35E+04	5.50E+03	2.00E+03	5.99E+02	1.55E+02	3.50E+01	6.69E+00	1.00E+00
3.00	4.20E+07	2.20E+07	7.40E+06	3.00E+06	1.65E+06	1.08E+06	4.99E+05	2.20E+05	9.80E+04	4.30E+04	1.80E+04	7.69E+03	3.35E+03	1.50E+03	6.29E+02	2.00E+02	4.00E+01	1.20E+00
3.20	4.70E+07	2.65E+07	9.39E+06	4.10E+06	2.40E+06	1.50E+06	7.40E+05	3.50E+05	1.55E+05	7.30E+04	3.29E+04	1.45E+04	5.39E+03	2.34E+03	6.29E+02	1.50E+02	2.95E+01	5.00E+00
3.40	5.30E+07	3.15E+07	1.17E+07	5.20E+06	3.00E+06	1.95E+06	9.50E+05	4.59E+05	2.34E+05	1.02E+05	4.49E+04	1.75E+04	5.79E+03	1.70E+03	3.90E+02	7.99E+01	1.50E+01	2.50E+00
3.50	5.70E+07	3.40E+07	1.25E+07	5.50E+06	3.40E+06	2.15E+06	1.05E+06	5.29E+05	2.55E+05	1.20E+05	4.99E+04	1.70E+04	5.09E+03	1.40E+03	3.10E+02	5.60E+01	1.05E+01	1.75E+00
3.60	6.00E+07	3.69E+07	1.45E+07	6.50E+06	3.69E+06	2.40E+06	1.30E+06	5.90E+05	2.95E+05	1.23E+05	4.99E+04	1.40E+04	3.85E+03	1.20E+03	2.50E+02	4.00E+01	7.30E+00	1.15E+00
3.80	6.50E+07	4.39E+07	1.70E+07	7.70E+06	4.29E+06	2.85E+06	1.35E+06	6.49E+05	3.29E+05	1.25E+05	4.59E+04	1.40E+04	3.85E+03	8.39E+02	1.55E+02	2.40E+01	3.00E+00	1.00E+00
4.00	7.20E+07	4.39E+07	2.05E+07	9.10E+06	4.99E+06	3.20E+06	1.60E+06	6.88E+05	3.15E+05	1.07E+05	4.00E+04	1.15E+04	3.00E+03	6.10E+02	9.50E+01	1.05E+01	1.00E+00	
4.40	7.60E+07	4.79E+07	2.45E+07	1.01E+07	5.70E+06	3.70E+06	1.60E+06	6.19E+05	2.59E+05	9.60E+04	3.35E+04	9.58E+03	2.40E+03	4.39E+02	5.79E+01	4.99E+00	1.00E+00	
4.50	8.00E+07	5.09E+07	2.45E+07	1.10E+07	5.99E+06	3.85E+06	1.48E+06	5.70E+05	2.20E+05	8.00E+04	2.74E+04	7.99E+03	1.90E+03	3.15E+02	3.50E+01	2.25E+00		
4.60	8.10E+07	5.20E+07	2.50E+07	1.11E+07	6.19E+06	3.80E+06	1.40E+06	5.20E+05	2.00E+05	7.50E+04	2.50E+04	7.09E+03	1.67E+03	2.65E+02	2.65E+01	1.45E+00		
4.80	8.30E+07	5.29E+07	2.85E+07	1.12E+07	5.99E+06	3.75E+06	1.32E+06	4.79E+05	1.80E+05	6.70E+04	2.30E+04	6.49E+03	1.49E+03	2.25E+02	2.05E+01	1.00E+00		
5.00	8.90E+07	5.39E+07	2.65E+07	1.09E+07	5.80E+06	3.35E+06	1.10E+06	4.00E+05	1.35E+05	5.30E+04	1.85E+04	5.09E+03	1.18E+03	1.55E+02	1.20E+01	1.00E+00		
5.50	8.10E+07	5.39E+07	2.50E+07	1.05E+07	4.79E+06	2.60E+06	9.00E+05	3.29E+05	1.20E+05	4.20E+04	1.45E+04	4.10E+03	9.10E+02	1.05E+02	6.99E+00	1.00E+00		
6.00	7.10E+07	4.29E+07	2.15E+07	7.60E+06	3.25E+06	1.75E+06	5.39E+05	1.85E+05	6.39E+04	2.30E+04	7.50E+03	2.15E+03	4.99E+02	4.20E+01	1.00E+00			
6.60	4.60E+07	3.15E+07	1.68E+07	5.30E+06	2.00E+06	9.69E+05	2.85E+05	9.69E+04	3.00E+04	1.11E+04	3.59E+03	1.05E+03	2.55E+02	1.60E+01				
7.00	3.90E+07	2.40E+07	1.10E+07	2.90E+06	1.15E+06	4.80E+05	9.00E+04	3.00E+04	1.05E+04	3.70E+03	1.55E+03	4.39E+02	1.15E+02	4.29E+01				
8.00	3.10E+07	1.58E+07	7.69E+06	1.85E+06	5.70E+05	2.60E+05	5.90E+04	1.70E+04	4.00E+03	1.55E+03	6.39E+02	2.34E+02	6.39E+01	4.00E+00				
9.00	2.40E+07	9.50E+06	4.49E+06	8.50E+05	2.40E+05	1.00E+05	1.95E+04	4.50E+03	1.13E+03	4.90E+02	2.20E+02	1.00E+02	2.85E+01	1.00E+00				
10.00	1.35E+07	2.34E+06	2.15E+06	3.15E+05	7.99E+04	2.90E+04	4.39E+03	9.50E+02	2.95E+02	1.40E+02	6.99E+01	3.90E+01	1.15E+01					
11.00	6.80E+06	2.79E+06	3.00E+05	1.55E+04	3.00E+03	7.50E+02	5.00E+01	2.50E+01	1.15E+01	6.80E+00	4.39E+00	2.65E+00	1.00E+00					
12.00	2.70E+06	1.20E+04	3.79E+01	1.22E+02	2.00E+01	5.00E+00	1.00E+00	2.50E+01										
15.60	1.00E+00	1.00E+00	1.00E+00	1.00E+00	1.00E+00	1.00E+00	1.00E+00	1.00E+00	1.00E+00	1.00E+00	1.00E+00	1.00E+00	1.00E+00	1.00E+00	1.00E+00	1.00E+00	1.00E+00	1.00E+00

Table 13B. AE-8MIN Equatorial Omnidirectional Fluxes Above Energy E

L\E	0.04 MeV	0.10 MeV	0.25 MeV	0.50 MeV	0.75 MeV	1.00 MeV	1.50 MeV	2.00 MeV	2.50 MeV	3.00 MeV	3.50 MeV	4.00 MeV	4.50 MeV	5.00 MeV	5.50 MeV	6.00 MeV	6.50 MeV	7.00 MeV
0.00	1.00E+00	1.00E+00	1.00E+00	1.00E+00	1.00E+00	1.00E+00	1.00E+00	1.00E+00	1.00E+00	1.00E+00	1.00E+00	1.00E+00	1.00E+00	1.00E+00	1.00E+00	1.00E+00	1.00E+00	1.00E+00
1.10	1.00E-00	1.00E-00	1.00E-00	1.00E-00	1.00E-00	1.00E-00	1.00E-00	1.00E-00	1.00E-00	1.00E-00	1.00E-00	1.00E+00						
1.20	5.87E+05	4.00E-05	1.45E-05	1.55E-04	3.25E-03	1.19E-03	3.25E-02	1.50E-02	5.30E+01	1.59E-01	3.99E-00	4.50E+00						
1.25	8.08E+06	5.29E-06	1.80E-06	2.20E-05	3.25E-05	1.00E-05	3.15E-04	1.35E-04	6.00E-03	3.06E-03	1.65E-02	1.60E-01	1.00E-00					
1.30	5.29E+06	2.82E-07	5.75E-06	9.00E-05	2.20E-05	2.30E-04	9.54E-04	4.25E-04	6.00E-04	1.70E-03	1.65E-02	3.67E-01	2.40E-00					
1.35	2.82E+07	4.30E-07	9.80E-06	1.81E-06	5.70E-05	1.00E-04	9.54E-04	4.25E-04	9.39E-02	1.70E-03	3.79E-02	3.67E-01	4.40E-00					
1.40	4.30E+07	6.00E-07	1.34E-07	2.90E-06	1.15E-06	2.85E-05	2.20E-05	9.50E-04	4.42E-04	7.50E-03	6.60E-02	5.80E-01	6.00E-00					
1.45	6.24E+07	6.85E-07	1.61E-07	3.70E-06	1.53E-06	8.39E-05	3.40E-05	1.53E-05	7.40E-04	1.10E-04	8.98E-02	7.30E-01	6.29E-00					
1.50	8.51E+07	7.45E-07	1.77E-07	4.10E-06	1.65E-06	8.60E-05	3.60E-05	1.70E-05	7.99E-04	1.10E-04	9.02E-02	7.40E-01	6.29E-00					
1.60	9.69E+07	8.47E-07	2.00E-07	4.10E-06	1.47E-06	8.99E-05	2.60E-05	1.12E-05	4.55E-04	6.00E-03	6.15E-02	9.02E-01	5.45E-00					
1.70	1.06E+08	9.31E-07	2.11E-07	3.45E-06	1.04E-06	4.65E-05	1.62E-04	5.86E-04	2.10E-04	2.70E-03	3.48E-02	6.15E-02	1.40E-00					
1.80	1.21E+08	9.20E-07	1.89E-07	2.36E-06	6.19E-05	2.68E-05	8.39E-04	2.10E-04	6.60E-03	1.02E-03	1.60E-02	2.50E-01	1.40E-00					
1.90	1.34E+08	7.79E-07	1.50E-07	1.49E-06	3.62E-05	1.35E-05	3.25E-04	6.90E-03	1.85E-03	3.10E-02	5.84E-01	1.10E-01	1.00E-00					
2.00	1.15E+08	6.75E-07	1.13E-07	1.01E-06	2.42E-05	7.81E-04	5.70E-03	1.25E-03	7.70E-03	1.09E-02	2.09E-01	1.10E-01	1.00E-00	1.00E+00				
2.20	1.02E+08	8.32E-07	7.20E-07	8.24E-05	1.71E-05	4.00E-04	5.70E-03	9.98E-02	2.72E-02	2.35E-01	2.03E-00	1.00E-00	1.00E-00	1.00E+00				
2.40	8.32E+07	5.26E-07	7.09E-06	7.40E-05	1.65E-05	5.00E-04	6.69E-03	1.70E-02	1.70E-02	1.00E-00	1.00E-00	1.00E-01	1.00E-00	1.00E+00				
2.50	6.37E+07	3.79E-07	5.09E-06	7.00E-05	2.05E-05	7.50E-04	1.40E-04	2.59E-03	4.79E-02	7.50E-01	1.00E-01	1.00E-00	1.00E-00	1.00E+00				
2.60	5.50E+07	3.25E-07	4.14E-06	6.70E-05	2.79E-05	1.15E-05	3.00E-04	6.79E-03	1.50E-03	2.50E-02	3.10E-01	4.00E-00	1.00E-00	1.00E+00				
2.69	4.70E+07	2.74E-07	3.59E-06															
2.70	3.80E+07	2.15E-07	3.10E-06	6.50E-05	3.00E-05	1.50E-05	4.99E-04	1.30E-04	3.59E-04	7.80E-02	1.50E-02	3.20E-01	4.99E-00	1.00E+00	1.00E+00	1.00E+00	1.00E+00	
2.79	3.20E+07														3.69E-00	1.00E+00	1.00E+00	
2.80	2.65E+07	1.65E-07	2.79E-06	6.50E-05	3.20E-05	1.90E-05	7.99E-04	2.50E-04	7.79E-04	2.00E-03	7.50E-02	2.50E-02	6.49E-01	1.60E-01				
2.89																		
2.90	2.25E+07	1.20E-07	2.59E-06	6.90E-05	3.51E-05	2.35E-05	9.39E-04	4.14E-04	1.55E-04	8.00E-03	4.45E-03	2.31E-03	1.14E-03	4.37E-02	1.43E-02	3.50E-01	6.69E-00	1.00E-00
3.00	1.55E+07	8.58E-06	2.50E-06	7.80E-05	4.28E-05	2.75E-05	1.15E-05	5.71E-04	2.45E-04	1.40E-04	7.74E-03	4.30E-03	2.38E-03	1.31E-03	6.29E-02	2.00E-02	4.00E-01	1.20E-00
3.20	1.42E+07	8.49E-06	2.55E-06	1.00E-06	6.24E-06	4.00E-06	1.92E-05	9.10E-04	4.49E-04	2.60E-04	1.55E-04	9.26E-03	4.36E-03	2.16E-03	6.29E-02	1.50E-02	2.95E-01	5.00E-00
3.40	1.45E+07	6.60E-06	3.04E-06	1.35E-06	7.79E-06	5.70E-05	2.70E-05	1.40E-04	7.09E-04	4.10E-04	2.34E-04	1.19E-04	4.87E-03	1.70E-03	3.90E-02	7.99E-01	1.50E-01	2.50E-00
3.50	1.55E+07	6.99E-06	3.38E-06	1.55E-06	9.18E-06	6.70E-05	3.20E-05	1.72E-05	8.02E-04	4.80E-04	2.59E-04	1.22E-04	4.55E-03	1.40E-03	3.10E-02	5.60E-01	1.05E-01	1.75E-00
3.60	1.85E+07	7.86E-06	3.79E-06	1.75E-06	1.20E-06	7.80E-06	3.69E-05	2.02E-05	9.87E-04	5.30E-04	2.79E-04	1.22E-04	4.36E-03	1.20E-03	2.50E-02	4.00E-01	7.30E-00	1.15E-00
3.80	2.16E+07	9.80E-06	4.92E-06	2.35E-06	1.25E-06	1.05E-06	5.20E-05	2.55E-05	1.32E-05	6.50E-04	3.00E-04	1.19E-04	3.67E-03	8.39E-02	1.55E-02	2.40E-01	3.00E-00	1.00E-00
4.00	2.58E+07	1.32E-07	6.75E-06	3.30E-06	1.40E-06	1.85E-06	6.49E-05	3.23E-05	1.65E-05	7.17E-04	3.10E-04	1.10E-04	3.00E-03	6.10E-02	9.50E-01	1.05E-01	1.00E-00	
4.20	2.58E+07	1.75E-07	8.70E-06	4.30E-06	2.94E-06	1.40E-06	8.19E-05	3.72E-05	1.87E-05	7.50E-04	2.90E-04	9.39E-04	2.40E-03	4.39E-02	5.79E-01	4.99E-00	1.00E-00	
4.40	3.36E+07	2.40E-07	1.18E-07	5.83E-06	3.38E-06	2.40E-06	1.02E-06	4.27E-05	1.88E-05	7.20E-04	2.70E-04	7.99E-03	1.94E-03	3.15E-02	3.50E-01	2.25E-00		
4.50	3.73E+07	2.79E-07	1.45E-07	6.90E-06	4.06E-06	2.65E-06	1.08E-06	4.31E-05	1.82E-05	7.00E-04	2.45E-04	7.09E-03	1.67E-03	2.65E-02	2.65E-01	1.45E-00		
4.60	4.15E+07	3.02E-07	1.67E-07	7.73E-06	4.40E-06	2.90E-06	1.12E-06	4.20E-05	1.75E-05	6.70E-04	2.30E-04	6.49E-03	1.49E-03	2.25E-02	2.05E-01	1.00E-00		
4.80	4.73E+07	3.54E-07	2.03E-07	8.83E-06	4.73E-06	2.95E-06	1.03E-06	3.79E-05	1.45E-05	5.30E-04	1.85E-04	5.09E-03	1.18E-03	1.55E-02	1.20E-01			
5.00	5.27E+07	3.93E-07	2.25E-07	9.40E-06	4.79E-06	2.75E-06	9.00E-06	3.29E-05	1.20E-05	4.20E-04	1.45E-04	4.10E-03	9.10E-02	1.05E-02	6.99E-00			
5.50	5.70E+07	4.02E-07	2.15E-07	7.80E-06	3.25E-06	1.75E-06	5.39E-05	2.01E-05	6.39E-04	2.30E-04	7.50E-03	2.15E-02	4.99E-02	4.29E-00	1.00E-00			
6.00	4.60E+07	3.74E-07	1.68E-07	1.85E-06	2.04E-06	1.00E-06	2.85E-06	9.89E-04	3.00E-04	1.11E-04	3.59E-03	1.05E-02	2.55E-02	1.60E-01				
6.60	3.80E+07	3.15E-07	1.10E-07	2.90E-06	1.15E-06	4.80E-05	1.20E-05	4.00E-04	1.05E-04	3.70E-03	7.30E-03	4.39E-02	1.15E-02	4.29E-00				
7.00	3.10E+07	2.40E-07	7.86E-06	1.85E-06	5.70E-05	1.75E-05	5.90E-04	1.70E-04	4.00E-03	1.55E-03	6.39E-02	2.34E-02	6.39E-01	2.65E-01				
7.50	2.40E+07	1.58E-07	4.49E-06	8.50E-05	2.40E-05	1.00E-05	1.95E-04	4.59E-02	1.13E-03	4.90E-02	2.20E-02	1.00E-02	3.90E-01	1.15E-01				
8.00	1.35E+07	9.50E-06	2.15E-06	3.15E-05	2.90E-04	2.90E-04	4.39E-03	9.50E-02	2.95E-02	1.40E-02	6.99E-01	2.20E-02	3.90E-01	1.00E-00				
9.00	6.90E+06	2.34E-08	3.00E-05	1.15E-04	3.00E-03	7.50E-02	9.50E-01	2.50E-01	1.15E-01	6.80E-00	4.39E-00	2.65E-00	1.15E-00	1.00E-00				
10.00	2.70E+06	2.79E-05	1.35E-05	1.22E-02	2.00E-01	5.00E-01	1.00E-00	1.00E-00	1.00E-00	1.00E-00	1.00E-00	1.00E-00						
11.00	1.00E-00	1.20E-04	1.00E-00															
12.00	1.00E-00	1.00E-00	1.00E-00	1.00E-00	1.00E-00	1.00E-00	1.00E-00	1.00E-00	1.00E-00	1.00E-00	1.00E-00	1.00E-00	1.00E-00	1.00E-00	1.00E-00	1.00E-00	1.00E-00	
15.60	1.00E-00	1.00E-00	1.00E-00	1.00E-00	1.00E-00	1.00E-00	1.00E-00	1.00E-00	1.00E-00	1.00E-00	1.00E-00	1.00E-00	1.00E-00	1.00E-00	1.00E-00	1.00E-00	1.00E-00	1.00E-00

Table 14. Four Circular Orbit Daily Fluence Summary Using AE-8MAX

Orbit Altitude - 150 n.mi. Accumulation Time - 36 Hrs. Sampling Interval - 30 s Units for Daily Fluence -e/cm²-day

Energy (MeV) E1	Energy (MeV) E2	Daily Fluence 0° Inclination *E1	Daily Fluence 0° Inclination E1-E2	Daily Fluence 30° Inclination *E1	Daily Fluence 30° Inclination E1-E2	Daily Fluence 60° Inclination *E1	Daily Fluence 60° Inclination E1-E2	Daily Fluence 90° Inclination *E1	Daily Fluence 90° Inclination E1-E2
0.00	0.25	0.0	0.0	0.229E+08	0.185E+08	0.453E+10	0.386E+10	0.531E+10	0.453E+10
0.25	0.50	0.0	0.0	0.438E+07	0.400E+07	0.666E+09	0.409E+09	0.776E+09	0.480E+09
0.50	0.75	0.0	0.0	0.375E+06	0.251E+06	0.258E+09	0.118E+09	0.295E+09	0.139E+09
0.75	1.00	0.0	0.0	0.123E+06	0.641E+05	0.140E+09	0.512E+08	0.156E+09	0.583E+08
1.00	1.25	0.0	0.0	0.593E+05	0.222E+05	0.884E+08	0.287E+08	0.981E+08	0.329E+08
1.25	1.50	0.0	0.0	0.371E+05	0.134E+05	0.597E+08	0.192E+08	0.652E+08	0.216E+08
1.50	1.75	0.0	0.0	0.236E+05	0.714E+04	0.405E+08	0.135E+08	0.436E+08	0.146E+08
1.75	2.00	0.0	0.0	0.165E+05	0.467E+04	0.270E+08	0.894E+07	0.286E+08	0.973E+07
2.00	2.25	0.0	0.0	0.118E+05	0.324E+04	0.181E+08	0.582E+07	0.190E+08	0.621E+07
2.25	2.50	0.0	0.0	0.859E+04	0.236E+04	0.123E+08	0.393E+07	0.128E+08	0.416E+07
2.50	2.75	0.0	0.0	0.623E+04	0.264E+04	0.836E+07	0.300E+07	0.865E+07	0.318E+07
2.75	3.00	0.0	0.0	0.359E+04	0.166E+04	0.536E+07	0.191E+07	0.548E+07	0.200E+07
3.00	3.25	0.0	0.0	0.193E+04	0.634E+03	0.345E+07	0.127E+07	0.348E+07	0.130E+07
3.25	3.50	0.0	0.0	0.129E+04	0.404E+03	0.218E+07	0.798E+06	0.218E+07	0.811E+06
3.50	3.75	0.0	0.0	0.889E+03	0.224E+03	0.138E+07	0.565E+06	0.137E+07	0.569E+06
3.75	4.00	0.0	0.0	0.665E+03	0.0	0.815E+06	0.331E+06	0.799E+06	0.330E+06
4.00	4.25	0.0	0.0	0.0	0.0	0.483E+06	0.217E+06	0.469E+06	0.212E+06
4.25	4.50	0.0	0.0	0.0	0.0	0.267E+06	0.119E+06	0.257E+06	0.116E+06
4.50	4.75	0.0	0.0	0.0	0.0	0.148E+06	0.686E+05	0.141E+06	0.666E+05
4.75	5.00	0.0	0.0	0.0	0.0	0.792E+05	0.367E+05	0.748E+05	0.352E+05
5.00	5.25	0.0	0.0	0.0	0.0	0.425E+05	0.221E+05	0.396E+05	0.208E+05
5.25	5.50	0.0	0.0	0.0	0.0	0.204E+05	0.114E+05	0.187E+05	0.104E+05
5.50	5.75	0.0	0.0	0.0	0.0	0.897E+04	0.547E+04	0.836E+04	0.485E+04
5.75	6.00	0.0	0.0	0.0	0.0	0.351E+04	0.225E+04	0.351E+04	0.232E+04
6.00	6.25	0.0	0.0	0.0	0.0	0.125E+04	0.924E+03	0.119E+04	0.852E+03
6.25	6.50	0.0	0.0	0.0	0.0	0.330E+03	0.0	0.294E+03	0.0
6.50	6.75	0.0	0.0	0.0	0.0	0.0	0.0	0.0	0.0
6.75	7.00	0.0	0.0	0.0	0.0	0.0	0.0	0.0	0.0

Table 14. Four Circular Orbit Daily Fluence Summary Using AE-8MAX (cont.)

Orbit Altitude - 300 n.mi.   Accumulation Time - 36 Hrs.   Sampling Interval - 30 s   Units for Daily Fluence -e/cm²-day

Energy (MeV)		Daily Fluence 0° Inclination		Daily Fluence 30° Inclination		Daily Fluence 60° Inclination		Daily Fluence 90° Inclination	
E1	E2	*E1	E1-E2	*E1	E1-E2	*E1	E1-E2	*E1	E1-E2
0.0	0.25	0.457E+06	0.171E+06	0.101E+11	0.873E+10	0.240E+11	0.210E+11	0.251E+11	0.220E+11
0.25	0.50	0.286E+06	0.171E+06	0.136E+10	0.125E+10	0.304E+10	0.228E+10	0.317E+10	0.235E+10
0.50	0.75	0.107E+05	0.433E+05	0.113E+09	0.808E+08	0.768E+09	0.389E+09	0.813E+09	0.417E+09
0.75	1.00	0.623E+05	0.189E+05	0.327E+08	0.179E+08	0.379E+09	0.146E+09	0.396E+09	0.154E+09
1.00	1.25	0.444E+05	0.884E+04	0.147E+08	0.566E+07	0.233E+09	0.773E+08	0.241E+09	0.830E+08
1.25	1.50	0.356E+05	0.653E+04	0.907E+07	0.347E+07	0.156E+09	0.510E+08	0.158E+09	0.536E+08
1.50	1.75	0.291E+05	0.372E+04	0.559E+07	0.186E+07	0.105E+09	0.350E+08	0.104E+09	0.360E+08
1.75	2.00	0.254E+05	0.287E+04	0.374E+07	0.124E+07	0.697E+08	0.232E+08	0.685E+08	0.234E+08
2.00	2.25	0.225E+05	0.287E+04	0.250E+07	0.802E+06	0.465E+08	0.150E+08	0.451E+08	0.149E+08
2.25	2.50	0.190E+05	0.287E+04	0.170E+07	0.543E+06	0.315E+08	0.101E+08	0.302E+08	0.990E+07
2.50	2.75	0.158E+05	0.268E+04	0.116E+07	0.543E+06	0.214E+08	0.805E+07	0.203E+08	0.773E+07
2.75	3.00	0.128E+05	0.227E+04	0.475E+06	0.276E+06	0.134E+08	0.494E+07	0.126E+08	0.471E+07
3.00	3.25	0.101E+05	0.222E+04	0.199E+06	0.135E+06	0.842E+07	0.317E+07	0.786E+07	0.300E+07
3.25	3.50	0.785E+04	0.180E+04	0.643E+05	0.432E+05	0.525E+07	0.195E+07	0.485E+07	0.183E+07
3.50	3.75	0.564E+04	0.0	0.211E+05	0.130E+05	0.330E+07	0.136E+07	0.302E+07	0.127E+07
3.75	4.00	0.383E+04	0.0	0.729E+04	0.645E+04	0.194E+07	0.793E+06	0.175E+07	0.731E+06
4.00	4.25	0.0	0.0	0.835E+03	0.0	0.115E+07	0.512E+06	0.102E+07	0.465E+06
4.25	4.50	0.0	0.0	0.0	0.0	0.635E+06	0.282E+06	0.556E+06	0.252E+06
4.50	4.75	0.0	0.0	0.0	0.0	0.354E+06	0.162E+06	0.304E+06	0.145E+06
4.75	5.00	0.0	0.0	0.0	0.0	0.191E+06	0.869E+05	0.159E+06	0.754E+05
5.00	5.25	0.0	0.0	0.0	0.0	0.104E+06	0.542E+05	0.838E+05	0.444E+05
5.25	5.50	0.0	0.0	0.0	0.0	0.502E+05	0.269E+05	0.393E+05	0.218E+05
5.50	5.75	0.0	0.0	0.0	0.0	0.232E+05	0.133E+05	0.176E+05	0.104E+05
5.75	6.00	0.0	0.0	0.0	0.0	0.993E+04	0.725E+04	0.720E+04	0.499E+04
6.00	6.25	0.0	0.0	0.0	0.0	0.268E+04	0.176E+04	0.222E+04	0.154E+04
6.25	6.50	0.0	0.0	0.0	0.0	0.919E+03	0.0	0.675E+03	0.0
6.50	6.75	0.0	0.0	0.0	0.0	0.0	0.0	0.0	0.0
6.75	7.00	0.0	0.0	0.0	0.0	0.0	0.0	0.0	0.0

Table 14. Four Circular Orbit Daily Fluence Summary Using AE-8MAX (cont.)

Orbit Altitude - 450 n.mi.   Accumulation Time - 36 Hrs.   Sampling Interval - 30 s   Units for Daily Fluence -e/cm²-day

Energy (MeV) E1	E2	Daily Fluence 0° Inclination *E1	E1-E2	Daily Fluence 30° Inclination *E1	E1-E2	Daily Fluence 60° Inclination *E1	E1-E2	Daily Fluence 90° Inclination *E1	E1-E2
0.0	0.25	0.607E+09	0.400E+09	0.696E+11	0.584E+11	0.843E+11	0.724E+11	0.815E+11	0.703E+11
0.25	0.50	0.207E+09	0.189E+09	0.113E+11	0.104E+11	0.119E+11	0.983E+10	0.112E+11	0.923E+10
0.50	0.75	0.180E+08	0.133E+08	0.904E+09	0.655E+09	0.205E+10	0.114E+10	0.196E+10	0.110E+10
0.75	1.00	0.475E+07	0.276E+07	0.249E+09	0.139E+09	0.909E+09	0.373E+09	0.858E+09	0.356E+09
1.00	1.25	0.155E+07	0.816E+06	0.110E+09	0.438E+08	0.537E+09	0.184E+09	0.502E+09	0.177E+09
1.25	1.50	0.117E+07	0.473E+06	0.657E+08	0.262E+08	0.353E+09	0.119E+09	0.325E+09	0.113E+09
1.50	1.75	0.701E+06	0.186E+06	0.355E+08	0.133E+08	0.234E+09	0.790E+08	0.213E+09	0.733E+08
1.75	2.00	0.515E+06	0.133E+06	0.262E+08	0.880E+07	0.155E+09	0.520E+08	0.139E+09	0.477E+08
2.00	2.25	0.382E+06	0.124E+06	0.174E+08	0.569E+07	0.103E+09	0.334E+08	0.916E+08	0.304E+08
2.25	2.50	0.258E+06	0.837E+05	0.118E+08	0.382E+07	0.694E+08	0.224E+08	0.612E+08	0.201E+08
2.50	2.75	0.174E+06	0.622E+05	0.793E+07	0.382E+07	0.469E+08	0.184E+08	0.411E+08	0.164E+08
2.75	3.00	0.112E+06	0.406E+05	0.336E+07	0.191E+07	0.286E+08	0.109E+08	0.247E+08	0.557E+07
3.00	3.25	0.713E+05	0.289E+05	0.145E+07	0.995E+06	0.177E+08	0.693E+07	0.151E+08	0.351E+07
3.25	3.50	0.424E+05	0.182E+05	0.454E+06	0.309E+06	0.108E+08	0.411E+07	0.912E+07	0.238E+07
3.50	3.75	0.242E+05	0.102E+05	0.145E+06	0.972E+05	0.670E+07	0.280E+07	0.560E+07	0.351E+07
3.75	4.00	0.140E+05	0.0	0.474E+05	0.351E+05	0.390E+07	0.161E+07	0.322E+07	0.238E+07
4.00	4.25	0.0	0.0	0.123E+05	0.101E+05	0.229E+07	0.103E+07	0.187E+07	0.135E+07
4.25	4.50	0.0	0.0	0.225E+04	0.0	0.125E+07	0.562E+06	0.101E+07	0.856E+06
4.50	4.75	0.0	0.0	0.0	0.0	0.692E+06	0.324E+06	0.554E+06	0.461E+06
4.75	5.00	0.0	0.0	0.0	0.0	0.368E+06	0.170E+06	0.289E+06	0.265E+06
5.00	5.25	0.0	0.0	0.0	0.0	0.198E+06	0.103E+06	0.152E+06	0.136E+06
5.25	5.50	0.0	0.0	0.0	0.0	0.949E+05	0.501E+05	0.722E+05	0.802E+05
5.50	5.75	0.0	0.0	0.0	0.0	0.448E+05	0.254E+05	0.336E+05	0.387E+05
5.75	6.00	0.0	0.0	0.0	0.0	0.194E+05	0.130E+05	0.146E+05	0.190E+05
6.00	6.25	0.0	0.0	0.0	0.0	0.632E+04	0.501E+04	0.484E+04	0.574E+04
6.25	6.50	0.0	0.0	0.0	0.0	0.131E+04	0.124E+04	0.141E+04	0.343E+04
6.50	6.75	0.0	0.0	0.0	0.0	0.646E+02	0.0	0.874E+02	0.132E+04
6.75	7.00	0.0	0.0	0.0	0.0	0.0	0.0	0.0	0.0
7.00									

Table 14. Four Circular Orbit Daily Fluence Summary Using AE-8MAX (cont.)

Orbit Altitude - 600 n.mi.   Accumulation Time - 24 Hrs.   Sampling Interval - 30 s   Units for Daily Fluence -e/cm²-day

Energy (MeV)		Daily Fluence 0° Inclination		Daily Fluence 30° Inclination		Daily Fluence 60° Inclination		Daily Fluence 90° Inclination	
E1	E2	*E1	E1-E2	*E1	E1-E2	*E1	E1-E2	*E1	E1-E2
0.0	0.25	0.677E+11	0.487E+11	0.676E+11	0.513E+11	0.258E+12	0.217E+12	0.216E+12	0.180E+12
0.25	0.50	0.190E+11	0.178E+11	0.162E+11	0.152E+11	0.416E+11	0.364E+11	0.357E+11	0.312E+11
0.50	0.75	0.121E+10	0.958E+09	0.106E+10	0.828E+09	0.512E+10	0.316E+10	0.443E+10	0.274E+10
0.75	1.00	0.250E+09	0.157E+09	0.236E+09	0.142E+09	0.197E+10	0.876E+09	0.170E+10	0.762E+09
1.00	1.25	0.934E+08	0.433E+08	0.937E+08	0.412E+08	0.109E+10	0.387E+09	0.936E+09	0.339E+09
1.25	1.50	0.500E+08	0.232E+08	0.526E+08	0.229E+08	0.704E+09	0.246E+09	0.596E+09	0.213E+09
1.50	1.75	0.268E+08	0.899E+07	0.297E+08	0.995E+07	0.458E+09	0.155E+09	0.383E+09	0.132E+09
1.75	2.00	0.178E+08	0.597E+07	0.158E+08	0.661E+07	0.303E+09	0.102E+09	0.251E+09	0.860E+08
2.00	2.25	0.119E+08	0.439E+07	0.132E+08	0.464E+07	0.201E+09	0.658E+08	0.165E+09	0.547E+08
2.25	2.50	0.748E+07	0.276E+07	0.853E+07	0.298E+07	0.135E+09	0.440E+08	0.111E+09	0.363E+08
2.50	2.75	0.473E+07	0.211E+07	0.554E+07	0.289E+07	0.912E+08	0.381E+08	0.743E+08	0.317E+08
2.75	3.00	0.262E+07	0.117E+07	0.266E+07	0.266E+07	0.530E+08	0.212E+08	0.426E+08	0.174E+08
3.00	3.25	0.145E+07	0.902E+06	0.131E+07	0.135E+07	0.318E+08	0.132E+08	0.252E+08	0.107E+08
3.25	3.50	0.549E+06	0.341E+06	0.451E+06	0.858E+06	0.186E+08	0.731E+07	0.145E+08	0.582E+07
3.50	3.75	0.208E+06	0.126E+06	0.156E+06	0.295E+06	0.113E+08	0.477E+07	0.872E+07	0.376E+07
3.75	4.00	0.819E+05	0.598E+05	0.536E+05	0.102E+06	0.656E+07	0.271E+07	0.496E+07	0.210E+07
4.00	4.25	0.221E+05	0.0	0.139E+05	0.397E+05	0.385E+07	0.173E+07	0.286E+07	0.131E+07
4.25	4.50	0.0	0.0	0.236E+04	0.115E+05	0.212E+07	0.943E+06	0.155E+07	0.704E+06
4.50	4.75	0.0	0.0	0.0	0.0	0.118E+07	0.540E+06	0.844E+06	0.405E+06
4.75	5.00	0.0	0.0	0.0	0.0	0.639E+06	0.286E+06	0.439E+06	0.206E+06
5.00	5.25	0.0	0.0	0.0	0.0	0.354E+06	0.181E+06	0.233E+06	0.122E+06
5.25	5.50	0.0	0.0	0.0	0.0	0.173E+06	0.889E+05	0.110E+06	0.582E+05
5.50	5.75	0.0	0.0	0.0	0.0	0.840E+05	0.453E+05	0.522E+05	0.291E+05
5.75	6.00	0.0	0.0	0.0	0.0	0.387E+05	0.229E+05	0.231E+05	0.140E+05
6.00	6.25	0.0	0.0	0.0	0.0	0.158E+05	0.113E+05	0.912E+04	0.616E+04
6.25	6.50	0.0	0.0	0.0	0.0	0.449E+04	0.387E+04	0.296E+04	0.277E+04
6.50	6.75	0.0	0.0	0.0	0.0	0.628E+03	0.0	0.187E+03	0.0
6.75	7.00	0.0	0.0	0.0	0.0	0.0	0.0	0.0	0.0

Table 14. Four Circular Orbit Daily Fluence Summary Using AE-8MAX (cont.)

Orbit Altitude - 800 n.mi.   Accumulation Time - 24 Hrs.   Sampling Interval - 30 s   Units for Daily Fluence -e/cm²-day

Energy (MeV)		Daily Fluence 0° Inclination		Daily Fluence 30° Inclination		Daily Fluence 60° Inclination		Daily Fluence 90° Inclination	
E1	E2	*E1	E1-E2	*E1	E1-E2	*E1	E1-E2	*E1	E1-E2
0.00	0.25	0.432E+13	0.330E+13	0.315E+13	0.256E+13	0.210E+13	0.173E+13	0.178E+13	0.146E+13
0.25	0.50	0.103E+13	0.944E+12	0.591E+12	0.542E+12	0.376E+12	0.340E+12	0.322E+12	0.291E+12
0.50	0.75	0.809E+11	0.578E+11	0.454E+11	0.348E+11	0.360E+11	0.242E+11	0.303E+11	0.206E+11
0.75	1.00	0.231E+11	0.129E+11	0.146E+11	0.801E+10	0.118E+11	0.596E+10	0.977E+10	0.501E+10
1.00	1.25	0.102E+11	0.426E+10	0.658E+10	0.263E+10	0.580E+10	0.219E+10	0.476E+10	0.183E+10
1.25	1.50	0.597E+10	0.248E+10	0.395E+10	0.157E+10	0.360E+10	0.135E+10	0.293E+10	0.112E+10
1.50	1.75	0.349E+10	0.118E+10	0.237E+10	0.795E+09	0.225E+10	0.760E+09	0.182E+10	0.617E+09
1.75	2.00	0.231E+10	0.782E+09	0.158E+10	0.528E+09	0.149E+10	0.502E+09	0.120E+10	0.407E+09
2.00	2.25	0.153E+10	0.491E+09	0.105E+10	0.335E+09	0.992E+09	0.320E+09	0.795E+09	0.258E+09
2.25	2.50	0.103E+10	0.333E+09	0.714E+09	0.228E+09	0.671E+09	0.216E+09	0.537E+09	0.174E+09
2.50	2.75	0.702E+09	0.383E+09	0.486E+09	0.279E+09	0.455E+09	0.229E+09	0.364E+09	0.188E+09
2.75	3.00	0.319E+09	0.172E+09	0.207E+09	0.118E+09	0.226E+09	0.108E+09	0.176E+09	0.866E+08
3.00	3.25	0.146E+09	0.102E+09	0.894E+08	0.626E+08	0.118E+09	0.612E+08	0.869E+08	0.483E+08
3.25	3.50	0.445E+08	0.310E+08	0.268E+08	0.187E+08	0.568E+08	0.262E+08	0.406E+08	0.157E+08
3.50	3.75	0.135E+08	0.940E+07	0.803E+07	0.562E+07	0.306E+08	0.139E+08	0.209E+08	0.993E+07
3.75	4.00	0.412E+07	0.287E+07	0.242E+07	0.169E+07	0.167E+08	0.721E+07	0.110E+08	0.453E+07
4.00	4.25	0.125E+07	0.909E+06	0.724E+06	0.529E+06	0.947E+07	0.435E+07	0.607E+07	0.286E+07
4.25	4.50	0.345E+06	0.275E+06	0.195E+06	0.159E+06	0.512E+07	0.231E+07	0.321E+07	0.148E+07
4.50	4.75	0.696E+05	0.0	0.354E+05	0.0	0.281E+07	0.131E+07	0.172E+07	0.832E+06
4.75	5.00	0.0	0.0	0.0	0.0	0.150E+07	0.676E+06	0.892E+06	0.415E+06
5.00	5.25	0.0	0.0	0.0	0.0	0.828E+06	0.425E+06	0.477E+06	0.249E+06
5.25	5.50	0.0	0.0	0.0	0.0	0.403E+06	0.205E+06	0.228E+06	0.118E+06
5.50	5.75	0.0	0.0	0.0	0.0	0.198E+06	0.107E+06	0.110E+06	0.600E+05
5.75	6.00	0.0	0.0	0.0	0.0	0.909E+05	0.502E+05	0.498E+05	0.281E+05
6.00	6.25	0.0	0.0	0.0	0.0	0.407E+05	0.241E+05	0.217E+05	0.130E+05
6.25	6.50	0.0	0.0	0.0	0.0	0.166E+05	0.135E+05	0.872E+04	0.709E+04
6.50	6.75	0.0	0.0	0.0	0.0	0.307E+04	0.297E+04	0.163E+04	0.0
6.75	7.00	0.0	0.0	0.0	0.0	0.913E+02	0.0	0.0	0.0

Table 14. Four Circular Orbit Daily Fluence Summary Using AE-8MAX (cont.)

Orbit Altitude - 1000 n.mi.   Accumulation Time - 24 Hrs.   Sampling Interval - 30 s   Units for Daily Fluence -e/cm²-day

Energy (MeV)		Daily Fluence 0° Inclination		Daily Fluence 30° Inclination		Daily Fluence 60° Inclination		Daily Fluence 90° Inclination	
E1	E2	*E1	E1-E2	*E1	E1-E2	*E1	E1-E2	*E1	E1-E2
0.0	0.25	0.111E+13	0.823E+12	0.800E+12	0.638E+12	0.848E+12	0.699E+12	0.714E+12	0.587E+12
0.25	0.50	0.284E+12	0.264E+12	0.162E+12	0.149E+12	0.149E+12	0.134E+12	0.127E+12	0.115E+12
0.50	0.75	0.200E+11	0.152E+11	0.122E+11	0.893E+10	0.150E+11	0.990E+10	0.127E+11	0.843E+10
0.75	1.00	0.482E+10	0.284E+10	0.331E+10	0.186E+10	0.505E+10	0.246E+10	0.422E+10	0.208E+10
1.00	1.25	0.158E+10	0.872E+09	0.144E+10	0.593E+09	0.259E+10	0.959E+09	0.215E+10	0.809E+09
1.25	1.50	0.111E+10	0.487E+09	0.850E+09	0.347E+09	0.163E+10	0.596E+09	0.134E+10	0.496E+09
1.50	1.75	0.624E+09	0.211E+09	0.502E+09	0.169E+09	0.104E+10	0.351E+09	0.838E+09	0.286E+09
1.75	2.00	0.413E+09	0.140E+09	0.333E+09	0.112E+09	0.687E+09	0.231E+09	0.552E+09	0.188E+09
2.00	2.25	0.273E+09	0.917E+08	0.221E+09	0.717E+08	0.456E+09	0.148E+09	0.364E+09	0.120E+09
2.25	2.50	0.182E+09	0.607E+08	0.149E+09	0.483E+08	0.308E+09	0.995E+08	0.245E+09	0.799E+08
2.50	2.75	0.121E+09	0.300E+08	0.101E+09	0.557E+08	0.208E+09	0.958E+08	0.165E+09	0.776E+08
2.75	3.00	0.601E+08	0.205E+08	0.451E+08	0.245E+08	0.112E+09	0.490E+08	0.869E+08	0.390E+08
3.00	3.25	0.301E+08	0.649E+07	0.205E+08	0.142E+08	0.633E+08	0.294E+08	0.479E+08	0.231E+08
3.25	3.50	0.953E+07	0.206E+07	0.632E+07	0.437E+07	0.339E+08	0.143E+08	0.248E+08	0.108E+08
3.50	3.75	0.304E+07	0.665E+06	0.155E+07	0.135E+07	0.196E+08	0.853E+07	0.139E+08	0.626E+07
3.75	4.00	0.977E+06	0.232E+06	0.603E+06	0.423E+06	0.111E+08	0.466E+07	0.768E+07	0.333E+07
4.00	4.25	0.313E+06	0.736E+05	0.180E+06	0.137E+06	0.642E+07	0.292E+07	0.435E+07	0.202E+07
4.25	4.50	0.804E+05	0.0	0.431E+05	0.393E+05	0.350E+07	0.157E+07	0.233E+07	0.107E+07
4.50	4.75	0.683E+04	0.0	0.379E+04	0.0	0.193E+07	0.896E+06	0.126E+07	0.604E+06
4.75	5.00	0.0	0.0	0.0	0.0	0.104E+07	0.468E+06	0.656E+06	0.307E+06
5.00	5.25	0.0	0.0	0.0	0.0	0.570E+06	0.294E+06	0.349E+06	0.183E+06
5.25	5.50	0.0	0.0	0.0	0.0	0.277E+06	0.142E+06	0.166E+06	0.866E+05
5.50	5.75	0.0	0.0	0.0	0.0	0.135E+06	0.730E+05	0.796E+05	0.439E+05
5.75	6.00	0.0	0.0	0.0	0.0	0.616E+05	0.348E+05	0.358E+05	0.207E+05
6.00	6.25	0.0	0.0	0.0	0.0	0.268E+05	0.161E+05	0.150E+05	0.926E+04
6.25	6.50	0.0	0.0	0.0	0.0	0.107E+05	0.989E+04	0.577E+04	0.521E+04
6.50	6.75	0.0	0.0	0.0	0.0	0.770E+03	0.0	0.562E+03	0.0
6.75	7.00	0.0	0.0	0.0	0.0	0.0	0.0	0.0	0.0
7.00		0.0	0.0	0.0	0.0	0.0	0.0	0.0	0.0

Table 14. Four Circular Orbit Daily Fluence Summary Using AE-8MAX (cont.)

Orbit Altitude - 1250 n.mi.   Accumulation Time - 24 Hrs.   Sampling Interval - 30 s   Units for Daily Fluence -e/cm²-day

Energy (MeV)		Daily Fluence 0° Inclination		Daily Fluence 30° Inclination		Daily Fluence 60° Inclination		Daily Fluence 90° Inclination	
E1	E2	*E1	E1-E2	*E1	E1-E2	*E1	E1-E2	*E1	E1-E2
0.0	0.25	0.103E+14	0.808E+13	0.692E+13	0.569E+13	0.420E+13	0.346E+13	0.356E+13	0.293E+13
0.25	0.50	0.225E+13	0.205E+13	0.123E+13	0.112E+13	0.735E+12	0.663E+12	0.627E+12	0.567E+12
0.50	0.75	0.200E+12	0.133E+12	0.110E+12	0.751E+11	0.719E+11	0.481E+11	0.605E+11	0.407E+11
0.75	1.00	0.661E+11	0.352E+11	0.346E+11	0.185E+11	0.238E+11	0.122E+11	0.198E+11	0.102E+11
1.00	1.25	0.309E+11	0.122E+11	0.161E+11	0.619E+10	0.117E+11	0.435E+10	0.958E+10	0.362E+10
1.25	1.50	0.187E+11	0.735E+10	0.989E+10	0.380E+10	0.730E+10	0.271E+10	0.596E+10	0.224E+10
1.50	1.75	0.114E+11	0.379E+10	0.609E+10	0.204E+10	0.460E+10	0.154E+10	0.373E+10	0.126E+10
1.75	2.00	0.758E+10	0.253E+10	0.406E+10	0.135E+10	0.306E+10	0.102E+10	0.247E+10	0.820E+09
2.00	2.25	0.505E+10	0.159E+10	0.270E+10	0.857E+09	0.203E+10	0.651E+09	0.164E+10	0.527E+09
2.25	2.50	0.347E+10	0.109E+10	0.184E+10	0.584E+09	0.138E+10	0.441E+09	0.111E+10	0.357E+09
2.50	2.75	0.238E+10	0.138E+10	0.506E+10	0.754E+09	0.942E+09	0.508E+09	0.757E+09	0.419E+09
2.75	3.00	0.954E+09	0.575E+09	0.205E+10	0.302E+09	0.434E+09	0.223E+09	0.388E+09	0.180E+09
3.00	3.25	0.419E+09	0.295E+09	0.6C3E+08	0.144E+09	0.211E+09	0.116E+09	0.158E+09	0.520E+08
3.25	3.50	0.123E+09	0.870E+08	0.178E+08	0.425E+08	0.944E+08	0.462E+08	0.664E+08	0.345E+08
3.50	3.75	0.364E+08	0.257E+08	0.525E+07	0.125E+08	0.482E+08	0.228E+08	0.319E+08	0.158E+08
3.75	4.00	0.108E+08	0.758E+07	0.155E+07	0.370E+07	0.253E+08	0.113E+08	0.161E+08	0.743E+07
4.00	4.25	0.318E+07	0.230E+07	0.436E+06	0.112E+07	0.141E+08	0.658E+07	0.868E+07	0.414E+07
4.25	4.50	0.874E+06	0.633E+06	0.109E+06	0.327E+06	0.750E+07	0.343E+07	0.454E+07	0.211E+07
4.50	4.75	0.240E+06	0.204E+06	0.122E+05	0.966E+05	0.407E+07	0.194E+07	0.243E+07	0.118E+07
4.75	5.00	0.363E+05	0.0	0.0	0.0	0.213E+07	0.982E+06	0.125E+07	0.584E+06
5.00	5.25	0.0	0.0	0.0	0.0	0.115E+07	0.595E+06	0.670E+06	0.348E+06
5.25	5.50	0.0	0.0	0.0	0.0	0.555E+06	0.285E+06	0.321E+06	0.165E+06
5.50	5.75	0.0	0.0	0.0	0.0	0.271E+06	0.147E+06	0.156E+06	0.848E+05
5.75	6.00	0.0	0.0	0.0	0.0	0.123E+06	0.683E+05	0.712E+05	0.353E+05
6.00	6.25	0.0	0.0	0.0	0.0	0.551E+05	0.330E+05	0.319E+05	0.191E+05
6.25	6.50	0.0	0.0	0.0	0.0	0.251E+05	0.159E+05	0.129E+05	0.901E+04
6.50	6.75	0.0	0.0	0.0	0.0	0.618E+04	0.587E+04	0.387E+04	0.367E+04
6.75	7.00	0.0	0.0	0.0	0.0	0.304E+03	0.0	0.197E+03	0.0
7.00		0.0	0.0	0.0	0.0	0.0	0.0	0.0	0.0

Table 14. Four Circular Orbit Daily Fluence Summary Using AE-8MAX (cont.)

Orbit Altitude - 1500 n.mi. Accumulation Time - 24 Hrs. Sampling Interval - 30 s Units for Daily Fluence -e/cm²-day

Energy (MeV)		Daily Fluence 0° Inclination		Daily Fluence 30° Inclination		Daily Fluence 60° Inclination		Daily Fluence 90° Inclination	
E2	E1	*E1	E1-E2	*E1	E1-E2	*E1	E1-E2	*E1	E1-E2
0.25	0.00	0.171E+14	0.136E+14	0.108E+14	0.896E+13	0.617E+13	0.512E+13	0.519E+13	0.430E+13
0.50	0.25	0.350E+13	0.318E+13	0.184E+13	0.167E+13	0.105E+13	0.944E+12	0.891E+12	0.803E+12
0.75	0.50	0.327E+12	0.212E+12	0.168E+12	0.119E+12	0.105E+12	0.717E+11	0.876E+11	0.603E+11
1.00	0.75	0.115E+12	0.601E+11	0.493E+11	0.269E+11	0.330E+11	0.170E+11	0.273E+11	0.143E+11
1.25	1.00	0.550E+11	0.205E+11	0.224E+11	0.836E+10	0.160E+11	0.582E+10	0.131E+11	0.461E+10
1.50	1.25	0.345E+11	0.129E+11	0.141E+11	0.523E+10	0.101E+11	0.368E+10	0.824E+10	0.202E+10
1.75	1.50	0.216E+11	0.714E+10	0.883E+10	0.292E+10	0.646E+10	0.215E+10	0.522E+10	0.175E+10
2.00	1.75	0.145E+11	0.478E+10	0.591E+10	0.195E+10	0.430E+10	0.143E+10	0.347E+10	0.116E+10
2.25	2.00	0.971E+10	0.306E+10	0.365E+10	0.127E+10	0.287E+10	0.927E+09	0.231E+10	0.750E+09
2.50	2.25	0.665E+10	0.209E+10	0.268E+10	0.861E+09	0.194E+10	0.625E+09	0.156E+10	0.505E+09
2.75	2.50	0.456E+10	0.108E+10	0.182E+10	0.113E+10	0.132E+10	0.732E+09	0.106E+10	0.403E+09
3.00	2.75	0.177E+10	0.488E+09	0.695E+09	0.429E+09	0.585E+09	0.309E+09	0.455E+09	0.249E+09
3.25	3.00	0.689E+09	0.142E+09	0.266E+09	0.188E+09	0.276E+09	0.152E+09	0.206E+09	0.119E+09
3.50	3.25	0.201E+09	0.414E+08	0.782E+08	0.552E+08	0.124E+09	0.605E+08	0.872E+08	0.449E+08
3.75	3.50	0.584E+08	0.121E+08	0.230E+08	0.162E+08	0.634E+08	0.300E+08	0.423E+08	0.206E+08
4.00	3.75	0.170E+08	0.355E+07	0.679E+07	0.479E+07	0.334E+08	0.149E+08	0.215E+08	0.903E+07
4.25	4.00	0.456E+07	0.101E+07	0.201E+07	0.143E+07	0.186E+08	0.862E+07	0.116E+08	0.551E+07
4.50	4.25	0.141E+07	0.295E+06	0.579E+06	0.423E+06	0.993E+07	0.451E+07	0.612E+07	0.158E+07
4.75	4.50	0.401E+06	0.123E+06	0.155E+06	0.123E+06	0.542E+07	0.255E+07	0.329E+07	0.796E+06
5.00	4.75	0.107E+06	0.0	0.321E+05	0.0	0.287E+07	0.131E+07	0.171E+07	0.473E+06
5.25	5.00	0.0	0.0	0.0	0.0	0.156E+07	0.799E+06	0.915E+06	0.225E+06
5.50	5.25	0.0	0.0	0.0	0.0	0.764E+06	0.385E+06	0.441E+06	0.117E+06
5.75	5.50	0.0	0.0	0.0	0.0	0.380E+06	0.203E+06	0.216E+06	0.544E+05
6.00	5.75	0.0	0.0	0.0	0.0	0.176E+06	0.957E+05	0.995E+05	0.243E+05
6.25	6.00	0.0	0.0	0.0	0.0	0.808E+05	0.476E+05	0.447E+05	0.118E+05
6.50	6.25	0.0	0.0	0.0	0.0	0.331E+05	0.213E+05	0.184E+05	0.569E+04
6.75	6.50	0.0	0.0	0.0	0.0	0.119E+05	0.993E+04	0.659E+04	0.0
7.00	6.75	0.0	0.0	0.0	0.0	0.194E+04	0.0	0.901E+03	0.0
	7.00	0.0		0.0		0.0		0.0	

Table 14. Four Circular Orbit Daily Fluence Summary Using AE-8MAX (cont.)

Orbit Altitude - 1750 n.ml. Accumulation Time - 48 Hrs. Sampling Interval - 60 s Units for Daily Fluence -e/cm²-day

Energy (MeV)		Daily Fluence 0° Inclination		Daily Fluence 30° Inclination		Daily Fluence 60° Inclination		Daily Fluence 90° Inclination	
E1	E2	*E1	E1-E2	*E1	E1-E2	*E1	E1-E2	*E1	E1-E2
0.0	0.25	0.306E+14	0.247E+14	0.189E+14	0.157E+14	0.987E+13	0.821E+13	0.835E+13	0.694E+13
0.25	0.50	0.588E+13	0.533E+13	0.317E+13	0.287E+13	0.166E+13	0.149E+13	0.141E+13	0.127E+13
0.50	0.75	0.551E+12	0.428E+12	0.256E+12	0.242E+12	0.169E+12	0.131E+12	0.140E+12	0.110E+12
0.75	1.00	0.123E+12	0.728E+11	0.546E+11	0.341E+11	0.375E+11	0.210E+11	0.300E+11	0.172E+11
1.00	1.25	0.497E+11	0.192E+11	0.205E+11	0.806E+10	0.165E+11	0.615E+10	0.128E+11	0.483E+10
1.25	1.50	0.306E+11	0.118E+11	0.125E+11	0.488E+10	0.104E+11	0.382E+10	0.793E+10	0.298E+10
1.50	1.75	0.188E+11	0.650E+10	0.759E+10	0.273E+10	0.655E+10	0.231E+10	0.496E+10	0.176E+10
1.75	2.00	0.123E+11	0.424E+10	0.406E+10	0.173E+10	0.425E+10	0.148E+10	0.320E+10	0.113E+10
2.00	2.25	0.804E+10	0.287E+10	0.313E+10	0.113E+10	0.276E+10	0.962E+09	0.208E+10	0.732E+09
2.25	2.50	0.517E+10	0.184E+10	0.199E+10	0.720E+09	0.180E+10	0.624E+09	0.134E+10	0.471E+09
2.50	2.75	0.335E+10	0.212E+10	0.127E+10	0.807E+09	0.118E+10	0.608E+09	0.873E+09	0.471E+09
2.75	3.00	0.121E+10	0.771E+09	0.466E+09	0.295E+09	0.570E+09	0.273E+09	0.402E+09	0.202E+09
3.00	3.25	0.443E+09	0.303E+09	0.171E+09	0.166E+09	0.297E+09	0.138E+09	0.200E+09	0.977E+08
3.25	3.50	0.144E+09	0.956E+08	0.550E+08	0.371E+08	0.160E+09	0.679E+08	0.102E+09	0.454E+08
3.50	3.75	0.444E+08	0.303E+08	0.179E+08	0.120E+08	0.916E+08	0.404E+08	0.566E+08	0.256E+08
3.75	4.00	0.141E+08	0.961E+07	0.589E+07	0.392E+07	0.512E+08	0.218E+08	0.310E+08	0.135E+08
4.00	4.25	0.448E+07	0.318E+07	0.197E+07	0.137E+07	0.294E+08	0.134E+08	0.176E+08	0.813E+07
4.25	4.50	0.130E+07	0.925E+06	0.601E+06	0.424E+06	0.159E+08	0.717E+07	0.944E+07	0.426E+07
4.50	4.75	0.380E+06	0.279E+06	0.177E+06	0.134E+06	0.876E+07	0.412E+07	0.516E+07	0.245E+07
4.75	5.00	0.100E+06	0.0	0.432E+05	0.386E+05	0.464E+07	0.211E+07	0.271E+07	0.124E+07
5.00	5.25	0.0	0.0	0.459E+04	0.224E+04	0.253E+07	0.130E+07	0.147E+07	0.755E+06
5.25	5.50	0.0	0.0	0.235E+04	0.916E+03	0.123E+07	0.621E+06	0.715E+06	0.361E+06
5.50	5.75	0.0	0.0	0.143E+04	0.527E+03	0.606E+06	0.326E+06	0.354E+06	0.190E+06
5.75	6.00	0.0	0.0	0.904E+03	0.0	0.280E+06	0.152E+06	0.164E+06	0.866E+05
6.00	6.25	0.0	0.0	0.0	0.0	0.128E+06	0.740E+05	0.755E+05	0.435E+05
6.25	6.50	0.0	0.0	0.0	0.0	0.544E+05	0.329E+05	0.320E+05	0.196E+05
6.50	6.75	0.0	0.0	0.0	0.0	0.215E+05	0.144E+05	0.124E+05	0.829E+04
6.75	7.00	0.0	0.0	0.0	0.0	0.707E+04	0.0	0.412E+04	0.0

Table 14. Four Circular Orbit Daily Fluence Summary Using AE-8MAX (cont.)

Orbit Altitude - 2250 n.ml. Accumulation Time - 48 Hrs. Sampling Interval - 60 s Units for Daily Fluence -e/cm²-day

Energy (MeV)		Daily Fluence 0° Inclination		Daily Fluence 30° Inclination		Daily Fluence 60° Inclination		Daily Fluence 90° Inclination	
E1	E2	*E1	E1-E2	*E1	E1-E2	*E1	E1-E2	*E1	E1-E2
0.00	0.25	0.241E+14	0.193E+14	0.159E+14	0.132E+14	0.814E+13	0.677E+13	0.687E+13	0.571E+13
0.25	0.50	0.476E+13	0.432E+13	0.270E+13	0.245E+13	0.137E+13	0.123E+13	0.116E+13	0.105E+13
0.50	0.75	0.444E+12	0.313E+12	0.249E+12	0.191E+12	0.138E+12	0.101E+12	0.115E+12	0.847E+11
0.75	1.00	0.130E+12	0.718E+11	0.586E+11	0.340E+11	0.372E+11	0.199E+11	0.303E+11	0.165E+11
1.00	1.25	0.527E+11	0.214E+11	0.246E+11	0.928E+10	0.173E+11	0.629E+10	0.138E+11	0.515E+10
1.25	1.50	0.373E+11	0.136E+11	0.154E+11	0.577E+10	0.110E+11	0.398E+10	0.871E+10	0.318E+10
1.50	1.75	0.237E+11	0.768E+10	0.958E+10	0.324E+10	0.702E+10	0.237E+10	0.552E+10	0.187E+10
1.75	2.00	0.160E+11	0.518E+10	0.674E+10	0.214E+10	0.465E+10	0.156E+10	0.365E+10	0.123E+10
2.00	2.25	0.108E+11	0.352E+10	0.420E+10	0.142E+10	0.309E+10	0.103E+10	0.242E+10	0.811E+09
2.25	2.50	0.728E+10	0.237E+10	0.278E+10	0.937E+09	0.206E+10	0.683E+09	0.161E+10	0.537E+09
2.50	2.75	0.451E+10	0.309E+10	0.184E+10	0.116E+10	0.138E+10	0.756E+09	0.107E+10	0.244E+09
2.75	3.00	0.182E+10	0.114E+10	0.683E+09	0.430E+09	0.622E+09	0.320E+09	0.463E+09	0.117E+09
3.00	3.25	0.675E+09	0.476E+09	0.253E+09	0.177E+09	0.301E+09	0.155E+09	0.214E+09	0.473E+08
3.25	3.50	0.199E+09	0.140E+09	0.767E+08	0.533E+08	0.146E+09	0.673E+08	0.969E+08	0.236E+08
3.50	3.75	0.586E+08	0.413E+08	0.233E+08	0.162E+08	0.787E+08	0.361E+08	0.497E+08	0.117E+08
3.75	4.00	0.173E+08	0.122E+08	0.714E+07	0.494E+07	0.425E+08	0.186E+08	0.261E+08	0.675E+07
4.00	4.25	0.513E+07	0.363E+07	0.220E+07	0.155E+07	0.239E+08	0.111E+08	0.144E+08	0.361E+07
4.25	4.50	0.149E+07	0.106E+07	0.644E+06	0.466E+06	0.129E+08	0.583E+07	0.766E+07	0.199E+07
4.50	4.75	0.436E+06	0.316E+06	0.178E+06	0.138E+06	0.703E+07	0.332E+07	0.415E+07	0.100E+07
4.75	5.00	0.119E+06	0.0	0.405E+05	0.404E+05	0.370E+07	0.170E+07	0.217E+07	0.601E+06
5.00	5.25	0.0	0.0	0.152E+03	0.0	0.200E+07	0.103E+07	0.117E+07	0.287E+06
5.25	5.50	0.0	0.0	0.0	0.0	0.973E+06	0.493E+06	0.565E+06	0.149E+06
5.50	5.75	0.0	0.0	0.0	0.0	0.481E+06	0.259E+06	0.278E+06	0.702E+05
5.75	6.00	0.0	0.0	0.0	0.0	0.222E+06	0.121E+06	0.129E+06	0.339E+05
6.00	6.25	0.0	0.0	0.0	0.0	0.101E+06	0.591E+05	0.585E+05	0.151E+05
6.25	6.50	0.0	0.0	0.0	0.0	0.421E+05	0.264E+05	0.246E+05	0.723E+04
6.50	6.75	0.0	0.0	0.0	0.0	0.157E+05	0.115E+05	0.950E+04	0.0
6.75	7.00	0.0	0.0	0.0	0.0	0.417E+04	0.0	0.227E+04	0.0

Table 14. Four Circular Orbit Daily Fluence Summary Using AE-8MAX (cont.)

Orbit Altitude - 2000 n.mi.   Accumulation Time - 36 Hrs.   Sampling Interval - 30 s   Units for Daily Fluence -e/cm²-day

Energy (MeV)		Daily Fluence 0° Inclination		Daily Fluence 30° Inclination		Daily Fluence 60° Inclination		Daily Fluence 90° Inclination	
E1	E2	*E1	E1-E2	*E1	E1-E2	*E1	E1-E2	*E1	E1-E2
0.00	0.25	0.363E+14	0.293E+14	0.211E+14	0.176E+14	0.110E+14	0.912E+13	0.926E+13	0.770E+13
0.25	0.50	0.693E+13	0.628E+13	0.353E+13	0.320E+13	0.184E+13	0.165E+13	0.156E+13	0.140E+13
0.50	0.75	0.650E+12	0.543E+12	0.336E+12	0.288E+12	0.191E+12	0.155E+12	0.158E+12	0.130E+12
0.75	1.00	0.108E+12	0.701E+11	0.475E+11	0.322E+11	0.363E+11	0.209E+11	0.282E+11	0.169E+11
1.00	1.25	0.377E+11	0.152E+11	0.152E+11	0.629E+10	0.154E+11	0.577E+10	0.113E+11	0.435E+10
1.25	1.50	0.224E+11	0.907E+10	0.895E+10	0.368E+10	0.959E+10	0.355E+10	0.696E+10	0.264E+10
1.50	1.75	0.134E+11	0.515E+10	0.527E+10	0.210E+10	0.603E+10	0.221E+10	0.432E+10	0.161E+10
1.75	2.00	0.822E+10	0.315E+10	0.317E+10	0.125E+10	0.382E+10	0.139E+10	0.271E+10	0.990E+09
2.00	2.25	0.507E+10	0.196E+10	0.192E+10	0.750E+09	0.244E+10	0.864E+09	0.171E+10	0.615E+09
2.25	2.50	0.311E+10	0.120E+10	0.117E+10	0.456E+09	0.157E+10	0.553E+09	0.105E+10	0.392E+09
2.50	2.75	0.191E+10	0.122E+10	0.714E+09	0.450E+09	0.102E+10	0.475E+09	0.701E+09	0.344E+09
2.75	3.00	0.691E+09	0.441E+09	0.264E+09	0.165E+09	0.544E+09	0.236E+09	0.357E+09	0.162E+09
3.00	3.25	0.251E+09	0.164E+09	0.984E+08	0.629E+08	0.309E+09	0.129E+09	0.195E+09	0.650E+08
3.25	3.50	0.861E+08	0.565E+08	0.355E+08	0.223E+08	0.179E+09	0.716E+08	0.110E+09	0.452E+08
3.50	3.75	0.297E+08	0.194E+08	0.132E+08	0.810E+07	0.107E+09	0.462E+08	0.648E+08	0.281E+08
3.75	4.00	0.102E+08	0.669E+07	0.511E+07	0.302E+07	0.613E+08	0.258E+08	0.366E+08	0.155E+08
4.00	4.25	0.353E+07	0.254E+07	0.209E+07	0.128E+07	0.355E+08	0.162E+08	0.211E+08	0.876E+07
4.25	4.50	0.996E+06	0.720E+06	0.808E+06	0.465E+06	0.193E+08	0.868E+07	0.115E+08	0.516E+07
4.50	4.75	0.276E+06	0.220E+06	0.344E+06	0.204E+06	0.106E+08	0.501E+07	0.631E+07	0.257E+07
4.75	5.00	0.554E+05	0.0	0.140E+06	0.721E+05	0.558E+07	0.255E+07	0.333E+07	0.151E+07
5.00	5.25	0.0	0.0	0.679E+05	0.274E+05	0.303E+07	0.156E+07	0.182E+07	0.631E+06
5.25	5.50	0.0	0.0	0.405E+05	0.166E+05	0.147E+07	0.745E+06	0.888E+06	0.447E+06
5.50	5.75	0.0	0.0	0.239E+05	0.112E+05	0.725E+06	0.390E+06	0.442E+06	0.236E+06
5.75	6.00	0.0	0.0	0.127E+05	0.686E+04	0.334E+06	0.181E+06	0.205E+06	0.110E+06
6.00	6.25	0.0	0.0	0.587E+04	0.374E+04	0.154E+06	0.891E+05	0.955E+05	0.550E+05
6.25	6.50	0.0	0.0	0.213E+04	0.122E+04	0.648E+05	0.387E+05	0.405E+05	0.243E+05
6.50	6.75	0.0	0.0	0.914E+03	0.666E+03	0.261E+05	0.170E+05	0.161E+05	0.103E+05
6.75	7.00	0.0	0.0	0.248E+03	0.0	0.914E+04	0.0	0.586E+04	0.0

Table 14. Four Circular Orbit Daily Fluence Summary Using AE-8MAX (cont.)

Orbit Altitude - 2500 n.mi.   Accumulation Time - 48 Hrs.   Sampling Interval - 60 s   Units for Daily Fluence -e/cm²-day

Energy (MeV)		Daily Fluence 0° Inclination		Daily Fluence 30° Inclination		Daily Fluence 60° Inclination		Daily Fluence 90° Inclination	
E1	E2	*E1	E1-E2	*E1	E1-E2	*E1	E1-E2	*E1	E1-E2
0.0	0.25	0.397E+14	0.322E+14	0.219E+14	0.183E+14	0.115E+14	0.957E+13	0.969E+13	0.809E+13
0.25	0.50	0.753E+13	0.681E+13	0.358E+13	0.323E+13	0.190E+13	0.169E+13	0.161E+13	0.144E+13
0.50	0.75	0.722E+12	0.631E+12	0.349E+12	0.308E+12	0.205E+12	0.171E+12	0.169E+12	0.143E+12
0.75	1.00	0.917E+11	0.651E+11	0.401E+11	0.292E+11	0.347E+11	0.203E+11	0.262E+11	0.161E+11
1.00	1.25	0.266E+11	0.113E+11	0.110E+11	0.471E+10	0.144E+11	0.539E+10	0.101E+11	0.365E+10
1.25	1.50	0.154E+11	0.649E+10	0.624E+10	0.266E+10	0.900E+10	0.331E+10	0.621E+10	0.214E+10
1.50	1.75	0.889E+10	0.387E+10	0.358E+10	0.157E+10	0.569E+10	0.213E+10	0.386E+10	0.148E+10
1.75	2.00	0.502E+10	0.217E+10	0.201E+10	0.870E+09	0.356E+10	0.131E+10	0.238E+10	0.897E+09
2.00	2.25	0.284E+10	0.118E+10	0.114E+10	0.470E+09	0.225E+10	0.790E+09	0.149E+10	0.533E+09
2.25	2.50	0.167E+10	0.689E+09	0.674E+09	0.276E+09	0.146E+10	0.506E+09	0.952E+09	0.339E+09
2.50	2.75	0.978E+09	0.617E+09	0.398E+09	0.240E+09	0.951E+09	0.398E+09	0.614E+09	0.267E+09
2.75	3.00	0.360E+09	0.227E+09	0.158E+09	0.925E+08	0.553E+09	0.220E+09	0.347E+09	0.142E+09
3.00	3.25	0.133E+09	0.837E+08	0.657E+08	0.370E+08	0.332E+09	0.131E+09	0.205E+09	0.824E+08
3.25	3.50	0.493E+08	0.310E+08	0.266E+08	0.152E+08	0.201E+09	0.776E+08	0.123E+09	0.478E+08
3.50	3.75	0.183E+08	0.115E+08	0.134E+08	0.670E+07	0.123E+09	0.522E+08	0.747E+08	0.316E+08
3.75	4.00	0.681E+07	0.428E+07	0.671E+07	0.312E+07	0.711E+08	0.297E+08	0.431E+08	0.180E+08
4.00	4.25	0.254E+07	0.185E+07	0.359E+07	0.171E+07	0.414E+08	0.188E+08	0.252E+08	0.114E+08
4.25	4.50	0.682E+06	0.498E+06	0.188E+07	0.819E+06	0.226E+08	0.101E+08	0.138E+08	0.415E+07
4.50	4.75	0.184E+06	0.0	0.166E+07	0.459E+06	0.124E+08	0.586E+07	0.761E+07	0.257E+07
4.75	5.00	0.0	0.0	0.597E+06	0.230E+06	0.655E+07	0.299E+07	0.404E+07	0.182E+07
5.00	5.25	0.0	0.0	0.367E+06	0.155E+06	0.356E+07	0.183E+07	0.222E+07	0.113E+07
5.25	5.50	0.0	0.0	0.211E+06	0.892E+05	0.173E+07	0.872E+06	0.109E+07	0.544E+06
5.50	5.75	0.0	0.0	0.122E+06	0.584E+05	0.854E+06	0.459E+06	0.543E+06	0.289E+06
5.75	6.00	0.0	0.0	0.638E+05	0.316E+05	0.395E+06	0.213E+06	0.253E+06	0.135E+06
6.00	6.25	0.0	0.0	0.322E+05	0.184E+05	0.182E+06	0.105E+06	0.118E+06	0.676E+05
6.25	6.50	0.0	0.0	0.139E+05	0.794E+04	0.775E+05	0.465E+05	0.505E+05	0.200E+05
6.50	6.75	0.0	0.0	0.592E+04	0.395E+04	0.310E+05	0.194E+05	0.205E+05	0.125E+05
6.75	7.00	0.0	0.0	0.197E+04	0.0	0.116E+05	0.0	0.763E+04	0.0

Table 14. Four Circular Orbit Daily Fluence Summary Using AE-8MAX (cont.)

Orbit Altitude - 2750 n.mi.   Accumulation Time - 48 Hrs.   Sampling Interval - 60 s   Units for Daily Fluence -e/cm²-day

Energy (MeV)		Daily Fluence 0° Inclination		Daily Fluence 30° Inclination		Daily Fluence 60° Inclination		Daily Fluence 90° Inclination	
E1	E2	*E1	E1-E2	*E1	E1-E2	*E1	E1-E2	*E1	E1-E2
0.0	0.25	0.392E+14	0.325E+14	0.211E+14	0.180E+14	0.110E+14	0.938E+13	0.932E+13	0.792E+13
0.25	0.50	0.673E+13	0.602E+13	0.310E+13	0.277E+13	0.166E+13	0.146E+13	0.140E+13	0.124E+13
0.50	0.75	0.709E+12	0.650E+12	0.323E+12	0.294E+12	0.200E+12	0.167E+12	0.162E+12	0.135E+12
0.75	1.00	0.585E+11	0.479E+11	0.289E+11	0.224E+11	0.332E+11	0.184E+11	0.235E+11	0.135E+11
1.00	1.25	0.106E+11	0.531E+10	0.655E+10	0.294E+11	0.148E+11	0.545E+10	0.955E+10	0.360E+10
1.25	1.50	0.527E+10	0.264E+10	0.360E+10	0.155E+10	0.933E+10	0.334E+10	0.595E+10	0.217E+10
1.50	1.75	0.264E+10	0.139E+10	0.205E+10	0.080E+09	0.599E+10	0.217E+10	0.378E+10	0.126E+10
1.75	2.00	0.125E+10	0.658E+09	0.117E+10	0.482E+09	0.382E+10	0.136E+10	0.240E+10	0.860E+09
2.00	2.25	0.593E+09	0.281E+09	0.651E+09	0.266E+09	0.246E+10	0.841E+09	0.154E+10	0.526E+09
2.25	2.50	0.312E+09	0.148E+09	0.424E+09	0.160E+09	0.162E+10	0.547E+09	0.101E+10	0.342E+09
2.50	2.75	0.164E+09	0.983E+08	0.265E+09	0.108E+09	0.107E+10	0.405E+09	0.668E+09	0.254E+09
2.75	3.00	0.660E+08	0.395E+08	0.157E+09	0.602E+08	0.670E+09	0.249E+09	0.417E+09	0.154E+09
3.00	3.25	0.265E+08	0.153E+08	0.965E+08	0.362E+08	0.421E+09	0.160E+09	0.262E+09	0.990E+08
3.25	3.50	0.112E+08	0.648E+07	0.603E+08	0.220E+08	0.261E+09	0.983E+08	0.163E+09	0.611E+08
3.50	3.75	0.476E+07	0.274E+07	0.304E+08	0.142E+08	0.163E+09	0.681E+08	0.598E+08	0.422E+08
3.75	4.00	0.201E+07	0.116E+07	0.241E+08	0.881E+07	0.946E+08	0.392E+08	0.353E+08	0.245E+08
4.00	4.25	0.853E+06	0.549E+06	0.153E+08	0.608E+07	0.554E+08	0.250E+08	0.195E+08	0.156E+08
4.25	4.50	0.304E+06	0.190E+06	0.922E+07	0.362E+07	0.304E+08	0.136E+08	0.109E+08	0.663E+07
4.50	4.75	0.114E+06	0.0	0.561E+07	0.220E+07	0.168E+08	0.794E+07	0.584E+07	0.507E+07
4.75	5.00	0.0	0.0	0.341E+07	0.128E+07	0.886E+07	0.403E+07	0.323E+07	0.261E+07
5.00	5.25	0.0	0.0	0.213E+07	0.956E+06	0.483E+07	0.248E+07	0.160E+07	0.163E+07
5.25	5.50	0.0	0.0	0.117E+07	0.519E+06	0.236E+07	0.118E+07	0.810E+06	0.790E+06
5.50	5.75	0.0	0.0	0.654E+06	0.321E+06	0.118E+07	0.630E+06	0.381E+06	0.429E+06
5.75	6.00	0.0	0.0	0.333E+06	0.163E+06	0.547E+06	0.291E+06	0.180E+06	0.201E+06
6.00	6.25	0.0	0.0	0.170E+06	0.951E+05	0.255E+06	0.146E+06	0.777E+05	0.103E+06
6.25	6.50	0.0	0.0	0.750E+05	0.428E+05	0.109E+06	0.642E+05	0.322E+05	0.455E+05
6.50	6.75	0.0	0.0	0.322E+05	0.191E+05	0.451E+05	0.286E+05	0.121E+05	0.201E+05
6.75	7.00	0.0	0.0	0.131E+05	0.130E+05	0.165E+05	0.153E+05	0.572E+03	0.115E+05
7.00		0.0	0.0	0.128E+03	0.128E+03	0.112E+04	0.112E+04		0.572E+03

Table 14. Four Circular Orbit Daily Fluence Summary Using AE-8MAX (cont.)

Orbit Altitude - 3000 n.ml.   Accumulation Time - 48 Hrs.   Sampling Interval - 60 s   Units for Daily Fluence -e/cm²-day

Energy (MeV)		Daily Fluence 0° Inclination		Daily Fluence 30° Inclination		Daily Fluence 60° Inclination		Daily Fluence 90° Inclination	
E1	E2	*E1	E1-E2	*E1	E1-E2	*E1	E1-E2	*E1	E1-E2
0.0	0.25	0.404E+14	0.330E+14	0.220E+14	0.185E+14	0.115E+14	0.967E+13	0.971E+13	0.817E+13
0.25	0.50	0.742E+13	0.667E+13	0.344E+13	0.309E+13	0.183E+13	0.162E+13	0.155E+13	0.136E+13
0.50	0.75	0.752E+12	0.678E+12	0.349E+12	0.315E+12	0.209E+12	0.176E+12	0.171E+12	0.147E+12
0.75	1.00	0.740E+11	0.571E+11	0.335E+11	0.257E+11	0.334E+11	0.193E+11	0.245E+11	0.151E+11
1.00	1.25	0.169E+11	0.767E+10	0.778E+10	0.350E+10	0.140E+11	0.525E+10	0.946E+10	0.362E+10
1.25	1.50	0.924E+10	0.418E+10	0.428E+10	0.189E+10	0.877E+10	0.320E+10	0.584E+10	0.217E+10
1.50	1.75	0.506E+10	0.252E+10	0.239E+10	0.110E+10	0.557E+10	0.207E+10	0.367E+10	0.139E+10
1.75	2.00	0.254E+10	0.126E+10	0.129E+10	0.582E+09	0.350E+10	0.127E+10	0.228E+10	0.844E+09
2.00	2.25	0.128E+10	0.566E+09	0.706E+09	0.293E+09	0.222E+10	0.770E+09	0.143E+10	0.502E+09
2.25	2.50	0.711E+09	0.315E+09	0.413E+09	0.169E+09	0.145E+10	0.497E+09	0.930E+09	0.321E+09
2.50	2.75	0.396E+09	0.241E+09	0.244E+09	0.124E+09	0.958E+09	0.372E+09	0.608E+09	0.240E+09
2.75	3.00	0.155E+09	0.944E+08	0.120E+09	0.567E+08	0.586E+09	0.222E+09	0.369E+09	0.141E+09
3.00	3.25	0.608E+08	0.366E+08	0.629E+08	0.280E+08	0.364E+09	0.140E+09	0.228E+09	0.876E+08
3.25	3.50	0.242E+08	0.146E+08	0.350E+08	0.146E+08	0.224E+09	0.851E+08	0.140E+09	0.532E+08
3.50	3.75	0.963E+07	0.579E+07	0.204E+08	0.826E+07	0.139E+09	0.584E+08	0.870E+08	0.363E+08
3.75	4.00	0.384E+07	0.231E+07	0.122E+08	0.473E+07	0.807E+08	0.335E+08	0.508E+08	0.209E+08
4.00	4.25	0.153E+07	0.112E+07	0.743E+07	0.308E+07	0.472E+08	0.214E+08	0.299E+08	0.134E+08
4.25	4.50	0.412E+06	0.296E+06	0.434E+07	0.174E+07	0.258E+08	0.116E+08	0.165E+08	0.733E+07
4.50	4.75	0.115E+06	0.0	0.261E+07	0.104E+07	0.143E+08	0.674E+07	0.915E+07	0.426E+07
4.75	5.00	0.0	0.0	0.157E+07	0.578E+06	0.752E+07	0.342E+07	0.439E+07	0.219E+07
5.00	5.25	0.0	0.0	0.990E+06	0.435E+06	0.410E+07	0.210E+07	0.270E+07	0.137E+07
5.25	5.50	0.0	0.0	0.554E+06	0.240E+06	0.200E+07	0.100E+07	0.133E+07	0.662E+06
5.50	5.75	0.0	0.0	0.314E+06	0.152E+06	0.995E+06	0.534E+06	0.671E+06	0.355E+06
5.75	6.00	0.0	0.0	0.162E+06	0.795E+05	0.461E+06	0.246E+06	0.315E+06	0.167E+06
6.00	6.25	0.0	0.0	0.829E+05	0.466E+05	0.215E+06	0.123E+06	0.148E+06	0.847E+05
6.25	6.50	0.0	0.0	0.363E+05	0.206E+05	0.919E+05	0.549E+05	0.636E+05	0.375E+05
6.50	6.75	0.0	0.0	0.157E+05	0.915E+04	0.370E+05	0.232E+05	0.260E+05	0.161E+05
6.75	7.00	0.0	0.0	0.655E+04	0.0	0.138E+05	0.136E+05	0.990E+04	0.571E+04
7.00		0.0	0.0	0.0	0.0	0.194E+03	0.194E+03	0.193E+03	0.193E+03

Table 14. Four Circular Orbit Daily Fluence Summary Using AE-8MAX (cont.)

Orbit Altitude - 3500 n.mi. Accumulation Time - 48 Hrs. Sampling Interval - 60 s Units for Daily Fluence -e/cm²-day

Energy (MeV)		Daily Fluence 0° Inclination		Daily Fluence 30° Inclination		Daily Fluence 60° Inclination		Daily Fluence 90° Inclination	
E1	E2	*E1	E1-E2	*E1	E1-E2	*E1	E1-E2	*E1	E1-E2
0.0	0.25	0.295E+14	0.259E+14	0.169E+14	0.150E+14	0.910E+13	0.801E+13	0.765E+13	0.674E+13
0.25	0.50	0.365E+13	0.331E+13	0.152E+13	0.169E+13	0.109E+13	0.926E+12	0.904E+12	0.776E+12
0.50	0.75	0.344E+12	0.322E+12	0.231E+12	0.194E+12	0.163E+12	0.120E+12	0.127E+12	0.969E+11
0.75	1.00	0.224E+11	0.191E+11	0.365E+11	0.218E+11	0.425E+11	0.201E+11	0.303E+11	0.148E+11
1.00	1.25	0.336E+10	0.206E+10	0.148E+11	0.512E+10	0.224E+11	0.796E+10	0.154E+11	0.543E+10
1.25	1.50	0.170E+10	0.797E+09	0.566E+10	0.321E+10	0.145E+11	0.501E+10	0.100E+11	0.342E+10
1.50	1.75	0.504E+09	0.275E+09	0.645E+10	0.220E+10	0.944E+10	0.331E+10	0.659E+10	0.229E+10
1.75	2.00	0.229E+09	0.124E+09	0.425E+10	0.142E+10	0.613E+10	0.213E+10	0.430E+10	0.148E+10
2.00	2.25	0.104E+09	0.564E+08	0.282E+10	0.942E+09	0.400E+10	0.136E+10	0.282E+10	0.952E+09
2.25	2.50	0.477E+08	0.258E+08	0.188E+10	0.618E+09	0.264E+10	0.889E+09	0.186E+10	0.623E+09
2.50	2.75	0.219E+08	0.154E+08	0.126E+10	0.449E+09	0.175E+10	0.646E+09	0.124E+10	0.456E+09
2.75	3.00	0.651E+07	0.457E+07	0.815E+09	0.286E+09	0.110E+10	0.404E+09	0.784E+09	0.266E+09
3.00	3.25	0.128E+07	0.663E+06	0.529E+09	0.192E+09	0.699E+09	0.263E+09	0.499E+09	0.187E+09
3.25	3.50	0.373E+06	0.391E+06	0.338E+09	0.121E+09	0.436E+09	0.163E+09	0.312E+09	0.116E+09
3.50	3.75	0.482E+06	0.214E+06	0.216E+09	0.839E+08	0.273E+09	0.113E+09	0.196E+09	0.802E+08
3.75	4.00	0.268E+06	0.788E+05	0.133E+09	0.509E+08	0.160E+09	0.655E+08	0.116E+09	0.469E+08
4.00	4.25	0.189E+06	0.554E+05	0.817E+08	0.342E+08	0.948E+08	0.421E+08	0.690E+08	0.304E+08
4.25	4.50	0.134E+06	0.290E+05	0.475E+08	0.197E+08	0.527E+08	0.231E+08	0.386E+08	0.166E+08
4.50	4.75	0.945E+05	0.0	0.278E+08	0.119E+08	0.295E+08	0.137E+08	0.218E+08	0.958E+07
4.75	5.00	0.0	0.0	0.158E+08	0.657E+07	0.158E+08	0.702E+07	0.118E+08	0.519E+07
5.00	5.25	0.0	0.0	0.926E+07	0.437E+07	0.880E+07	0.440E+07	0.665E+07	0.330E+07
5.25	5.50	0.0	0.0	0.489E+07	0.226E+07	0.440E+07	0.214E+07	0.336E+07	0.162E+07
5.50	5.75	0.0	0.0	0.264E+07	0.135E+07	0.226E+07	0.119E+07	0.174E+07	0.831E+06
5.75	6.00	0.0	0.0	0.129E+07	0.655E+06	0.107E+07	0.558E+06	0.831E+06	0.431E+06
6.00	6.25	0.0	0.0	0.636E+06	0.355E+06	0.514E+06	0.291E+06	0.400E+06	0.226E+06
6.25	6.50	0.0	0.0	0.280E+06	0.159E+06	0.223E+06	0.128E+06	0.174E+06	0.555E+05
6.50	6.75	0.0	0.0	0.122E+06	0.786E+05	0.951E+05	0.612E+05	0.746E+05	0.481E+05
6.75	7.00	0.0	0.0	0.431E+05	0.329E+05	0.339E+05	0.254E+05	0.265E+05	0.192E+05
7.00		0.0	0.0	0.102E+05	0.102E+05	0.851E+04	0.851E+04	0.671E+04	0.671E+04

Table 14. Four Circular Orbit Daily Fluence Summary Using AE-8MAX (cont.)

Orbit Altitude - 4000 n.ml. Accumulation Time - 48 Hrs. Sampling Interval - 60 s Units for Daily Fluence -e/cm²-day

Energy (MeV)		Daily Fluence 0° Inclination		Daily Fluence 30° Inclination		Daily Fluence 60° Inclination		Daily Fluence 90° Inclination	
E1	E2	*E1	E1-E2	*E1	E1-E2	*E1	E1-E2	*E1	E1-E2
0.00	0.25	0.340E+14	0.290E+14	0.191E+14	0.167E+14	0.101E+14	0.873E+13	0.846E+13	0.735E+13
0.25	0.50	0.497E+13	0.448E+13	0.243E+13	0.217E+13	0.133E+13	0.116E+13	0.112E+13	0.978E+12
0.50	0.75	0.490E+12	0.457E+12	0.259E+12	0.231E+12	0.173E+12	0.137E+12	0.137E+12	0.112E+12
0.75	1.00	0.333E+11	0.284E+11	0.276E+11	0.191E+11	0.359E+11	0.180E+11	0.249E+11	0.132E+11
1.00	1.25	0.467E+10	0.288E+10	0.847E+10	0.329E+10	0.179E+11	0.645E+10	0.117E+11	0.425E+10
1.25	1.50	0.198E+10	0.117E+10	0.518E+10	0.188E+10	0.114E+11	0.400E+10	0.748E+10	0.262E+10
1.50	1.75	0.808E+09	0.418E+09	0.330E+10	0.116E+10	0.742E+10	0.261E+10	0.486E+10	0.171E+10
1.75	2.00	0.340E+09	0.202E+09	0.214E+10	0.732E+09	0.481E+10	0.168E+10	0.316E+10	0.109E+10
2.00	2.25	0.188E+09	0.968E+08	0.141E+10	0.486E+09	0.313E+10	0.106E+10	0.206E+10	0.693E+09
2.25	2.50	0.915E+08	0.471E+08	0.924E+09	0.312E+09	0.207E+10	0.695E+09	0.137E+10	0.456E+09
2.50	2.75	0.445E+08	0.285E+08	0.612E+09	0.215E+09	0.137E+10	0.510E+09	0.905E+09	0.210E+09
2.75	3.00	0.160E+08	0.102E+08	0.367E+09	0.136E+09	0.865E+09	0.318E+09	0.574E+09	0.176E+09
3.00	3.25	0.574E+07	0.304E+07	0.261E+09	0.922E+08	0.546E+09	0.206E+09	0.364E+09	0.847E+08
3.25	3.50	0.270E+07	0.142E+07	0.169E+09	0.590E+08	0.340E+09	0.128E+09	0.228E+09	0.588E+08
3.50	3.75	0.128E+07	0.673E+06	0.110E+09	0.410E+08	0.213E+09	0.884E+08	0.143E+09	0.343E+08
3.75	4.00	0.604E+06	0.316E+06	0.689E+08	0.255E+08	0.124E+09	0.512E+08	0.841E+08	0.221E+08
4.00	4.25	0.288E+06	0.988E+05	0.434E+08	0.177E+08	0.732E+08	0.328E+08	0.499E+08	0.122E+08
4.25	4.50	0.189E+06	0.645E+05	0.257E+08	0.104E+08	0.404E+08	0.179E+08	0.278E+08	0.720E+07
4.50	4.75	0.124E+06	0.105E+06	0.153E+08	0.621E+07	0.225E+08	0.105E+08	0.156E+08	0.372E+07
4.75	5.00	0.195E+05	0.0	0.905E+07	0.358E+07	0.119E+08	0.537E+07	0.839E+07	0.234E+07
5.00	5.25	0.0	0.0	0.547E+07	0.257E+07	0.657E+07	0.333E+07	0.467E+07	0.114E+07
5.25	5.50	0.0	0.0	0.291E+07	0.134E+07	0.324E+07	0.160E+07	0.233E+07	0.629E+06
5.50	5.75	0.0	0.0	0.156E+07	0.790E+06	0.164E+07	0.871E+06	0.119E+07	0.255E+06
5.75	6.00	0.0	0.0	0.772E+06	0.389E+06	0.771E+06	0.406E+06	0.565E+06	0.153E+06
6.00	6.25	0.0	0.0	0.383E+06	0.214E+06	0.364E+06	0.207E+06	0.270E+06	0.678E+05
6.25	6.50	0.0	0.0	0.169E+06	0.952E+05	0.157E+06	0.910E+05	0.117E+06	0.312E+05
6.50	6.75	0.0	0.0	0.741E+05	0.456E+05	0.664E+05	0.423E+05	0.492E+05	0.144E+05
6.75	7.00	0.0	0.0	0.285E+05	0.229E+05	0.241E+05	0.197E+05	0.179E+05	0.356E+04
7.00		0.0	0.0	0.557E+04	0.557E+04	0.443E+04	0.443E+04	0.356E+04	

Table 14. Four Circular Orbit Daily Fluence Summary Using AE-8MAX (cont.)

Orbit Altitude - 4500 n.mi.   Accumulation Time - 48 Hrs.   Sampling Interval - 60 s   Units for Daily Fluence -e/cm²-day

Energy (MeV)		Daily Fluence 0° Inclination		Daily Fluence 30° Inclination		Daily Fluence 60° Inclination		Daily Fluence 90° Inclination	
E1	E2	*E1	E1-E2	*E1	E1-E2	*E1	E1-E2	*E1	E1-E2
0.0	0.25	0.255E+14	0.226E+14	0.142E+14	0.127E+14	0.779E+13	0.692E+13	0.653E+13	0.581E+13
0.25	0.50	0.283E+13	0.251E+13	0.148E+13	0.125E+13	0.874E+12	0.708E+12	0.719E+12	0.589E+12
0.50	0.75	0.320E+12	0.291E+12	0.231E+12	0.176E+12	0.166E+12	0.113E+12	0.130E+12	0.905E+11
0.75	1.00	0.267E+11	0.243E+11	0.554E+11	0.293E+11	0.532E+11	0.245E+11	0.393E+11	0.165E+11
1.00	1.25	0.440E+10	0.245E+10	0.260E+11	0.854E+10	0.287E+11	0.100E+11	0.208E+11	0.716E+10
1.25	1.50	0.195E+10	0.107E+10	0.175E+11	0.563E+10	0.187E+11	0.640E+10	0.136E+11	0.460E+10
1.50	1.75	0.883E+09	0.519E+09	0.119E+11	0.403E+10	0.123E+11	0.429E+10	0.902E+10	0.312E+10
1.75	2.00	0.364E+09	0.213E+09	0.783E+10	0.263E+10	0.801E+10	0.277E+10	0.589E+10	0.202E+10
2.00	2.25	0.151E+09	0.894E+08	0.520E+10	0.175E+10	0.524E+10	0.178E+10	0.387E+10	0.131E+10
2.25	2.50	0.617E+08	0.365E+08	0.345E+10	0.115E+10	0.346E+10	0.116E+10	0.256E+10	0.857E+09
2.50	2.75	0.253E+08	0.179E+08	0.231E+10	0.831E+09	0.230E+10	0.844E+09	0.171E+10	0.624E+09
2.75	3.00	0.740E+07	0.520E+07	0.148E+10	0.525E+09	0.145E+10	0.530E+09	0.108E+10	0.393E+09
3.00	3.25	0.220E+07	0.194E+07	0.951E+09	0.348E+09	0.924E+09	0.346E+09	0.690E+09	0.257E+09
3.25	3.50	0.148E+07	0.875E+06	0.603E+09	0.219E+09	0.578E+09	0.215E+09	0.432E+09	0.160E+09
3.50	3.75	0.601E+06	0.351E+06	0.384E+09	0.149E+09	0.362E+09	0.148E+09	0.272E+09	0.111E+09
3.75	4.00	0.250E+06	0.614E+05	0.235E+09	0.901E+08	0.214E+09	0.866E+08	0.162E+09	0.645E+08
4.00	4.25	0.188E+06	0.462E+05	0.145E+09	0.600E+08	0.127E+09	0.561E+08	0.966E+08	0.422E+08
4.25	4.50	0.142E+06	0.351E+05	0.851E+08	0.348E+08	0.714E+08	0.311E+08	0.544E+08	0.235E+08
4.50	4.75	0.107E+06	0.0	0.503E+08	0.211E+08	0.403E+08	0.185E+08	0.309E+08	0.140E+08
4.75	5.00	0.0	0.0	0.253E+08	0.117E+08	0.218E+08	0.954E+07	0.169E+08	0.731E+07
5.00	5.25	0.0	0.0	0.175E+08	0.807E+07	0.123E+08	0.605E+07	0.954E+07	0.462E+07
5.25	5.50	0.0	0.0	0.947E+07	0.424E+07	0.620E+07	0.297E+07	0.488E+07	0.222E+07
5.50	5.75	0.0	0.0	0.523E+07	0.261E+07	0.323E+07	0.169E+07	0.256E+07	0.133E+07
5.75	6.00	0.0	0.0	0.261E+07	0.130E+07	0.154E+07	0.798E+06	0.123E+07	0.632E+06
6.00	6.25	0.0	0.0	0.132E+07	0.739E+06	0.746E+06	0.422E+06	0.596E+06	0.337E+06
6.25	6.50	0.0	0.0	0.580E+06	0.327E+06	0.324E+06	0.185E+06	0.259E+06	0.148E+06
6.50	6.75	0.0	0.0	0.253E+06	0.166E+06	0.140E+06	0.903E+05	0.112E+06	0.721E+05
6.75	7.00	0.0	0.0	0.867E+05	0.607E+05	0.493E+05	0.351E+05	0.395E+05	0.281E+05
7.00		0.0	0.0	0.260E+05	0.260E+05	0.142E+05	0.142E+05	0.114E+05	0.114E+05

Table 14. Four Circular Orbit Daily Fluence Summary Using AE-8MAX (cont.)

Orbit Altitude - 5000 n.mi. Accumulation Time - 96 Hrs. Sampling Interval - 120 s Units for Daily Fluence -e/cm²-day

Energy (MeV)		Daily Fluence 0° Inclination		Daily Fluence 30° Inclination		Daily Fluence 60° Inclination		Daily Fluence 90° Inclination	
E1	E2	*E1	E1-E2	*E1	E1-E2	*E1	E1-E2	*E1	E1-E2
0.0	0.25	0.206E+14	0.186E+14	0.112E+14	0.101E+14	0.630E+13	0.563E+13	0.524E+13	0.470E+13
0.25	0.50	0.195E+13	0.167E+13	0.104E+13	0.815E+12	0.665E+12	0.498E+12	0.536E+12	0.407E+12
0.50	0.75	0.230E+12	0.238E+12	0.229E+12	0.149E+12	0.167E+12	0.102E+12	0.130E+12	0.804E+11
0.75	1.00	0.419E+11	0.329E+11	0.798E+11	0.379E+11	0.657E+11	0.291E+11	0.498E+11	0.224E+11
1.00	1.25	0.895E+10	0.344E+10	0.419E+11	0.134E+11	0.366E+11	0.125E+11	0.275E+11	0.926E+10
1.25	1.50	0.552E+10	0.208E+10	0.285E+11	0.905E+10	0.241E+11	0.813E+10	0.182E+11	0.606E+10
1.50	1.75	0.344E+10	0.158E+10	0.155E+11	0.656E+10	0.160E+11	0.554E+10	0.121E+11	0.418E+10
1.75	2.00	0.185E+10	0.836E+09	0.129E+11	0.432E+10	0.104E+11	0.359E+10	0.796E+10	0.272E+10
2.00	2.25	0.102E+10	0.510E+09	0.860E+10	0.288E+10	0.686E+10	0.233E+10	0.524E+10	0.178E+10
2.25	2.50	0.507E+09	0.251E+09	0.572E+10	0.190E+10	0.452E+10	0.152E+10	0.347E+10	0.116E+10
2.50	2.75	0.256E+09	0.142E+09	0.382E+10	0.138E+10	0.300E+10	0.110E+10	0.230E+10	0.642E+09
2.75	3.00	0.114E+09	0.622E+08	0.244E+10	0.873E+09	0.190E+10	0.691E+09	0.146E+10	0.572E+09
3.00	3.25	0.520E+08	0.306E+08	0.157E+10	0.580E+09	0.121E+10	0.453E+09	0.932E+09	0.348E+09
3.25	3.50	0.215E+08	0.124E+08	0.987E+09	0.362E+09	0.755E+09	0.281E+09	0.584E+09	0.216E+09
3.50	3.75	0.904E+07	0.622E+07	0.625E+09	0.247E+09	0.474E+09	0.193E+09	0.368E+09	0.149E+09
3.75	4.00	0.282E+07	0.194E+07	0.377E+09	0.148E+09	0.281E+09	0.113E+09	0.215E+09	0.875E+08
4.00	4.25	0.883E+06	0.529E+06	0.230E+09	0.975E+08	0.168E+09	0.734E+08	0.131E+09	0.570E+08
4.25	4.50	0.354E+06	0.176E+06	0.132E+09	0.555E+08	0.944E+08	0.408E+08	0.741E+08	0.319E+08
4.50	4.75	0.178E+06	0.816E+05	0.769E+08	0.338E+08	0.536E+08	0.244E+08	0.423E+08	0.191E+08
4.75	5.00	0.961E+05	0.0	0.431E+08	0.180E+08	0.292E+08	0.127E+08	0.232E+08	0.997E+07
5.00	5.25	0.0	0.0	0.251E+08	0.119E+08	0.165E+08	0.807E+07	0.132E+08	0.643E+07
5.25	5.50	0.0	0.0	0.132E+08	0.605E+07	0.843E+07	0.399E+07	0.680E+07	0.320E+07
5.50	5.75	0.0	0.0	0.718E+07	0.367E+07	0.443E+07	0.230E+07	0.359E+07	0.186E+07
5.75	6.00	0.0	0.0	0.351E+07	0.178E+07	0.213E+07	0.109E+07	0.173E+07	0.867E+06
6.00	6.25	0.0	0.0	0.173E+07	0.974E+06	0.104E+07	0.585E+06	0.847E+06	0.477E+06
6.25	6.50	0.0	0.0	0.758E+06	0.427E+06	0.452E+06	0.256E+06	0.369E+06	0.209E+06
6.50	6.75	0.0	0.0	0.332E+06	0.216E+06	0.196E+06	0.127E+06	0.160E+06	0.104E+06
6.75	7.00	0.0	0.0	0.116E+06	0.804E+05	0.687E+05	0.475E+05	0.562E+05	0.389E+05
7.00				0.356E+05	0.356E+05	0.213E+05	0.213E+05	0.173E+05	0.173E+05

Table 14. Four Circular Orbit Daily Fluence Summary Using AE-8MAX (cont.)

Orbit Altitude - 5500 n.mi.   Accumulation Time - 96 Hrs.   Sampling Interval - 120 s   Units for Daily Fluence -e/cm²-day

Energy (MeV)		Daily Fluence 0° Inclination		Daily Fluence 30° Inclination		Daily Fluence 60° Inclination		Daily Fluence 90° Inclination	
E1	E2	*E1	E1-E2	*E1	E1-E2	*E1	E1-E2	*E1	E1-E2
0.0	0.25	0.109E+14	0.103E+14	0.661E+13	0.592E+13	0.398E+13	0.351E+13	0.326E+13	0.289E+13
0.25	0.50	0.685E+12	0.471E+12	0.651E+12	0.420E+12	0.470E+12	0.286E+12	0.370E+12	0.225E+12
0.50	0.75	0.214E+12	0.124E+12	0.271E+12	0.129E+12	0.184E+12	0.898E+11	0.145E+12	0.704E+11
0.75	1.00	0.902E+11	0.442E+11	0.142E+12	0.546E+11	0.945E+11	0.370E+11	0.746E+11	0.251E+11
1.00	1.25	0.460E+11	0.158E+11	0.874E+11	0.280E+11	0.575E+11	0.194E+11	0.455E+11	0.152E+11
1.25	1.50	0.302E+11	0.104E+11	0.595E+11	0.189E+11	0.381E+11	0.127E+11	0.303E+11	0.100E+11
1.50	1.75	0.198E+11	0.678E+10	0.405E+11	0.134E+11	0.254E+11	0.862E+10	0.203E+11	0.685E+10
1.75	2.00	0.130E+11	0.446E+10	0.271E+11	0.895E+10	0.168E+11	0.566E+10	0.135E+11	0.452E+10
2.00	2.25	0.857E+10	0.210E+10	0.162E+11	0.594E+10	0.111E+11	0.372E+10	0.895E+10	0.297E+10
2.25	2.50	0.547E+10	0.198E+10	0.122E+11	0.398E+10	0.743E+10	0.246E+10	0.598E+10	0.157E+10
2.50	2.75	0.345E+10	0.131E+10	0.824E+10	0.292E+10	0.496E+10	0.179E+10	0.400E+10	0.144E+10
2.75	3.00	0.218E+10	0.816E+09	0.532E+10	0.188E+10	0.318E+10	0.114E+10	0.256E+10	0.607E+09
3.00	3.25	0.136E+10	0.530E+09	0.344E+10	0.126E+10	0.204E+10	0.753E+09	0.165E+10	0.382E+09
3.25	3.50	0.832E+09	0.323E+09	0.218E+10	0.795E+09	0.128E+10	0.473E+09	0.104E+10	0.263E+09
3.50	3.75	0.509E+09	0.212E+09	0.139E+10	0.545E+09	0.811E+09	0.326E+09	0.658E+09	0.157E+09
3.75	4.00	0.309E+09	0.123E+09	0.841E+09	0.328E+09	0.485E+09	0.193E+09	0.395E+09	0.103E+09
4.00	4.25	0.174E+09	0.778E+08	0.513E+09	0.216E+09	0.292E+09	0.126E+09	0.239E+09	0.579E+08
4.25	4.50	0.967E+08	0.427E+08	0.297E+09	0.124E+09	0.166E+09	0.709E+08	0.136E+09	0.355E+08
4.50	4.75	0.540E+08	0.324E+08	0.173E+09	0.757E+08	0.950E+08	0.434E+08	0.780E+08	0.183E+08
4.75	5.00	0.216E+08	0.113E+08	0.974E+08	0.402E+08	0.516E+08	0.222E+08	0.426E+08	0.116E+08
5.00	5.25	0.103E+08	0.452E+07	0.572E+08	0.266E+08	0.293E+08	0.141E+08	0.243E+08	0.585E+07
5.25	5.50	0.577E+07	0.212E+07	0.306E+08	0.137E+08	0.153E+08	0.706E+07	0.127E+08	0.353E+07
5.50	5.75	0.365E+07	0.208E+07	0.169E+08	0.852E+07	0.821E+07	0.423E+07	0.686E+07	0.170E+07
5.75	6.00	0.157E+07	0.906E+06	0.838E+07	0.418E+07	0.398E+07	0.203E+07	0.334E+07	0.723E+06
6.00	6.25	0.665E+06	0.379E+06	0.420E+07	0.236E+07	0.195E+07	0.110E+07	0.164E+07	0.404E+06
6.25	6.50	0.286E+06	0.163E+06	0.185E+07	0.103E+07	0.854E+06	0.481E+06	0.718E+06	0.204E+06
6.50	6.75	0.123E+06	0.809E+05	0.811E+06	0.533E+06	0.373E+06	0.242E+06	0.314E+06	0.732E+05
6.75	7.00	0.424E+05	0.305E+05	0.277E+06	0.187E+06	0.130E+06	0.872E+05	0.110E+06	0.363E+05
7.00		0.119E+05	0.119E+05	0.906E+05	0.906E+05	0.433E+05	0.433E+05	0.363E+05	

Table 14. Four Circular Orbit Daily Fluence Summary Using AE-8MAX (cont.)

Orbit Altitude - 6000 n.mi.　　Accumulation Time - 96 Hrs.　　Sampling Interval - 120 s　　Units for Daily Fluence -e/cm²-day

Energy (MeV)		Daily Fluence 0° Inclination		Daily Fluence 30° Inclination		Daily Fluence 60° Inclination		Daily Fluence 90° Inclination	
E1	E2	*E1	E1-E2	*E1	E1-E2	*E1	E1-E2	*E1	E1-E2
0.0	0.25	0.155E+14	0.144E+14	0.863E+13	0.786E+13	0.499E+13	0.447E+13	0.413E+13	0.372E+13
0.25	0.50	0.114E+13	0.904E+12	0.777E+12	0.536E+12	0.522E+12	0.350E+12	0.413E+12	0.280E+12
0.50	0.75	0.233E+12	0.170E+12	0.241E+12	0.132E+12	0.172E+12	0.921E+11	0.134E+12	0.722E+11
0.75	1.00	0.630E+11	0.400E+11	0.109E+12	0.463E+11	0.797E+11	0.333E+11	0.617E+11	0.255E+11
1.00	1.25	0.223E+11	0.720E+10	0.626E+11	0.199E+11	0.463E+11	0.156E+11	0.357E+11	0.115E+11
1.25	1.50	0.151E+11	0.487E+10	0.427E+11	0.135E+11	0.307E+11	0.102E+11	0.238E+11	0.765E+10
1.50	1.75	0.102E+11	0.371E+10	0.292E+11	0.971E+10	0.205E+11	0.700E+10	0.160E+11	0.544E+10
1.75	2.00	0.648E+10	0.236E+10	0.195E+11	0.646E+10	0.135E+11	0.458E+10	0.106E+11	0.357E+10
2.00	2.25	0.413E+10	0.169E+10	0.130E+11	0.432E+10	0.888E+10	0.300E+10	0.698E+10	0.235E+10
2.25	2.50	0.243E+10	0.995E+09	0.872E+10	0.287E+10	0.391E+10	0.197E+10	0.463E+10	0.155E+10
2.50	2.75	0.144E+10	0.649E+09	0.585E+10	0.212E+10	0.248E+10	0.143E+10	0.302E+10	0.113E+10
2.75	3.00	0.788E+09	0.353E+09	0.373E+10	0.134E+10	0.158E+10	0.900E+09	0.196E+10	0.705E+09
3.00	3.25	0.435E+09	0.214E+09	0.239E+10	0.890E+09	0.986E+09	0.591E+09	0.125E+10	0.467E+09
3.25	3.50	0.222E+09	0.107E+09	0.150E+10	0.555E+09	0.619E+09	0.367E+09	0.782E+09	0.290E+09
3.50	3.75	0.115E+09	0.610E+08	0.948E+09	0.379E+09	0.252E+09	0.252E+09	0.491E+09	0.199E+09
3.75	4.00	0.539E+08	0.276E+08	0.569E+09	0.225E+09	0.367E+09	0.148E+09	0.293E+09	0.117E+09
4.00	4.25	0.263E+08	0.142E+08	0.344E+09	0.147E+09	0.220E+09	0.958E+08	0.176E+09	0.762E+08
4.25	4.50	0.122E+08	0.640E+07	0.197E+09	0.833E+08	0.124E+09	0.534E+08	0.994E+08	0.426E+08
4.50	4.75	0.577E+07	0.353E+07	0.114E+09	0.511E+08	0.704E+08	0.320E+08	0.568E+08	0.256E+08
4.75	5.00	0.224E+07	0.101E+07	0.630E+08	0.268E+08	0.385E+08	0.166E+08	0.312E+08	0.133E+08
5.00	5.25	0.124E+07	0.826E+06	0.362E+08	0.171E+08	0.219E+08	0.107E+08	0.179E+08	0.867E+07
5.25	5.50	0.413E+06	0.200E+06	0.151E+08	0.870E+07	0.112E+08	0.529E+07	0.921E+07	0.431E+07
5.50	5.75	0.213E+06	0.161E+06	0.104E+08	0.532E+07	0.594E+07	0.307E+07	0.489E+07	0.253E+07
5.75	6.00	0.518E+05	0.0	0.512E+07	0.258E+07	0.286E+07	0.146E+07	0.237E+07	0.121E+07
6.00	6.25	0.0	0.0	0.255E+07	0.143E+07	0.140E+07	0.788E+06	0.116E+07	0.652E+06
6.25	6.50	0.0	0.0	0.112E+07	0.628E+06	0.610E+06	0.345E+06	0.507E+06	0.286E+06
6.50	6.75	0.0	0.0	0.488E+06	0.321E+06	0.266E+06	0.172E+06	0.221E+06	0.143E+06
6.75	7.00	0.0	0.0	0.166E+06	0.115E+06	0.934E+05	0.630E+05	0.778E+05	0.523E+05
				0.511E+05	0.511E+05	0.305E+05	0.305E+05	0.255E+05	0.255E+05

Table 14. Four Circular Orbit Daily Fluence Summary Using AE-8MAX (cont.)

Orbit Altitude - 7000 n.mi.　　Accumulation Time - 96 Hrs.　　Sampling Interval - 120 s　　Units for Daily Fluence -e/cm²-day

Energy (MeV) E1	E2	Daily Fluence 0° Inclination *E1	E1-E2	Daily Fluence 30° Inclination *E1	E1-E2	Daily Fluence 60° Inclination *E1	E1-E2	Daily Fluence 90° Inclination *E1	E1-E2
0.0	0.25	0.562E+13	0.491E+13	0.532E+13	0.447E+13	0.324E+13	0.270E+13	0.261E+13	0.216E+13
0.25	0.50	0.702E+12	0.407E+12	0.657E+12	0.482E+12	0.539E+12	0.311E+12	0.429E+12	0.246E+12
0.50	0.75	0.295E+12	0.128E+12	0.376E+12	0.165E+12	0.228E+12	0.104E+12	0.183E+12	0.829E+11
0.75	1.00	0.167E+12	0.603E+11	0.210E+12	0.762E+11	0.124E+12	0.459E+11	0.999E+11	0.366E+11
1.00	1.25	0.107E+12	0.331E+11	0.134E+12	0.423E+11	0.779E+11	0.258E+11	0.631E+11	0.207E+11
1.25	1.50	0.741E+11	0.229E+11	0.919E+11	0.288E+11	0.522E+11	0.170E+11	0.424E+11	0.137E+11
1.50	1.75	0.512E+11	0.166E+11	0.631E+11	0.205E+11	0.351E+11	0.118E+11	0.287E+11	0.955E+10
1.75	2.00	0.346E+11	0.112E+11	0.425E+11	0.138E+11	0.233E+11	0.779E+10	0.191E+11	0.635E+10
2.00	2.25	0.234E+11	0.779E+10	0.287E+11	0.919E+10	0.155E+11	0.509E+10	0.127E+11	0.416E+10
2.25	2.50	0.156E+11	0.520E+10	0.195E+11	0.623E+10	0.104E+11	0.340E+10	0.858E+10	0.279E+10
2.50	2.75	0.104E+11	0.340E+10	0.133E+11	0.463E+10	0.704E+10	0.250E+10	0.579E+10	0.265E+10
2.75	3.00	0.703E+10	0.229E+10	0.869E+10	0.301E+10	0.454E+10	0.160E+10	0.375E+10	0.126E+10
3.00	3.25	0.474E+10	0.161E+10	0.568E+10	0.203E+10	0.294E+10	0.107E+10	0.243E+10	0.879E+09
3.25	3.50	0.313E+10	0.106E+10	0.366E+10	0.130E+10	0.187E+10	0.677E+09	0.155E+10	0.559E+09
3.50	3.75	0.206E+10	0.706E+09	0.235E+10	0.914E+09	0.119E+10	0.470E+09	0.990E+09	0.386E+09
3.75	4.00	0.863E+09	0.329E+09	0.144E+10	0.555E+09	0.723E+09	0.282E+09	0.601E+09	0.234E+09
4.00	4.25	0.565E+09	0.207E+09	0.886E+09	0.374E+09	0.441E+09	0.187E+09	0.368E+09	0.156E+09
4.25	4.50	0.357E+09	0.121E+09	0.512E+09	0.214E+09	0.254E+09	0.107E+09	0.212E+09	0.886E+08
4.50	4.75	0.236E+09	0.799E+08	0.298E+09	0.124E+09	0.147E+09	0.619E+08	0.123E+09	0.516E+08
4.75	5.00	0.156E+09	0.656E+08	0.173E+09	0.705E+08	0.852E+08	0.346E+08	0.719E+08	0.291E+08
5.00	5.25	0.905E+08	0.379E+08	0.103E+09	0.493E+08	0.505E+08	0.240E+08	0.428E+08	0.203E+08
5.25	5.50	0.526E+08	0.249E+08	0.536E+08	0.253E+08	0.265E+08	0.123E+08	0.226E+08	0.105E+08
5.50	5.75	0.277E+08	0.131E+08	0.264E+08	0.145E+08	0.142E+08	0.717E+07	0.121E+08	0.610E+07
5.75	6.00	0.146E+08	0.809E+07	0.139E+08	0.702E+07	0.700E+07	0.350E+07	0.598E+07	0.299E+07
6.00	6.25	0.650E+07	0.360E+07	0.684E+07	0.383E+07	0.350E+07	0.196E+07	0.299E+07	0.168E+07
6.25	6.50	0.289E+07	0.192E+07	0.301E+07	0.169E+07	0.154E+07	0.861E+06	0.132E+07	0.737E+06
6.50	6.75	0.974E+06	0.643E+06	0.132E+07	0.845E+06	0.675E+06	0.437E+06	0.578E+06	0.374E+06
6.75	7.00	0.331E+06	0.331E+06	0.477E+06	0.305E+06	0.230E+06	0.155E+06	0.204E+06	0.133E+06
7.00				0.172E+06	0.172E+06	0.833E+05	0.833E+05	0.714E+05	0.714E+05

T-34

Table 14. Four Circular Orbit Daily Fluence Summary Using AE-8MAX (cont.)

Orbit Altitude - 8000 n.mi.　　Accumulation Time - 192 Hrs.　　Sampling Interval - 180 s　　Units for Daily Fluence -e/cm²-day

Energy (MeV)		Daily Fluence 0° Inclination		Daily Fluence 30° Inclination		Daily Fluence 60° Inclination		Daily Fluence 90° Inclination	
E1	E2	*E1	E1-E2	*E1	E1-E2	*E1	E1-E2	*E1	E1-E2
0.0	0.25	0.634E+13	0.536E+13	0.592E+13	0.483E+13	0.353E+13	0.288E+13	0.288E+13	0.235E+13
0.25	0.50	0.973E+12	0.537E+12	0.109E+13	0.608E+12	0.644E+12	0.368E+12	0.525E+12	0.298E+12
0.50	0.75	0.436E+12	0.184E+12	0.461E+12	0.215E+12	0.276E+12	0.127E+12	0.227E+12	0.102E+12
0.75	1.00	0.252E+12	0.899E+11	0.266E+12	0.962E+11	0.150E+12	0.553E+11	0.124E+12	0.455E+11
1.00	1.25	0.162E+12	0.485E+11	0.170E+12	0.542E+11	0.943E+11	0.313E+11	0.781E+11	0.257E+11
1.25	1.50	0.113E+12	0.340E+11	0.115E+12	0.365E+11	0.630E+11	0.206E+11	0.524E+11	0.170E+11
1.50	1.75	0.795E+11	0.241E+11	0.790E+11	0.259E+11	0.424E+11	0.142E+11	0.353E+11	0.118E+11
1.75	2.00	0.553E+11	0.168E+11	0.531E+11	0.173E+11	0.282E+11	0.938E+10	0.236E+11	0.761E+10
2.00	2.25	0.385E+11	0.114E+11	0.358E+11	0.112E+11	0.188E+11	0.602E+10	0.157E+11	0.501E+10
2.25	2.50	0.271E+11	0.803E+10	0.246E+11	0.764E+10	0.128E+11	0.406E+10	0.107E+11	0.339E+10
2.50	2.75	0.191E+11	0.635E+10	0.170E+11	0.609E+10	0.874E+10	0.316E+10	0.734E+10	0.246E+10
2.75	3.00	0.127E+11	0.423E+10	0.109E+11	0.389E+10	0.558E+10	0.201E+10	0.469E+10	0.165E+10
3.00	3.25	0.849E+10	0.288E+10	0.659E+10	0.257E+10	0.357E+10	0.132E+10	0.300E+10	0.111E+10
3.25	3.50	0.561E+10	0.190E+10	0.442E+10	0.162E+10	0.225E+10	0.826E+09	0.190E+10	0.696E+09
3.50	3.75	0.370E+10	0.870E+09	0.280E+10	0.116E+10	0.142E+10	0.589E+09	0.120E+10	0.466E+09
3.75	4.00	0.230E+10	0.612E+09	0.164E+10	0.675E+09	0.832E+09	0.343E+09	0.703E+09	0.246E+09
4.00	4.25	0.144E+10	0.351E+09	0.968E+09	0.439E+09	0.489E+09	0.222E+09	0.414E+09	0.188E+09
4.25	4.50	0.923E+09	0.211E+09	0.528E+09	0.239E+09	0.266E+09	0.121E+09	0.226E+09	0.102E+09
4.50	4.75	0.473E+09	0.117E+09	0.290E+09	0.140E+09	0.146E+09	0.707E+08	0.124E+09	0.599E+08
4.75	5.00	0.262E+09	0.751E+08	0.150E+09	0.714E+08	0.750E+08	0.359E+08	0.634E+08	0.304E+08
5.00	5.25	0.145E+09	0.363E+08	0.786E+08	0.421E+08	0.391E+08	0.210E+08	0.334E+08	0.179E+08
5.25	5.50	0.704E+08	0.186E+08	0.365E+08	0.194E+08	0.181E+08	0.966E+07	0.154E+08	0.824E+07
5.50	5.75	0.341E+08	0.844E+07	0.171E+08	0.968E+07	0.844E+07	0.479E+07	0.721E+07	0.409E+07
5.75	6.00	0.155E+08	0.397E+07	0.738E+07	0.417E+07	0.365E+07	0.206E+07	0.312E+07	0.174E+07
6.00	6.25	0.703E+07	0.173E+07	0.322E+07	0.185E+07	0.159E+07	0.916E+06	0.136E+07	0.785E+06
6.25	6.50	0.306E+07	0.786E+06	0.136E+07	0.786E+06	0.674E+06	0.389E+06	0.578E+06	0.333E+06
6.50	6.75	0.133E+07	0.321E+06	0.577E+06	0.349E+06	0.286E+06	0.172E+06	0.245E+06	0.148E+06
6.75	7.00	0.543E+06	0.222E+06	0.228E+06	0.145E+06	0.113E+06	0.708E+05	0.972E+05	0.607E+05
7.00		0.222E+06		0.833E+05	0.833E+05	0.425E+05	0.425E+05	0.365E+05	0.365E+05

Table 14. Four Circular Orbit Daily Fluence Summary Using AE-8MAX (cont.)

Orbit Altitude - 9000 n.mi.   Accumulation Time - 192 Hrs.   Sampling Interval - 180 s   Units for Daily Fluence -e/cm²-day

Energy (MeV)		Daily Fluence 0° Inclination		Daily Fluence 30° Inclination		Daily Fluence 60° Inclination		Daily Fluence 90° Inclination	
E1	E2	*E1	E1-E2	*E1	E1-E2	*E1	E1-E2	*E1	E1-E2
0.00	0.25	0.727E+13	0.595E+13	0.655E+13	0.521E+13	0.376E+13	0.303E+13	0.306E+13	0.246E+13
0.25	0.50	0.132E+13	0.727E+12	0.134E+13	0.758E+12	0.736E+12	0.423E+12	0.607E+12	0.347E+12
0.50	0.75	0.596E+12	0.260E+12	0.586E+12	0.268E+12	0.313E+12	0.146E+12	0.260E+12	0.121E+12
0.75	1.00	0.336E+12	0.116E+12	0.318E+12	0.115E+12	0.167E+12	0.615E+11	0.139E+12	0.511E+11
1.00	1.25	0.220E+12	0.631E+11	0.203E+12	0.668E+11	0.105E+12	0.355E+11	0.878E+11	0.295E+11
1.25	1.50	0.157E+12	0.450E+11	0.136E+12	0.442E+11	0.695E+11	0.231E+11	0.583E+11	0.193E+11
1.50	1.75	0.112E+12	0.356E+11	0.917E+11	0.316E+11	0.464E+11	0.161E+11	0.390E+11	0.135E+11
1.75	2.00	0.764E+11	0.243E+11	0.601E+11	0.206E+11	0.303E+11	0.105E+11	0.255E+11	0.875E+10
2.00	2.25	0.522E+11	0.152E+11	0.395E+11	0.127E+11	0.199E+11	0.646E+10	0.168E+11	0.543E+10
2.25	2.50	0.370E+11	0.108E+11	0.268E+11	0.858E+10	0.134E+11	0.432E+10	0.113E+11	0.364E+10
2.50	2.75	0.262E+11	0.960E+10	0.182E+11	0.699E+10	0.907E+10	0.346E+10	0.768E+10	0.253E+10
2.75	3.00	0.166E+11	0.608E+10	0.112E+11	0.429E+10	0.561E+10	0.214E+10	0.475E+10	0.161E+10
3.00	3.25	0.105E+11	0.400E+10	0.690E+10	0.269E+10	0.347E+10	0.135E+10	0.294E+10	0.115E+10
3.25	3.50	0.653E+10	0.175E+10	0.421E+10	0.164E+10	0.212E+10	0.825E+09	0.179E+10	0.655E+09
3.50	3.75	0.405E+10	0.994E+09	0.257E+10	0.114E+10	0.129E+10	0.574E+09	0.109E+10	0.487E+09
3.75	4.00	0.230E+10	0.618E+09	0.142E+10	0.633E+09	0.716E+09	0.318E+09	0.608E+09	0.27E+09
4.00	4.25	0.131E+10	0.326E+09	0.788E+09	0.380E+09	0.398E+09	0.192E+09	0.33E+09	0.143E+09
4.25	4.50	0.692E+09	0.188E+09	0.407E+09	0.196E+09	0.206E+09	0.993E+08	0.175E+09	0.842E+08
4.50	4.75	0.366E+09	0.913E+08	0.211E+09	0.113E+09	0.107E+09	0.574E+08	0.905E+08	0.487E+08
4.75	5.00	0.177E+09	0.479E+08	0.975E+08	0.521E+08	0.492E+08	0.263E+08	0.419E+08	0.223E+08
5.00	5.25	0.862E+08	0.213E+08	0.454E+08	0.263E+08	0.229E+08	0.133E+08	0.195E+08	0.113E+08
5.25	5.50	0.383E+08	0.107E+08	0.191E+08	0.110E+08	0.963E+07	0.554E+07	0.823E+07	0.473E+07
5.50	5.75	0.170E+08	0.407E+07	0.807E+07	0.503E+07	0.410E+07	0.962E+06	0.350E+07	0.217E+07
5.75	6.00	0.675E+07	0.162E+07	0.304E+07	0.189E+07	0.155E+07	0.962E+06	0.133E+07	0.824E+06
6.00	6.25	0.260E+07	0.638E+06	0.115E+07	0.719E+06	0.590E+06	0.366E+06	0.506E+06	0.314E+06
6.25	6.50	0.106E+07	0.251E+06	0.430E+06	0.273E+06	0.224E+06	0.140E+06	0.192E+06	0.120E+06
6.50	6.75	0.421E+06	0.104E+06	0.156E+06	0.101E+06	0.834E+05	0.527E+05	0.716E+05	0.452E+05
6.75	7.00	0.169E+06	0.648E+05	0.555E+05	0.362E+05	0.307E+05	0.195E+05	0.264E+05	0.168E+05
7.00		0.648E+05		0.193E+05	0.193E+05	0.112E+05	0.112E+05	0.966E+04	0.966E+04

T-36

Table 14. Four Circular Orbit Daily Fluence Summary Using AE-8MAX (cont.)

Orbit Altitude - 10,000 n.mi.   Accumulation Time - 192 Hrs.   Sampling Interval - 180 s   Units for Daily Fluence -e/cm²-day

Energy (MeV)		Daily Fluence 0° Inclination		Daily Fluence 30° Inclination		Daily Fluence 60° Inclination		Daily Fluence 90° Inclination	
E1	E2	*E1	E1-E2	*E1	E1-E2	*E1	E1-E2	*E1	E1-E2
0.0	0.25	0.833E+13	0.663E+13	0.650E+13	0.539E+13	0.394E+13	0.313E+13	0.324E+13	0.256E+13
0.25	0.50	0.170E+13	0.946E+12	0.151E+13	0.867E+12	0.811E+12	0.470E+12	0.678E+12	0.392E+12
0.50	0.75	0.759E+12	0.340E+12	0.648E+12	0.303E+12	0.340E+12	0.162E+12	0.286E+12	0.136E+12
0.75	1.00	0.419E+12	0.149E+12	0.344E+12	0.128E+12	0.178E+12	0.672E+11	0.150E+12	0.565E+11
1.00	1.25	0.270E+12	0.813E+11	0.216E+12	0.768E+11	0.111E+12	0.395E+11	0.935E+11	0.332E+11
1.25	1.50	0.189E+12	0.568E+11	0.139E+12	0.489E+11	0.712E+11	0.251E+11	0.603E+11	0.211E+11
1.50	1.75	0.132E+12	0.451E+11	0.903E+11	0.330E+11	0.462E+11	0.169E+11	0.392E+11	0.143E+11
1.75	2.00	0.867E+11	0.296E+11	0.572E+11	0.209E+11	0.293E+11	0.107E+11	0.249E+11	0.904E+10
2.00	2.25	0.571E+11	0.183E+11	0.363E+11	0.127E+11	0.186E+11	0.651E+10	0.158E+11	0.552E+10
2.25	2.50	0.387E+11	0.124E+11	0.236E+11	0.823E+10	0.121E+11	0.421E+10	0.103E+11	0.357E+10
2.50	2.75	0.263E+11	0.108E+11	0.154E+11	0.616E+10	0.792E+10	0.318E+10	0.674E+10	0.271E+10
2.75	3.00	0.155E+11	0.636E+10	0.922E+10	0.369E+10	0.474E+10	0.190E+10	0.403E+10	0.162E+10
3.00	3.25	0.917E+10	0.359E+10	0.553E+10	0.222E+10	0.284E+10	0.114E+10	0.241E+10	0.966E+09
3.25	3.50	0.558E+10	0.219E+10	0.330E+10	0.133E+10	0.170E+10	0.681E+09	0.145E+10	0.580E+09
3.50	3.75	0.339E+10	0.157E+10	0.198E+10	0.915E+09	0.102E+10	0.471E+09	0.866E+09	0.401E+09
3.75	4.00	0.183E+10	0.844E+09	0.106E+10	0.491E+09	0.547E+09	0.253E+09	0.466E+09	0.215E+09
4.00	4.25	0.985E+09	0.481E+09	0.570E+09	0.284E+09	0.294E+09	0.146E+09	0.250E+09	0.124E+09
4.25	4.50	0.504E+09	0.246E+09	0.286E+09	0.143E+09	0.148E+09	0.734E+08	0.126E+09	0.622E+08
4.50	4.75	0.258E+09	0.142E+09	0.144E+09	0.822E+08	0.743E+08	0.425E+08	0.633E+08	0.362E+08
4.75	5.00	0.117E+09	0.639E+08	0.616E+08	0.350E+08	0.319E+08	0.181E+08	0.272E+08	0.154E+08
5.00	5.25	0.526E+08	0.317E+08	0.266E+08	0.167E+08	0.138E+08	0.860E+07	0.118E+08	0.734E+07
5.25	5.50	0.209E+08	0.126E+08	0.994E+07	0.619E+07	0.517E+07	0.321E+07	0.442E+07	0.274E+07
5.50	5.75	0.833E+07	0.550E+07	0.375E+07	0.255E+07	0.196E+07	0.133E+07	0.168E+07	0.114E+07
5.75	6.00	0.283E+07	0.187E+07	0.120E+07	0.823E+06	0.638E+06	0.433E+06	0.546E+06	0.371E+06
6.00	6.25	0.962E+06	0.656E+06	0.382E+06	0.271E+06	0.205E+06	0.143E+06	0.176E+06	0.123E+06
6.25	6.50	0.306E+06	0.226E+06	0.111E+06	0.887E+05	0.617E+05	0.486E+05	0.528E+05	0.416E+05
6.50	6.75	0.800E+05	0.0	0.222E+05	0.0	0.131E+05	0.0	0.112E+05	0.0
6.75	7.00	0.0	0.0	0.0	0.0	0.0	0.0	0.0	0.0
7.00		0.0	0.0	0.0	0.0	0.0	0.0	0.0	0.0

T-37

Table 14. Four Circular Orbit Daily Fluence Summary Using AE-8MAX (cont.)

Orbit Altitude - 11,000 n.mi.   Accumulation Time - 432 Hrs.   Sampling Interval - 360 s   Units for Daily Fluence -e/cm²-day

Energy (MeV)		Daily Fluence 0° Inclination		Daily Fluence 30° Inclination		Daily Fluence 60° Inclination		Daily Fluence 90° Inclination	
E1	E2	*E1	E1-E2	*E1	E1-E2	*E1	E1-E2	*E1	E1-E2
0.00	0.25	0.889E+13	0.689E+13	0.715E+13	0.551E+13	0.393E+13	0.309E+13	0.320E+13	0.251E+13
0.25	0.50	0.200E+13	0.111E+13	0.164E+13	0.949E+12	0.838E+12	0.493E+12	0.691E+12	0.405E+12
0.50	0.75	0.886E+12	0.393E+12	0.687E+12	0.330E+12	0.345E+12	0.168E+12	0.286E+12	0.139E+12
0.75	1.00	0.453E+12	0.176E+12	0.357E+12	0.137E+12	0.177E+12	0.687E+11	0.148E+12	0.565E+11
1.00	1.25	0.317E+12	0.114E+12	0.220E+12	0.861E+11	0.109E+12	0.424E+11	0.907E+11	0.352E+11
1.25	1.50	0.204E+12	0.730E+11	0.134E+12	0.521E+11	0.663E+11	0.257E+11	0.555E+11	0.214E+11
1.50	1.75	0.131E+12	0.494E+11	0.817E+11	0.316E+11	0.406E+11	0.157E+11	0.341E+11	0.132E+11
1.75	2.00	0.811E+11	0.307E+11	0.500E+11	0.194E+11	0.249E+11	0.963E+10	0.209E+11	0.807E+10
2.00	2.25	0.504E+11	0.183E+11	0.307E+11	0.117E+11	0.153E+11	0.579E+10	0.128E+11	0.465E+10
2.25	2.50	0.321E+11	0.117E+11	0.190E+11	0.721E+10	0.949E+10	0.359E+10	0.798E+10	0.301E+10
2.50	2.75	0.204E+11	0.804E+10	0.118E+11	0.463E+10	0.590E+10	0.232E+10	0.497E+10	0.155E+10
2.75	3.00	0.124E+11	0.487E+10	0.715E+10	0.281E+10	0.358E+10	0.141E+10	0.301E+10	0.115E+10
3.00	3.25	0.749E+10	0.308E+10	0.434E+10	0.179E+10	0.217E+10	0.897E+09	0.183E+10	0.754E+09
3.25	3.50	0.441E+10	0.181E+10	0.255E+10	0.105E+10	0.128E+10	0.527E+09	0.107E+10	0.443E+09
3.50	3.75	0.260E+10	0.120E+10	0.150E+10	0.697E+09	0.750E+09	0.349E+09	0.631E+09	0.257E+09
3.75	4.00	0.139E+10	0.646E+09	0.800E+09	0.372E+09	0.401E+09	0.186E+09	0.337E+09	0.157E+09
4.00	4.25	0.748E+09	0.378E+09	0.427E+09	0.219E+09	0.214E+09	0.109E+09	0.180E+09	0.520E+08
4.25	4.50	0.370E+09	0.187E+09	0.209E+09	0.107E+09	0.105E+09	0.536E+08	0.885E+08	0.451E+08
4.50	4.75	0.183E+09	0.106E+09	0.102E+09	0.616E+08	0.515E+08	0.310E+08	0.434E+08	0.261E+08
4.75	5.00	0.768E+08	0.446E+08	0.404E+08	0.243E+08	0.204E+08	0.122E+08	0.173E+08	0.103E+08
5.00	5.25	0.322E+08	0.209E+08	0.161E+08	0.108E+08	0.819E+07	0.548E+07	0.695E+07	0.464E+07
5.25	5.50	0.113E+08	0.733E+07	0.529E+07	0.354E+07	0.272E+07	0.181E+07	0.231E+07	0.154E+07
5.50	5.75	0.397E+07	0.287E+07	0.175E+07	0.128E+07	0.906E+06	0.662E+06	0.774E+06	0.555E+06
5.75	6.00	0.110E+07	0.795E+06	0.465E+06	0.356E+06	0.245E+06	0.184E+06	0.210E+06	0.158E+06
6.00	6.25	0.307E+06	0.254E+06	0.108E+06	0.923E+05	0.602E+05	0.502E+05	0.518E+05	0.429E+05
6.25	6.50	0.532E+05	0.0	0.158E+05	0.0	0.101E+05	0.0	0.894E+04	0.0
6.50	6.75	0.0	0.0	0.0	0.0	0.0	0.0	0.0	0.0
6.75	7.00	0.0	0.0	0.0	0.0	0.0	0.0	0.0	0.0
7.00		0.0	0.0	0.0	0.0	0.0	0.0	0.0	0.0

Table 14. Four Circular Orbit Daily Fluence Summary Using AE-8MAX (cont.)

Orbit Altitude - 12,000 n.mi.   Accumulation Time - 432 Hrs.   Sampling Interval - 360 s   Units for Daily Fluence -e/cm²-day

Energy (MeV)		Daily Fluence 0° Inclination		Daily Fluence 30° Inclination		Daily Fluence 60° Inclination		Daily Fluence 90° Inclination	
E1	E2	*E1	E1-E2	*E1	E1-E2	*E1	E1-E2	*E1	E1-E2
0.0	0.25	0.937E+13	0.717E+13	0.654E+13	0.534E+13	0.385E+13	0.304E+13	0.316E+13	0.247E+13
0.25	0.50	0.219E+13	0.125E+13	0.160E+13	0.953E+12	0.813E+12	0.489E+12	0.685E+12	0.411E+12
0.50	0.75	0.942E+12	0.432E+12	0.647E+12	0.328E+12	0.324E+12	0.164E+12	0.274E+12	0.139E+12
0.75	1.00	0.509E+12	0.194E+12	0.320E+12	0.130E+12	0.160E+12	0.652E+11	0.136E+12	0.552E+11
1.00	1.25	0.315E+12	0.127E+12	0.190E+12	0.793E+11	0.946E+11	0.396E+11	0.803E+11	0.356E+11
1.25	1.50	0.188E+12	0.757E+11	0.110E+12	0.460E+11	0.550E+11	0.230E+11	0.468E+11	0.210E+11
1.50	1.75	0.112E+12	0.442E+11	0.641E+11	0.255E+11	0.321E+11	0.127E+11	0.273E+11	0.652E+10
1.75	2.00	0.680E+11	0.268E+11	0.387E+11	0.153E+11	0.193E+11	0.767E+10	0.164E+11	0.394E+10
2.00	2.25	0.412E+11	0.160E+11	0.233E+11	0.928E+10	0.117E+11	0.464E+10	0.992E+10	0.237E+10
2.25	2.50	0.252E+11	0.977E+10	0.141E+11	0.558E+10	0.702E+10	0.279E+10	0.598E+10	0.141E+10
2.50	2.75	0.154E+11	0.599E+10	0.848E+10	0.332E+10	0.423E+10	0.165E+10	0.361E+10	0.856E+09
2.75	3.00	0.945E+10	0.367E+10	0.516E+10	0.202E+10	0.258E+10	0.101E+10	0.220E+10	0.557E+09
3.00	3.25	0.578E+10	0.241E+10	0.314E+10	0.131E+10	0.157E+10	0.654E+09	0.134E+10	0.325E+09
3.25	3.50	0.337E+10	0.141E+10	0.184E+10	0.763E+09	0.918E+09	0.382E+09	0.782E+09	0.214E+09
3.50	3.75	0.197E+10	0.922E+09	0.107E+10	0.502E+09	0.536E+09	0.251E+09	0.457E+09	0.114E+09
3.75	4.00	0.105E+10	0.490E+09	0.570E+09	0.267E+09	0.285E+09	0.134E+09	0.243E+09	0.671E+08
4.00	4.25	0.557E+09	0.288E+09	0.303E+09	0.157E+09	0.152E+09	0.787E+08	0.129E+09	0.343E+08
4.25	4.50	0.268E+09	0.139E+09	0.146E+09	0.756E+08	0.730E+08	0.379E+08	0.622E+08	0.189E+08
4.50	4.75	0.129E+09	0.788E+08	0.699E+08	0.443E+08	0.351E+08	0.222E+08	0.299E+08	0.691E+07
4.75	5.00	0.5C3E+08	0.307E+08	0.256E+08	0.161E+08	0.129E+08	0.811E+07	0.110E+08	0.289E+07
5.00	5.25	0.196E+08	0.136E+08	0.946E+07	0.674E+07	0.477E+07	0.339E+07	0.408E+07	0.840E+06
5.25	5.50	0.601E+07	0.417E+07	0.272E+07	0.194E+07	0.138E+07	0.983E+06	0.118E+07	0.262E+06
5.50	5.75	0.1C4E+07	0.141E+07	0.783E+06	0.600E+06	0.400E+06	0.306E+06	0.343E+06	0.70CE+05
5.75	6.00	0.429E+06	0.364E+06	0.183E+06	0.162E+06	0.936E+05	0.817E+05	0.802E+05	0.0
6.00	6.25	0.657E+05	0.0	0.213E+05	0.0	0.119E+05	0.0	0.102E+05	0.0
6.25	6.50	0.0	0.0	0.0	0.0	0.0	0.0	0.0	0.0
6.50	6.75	0.0	0.0	0.0	0.0	0.0	0.0	0.0	0.0
6.75	7.00	0.0	0.0	0.0	0.0	0.0	0.0	0.0	0.0
7.00		0.0	0	0.0		0.0		0.0	

Table 14. Four Circular Orbit Daily Fluence Summary Using AE-8MAX (cont.)

Orbit Altitude - 13,000 n.mi.　Accumulation Time - 576 Hrs.　Sampling Interval - 480 s　Units for Daily Fluence -e/cm²-day

Energy (MeV)		Daily Fluence 0° Inclination		Daily Fluence 30° Inclination		Daily Fluence 60° Inclination		Daily Fluence 90° Inclination	
E1	E2	*E1	E1-E2	*E1	E1-E2	*E1	E1-E2	*E1	E1-E2
0.0	0.25	0.854E+13	0.653E+13	0.592E+13	0.461E+13	0.328E+13	0.263E+13	0.270E+13	0.215E+13
0.25	0.50	0.200E+13	0.120E+13	0.131E+13	0.831E+12	0.653E+12	0.416E+12	0.553E+12	0.352E+12
0.50	0.75	0.798E+12	0.445E+12	0.476E+12	0.274E+12	0.237E+12	0.137E+12	0.202E+12	0.116E+12
0.75	1.00	0.353E+12	0.153E+12	0.202E+12	0.920E+11	0.100E+12	0.457E+11	0.855E+11	0.388E+11
1.00	1.25	0.200E+12	0.874E+11	0.110E+12	0.488E+11	0.548E+11	0.244E+11	0.467E+11	0.208E+11
1.25	1.50	0.113E+12	0.492E+11	0.608E+11	0.270E+11	0.304E+11	0.135E+11	0.259E+11	0.115E+11
1.50	1.75	0.634E+11	0.255E+11	0.338E+11	0.137E+11	0.169E+11	0.686E+10	0.144E+11	0.585E+10
1.75	2.00	0.379E+11	0.152E+11	0.201E+11	0.815E+10	0.100E+11	0.407E+10	0.856E+10	0.346E+10
2.00	2.25	0.227E+11	0.912E+10	0.119E+11	0.491E+10	0.596E+10	0.245E+10	0.509E+10	0.209E+10
2.25	2.50	0.136E+11	0.546E+10	0.700E+10	0.288E+10	0.351E+10	0.144E+10	0.300E+10	0.123E+10
2.50	2.75	0.812E+10	0.330E+10	0.412E+10	0.166E+10	0.207E+10	0.834E+09	0.177E+10	0.713E+09
2.75	3.00	0.483E+10	0.196E+10	0.246E+10	0.991E+09	0.123E+10	0.498E+09	0.105E+10	0.425E+09
3.00	3.25	0.287E+10	0.120E+10	0.147E+10	0.616E+09	0.736E+09	0.308E+09	0.625E+09	0.264E+09
3.25	3.50	0.167E+10	0.698E+09	0.851E+09	0.357E+09	0.427E+09	0.179E+09	0.365E+09	0.153E+09
3.50	3.75	0.971E+09	0.454E+09	0.494E+09	0.230E+09	0.248E+09	0.116E+09	0.212E+09	0.966E+08
3.75	4.00	0.518E+09	0.242E+09	0.264E+09	0.123E+09	0.133E+09	0.618E+08	0.113E+09	0.526E+08
4.00	4.25	0.276E+09	0.145E+09	0.141E+09	0.734E+08	0.710E+08	0.370E+08	0.607E+08	0.316E+08
4.25	4.50	0.131E+09	0.688E+08	0.676E+08	0.352E+08	0.340E+08	0.177E+08	0.291E+08	0.151E+08
4.50	4.75	0.622E+08	0.422E+08	0.324E+08	0.226E+08	0.163E+08	0.113E+08	0.139E+08	0.967E+07
4.75	5.00	0.200E+08	0.136E+08	0.982E+07	0.683E+07	0.497E+07	0.345E+07	0.425E+07	0.255E+07
5.00	5.25	0.643E+07	0.505E+07	0.300E+07	0.238E+07	0.152E+07	0.120E+07	0.130E+07	0.103E+07
5.25	5.50	0.138E+07	0.108E+07	0.620E+06	0.515E+06	0.318E+06	0.261E+06	0.273E+06	0.224E+06
5.50	5.75	0.298E+06	0.277E+06	0.105E+06	0.951E+05	0.575E+05	0.518E+05	0.494E+05	0.445E+05
5.75	6.00	0.202E+05	0.0	0.101E+05	0.0	0.569E+04	0.0	0.493E+04	0.0
6.00	6.25	0.0	0.0	0.0	0.0	0.0	0.0	0.0	0.0
6.25	6.50	0.0	0.0	0.0	0.0	0.0	0.0	0.0	0.0
6.50	6.75	0.0	0.0	0.0	0.0	0.0	0.0	0.0	0.0
6.75	7.00	0.0	0.0	0.0	0.0	0.0	0.0	0.0	0.0
7.00		0.0	0.0	0.0	0.0	0.0	0.0	0.0	0.0

Table 14. Four Circular Orbit Daily Fluence Summary Using AE-8MAX (cont.)

Orbit Altitude - 14,000 n.mi. Accumulation Time - 576 Hrs. Sampling Interval - 480 s Units for Daily Fluence -e/cm²-day

Energy (MeV)		Daily Fluence 0° Inclination		Daily Fluence 30° Inclination		Daily Fluence 60° Inclination		Daily Fluence 90° Inclination	
E1	E2	*E1	E1-E2	*E1	E1-E2	*E1	E1-E2	*E1	E1-E2
0.0	0.25	0.920E+13	0.702E+13	0.649E+13	0.502E+13	0.362E+13	0.287E+13	0.297E+13	0.234E+13
0.25	0.50	0.219E+13	0.128E+13	0.148E+13	0.908E+12	0.750E+12	0.463E+12	0.634E+12	0.351E+12
0.50	0.75	0.906E+12	0.462E+12	0.570E+12	0.310E+12	0.287E+12	0.156E+12	0.243E+12	0.132E+12
0.75	1.00	0.444E+12	0.181E+12	0.260E+12	0.112E+12	0.131E+12	0.565E+11	0.111E+12	0.477E+11
1.00	1.25	0.263E+12	0.113E+12	0.148E+12	0.646E+11	0.745E+11	0.325E+11	0.634E+11	0.277E+11
1.25	1.50	0.150E+12	0.644E+11	0.836E+11	0.364E+11	0.420E+11	0.183E+11	0.358E+11	0.156E+11
1.50	1.75	0.858E+11	0.340E+11	0.472E+11	0.189E+11	0.237E+11	0.951E+10	0.202E+11	0.810E+10
1.75	2.00	0.518E+11	0.205E+11	0.283E+11	0.113E+11	0.142E+11	0.570E+10	0.121E+11	0.485E+10
2.00	2.25	0.312E+11	0.128E+11	0.169E+11	0.696E+10	0.851E+10	0.351E+10	0.726E+10	0.299E+10
2.25	2.50	0.184E+11	0.755E+10	0.997E+10	0.409E+10	0.501E+10	0.206E+10	0.427E+10	0.176E+10
2.50	2.75	0.109E+11	0.423E+10	0.588E+10	0.231E+10	0.295E+10	0.116E+10	0.251E+10	0.987E+09
2.75	3.00	0.667E+10	0.259E+10	0.356E+10	0.140E+10	0.179E+10	0.702E+09	0.153E+10	0.597E+09
3.00	3.25	0.408E+10	0.168E+10	0.216E+10	0.896E+09	0.109E+10	0.450E+09	0.927E+09	0.384E+09
3.25	3.50	0.241E+10	0.988E+09	0.126E+10	0.524E+09	0.637E+09	0.264E+09	0.543E+09	0.225E+09
3.50	3.75	0.142E+10	0.669E+09	0.741E+09	0.348E+09	0.374E+09	0.175E+09	0.319E+09	0.150E+09
3.75	4.00	0.748E+09	0.353E+09	0.393E+09	0.184E+09	0.198E+09	0.930E+08	0.169E+09	0.794E+08
4.00	4.25	0.355E+09	0.206E+09	0.208E+09	0.109E+09	0.105E+09	0.548E+08	0.897E+08	0.467E+08
4.25	4.50	0.188E+09	0.985E+08	0.998E+08	0.520E+08	0.503E+08	0.262E+08	0.429E+08	0.224E+08
4.50	4.75	0.899E+08	0.581E+08	0.477E+08	0.318E+08	0.241E+08	0.161E+08	0.206E+08	0.137E+08
4.75	5.00	0.318E+08	0.205E+08	0.159E+08	0.106E+08	0.806E+07	0.534E+07	0.688E+07	0.456E+07
5.00	5.25	0.112E+08	0.820E+07	0.534E+07	0.401E+07	0.271E+07	0.203E+07	0.232E+07	0.173E+07
5.25	5.50	0.304E+07	0.222E+07	0.133E+07	0.101E+07	0.687E+06	0.518E+06	0.588E+06	0.443E+06
5.50	5.75	0.823E+06	0.601E+06	0.324E+06	0.248E+06	0.169E+06	0.128E+06	0.145E+06	0.110E+06
5.75	6.00	0.222E+06	0.0	0.755E+05	0.0	0.409E+05	0.0	0.351E+05	0.0
6.00	6.25	0.0	0.0	0.0	0.0	0.0	0.0	0.0	0.0
6.25	6.50	0.0	0.0	0.0	0.0	0.0	0.0	0.0	0.0
6.50	6.75	0.0	0.0	0.0	0.0	0.0	0.0	0.0	0.0
6.75	7.00	0.0	0.0	0.0	0.0	0.0	0.0	0.0	0.0
7.00		0.0	0.0	0.0	0.0	0.0	0.0	0.0	0.0

Table 14. Four Circular Orbit Daily Fluence Summary Using AE-8MAX (cont.)

Orbit Altitude - 15,000 n.mi. Accumulation Time - 1152 Hrs. Sampling Interval - 720 s Units for Daily Fluence -e/cm²-day

Energy (MeV) E1	Energy (MeV) E2	Daily Fluence 0° Inclination *E1	Daily Fluence 0° Inclination E1-E2	Daily Fluence 30° Inclination *E1	Daily Fluence 30° Inclination E1-E2	Daily Fluence 60° Inclination *E1	Daily Fluence 60° Inclination E1-E2	Daily Fluence 90° Inclination *E1	Daily Fluence 90° Inclination E1-E2
0.0	0.25	0.696E+13	0.537E+13	0.478E+13	0.385E+13	0.268E+13	0.221E+13	0.222E+13	0.182E+13
0.25	0.50	0.159E+13	0.105E+13	0.933E+12	0.643E+12	0.466E+12	0.321E+12	0.397E+12	0.273E+12
0.50	0.75	0.535E+12	0.323E+12	0.290E+12	0.178E+12	0.145E+12	0.890E+11	0.124E+12	0.755E+11
0.75	1.00	0.211E+12	0.102E+12	0.112E+12	0.567E+11	0.561E+11	0.282E+11	0.479E+11	0.240E+11
1.00	1.25	0.109E+12	0.498E+11	0.555E+11	0.259E+11	0.279E+11	0.130E+11	0.238E+11	0.111E+11
1.25	1.50	0.594E+11	0.271E+11	0.296E+11	0.138E+11	0.149E+11	0.694E+10	0.127E+11	0.593E+10
1.50	1.75	0.323E+11	0.133E+11	0.158E+11	0.657E+10	0.798E+10	0.332E+10	0.682E+10	0.283E+10
1.75	2.00	0.190E+11	0.784E+10	0.925E+10	0.384E+10	0.467E+10	0.194E+10	0.399E+10	0.166E+10
2.00	2.25	0.112E+11	0.482E+10	0.541E+10	0.240E+10	0.273E+10	0.121E+10	0.233E+10	0.103E+10
2.25	2.50	0.634E+10	0.274E+10	0.301E+10	0.133E+10	0.152E+10	0.672E+09	0.130E+10	0.574E+09
2.50	2.75	0.360E+10	0.143E+10	0.168E+10	0.664E+09	0.852E+09	0.337E+09	0.729E+09	0.288E+09
2.75	3.00	0.218E+10	0.862E+09	0.101E+10	0.401E+09	0.515E+09	0.204E+09	0.440E+09	0.174E+09
3.00	3.25	0.132E+10	0.565E+09	0.612E+09	0.257E+09	0.311E+09	0.131E+09	0.266E+09	0.112E+09
3.25	3.50	0.750E+09	0.322E+09	0.355E+09	0.149E+09	0.180E+09	0.757E+08	0.154E+09	0.646E+08
3.50	3.75	0.428E+09	0.198E+09	0.206E+09	0.949E+08	0.104E+09	0.479E+08	0.891E+08	0.410E+08
3.75	4.00	0.230E+09	0.106E+09	0.111E+09	0.512E+08	0.563E+08	0.259E+08	0.481E+08	0.221E+08
4.00	4.25	0.124E+09	0.633E+08	0.601E+08	0.305E+08	0.305E+08	0.155E+08	0.260E+08	0.132E+08
4.25	4.50	0.603E+08	0.309E+08	0.296E+08	0.150E+08	0.150E+08	0.761E+07	0.128E+08	0.650E+07
4.50	4.75	0.294E+08	0.215E+08	0.146E+08	0.109E+08	0.738E+07	0.550E+07	0.630E+07	0.469E+07
4.75	5.00	0.790E+07	0.578E+07	0.369E+07	0.276E+07	0.188E+07	0.141E+07	0.161E+07	0.120E+07
5.00	5.25	0.212E+07	0.170E+07	0.928E+06	0.745E+06	0.475E+06	0.381E+06	0.407E+06	0.327E+06
5.25	5.50	0.426E+06	0.0	0.183E+06	0.0	0.938E+05	0.0	0.804E+05	0.0
5.50	5.75	0.0	0.0	0.0	0.0	0.0	0.0	0.0	0.0
5.75	6.00	0.0	0.0	0.0	0.0	0.0	0.0	0.0	0.0
6.00	6.25	0.0	0.0	0.0	0.0	0.0	0.0	0.0	0.0
6.25	6.50	0.0	0.0	0.0	0.0	0.0	0.0	0.0	0.0
6.50	6.75	0.0	0.0	0.0	0.0	0.0	0.0	0.0	0.0
6.75	7.00	0.0	0.0	0.0	0.0	0.0	0.0	0.0	0.0

Table 14. Four Circular Orbit Daily Fluence Summary Using AE-8MAX (cont.)

Orbit Altitude - 16,000 n.mi.   Accumulation Time - 1152 Hrs.   Sampling Interval - 720 s   Units for Daily Fluence -e/cm²-day

Energy (MeV)		Daily Fluence 0° Inclination		Daily Fluence 30° Inclination		Daily Fluence 60° Inclination		Daily Fluence 90° Inclination	
E1	E2	*E1	E1-E2	*E1	E1-E2	*E1	E1-E2	*E1	E1-E2
0.0	0.25	0.782E+13	0.600E+13	0.533E+13	0.421E+13	0.297E+13	0.241E+13	0.247E+13	0.199E+13
0.25	0.50	0.182E+13	0.116E+13	0.112E+13	0.745E+12	0.562E+12	0.373E+12	0.477E+12	0.317E+12
0.50	0.75	0.667E+12	0.388E+12	0.378E+12	0.225E+12	0.189E+12	0.113E+12	0.161E+12	0.957E+11
0.75	1.00	0.280E+12	0.129E+12	0.153E+12	0.733E+11	0.764E+11	0.366E+11	0.651E+11	0.712E+11
1.00	1.25	0.151E+12	0.671E+11	0.793E+11	0.360E+11	0.398E+11	0.180E+11	0.339E+11	0.154E+11
1.25	1.50	0.840E+11	0.373E+11	0.433E+11	0.196E+11	0.217E+11	0.985E+10	0.186E+11	0.640E+10
1.50	1.75	0.467E+11	0.192E+11	0.237E+11	0.978E+10	0.119E+11	0.491E+10	0.102E+11	0.420E+10
1.75	2.00	0.274E+11	0.113E+11	0.139E+11	0.574E+10	0.697E+10	0.288E+10	0.595E+10	0.246E+10
2.00	2.25	0.161E+11	0.664E+10	0.816E+10	0.347E+10	0.409E+10	0.173E+10	0.349E+10	0.148E+10
2.25	2.50	0.948E+10	0.390E+10	0.469E+10	0.199E+10	0.236E+10	0.996E+09	0.201E+10	0.851E+09
2.50	2.75	0.558E+10	0.224E+10	0.270E+10	0.108E+10	0.136E+10	0.543E+09	0.116E+10	0.465E+09
2.75	3.00	0.334E+10	0.134E+10	0.162E+10	0.648E+09	0.817E+09	0.326E+09	0.699E+09	0.279E+09
3.00	3.25	0.200E+10	0.855E+09	0.975E+09	0.414E+09	0.491E+09	0.208E+09	0.420E+09	0.176E+09
3.25	3.50	0.115E+10	0.490E+09	0.562E+09	0.238E+09	0.283E+09	0.120E+09	0.242E+09	0.102E+09
3.50	3.75	0.657E+09	0.306E+09	0.324E+09	0.150E+09	0.163E+09	0.755E+08	0.139E+09	0.645E+08
3.75	4.00	0.352E+09	0.163E+09	0.174E+09	0.805E+08	0.877E+08	0.406E+08	0.749E+08	0.347E+08
4.00	4.25	0.188E+09	0.975E+08	0.934E+08	0.480E+08	0.471E+08	0.242E+08	0.402E+08	0.207E+08
4.25	4.50	0.905E+08	0.470E+08	0.454E+08	0.233E+08	0.229E+08	0.118E+08	0.195E+08	0.100E+08
4.50	4.75	0.436E+08	0.308E+08	0.220E+08	0.159E+08	0.111E+08	0.801E+07	0.949E+07	0.684E+07
4.75	5.00	0.128E+08	0.903E+07	0.611E+07	0.441E+07	0.310E+07	0.223E+07	0.265E+07	0.191E+07
5.00	5.25	0.374E+07	0.313E+07	0.170E+07	0.140E+07	0.862E+06	0.711E+06	0.738E+06	0.605E+06
5.25	5.50	0.610E+06	0.551E+06	0.304E+06	0.282E+06	0.151E+06	0.139E+06	0.129E+06	0.119E+06
5.50	5.75	0.588E+05	0.0	0.219E+05	0.0	0.119E+05	0.0	0.102E+05	0.0
5.75	6.00	0.0	0.0	0.0	0.0	0.0	0.0	0.0	0.0
6.00	6.25	0.0	0.0	0.0	0.0	0.0	0.0	0.0	0.0
6.25	6.50	0.0	0.0	0.0	0.0	0.0	0.0	0.0	0.0
6.50	6.75	0.0	0.0	0.0	0.0	0.0	0.0	0.0	0.0
6.75	7.00	0.0	0.0	0.0	0.0	0.0	0.0	0.0	0.0
7.00		0.0	0.0	0.0	0.0	0.0	0.0	0.0	0.0

Table 14. Four Circular Orbit Daily Fluence Summary Using AE-8MAX (cont.)

Orbit Altitude - 17,000 n.mi.   Accumulation Time - 2304 Hrs.   Sampling Interval - 1440 s   Units for Daily Fluence -e/cm²-day

Energy (MeV)		Daily Fluence 0° Inclination		Daily Fluence 30° Inclination		Daily Fluence 60° Inclination		Daily Fluence 90° Inclination	
E1	E2	*E1	E1-E2	*E1	E1-E2	*E1	E1-E2	*E1	E1-E2
0.00	0.25	0.616E+13	0.481E+13	0.435E+13	0.360E+13	0.242E+13	0.205E+13	0.201E+13	0.169E+13
0.25	0.50	0.135E+13	0.933E+12	0.753E+12	0.537E+12	0.377E+12	0.269E+12	0.322E+12	0.229E+12
0.50	0.75	0.418E+12	0.259E+12	0.216E+12	0.135E+12	0.109E+12	0.679E+11	0.927E+11	0.575E+11
0.75	1.00	0.159E+12	0.813E+11	0.810E+11	0.429E+11	0.406E+11	0.214E+11	0.347E+11	0.183E+11
1.00	1.25	0.778E+11	0.366E+11	0.380E+11	0.183E+11	0.192E+11	0.921E+10	0.164E+11	0.766E+10
1.25	1.50	0.413E+11	0.194E+11	0.158E+11	0.948E+10	0.100E+11	0.479E+10	0.857E+10	0.410E+10
1.50	1.75	0.219E+11	0.902E+10	0.103E+11	0.430E+10	0.522E+10	0.218E+10	0.447E+10	0.187E+10
1.75	2.00	0.129E+11	0.530E+10	0.598E+10	0.250E+10	0.304E+10	0.127E+10	0.260E+10	0.109E+10
2.00	2.25	0.757E+10	0.343E+10	0.348E+10	0.161E+10	0.177E+10	0.815E+09	0.152E+10	0.695E+09
2.25	2.50	0.414E+10	0.188E+10	0.187E+10	0.864E+09	0.955E+09	0.439E+09	0.818E+09	0.374E+09
2.50	2.75	0.226E+10	0.890E+09	0.101E+10	0.397E+09	0.516E+09	0.203E+09	0.442E+09	0.174E+09
2.75	3.00	0.137E+10	0.540E+09	0.605E+09	0.240E+09	0.312E+09	0.123E+09	0.268E+09	0.106E+09
3.00	3.25	0.832E+09	0.351E+09	0.369E+09	0.150E+09	0.189E+09	0.777E+08	0.162E+09	0.666E+08
3.25	3.50	0.481E+09	0.203E+09	0.219E+09	0.888E+08	0.112E+09	0.457E+08	0.956E+08	0.391E+08
3.50	3.75	0.278E+09	0.128E+09	0.130E+09	0.593E+08	0.660E+08	0.301E+08	0.565E+08	0.256E+08
3.75	4.00	0.150E+09	0.690E+08	0.705E+08	0.322E+08	0.359E+08	0.163E+08	0.307E+08	0.140E+08
4.00	4.25	0.807E+08	0.408E+08	0.383E+08	0.192E+08	0.195E+08	0.976E+07	0.167E+08	0.836E+07
4.25	4.50	0.400E+08	0.202E+08	0.192E+08	0.958E+07	0.975E+07	0.488E+07	0.834E+07	0.417E+07
4.50	4.75	0.198E+08	0.150E+08	0.560E+07	0.740E+07	0.487E+07	0.374E+07	0.417E+07	0.320E+07
4.75	5.00	0.462E+07	0.364E+07	0.219E+07	0.170E+07	0.113E+07	0.874E+06	0.966E+06	0.748E+06
5.00	5.25	0.118E+07	0.893E+06	0.452E+06	0.388E+06	0.255E+06	0.199E+06	0.218E+06	0.171E+06
5.25	5.50	0.283E+06	0.0	0.104E+06	0.0	0.554E+05	0.0	0.476E+05	0.0
5.50	5.75	0.0	0.0	0.0	0.0	0.0	0.0	0.0	0.0
5.75	6.00	0.0	0.0	0.0	0.0	0.0	0.0	0.0	0.0
6.00	6.25	0.0	0.0	0.0	0.0	0.0	0.0	0.0	0.0
6.25	6.50	0.0	0.0	0.0	0.0	0.0	0.0	0.0	0.0
6.50	6.75	0.0	0.0	0.0	0.0	0.0	0.0	0.0	0.0
6.75	7.00	0.0	0.0	0.0	0.0	0.0	0.0	0.0	0.0
7.00		0.0	0.0	0.0	0.0	0.0	0.0	0.0	0.0

Table 14. Four Circular Orbit Daily Fluence Summary Using AE-8MAX (cont.)

Orbit Altitude - 18,000 n.mi.   Accumulation Time - 4608 Hrs.   Sampling Interval - 2880 s   Units for Daily Fluence -e/cm²-day

Energy (MeV)		Daily Fluence 0° Inclination		Daily Fluence 30° Inclination		Daily Fluence 60° Inclination		Daily Fluence 90° Inclination	
E1	E2	*E1	E1-E2	*E1	E1-E2	*E1	E1-E2	*E1	E1-E2
0.0	0.25	0.550E+13	0.439E+13	0.406E+13	0.347E+13	0.222E+13	0.192E+13	0.184E+13	0.155E+13
0.25	0.50	0.110E+13	0.790E+12	0.589E+12	0.434E+12	0.294E+12	0.216E+12	0.251E+12	0.185E+12
0.50	0.75	0.313E+12	0.191E+12	0.155E+12	0.979E+11	0.780E+11	0.490E+11	0.667E+11	0.419E+11
0.75	1.00	0.122E+12	0.670E+11	0.575E+11	0.319E+11	0.290E+11	0.161E+11	0.246E+11	0.132E+11
1.00	1.25	0.546E+11	0.265E+11	0.255E+11	0.127E+11	0.129E+11	0.638E+10	0.110E+11	0.540E+10
1.25	1.50	0.280E+11	0.136E+11	0.129E+11	0.637E+10	0.651E+10	0.322E+10	0.558E+10	0.276E+10
1.50	1.75	0.144E+11	0.602E+10	0.649E+10	0.277E+10	0.330E+10	0.140E+10	0.282E+10	0.120E+10
1.75	2.00	0.839E+10	0.351E+10	0.372E+10	0.159E+10	0.189E+10	0.805E+09	0.162E+10	0.689E+09
2.00	2.25	0.489E+10	0.231E+10	0.213E+10	0.102E+10	0.109E+10	0.519E+09	0.932E+09	0.445E+09
2.25	2.50	0.258E+10	0.122E+10	0.111E+10	0.532E+09	0.568E+09	0.271E+09	0.487E+09	0.232E+09
2.50	2.75	0.136E+10	0.545E+09	0.579E+09	0.230E+09	0.297E+09	0.118E+09	0.255E+09	0.101E+09
2.75	3.00	0.816E+09	0.727E+09	0.349E+09	0.139E+09	0.179E+09	0.712E+08	0.154E+09	0.610E+08
3.00	3.25	0.500E+09	0.189E+09	0.211E+09	0.799E+08	0.108E+09	0.411E+08	0.926E+08	0.352E+08
3.25	3.50	0.300E+09	0.116E+09	0.131E+09	0.495E+08	0.669E+08	0.254E+08	0.573E+08	0.218E+08
3.50	3.75	0.184E+09	0.855E+08	0.813E+08	0.368E+08	0.415E+08	0.188E+08	0.355E+08	0.161E+08
3.75	4.00	0.987E+08	0.458E+08	0.446E+08	0.201E+08	0.227E+08	0.102E+08	0.194E+08	0.878E+07
4.00	4.25	0.529E+08	0.262E+08	0.245E+08	0.120E+08	0.124E+08	0.612E+07	0.106E+08	0.524E+07
4.25	4.50	0.267E+08	0.132E+08	0.125E+08	0.612E+07	0.631E+07	0.310E+07	0.540E+07	0.266E+07
4.50	4.75	0.134E+08	0.105E+08	0.634E+07	0.504E+07	0.321E+07	0.254E+07	0.274E+07	0.217E+07
4.75	5.00	0.289E+07	0.227E+07	0.130E+07	0.105E+07	0.666E+06	0.537E+06	0.570E+06	0.455E+06
5.00	5.25	0.623E+06	0.497E+06	0.250E+06	0.209E+06	0.129E+06	0.107E+06	0.111E+06	0.919E+05
5.25	5.50	0.126E+06	0.0	0.413E+05	0.0	0.222E+05	0.0	0.193E+05	0.0
5.50	5.75	0.0	0.0	0.0	0.0	0.0	0.0	0.0	0.0
5.75	6.00	0.0	0.0	0.0	0.0	0.0	0.0	0.0	0.0
6.00	6.25	0.0	0.0	0.0	0.0	0.0	0.0	0.0	0.0
6.25	6.50	0.0	0.0	0.0	0.0	0.0	0.0	0.0	0.0
6.50	6.75	0.0	0.0	0.0	0.0	0.0	0.0	0.0	0.0
6.75	7.00	0.0	0.0	0.0	0.0	0.0	0.0	0.0	0.0
7.00		0.0		0.0		0.0		0.0	

Figures

Figure 1. Local Time Variations for E > 1.5 MeV
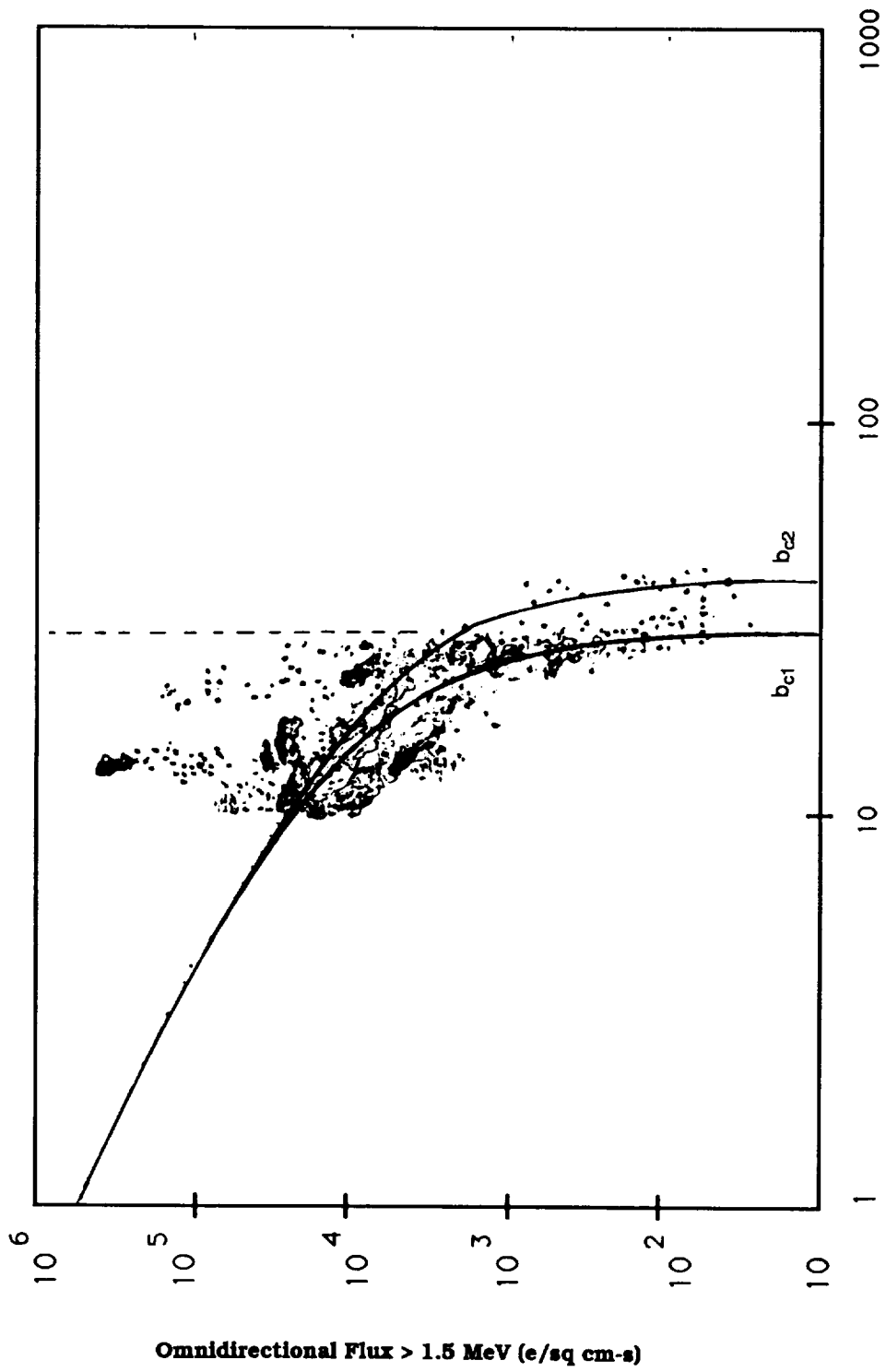
Figure 2. Azur Data at L = 3.0 and the Determination of Atmospheric Cutoffs

Omnidirectional Flux > 1.5 MeV (e/sq cm-s)

Omnidirectional Flux > 1.5 MeV (e/sq cm-s)
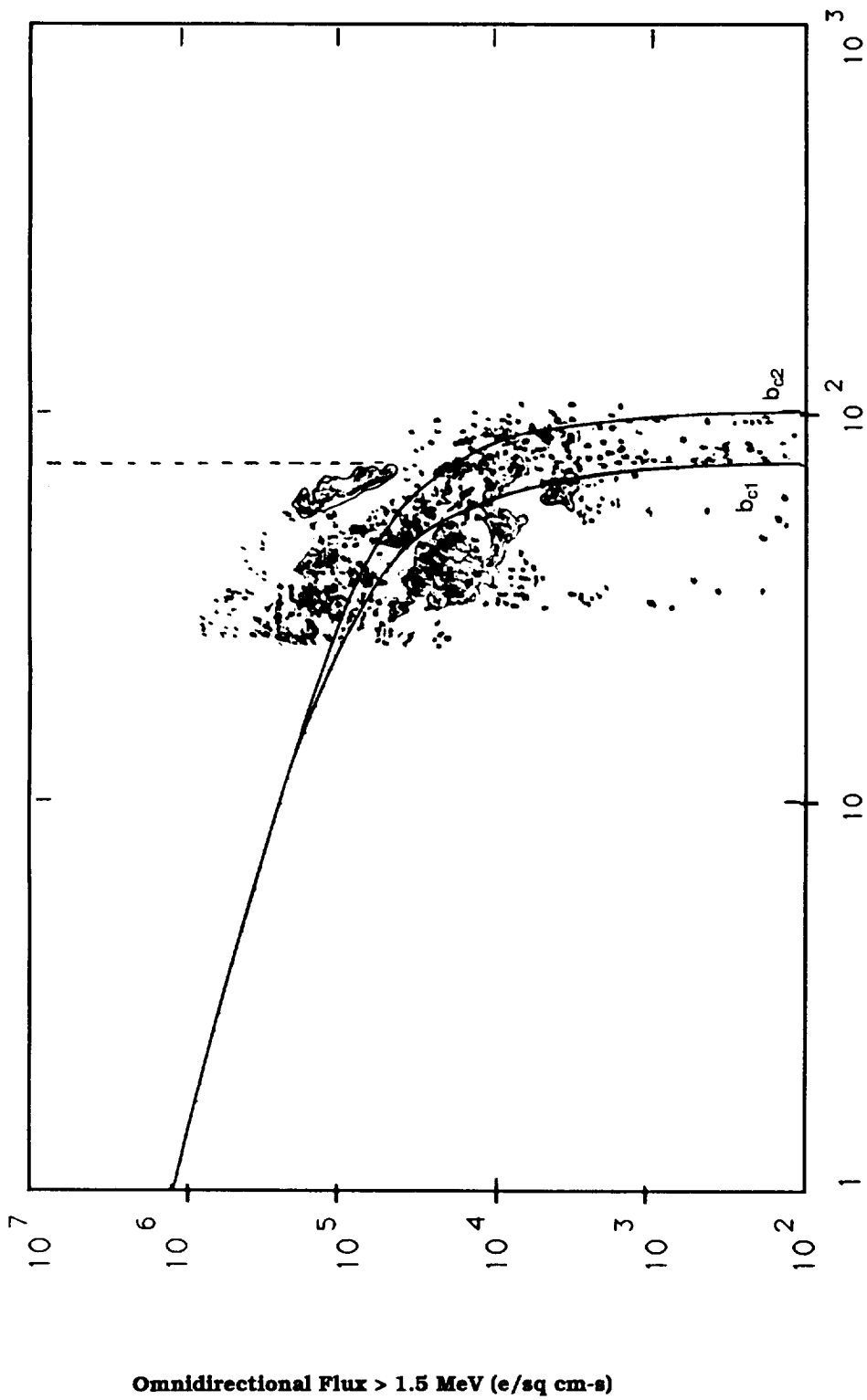
Figure 3. Azur Data at L = 4.0 and the Determination of Atmospheric Cutoffs
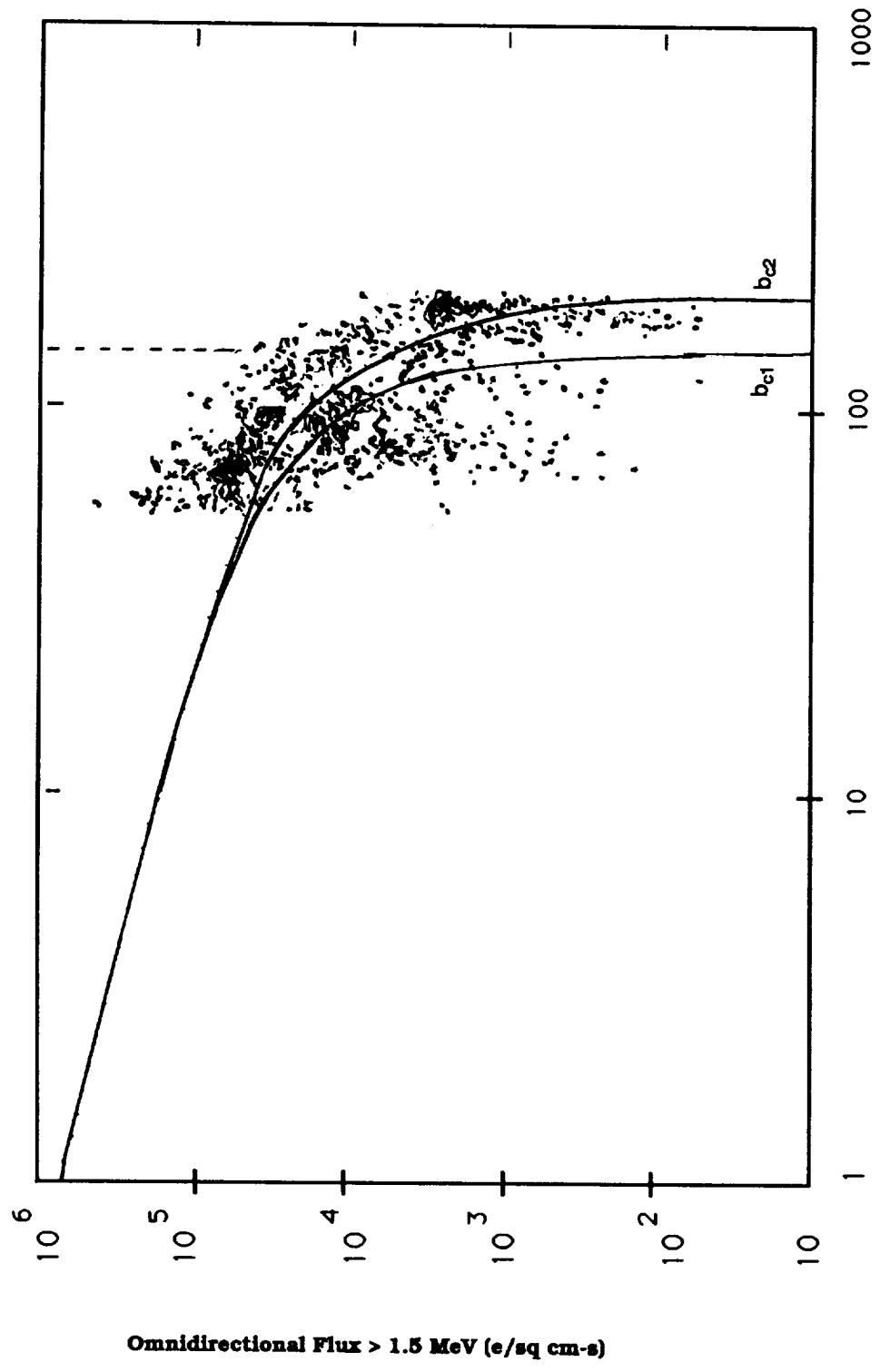
Figure 4. Azur Data at L = 5.0 and the Determination of Atmospheric Cutoffs

Omnidirectional Flux > 1.5 MeV (e/sq cm-s)
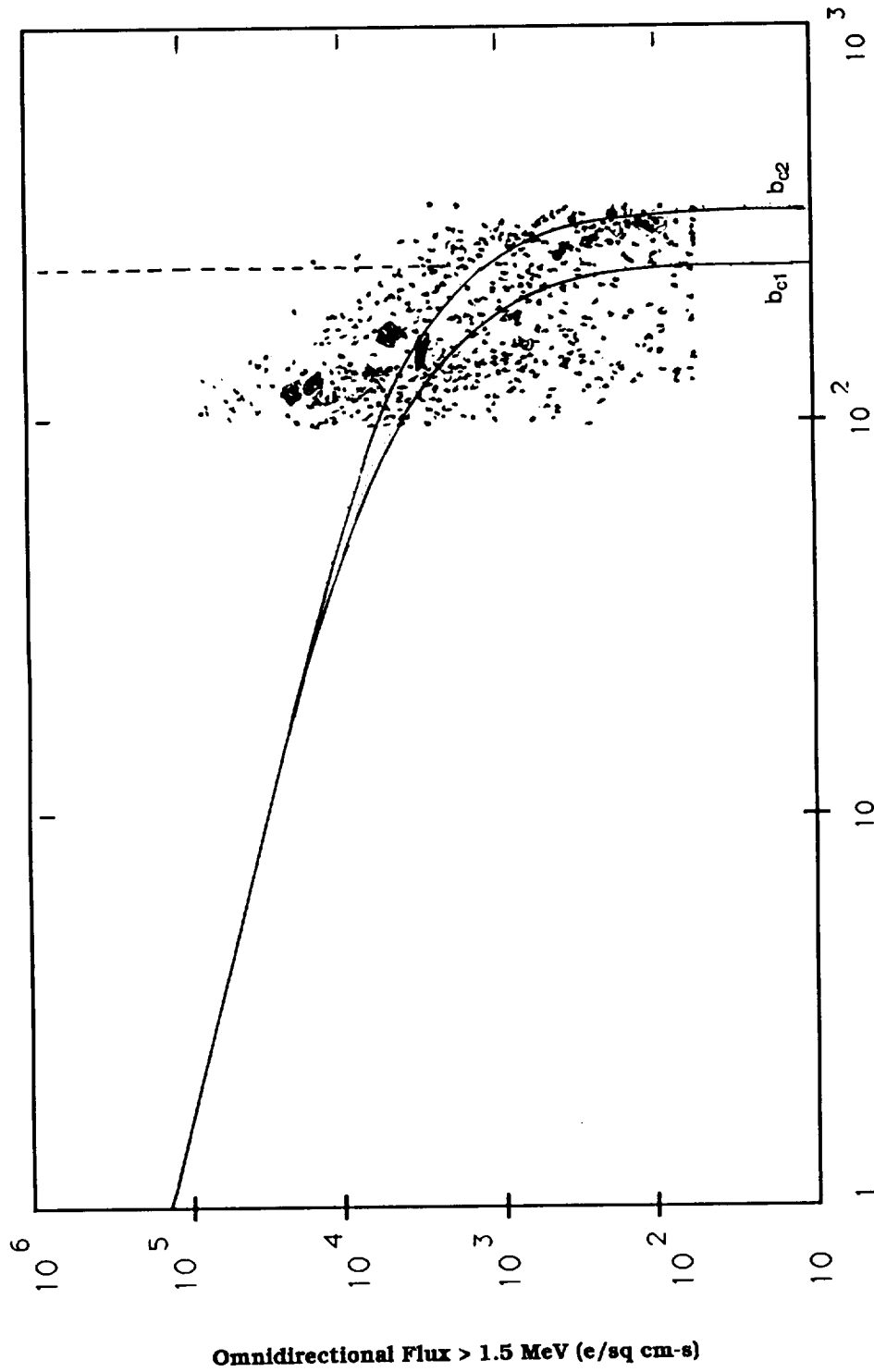
Figure 5. Azur Data at L = 6.0 and the Determination of Atmospheric Cutoffs

F-5
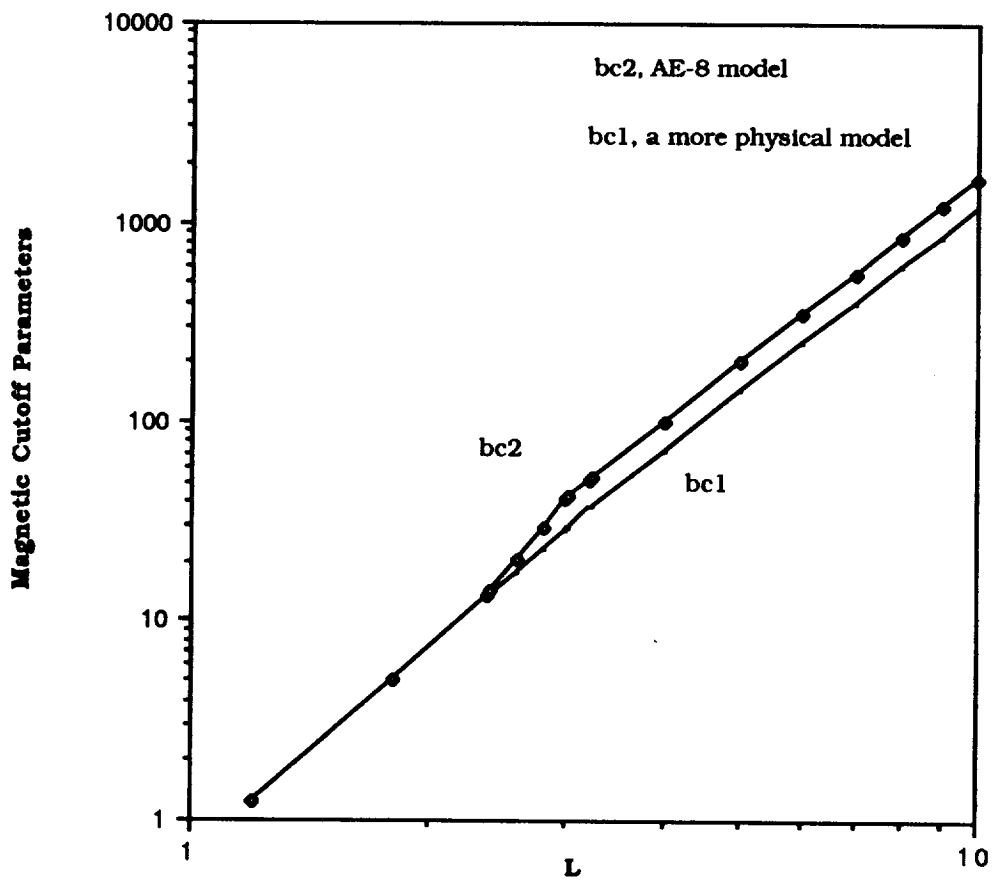
Figure 6. Magnetic (Atmospheric) Cutoff Models
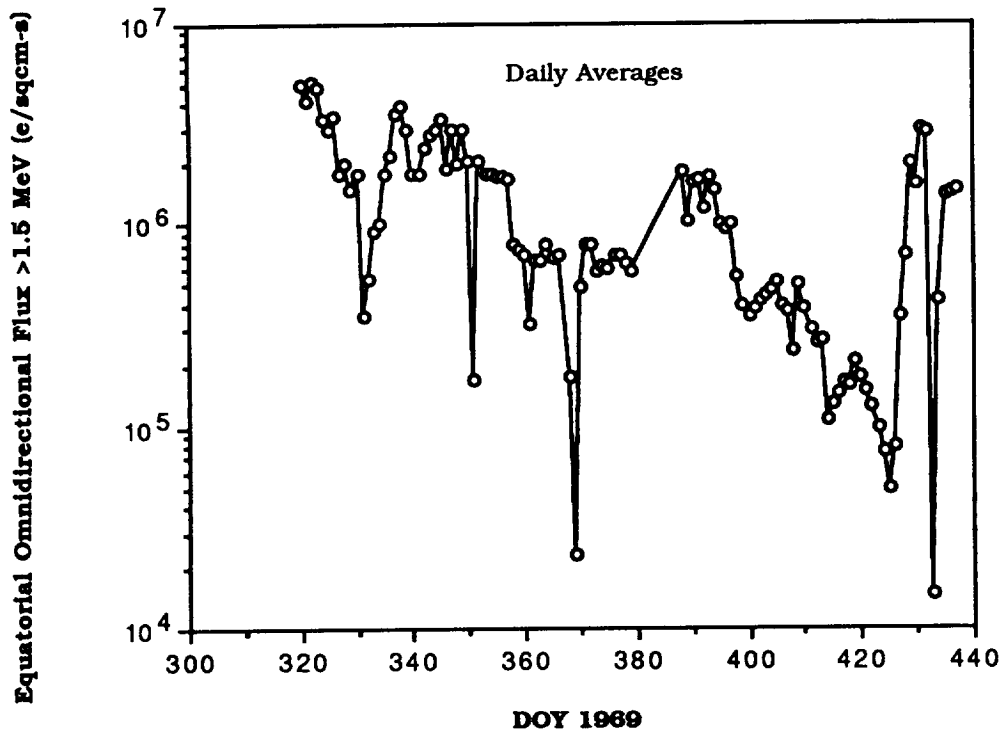
Figure 7. Azur Data Greater Than 1.5 MeV Versus Time at L = 4.4
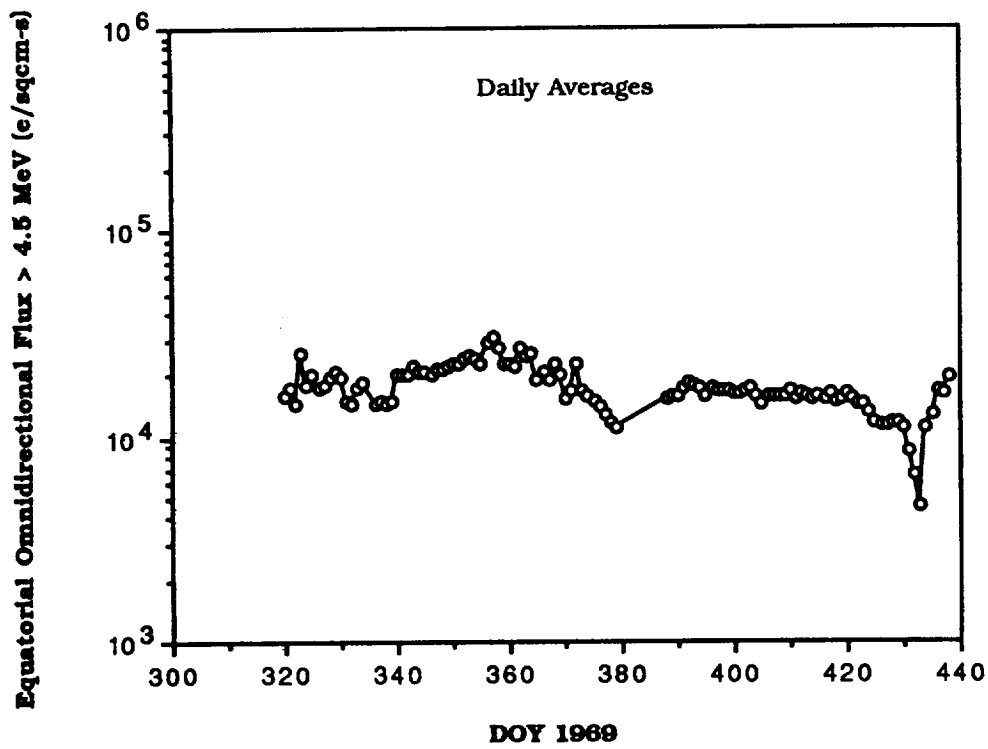
Figure 8. Azur Data Greater Than 4.5 MeV Versus Time at L = 3.0
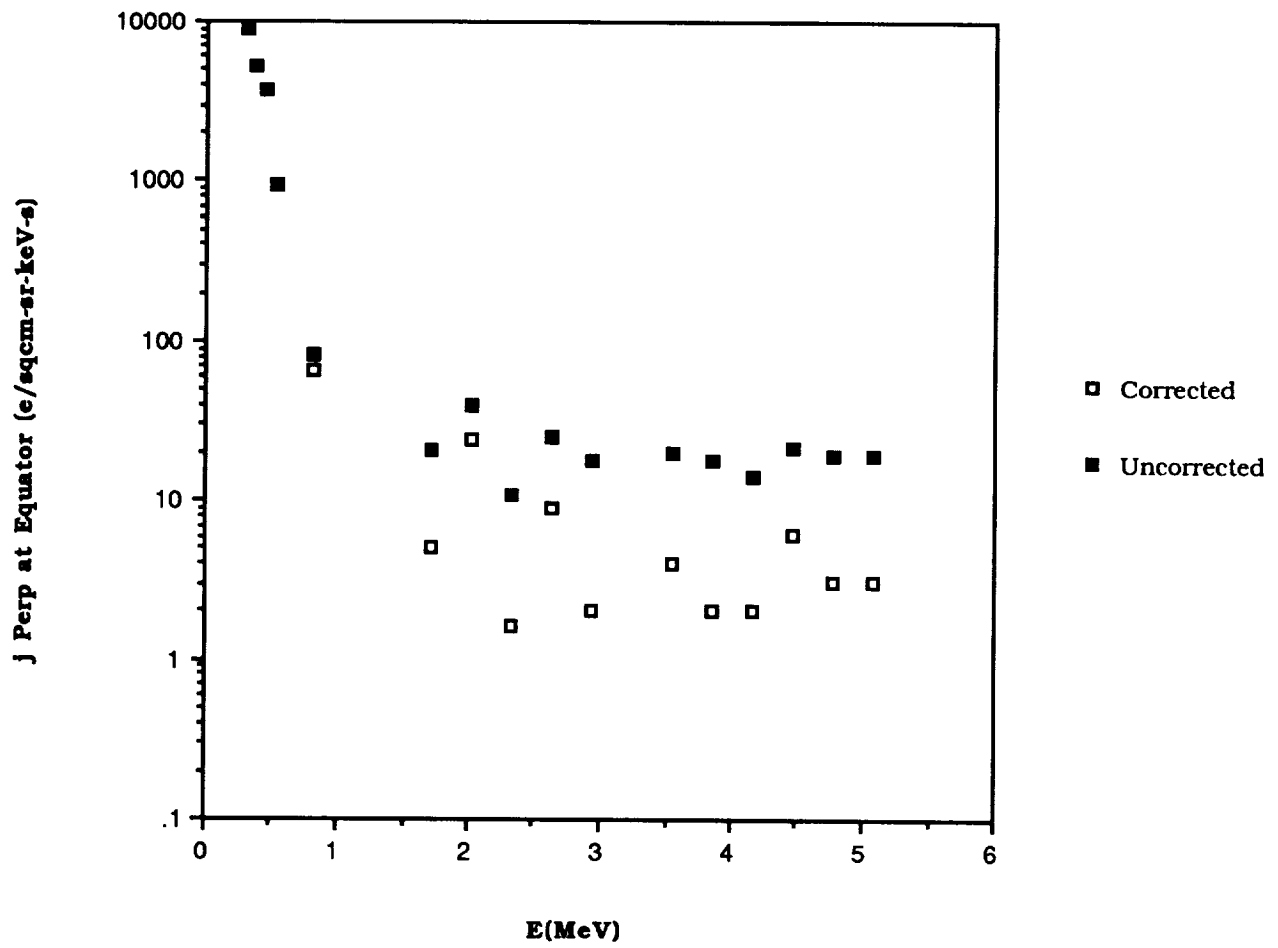
Figure 9. OV1-19 Data at L = 3
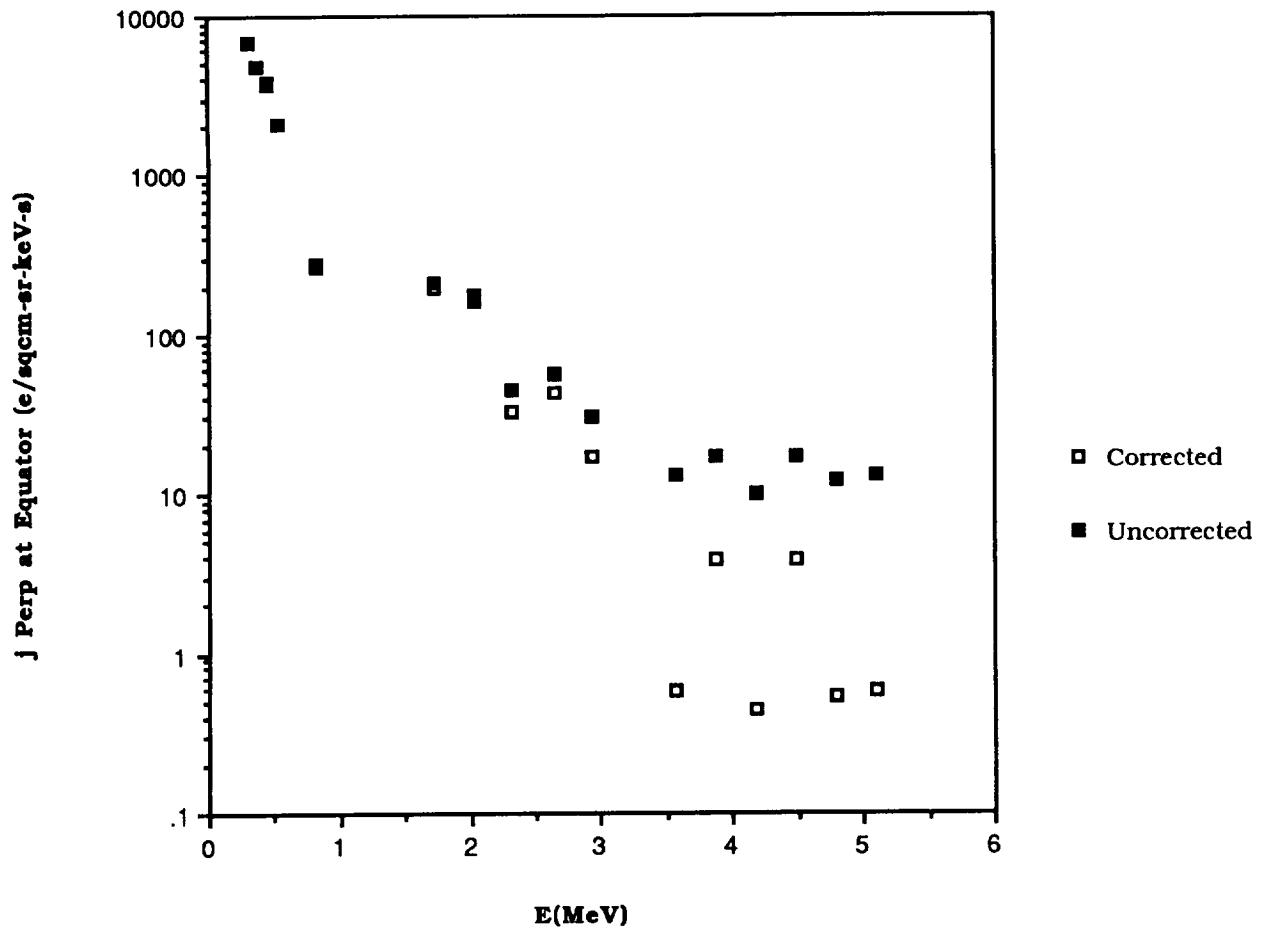
Figure 10. OV1-19 Data at L = 4.5
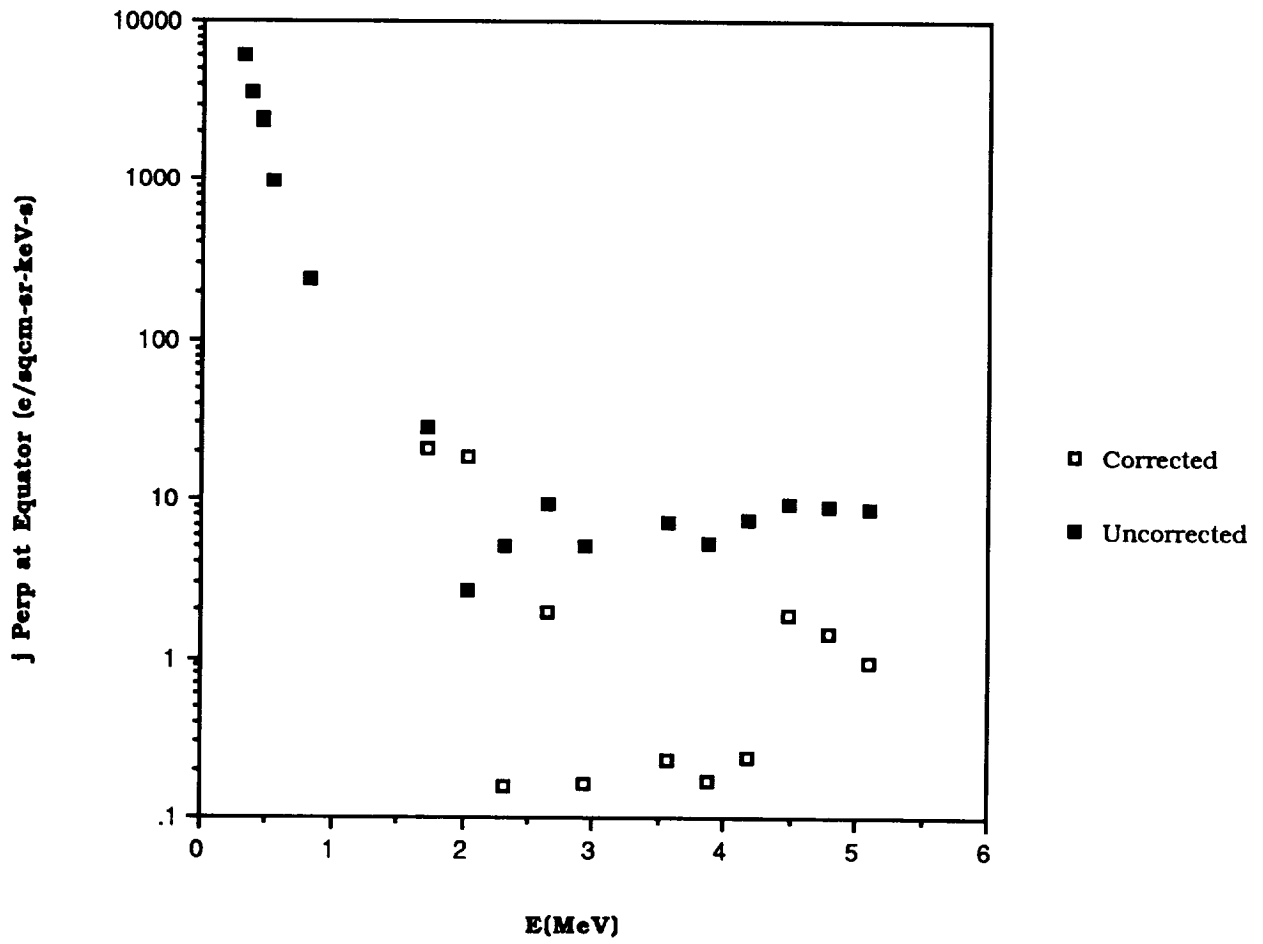
Figure 11. OV1-19 Data at L = 6.0
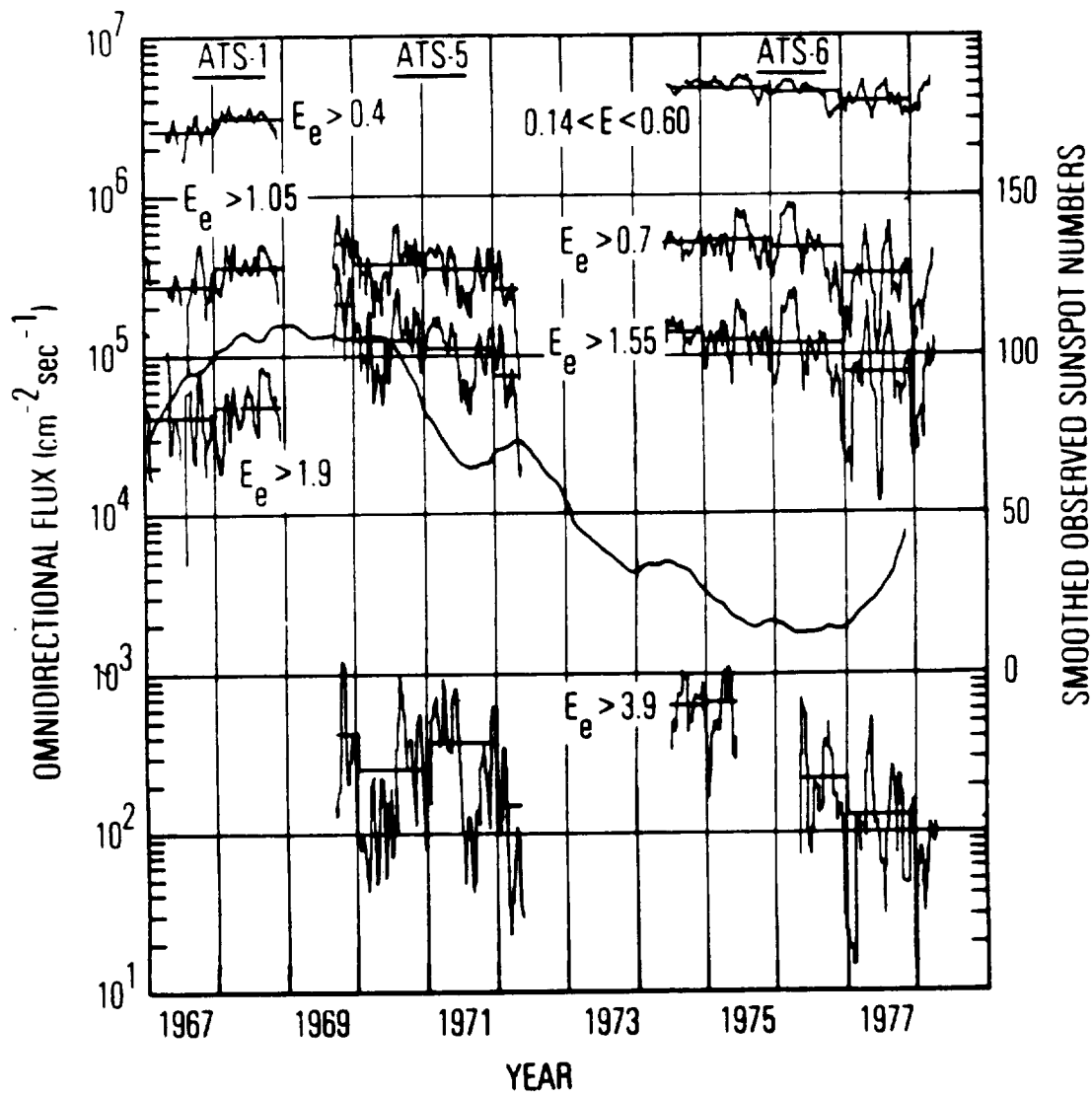
Figure 12. ATS Long-Term Electron Observations at L ~ 6.6

C-2
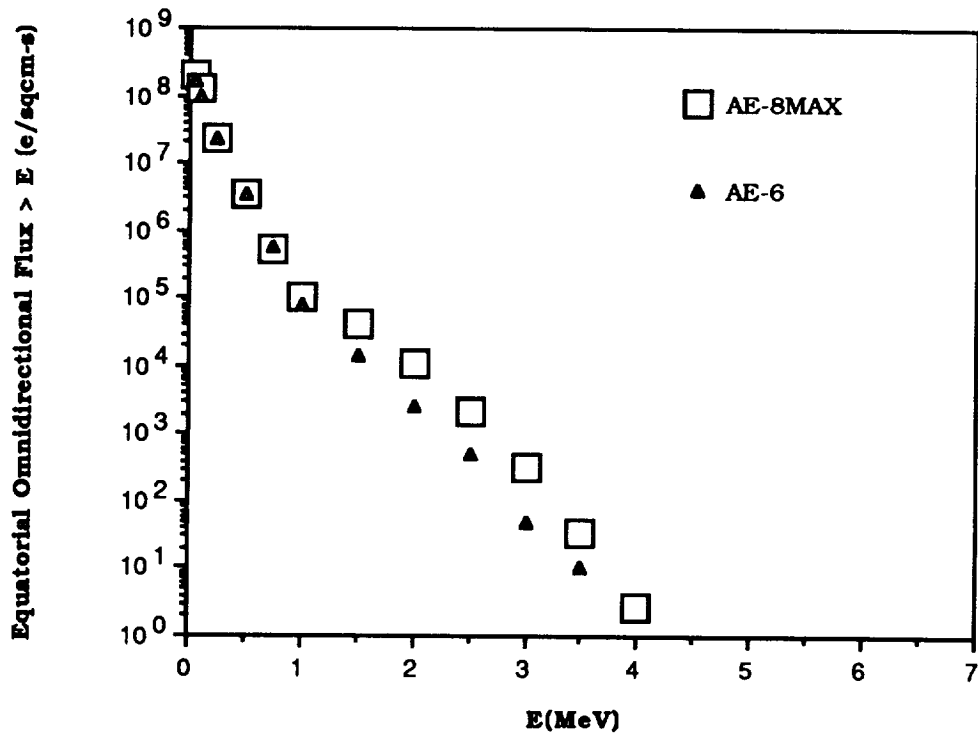
Figure 13a. Comparison of SOLMAX Models at L = 2.5
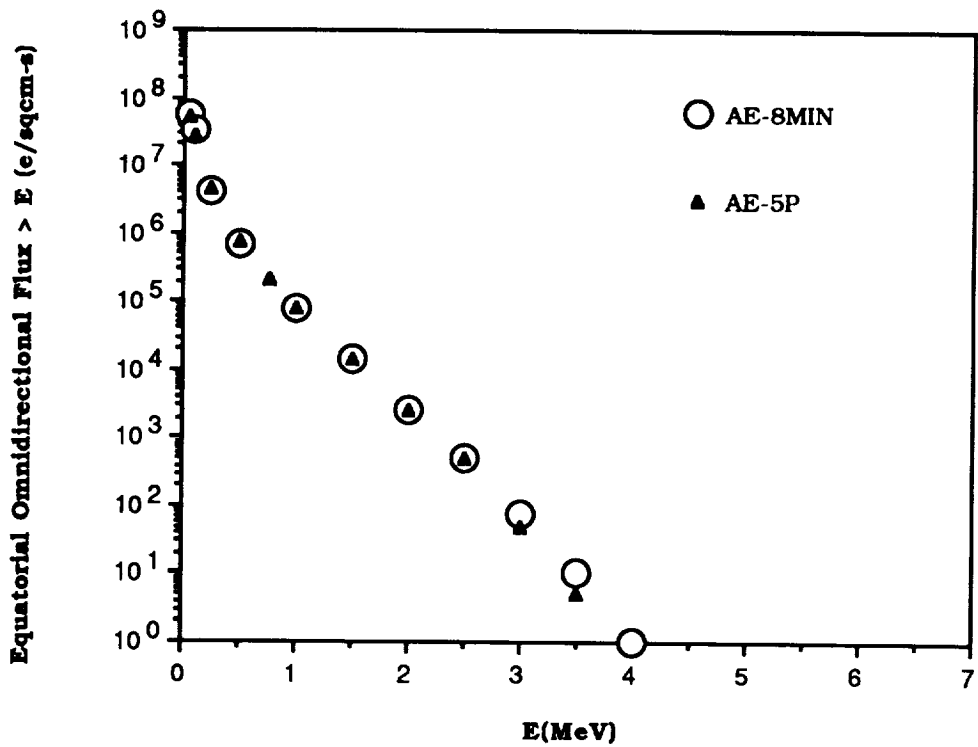
Figure 13b. Comparison of SOLMIN Models at L = 2.5
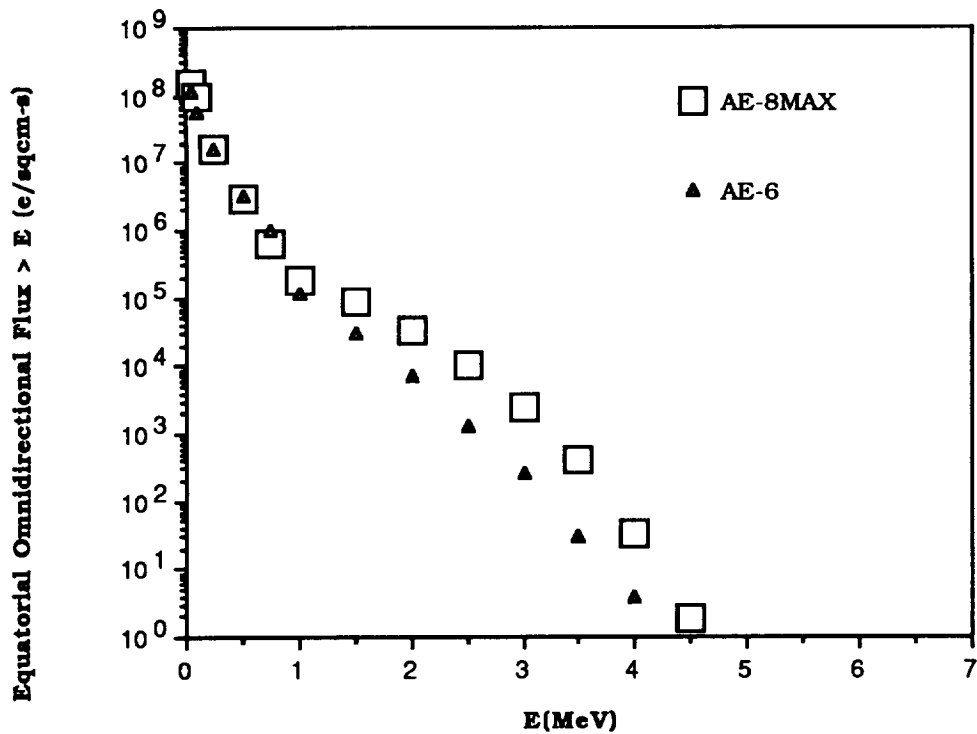
Figure 14a. Comparison of SOLMAX Models at L = 2.6
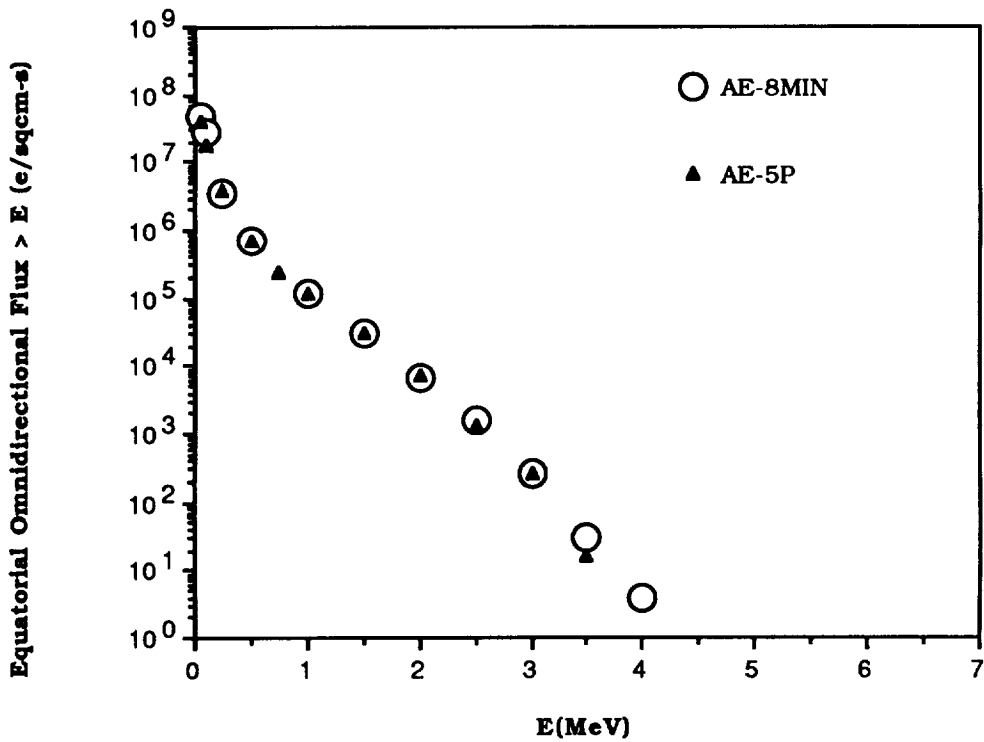
Figure 14b. Comparison of SOLMIN Models at L = 2.6
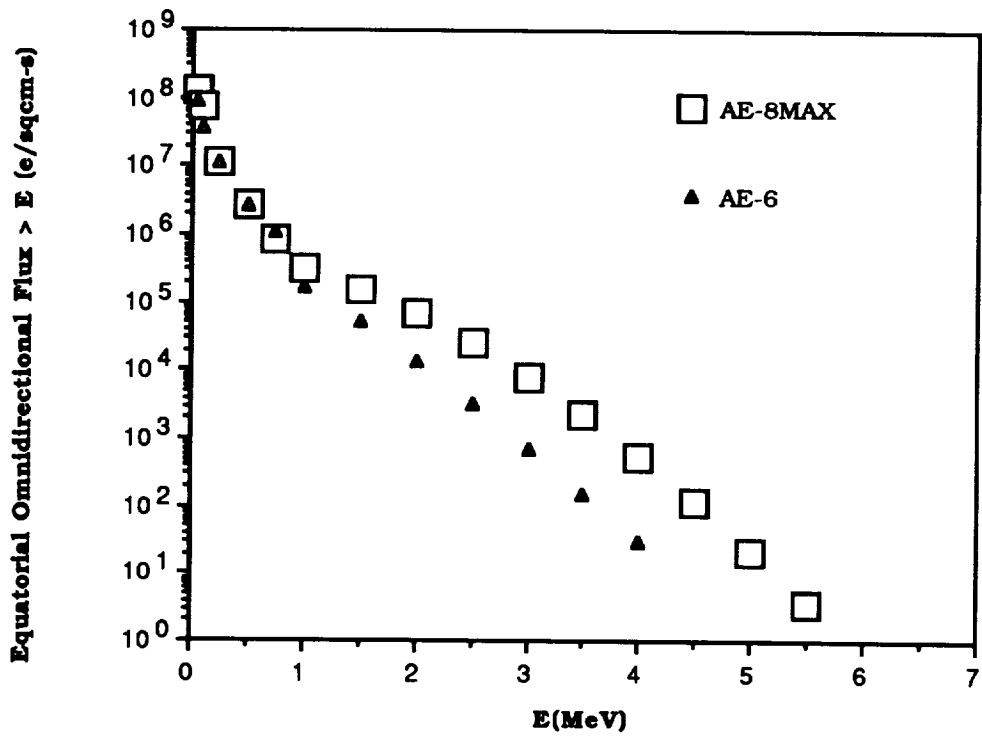
Figure 15a. Comparison of SOLMAX Models at L = 2.7
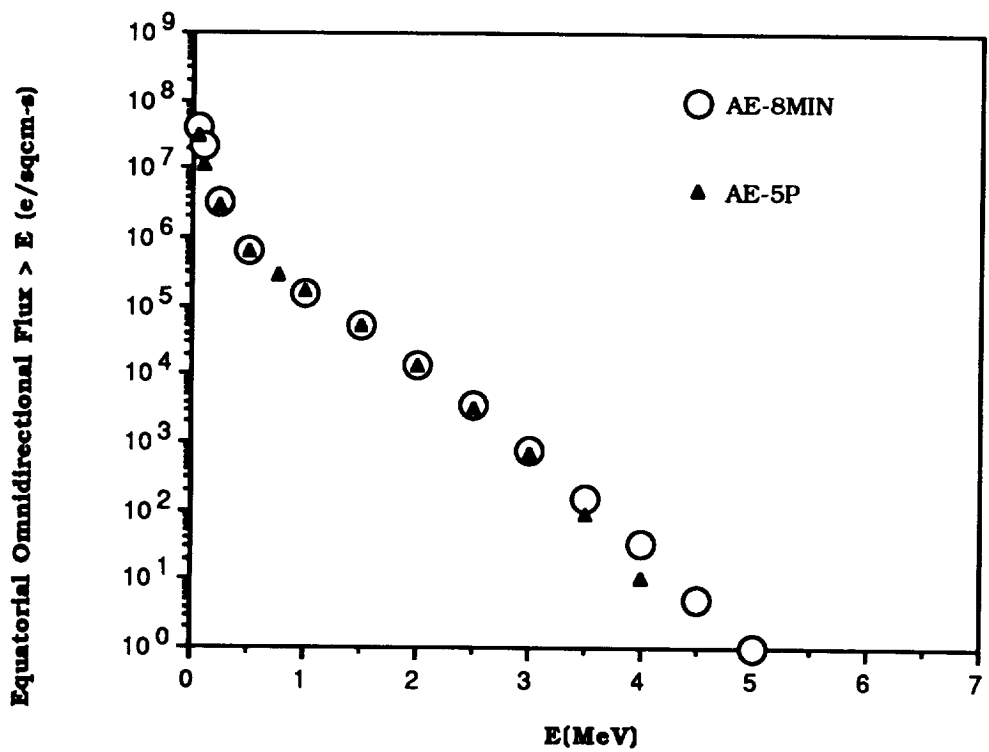
Figure 15b. Comparison of SOLMIN Models at L = 2.7
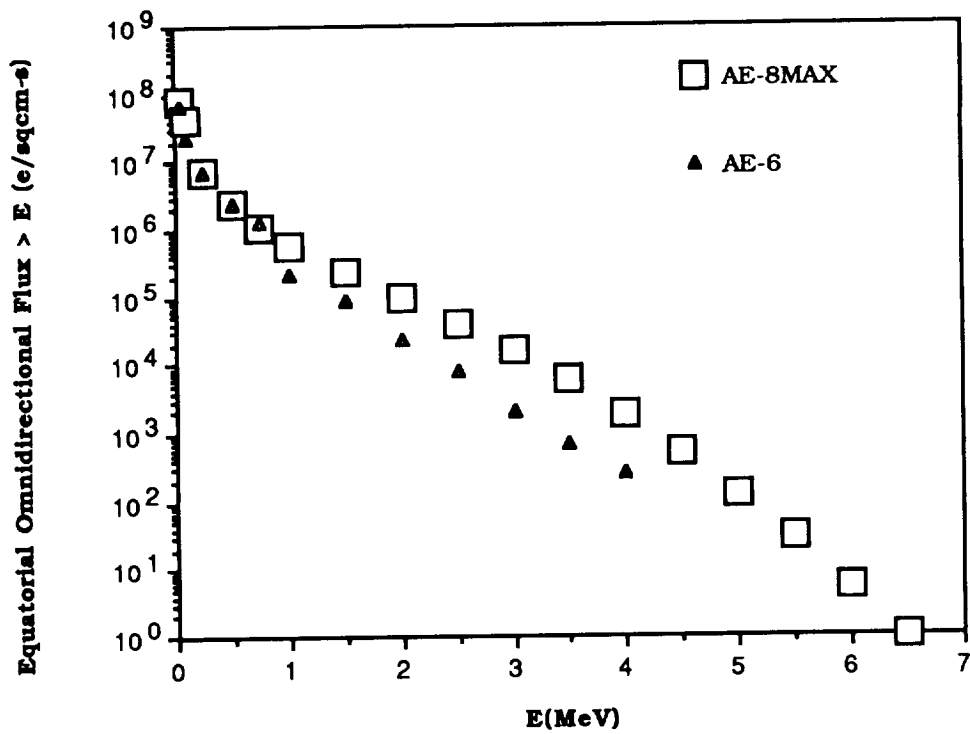
Figure 16a. Comparison of SOLMAX Models at L = 2.8
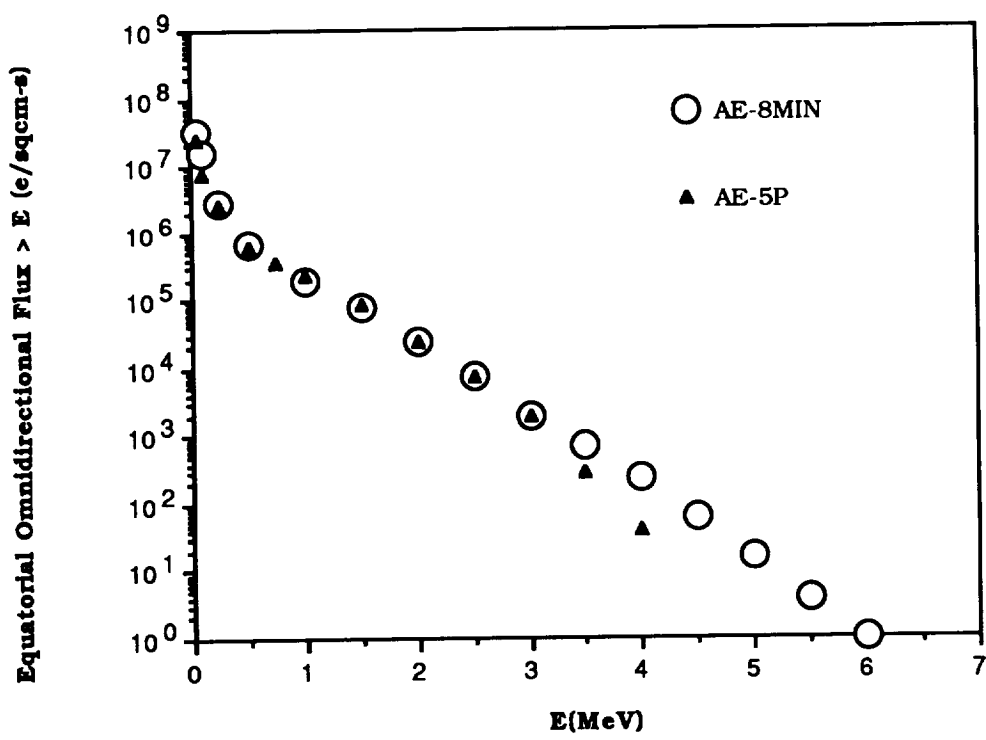
Figure 16b. Comparison of SOLMIN Models at L = 2.8
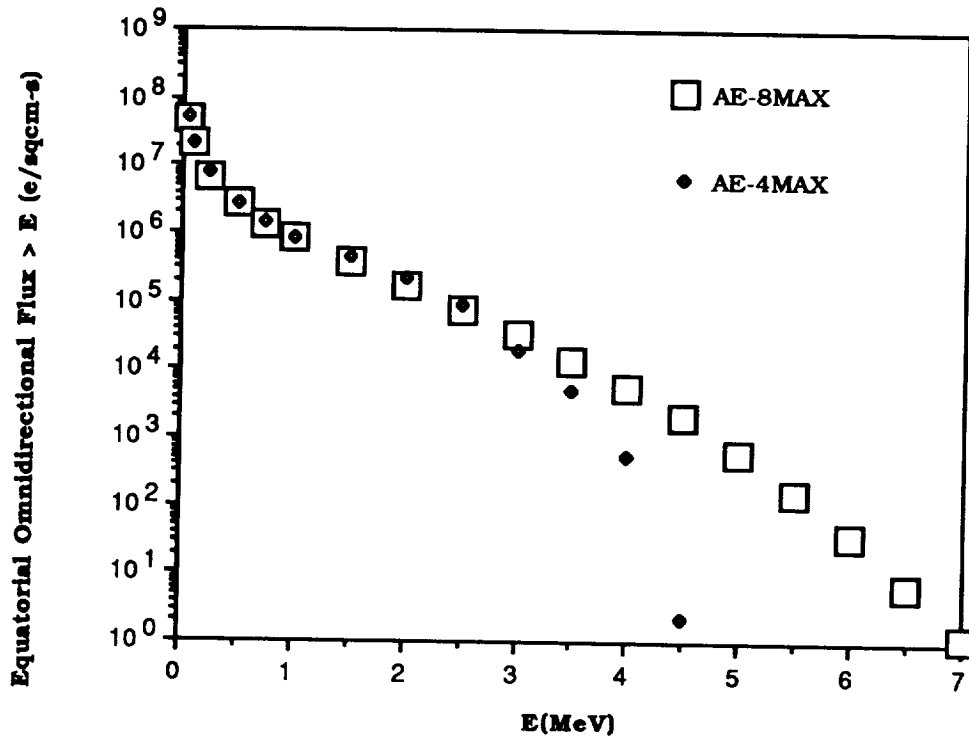
Figure 17a. Comparison of SOLMAX Models at L = 2.9
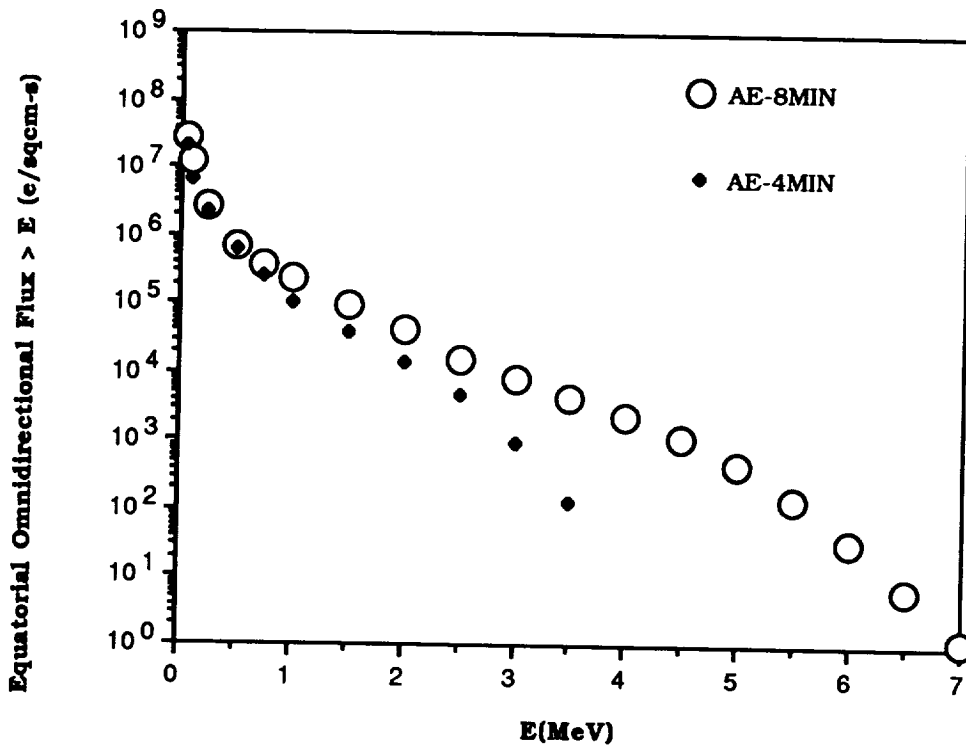
Figure 17b. Comparison of SOLMIN Models at L = 2.9
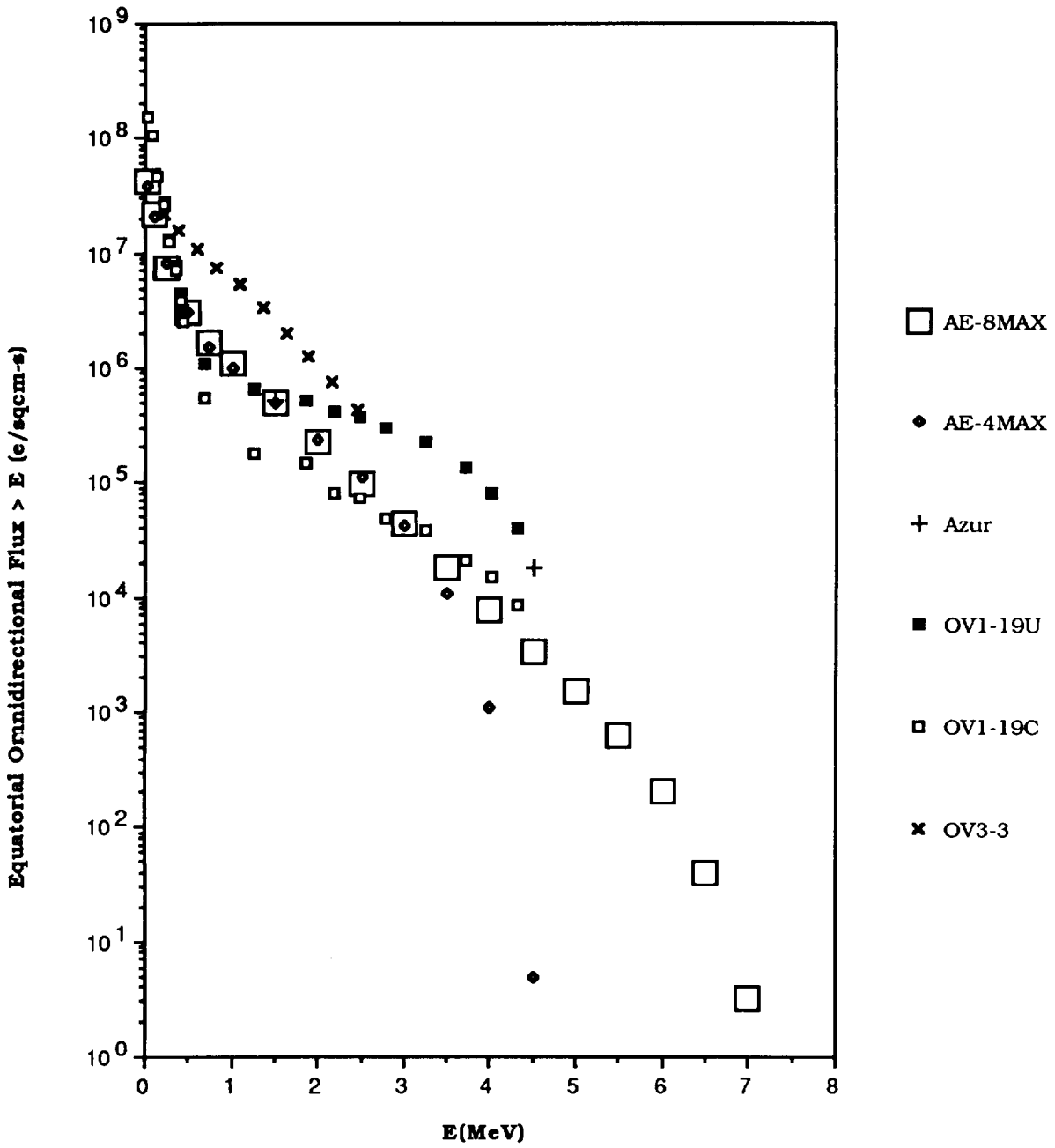
Figure 18. Comparison of AE-8MAX with Outer Zone Data at L = 3.0
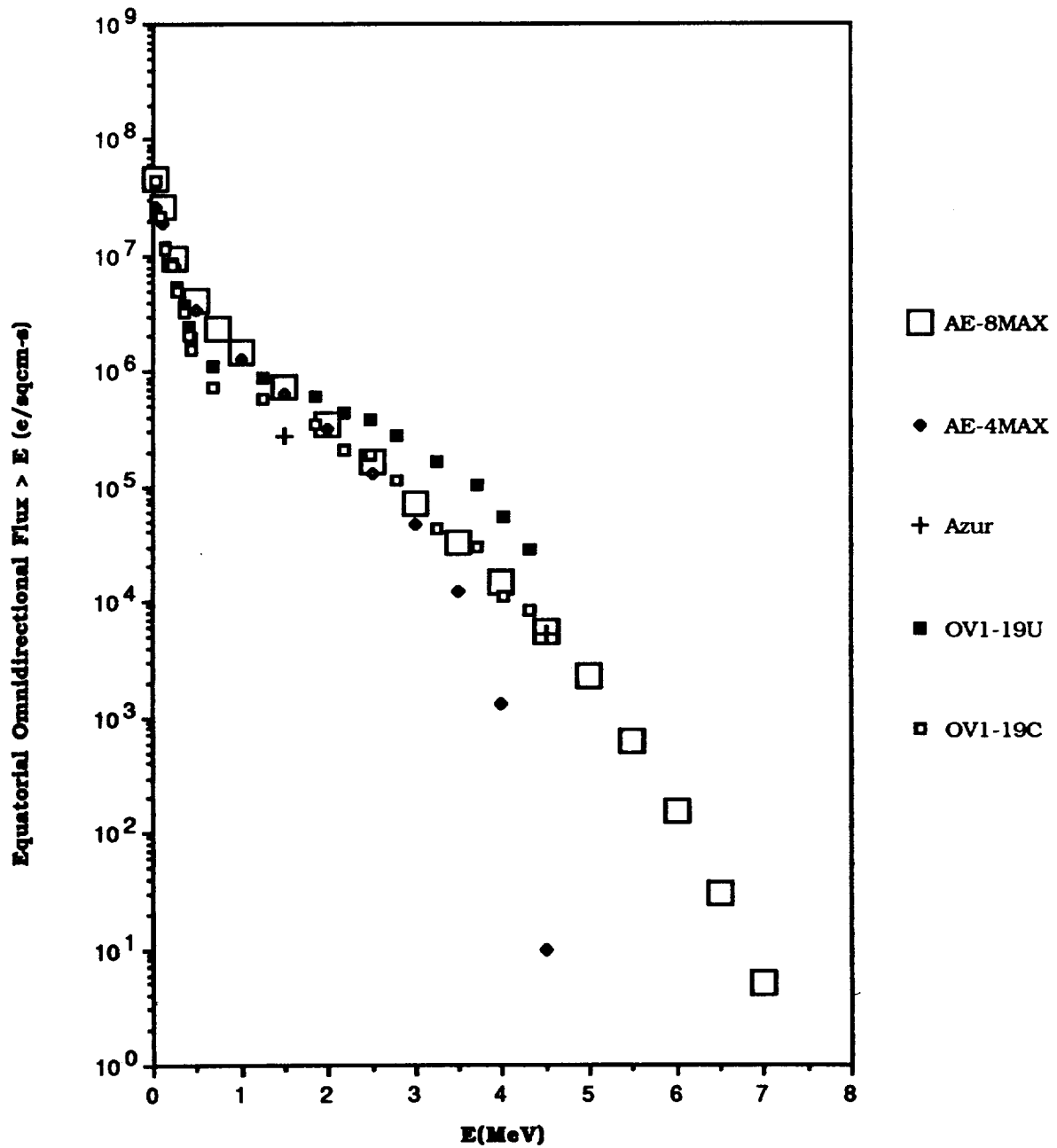
Figure 19. Comparison of AE-8MAX with Outer Zone Data at L = 3.2
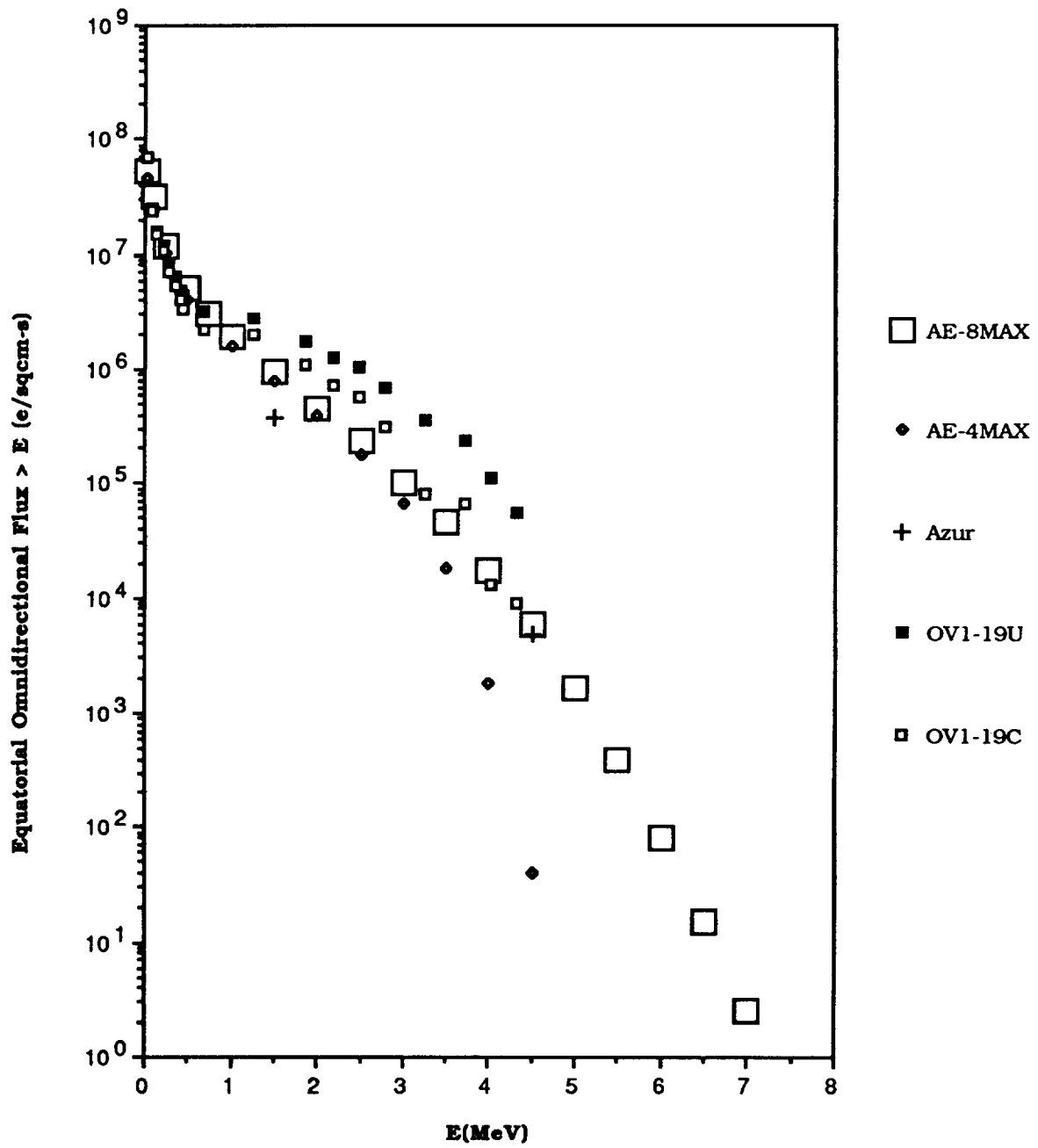
Figure 20. Comparison of AE-8MAX with Outer Zone Data at L = 3.4
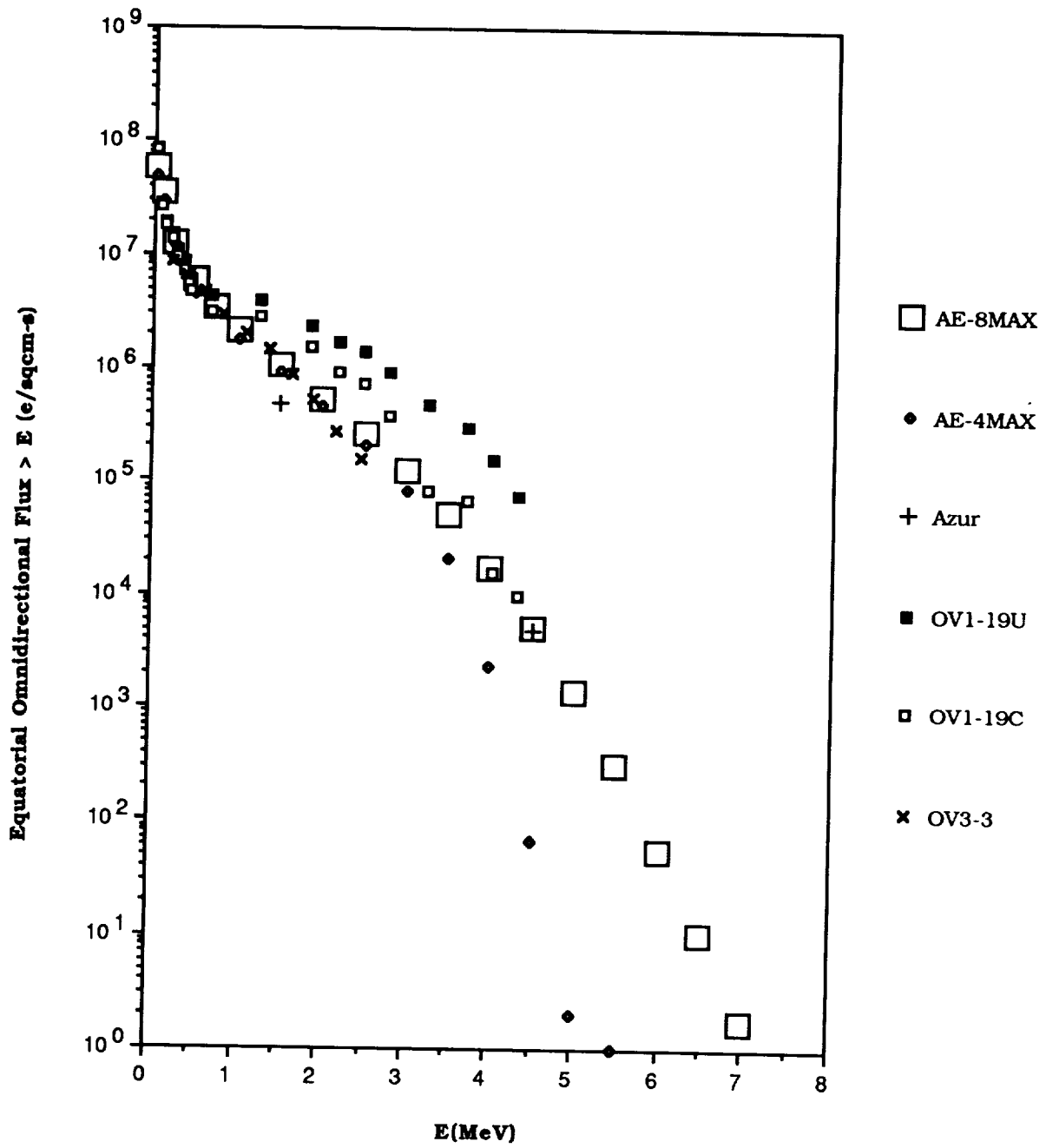
Figure 21. Comparison of AE-8MAX with Outer Zone Data at L = 3.5
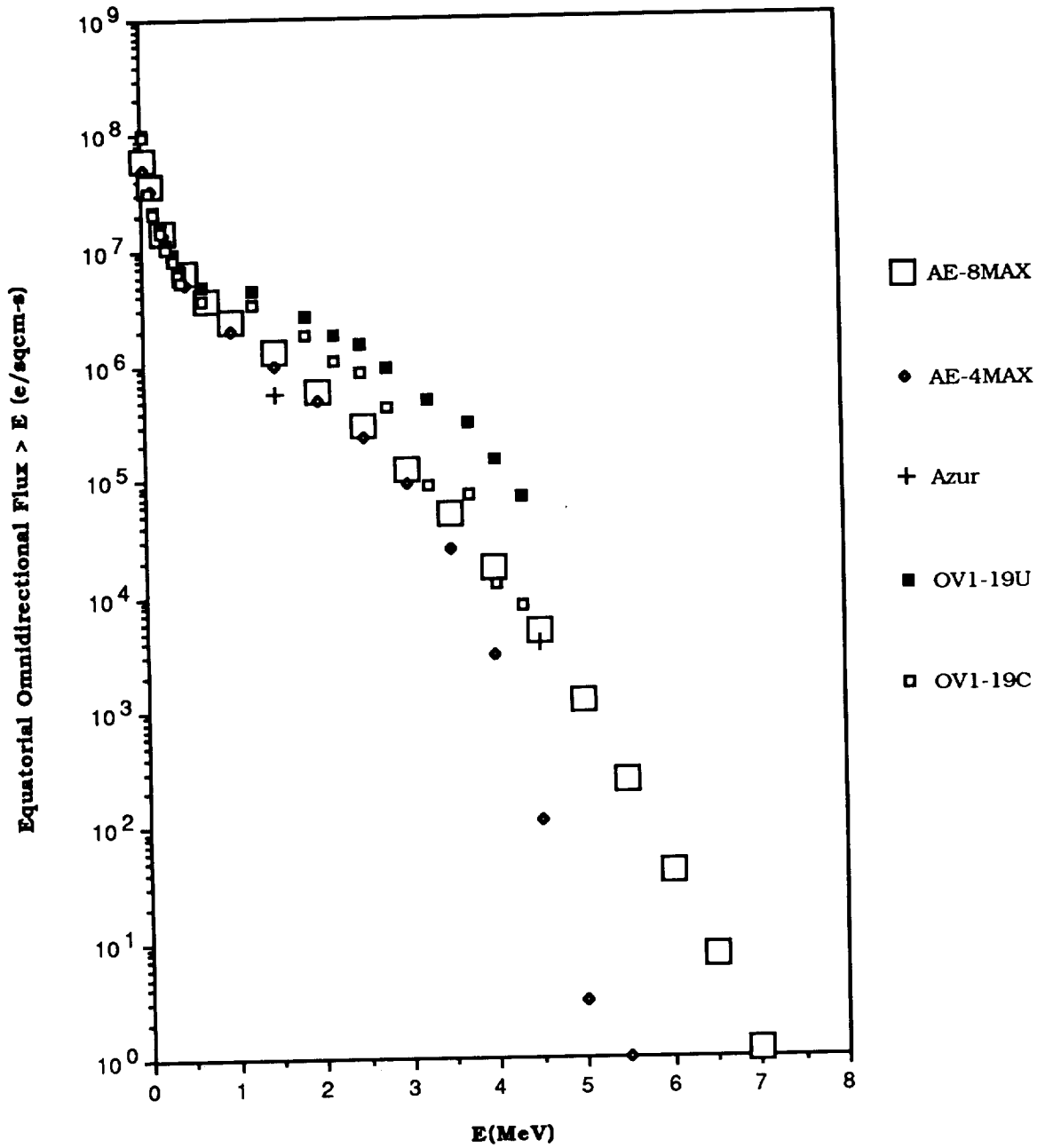
Figure 22. Comparison of AE-8MAX with Outer Zone Data at L = 3.6
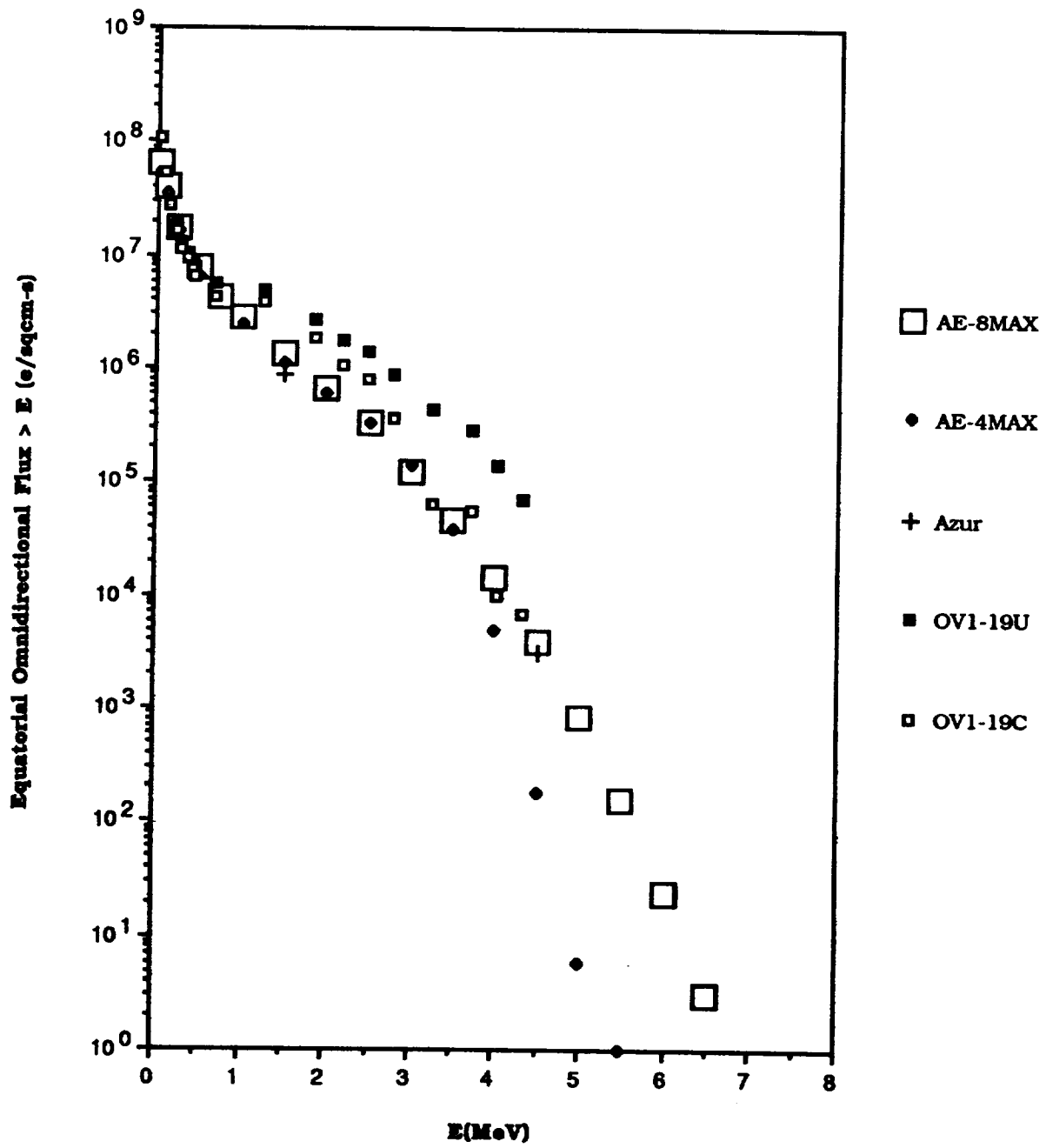
Figure 23. Comparison of AE-8MAX with Outer Zone Data at L = 3.8
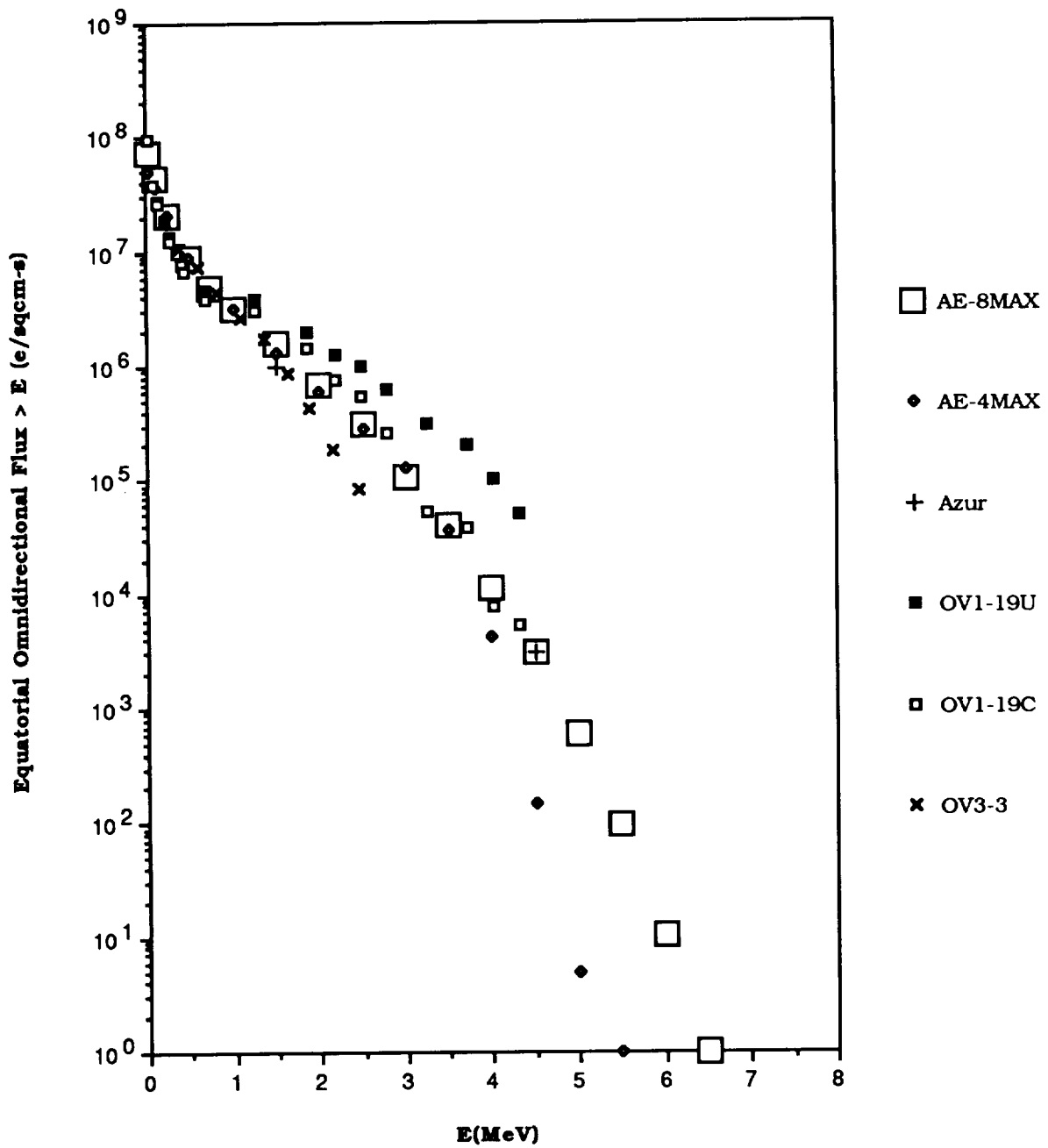
Figure 24. Comparison of AE-8MAX with Outer Zone Data at L = 4.0
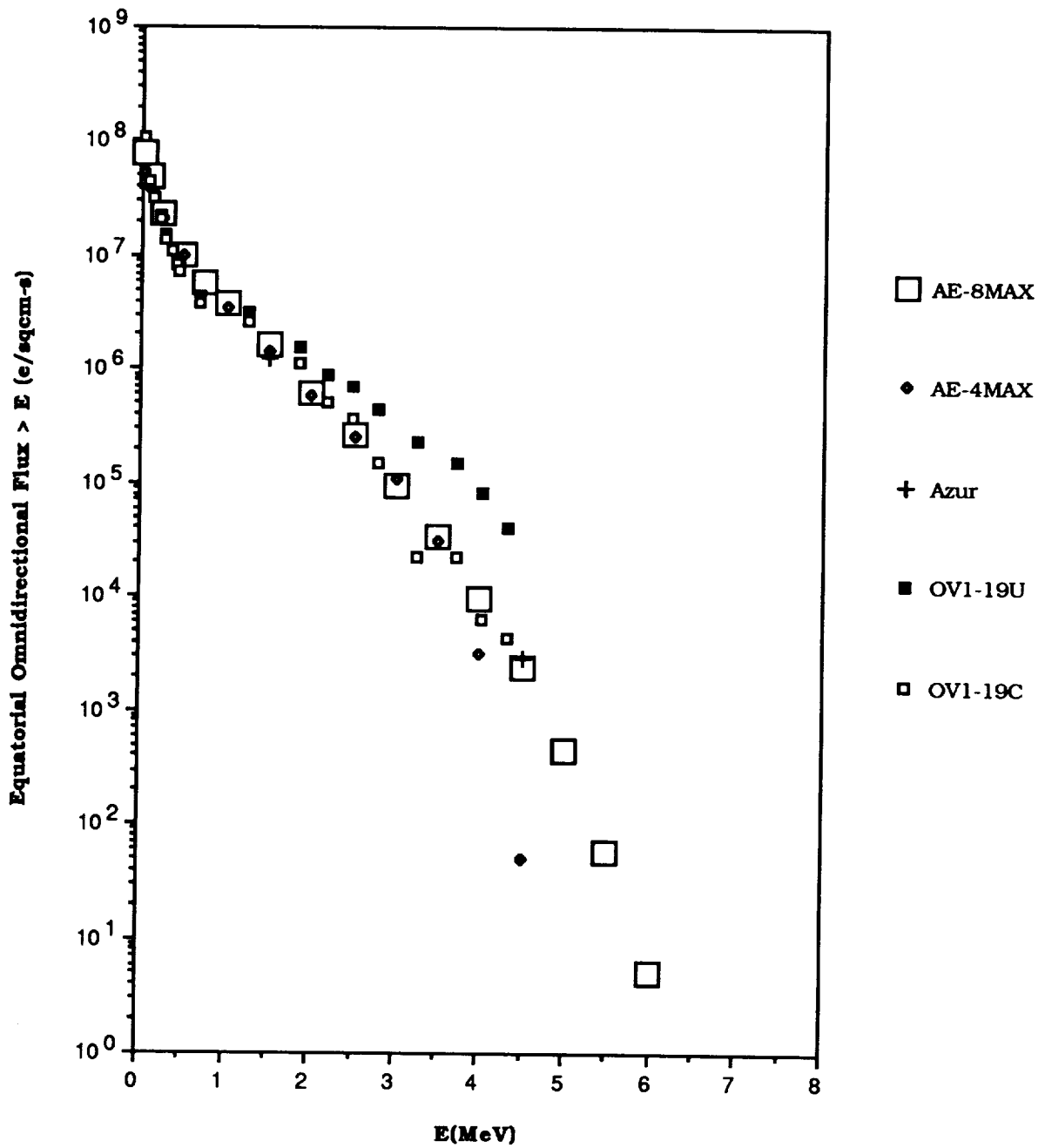
Figure 25. Comparison of AE-8MAX with Outer Zone Data at L = 4.2
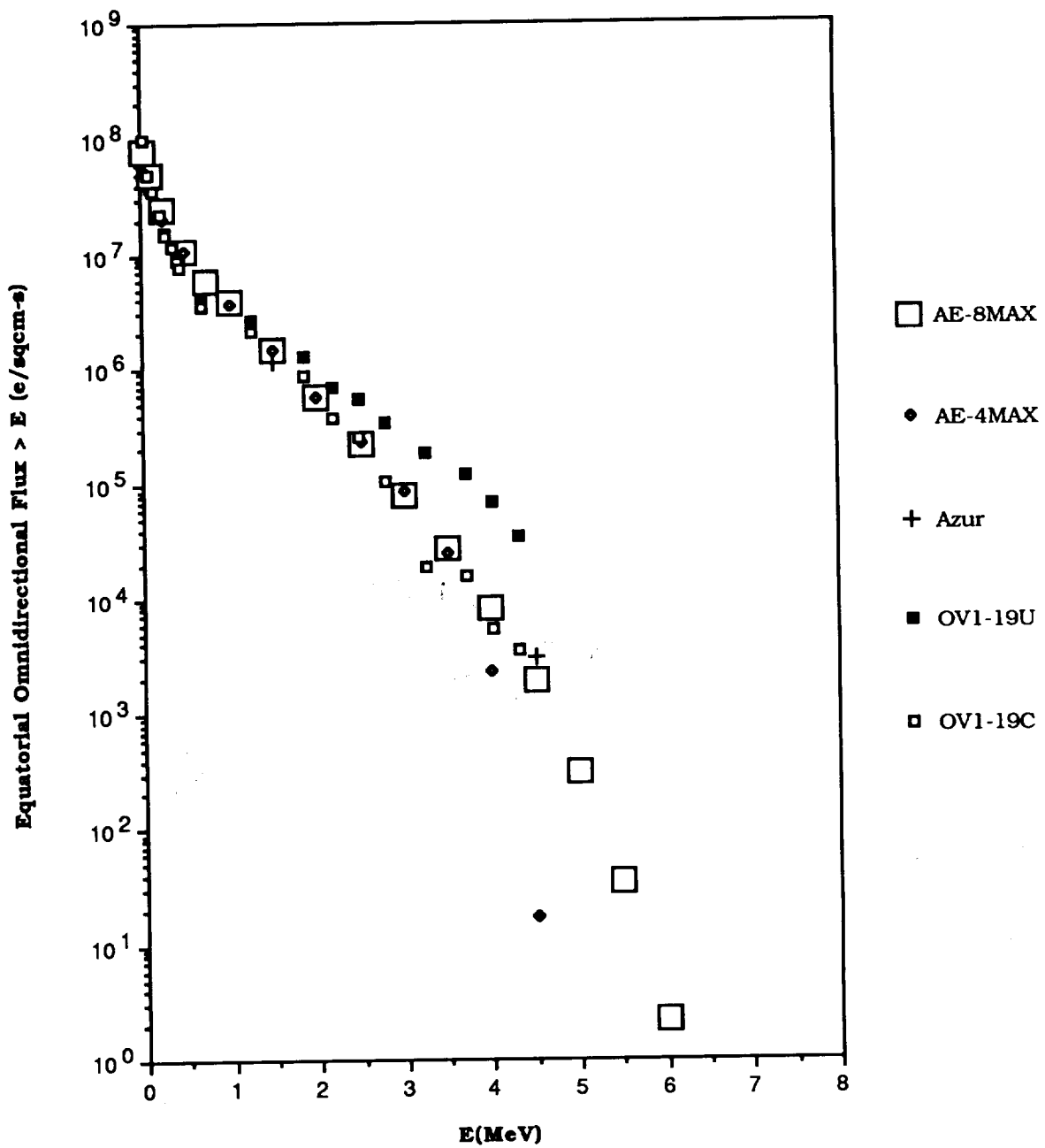
Figure 26. Comparison of AE-8MAX with Outer Zone Data at L = 4.4
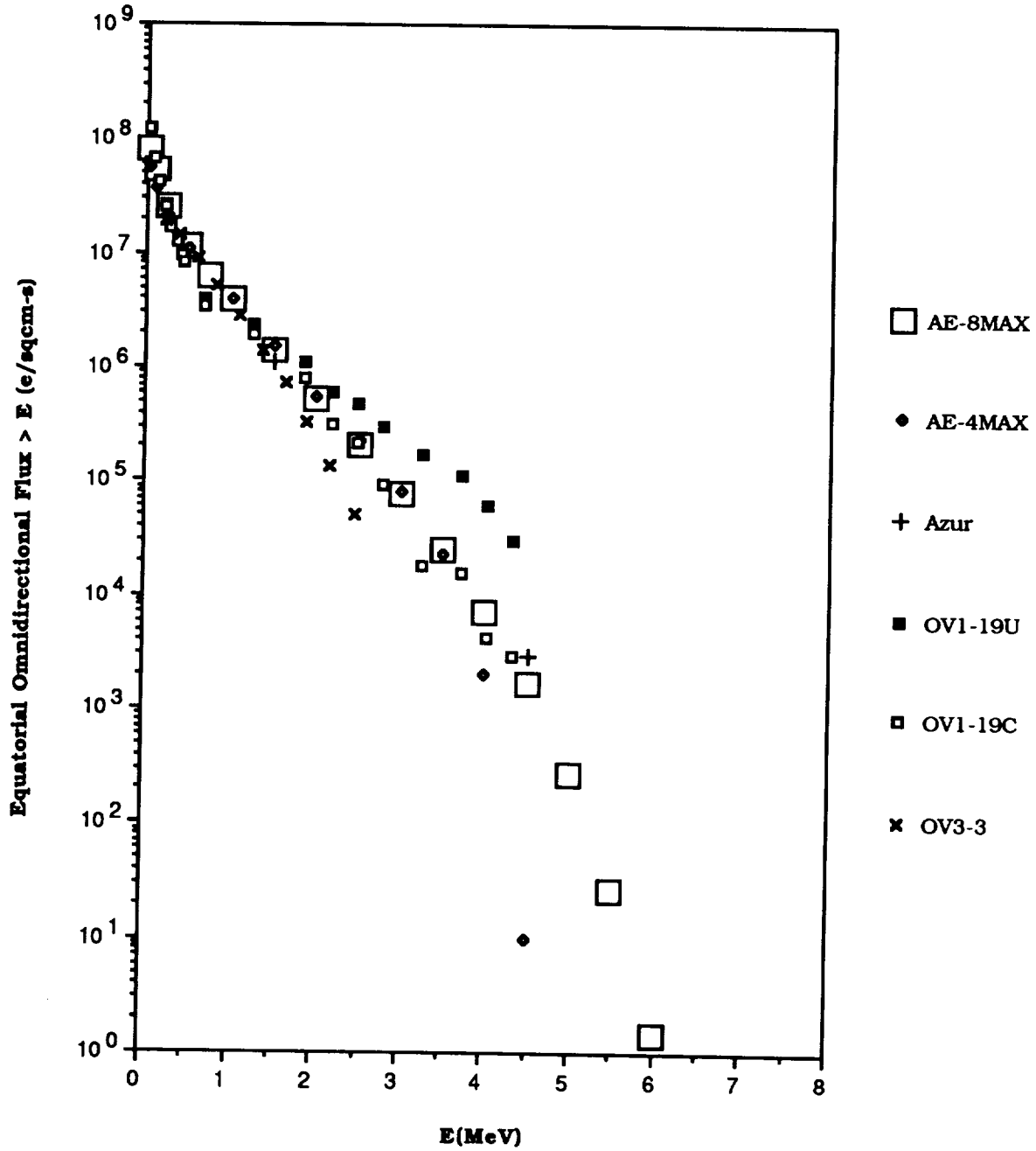
Figure 27. Comparison of AE-8MAX with Outer Zone Data at L = 4.5
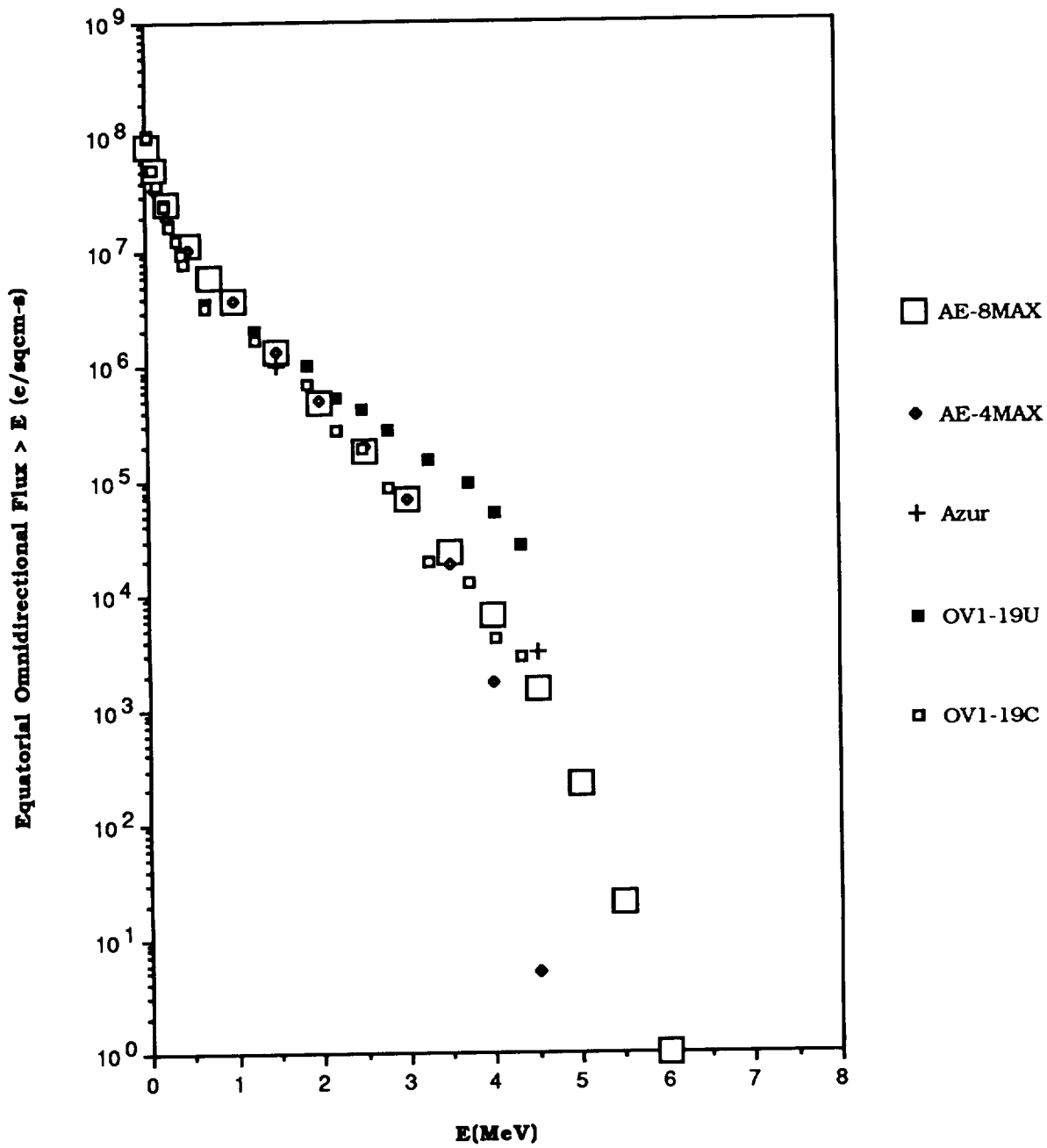
Figure 28. Comparison of AE-8MAX with Outer Zone Data at L = 4.6
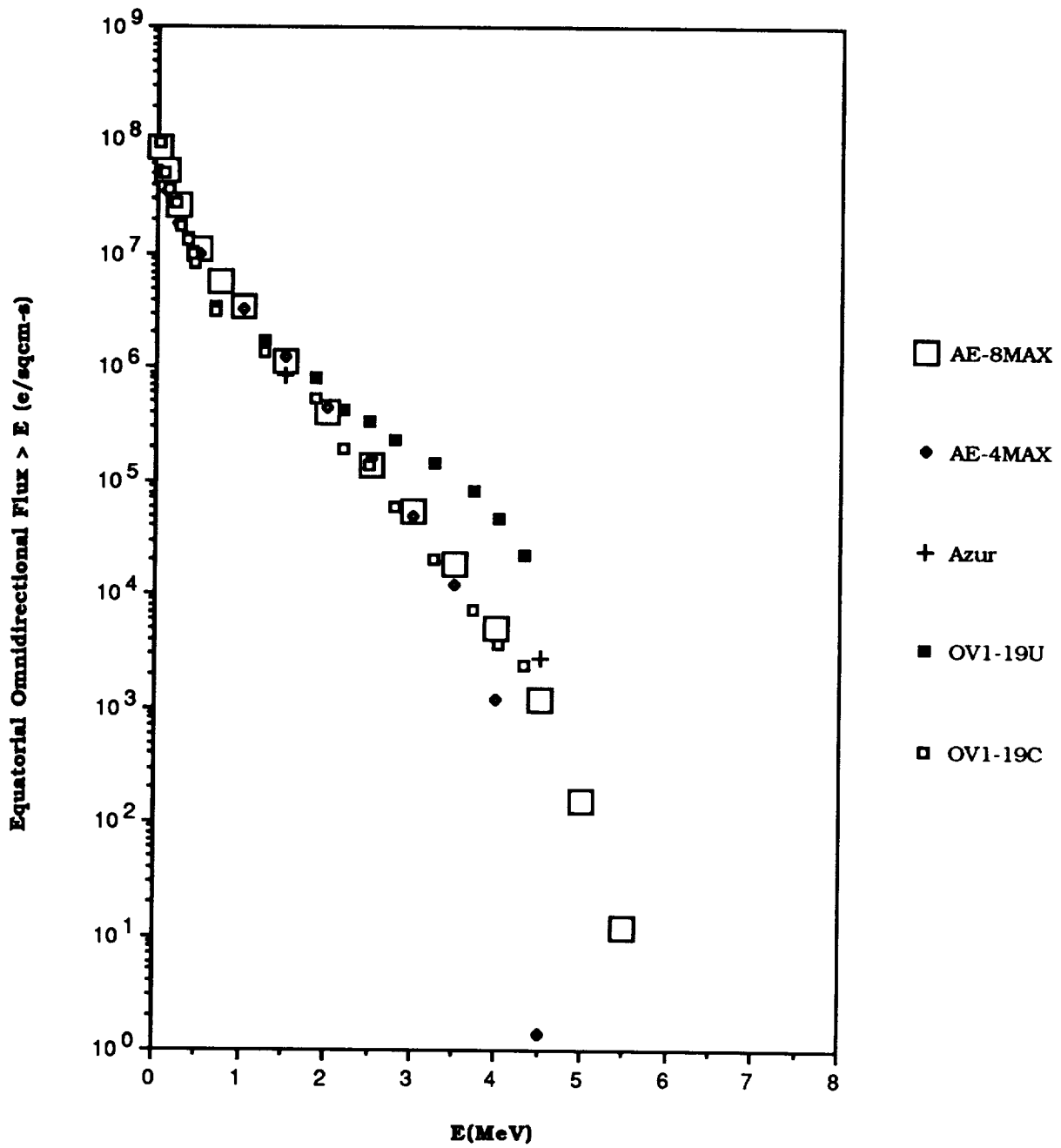
Figure 29. Comparison of AE-8MAX with Outer Zone Data at L = 4.8
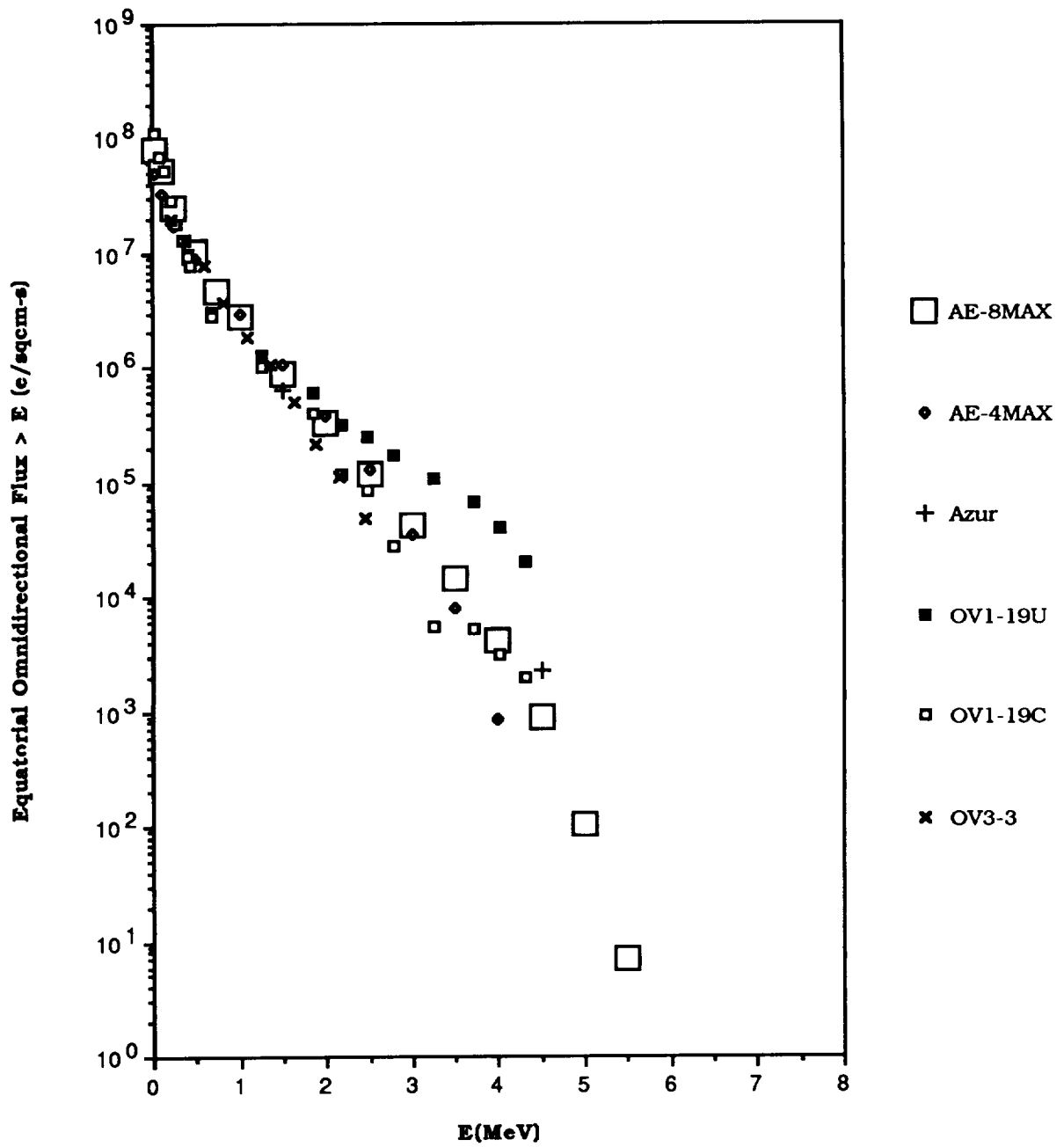
Figure 30. Comparison of AE-8MAX with Outer Zone Data at L = 5.0
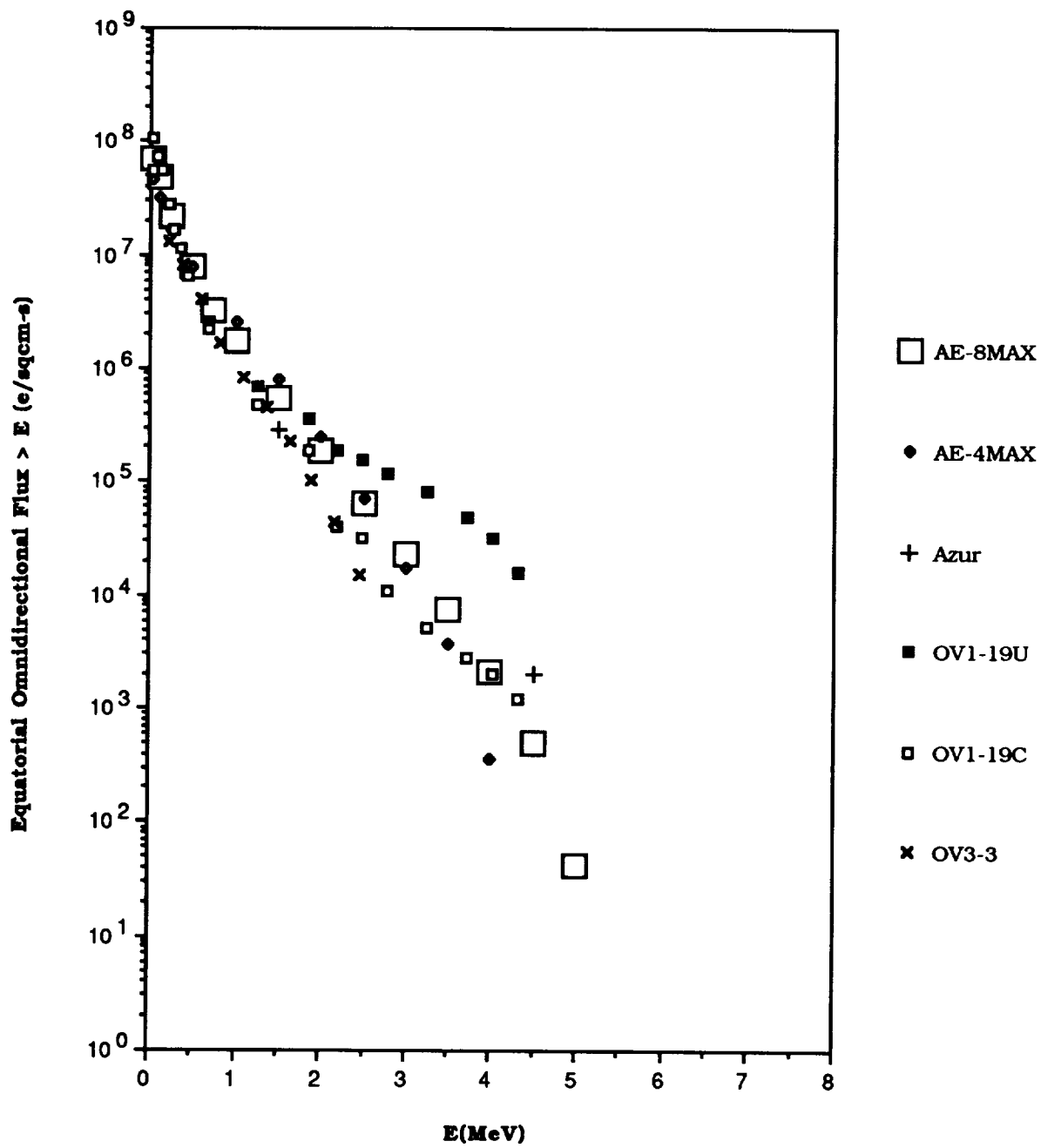
Figure 31. Comparison of AE-8MAX with Outer Zone Data at L = 5.5
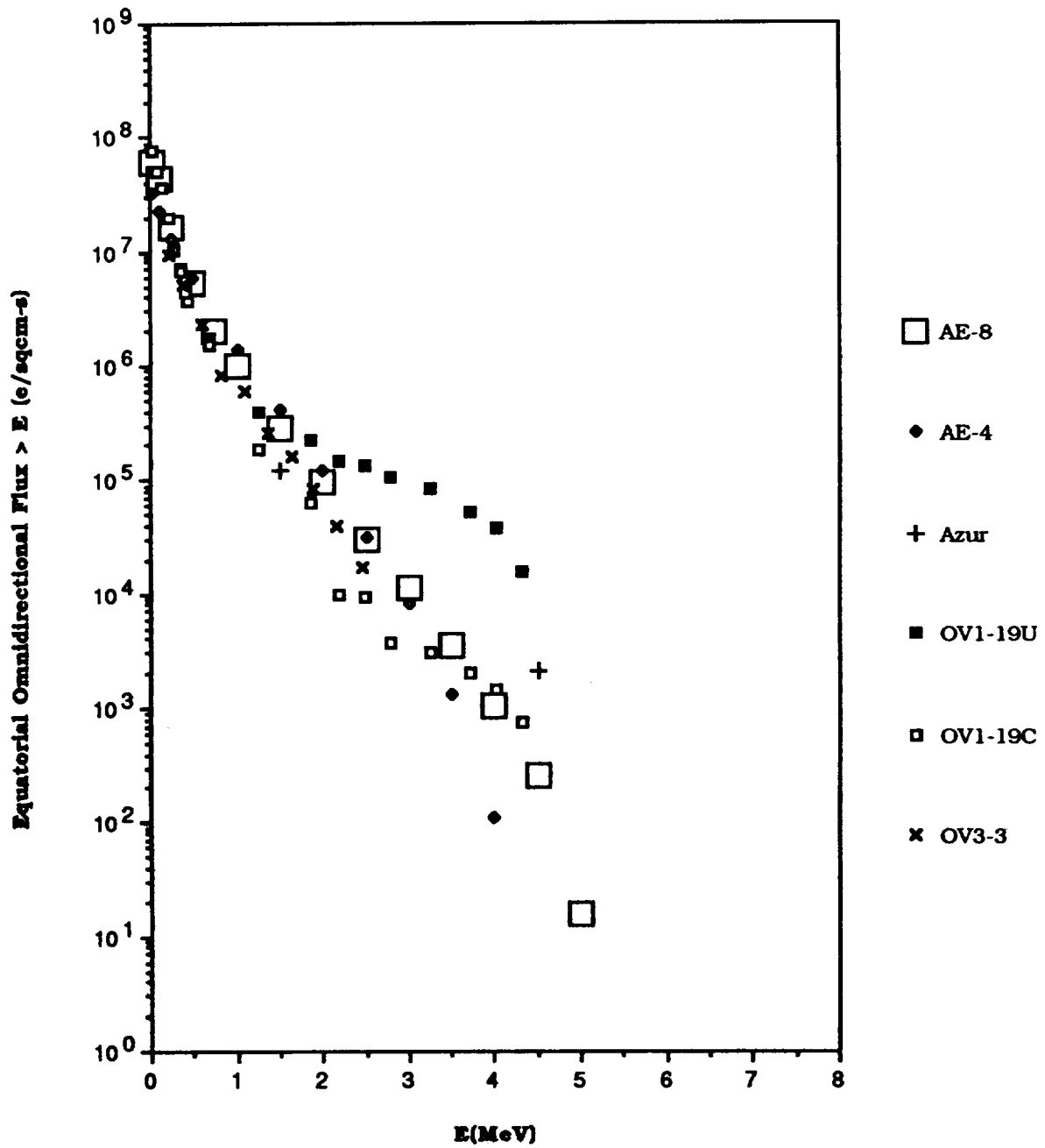
Figure 32. Comparison of AE-8 with Outer Zone Data at L = 6.0
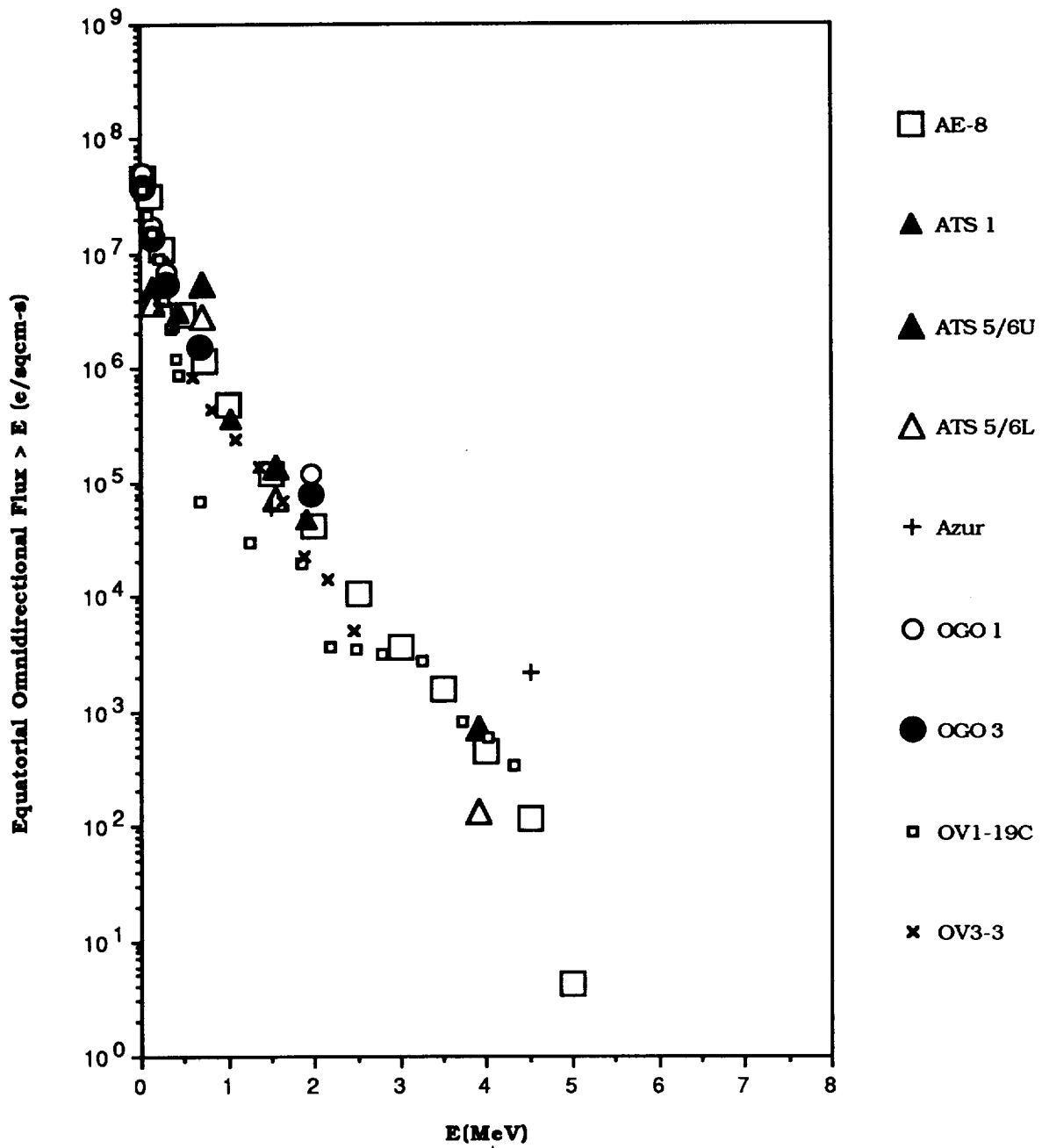
Figure 33a. Comparison of AE-8 with Some Outer Zone Data at L = 6.6
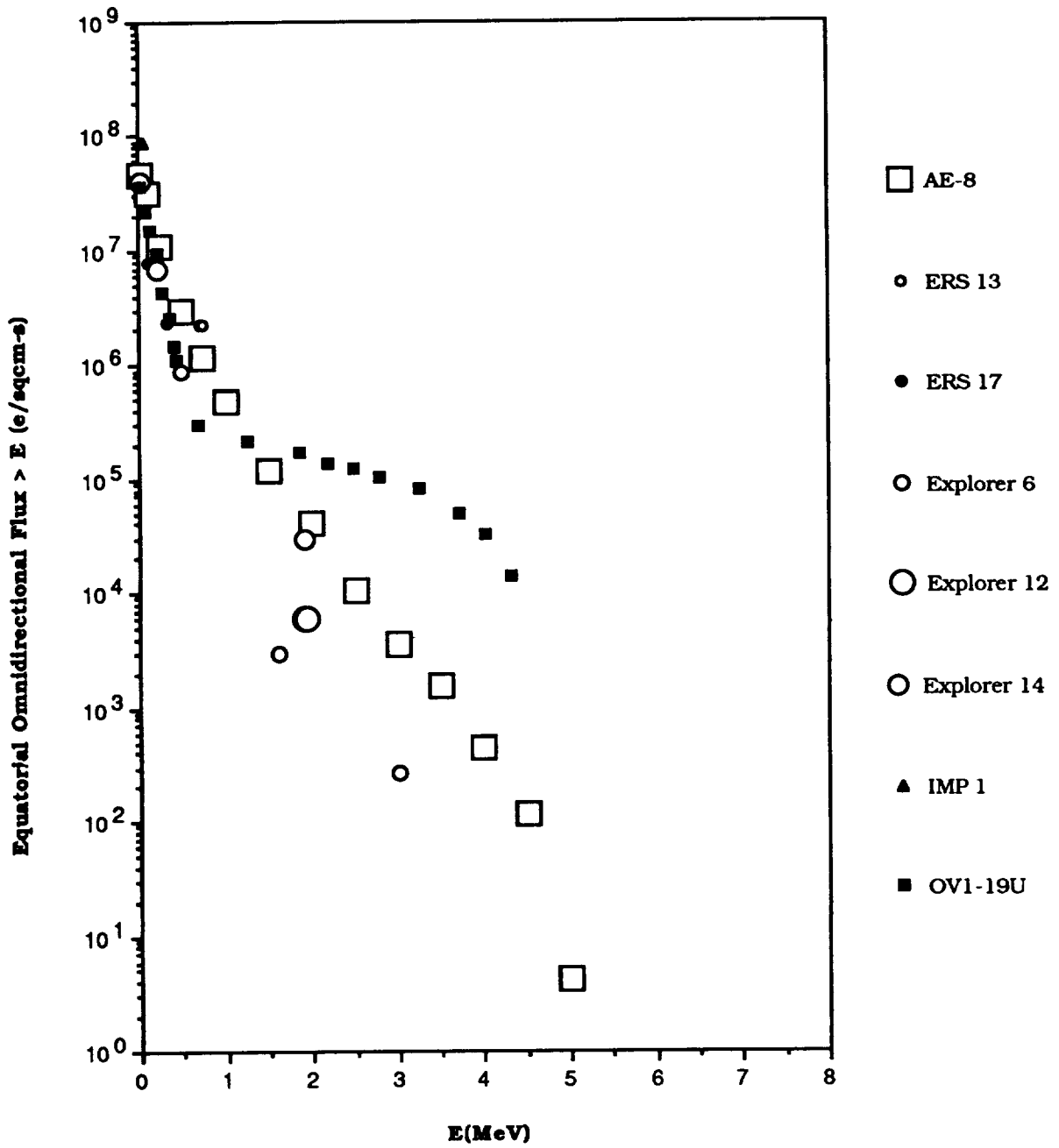
Figure 33b. Comparison of AE-8 with Some Outer Zone Data at L = 6.6
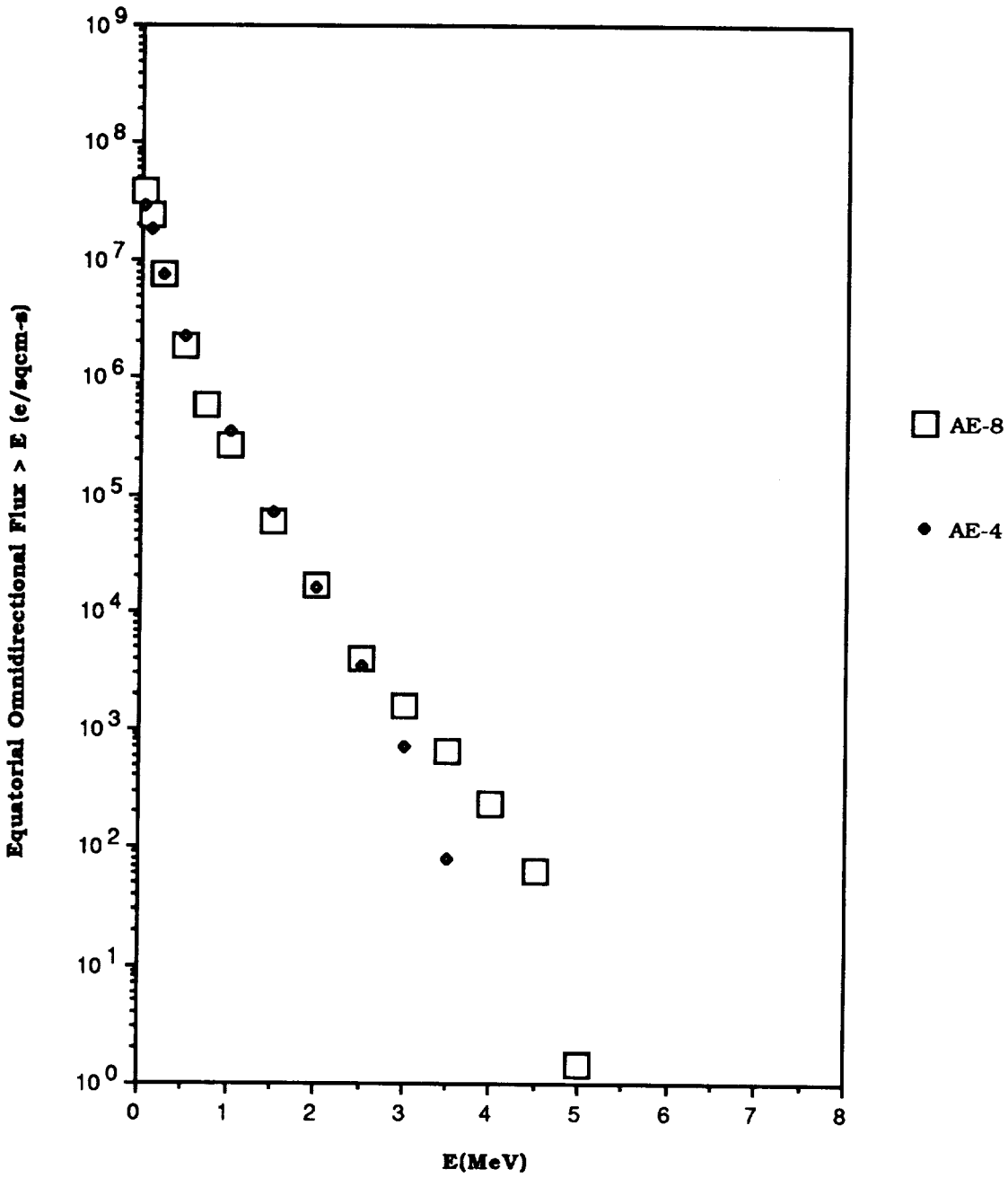
Figure 34. Comparison of AE-8 and AE-4 at L = 7.0
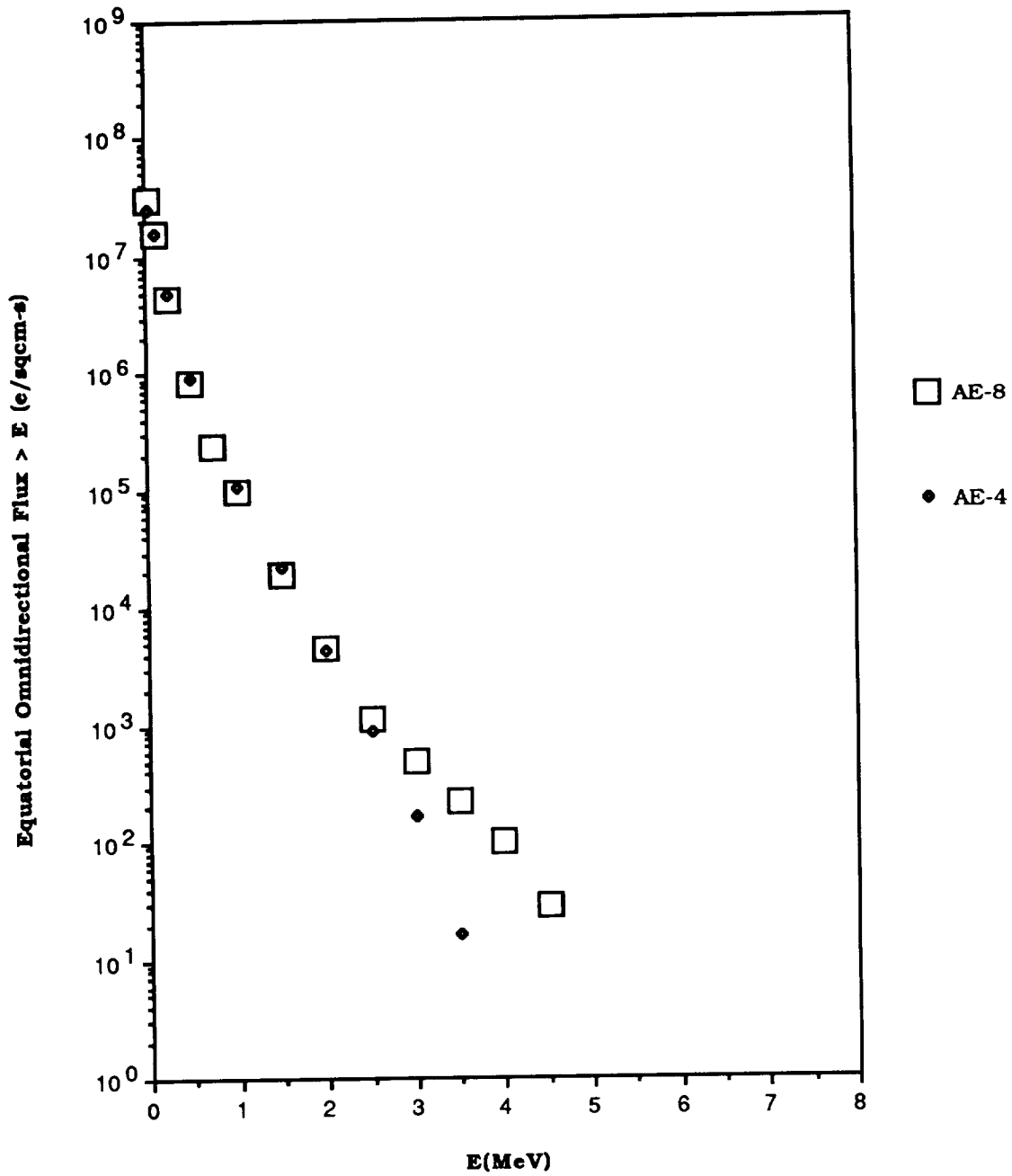
Figure 35. Comparison of AE-8 and AE-4 at L = 7.5
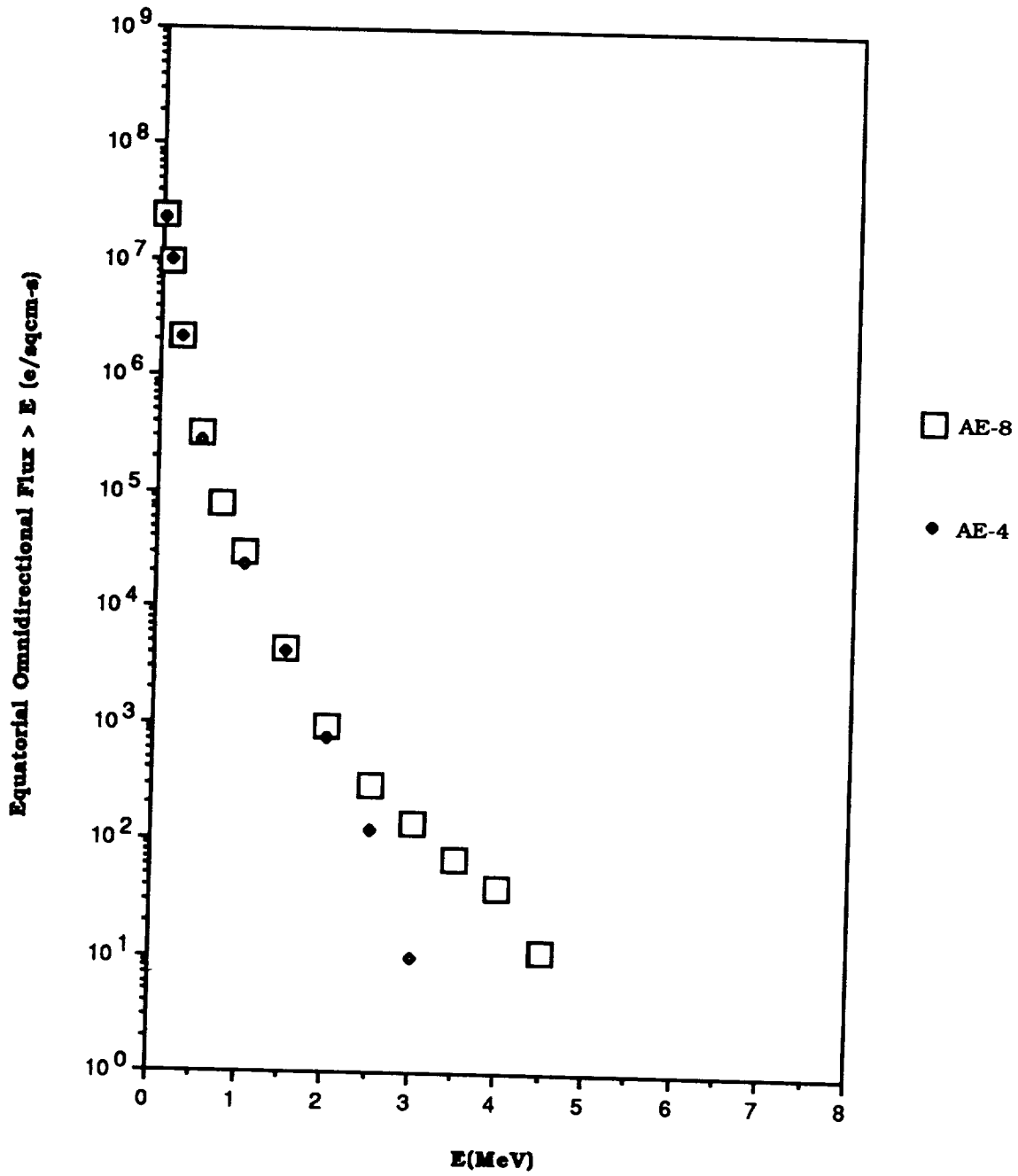
Figure 36. Comparison of AE-8 and AE-4 at L = 8.0
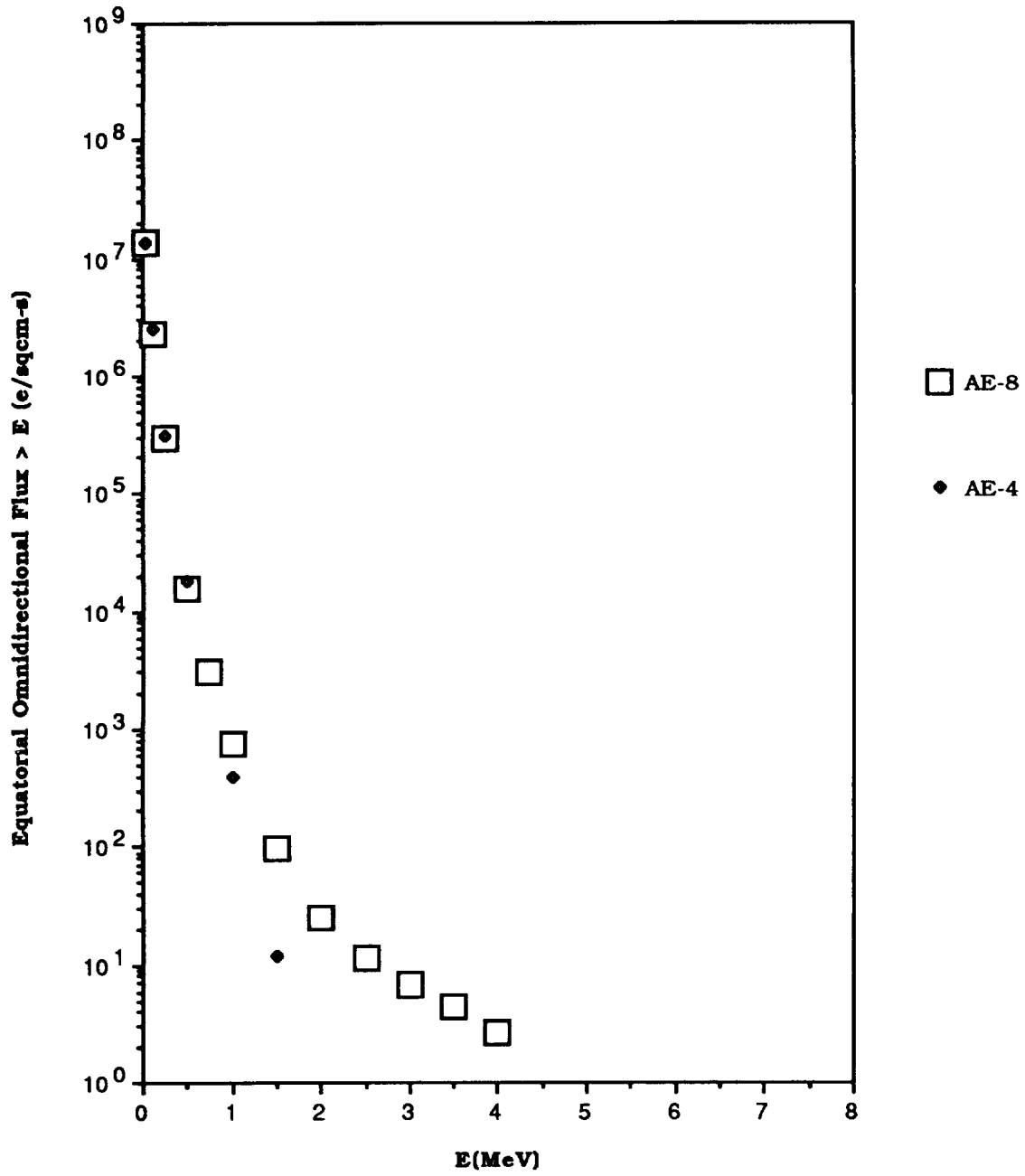
Figure 37. Comparison of AE-8 and AE-4 at L = 9.0
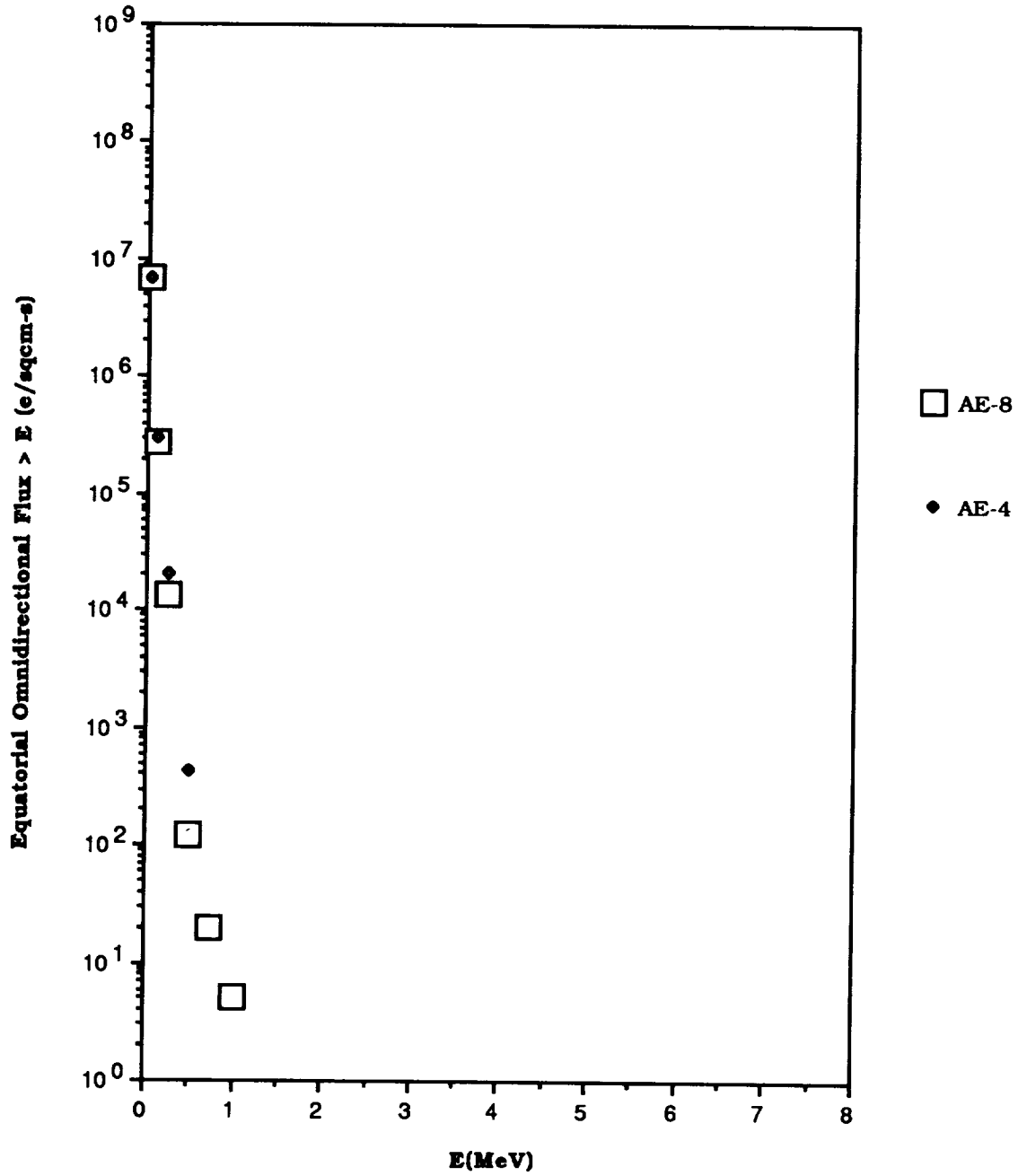
Figure 38. Comparison of AE-8 and AE-4 at L = 10.0
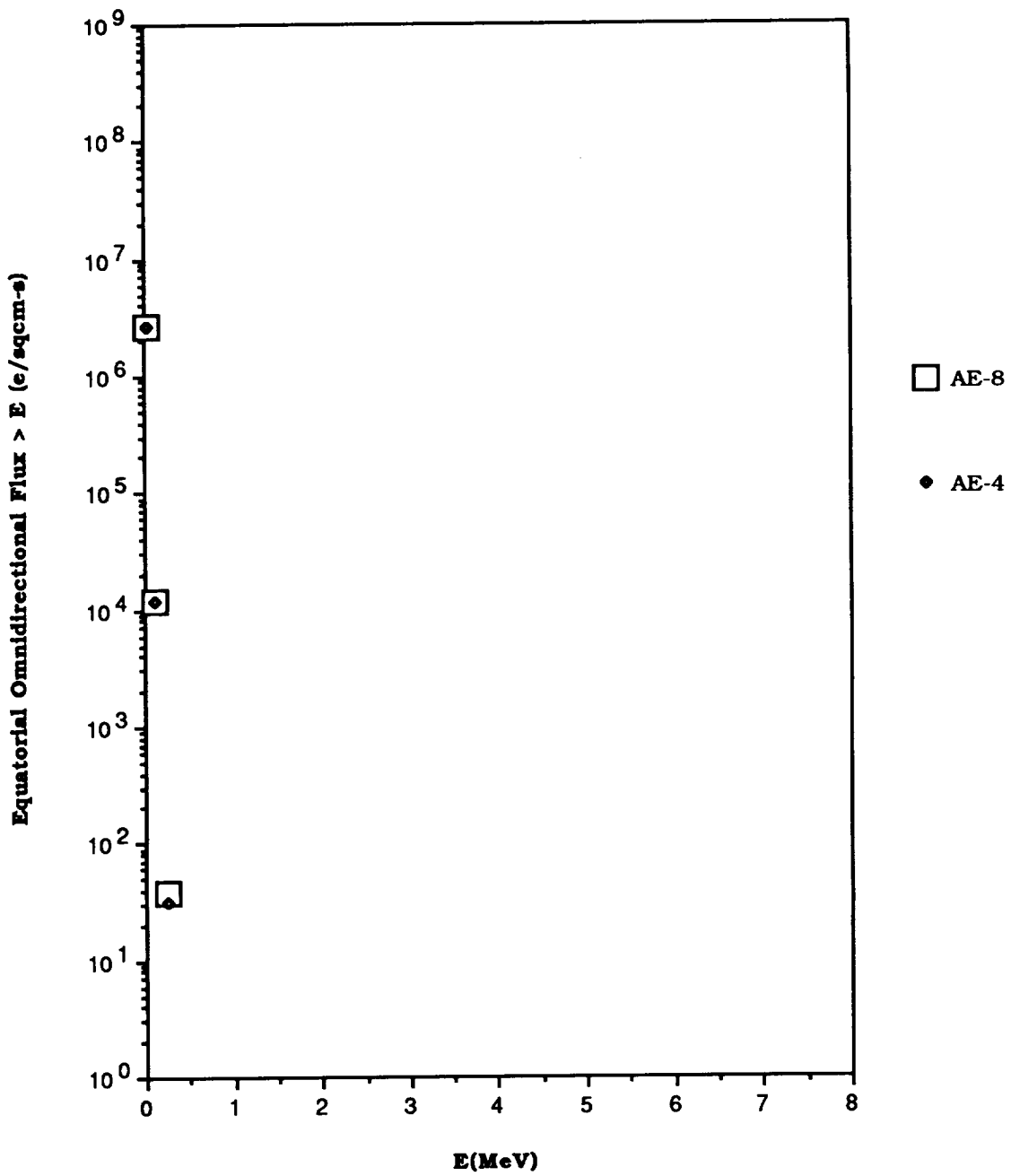
Figure 39. Comparison of AE-8 and AE-4 at L = 11.0
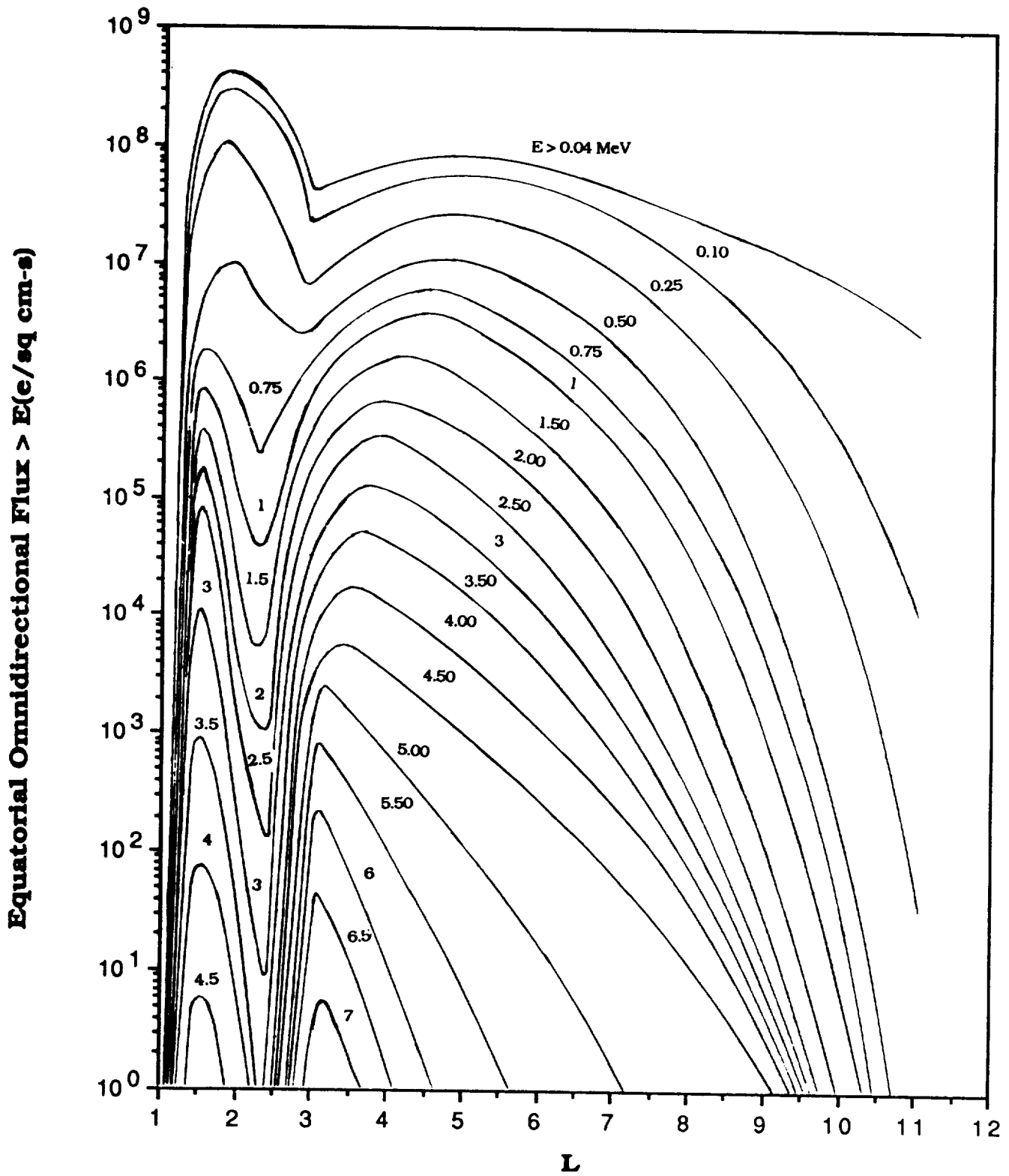
Figure 40. AE-8 MAX Equatorial Radial Profile
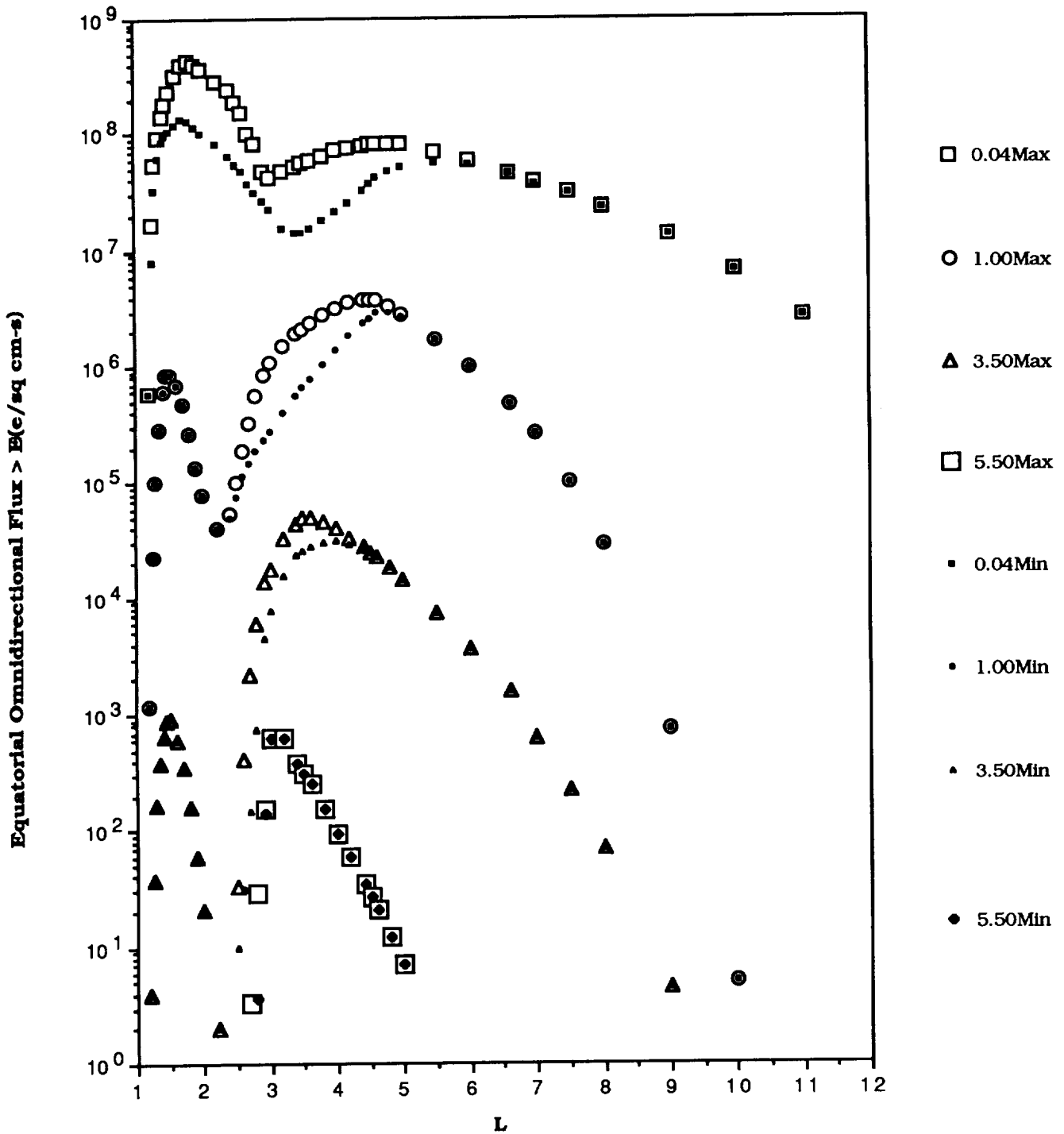
Figure 41. AE-8MAX/MIN Comparison at 0.04, 1.00, 3.50, and 5.50 MeV
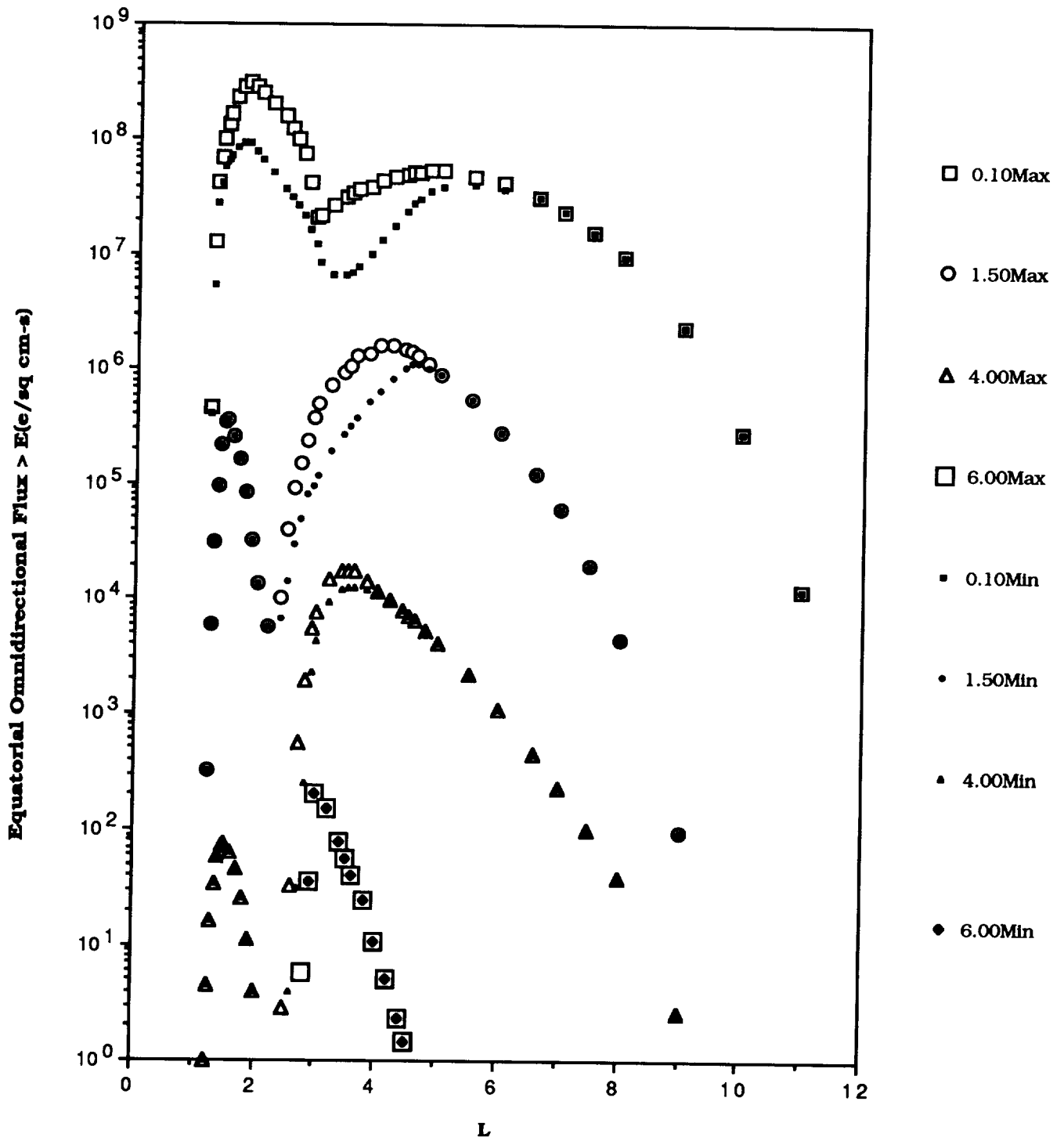
Figure 42. AE-8MAX/MIN Comparison at 0.10, 1.50, 4.00, and 6.00 MeV
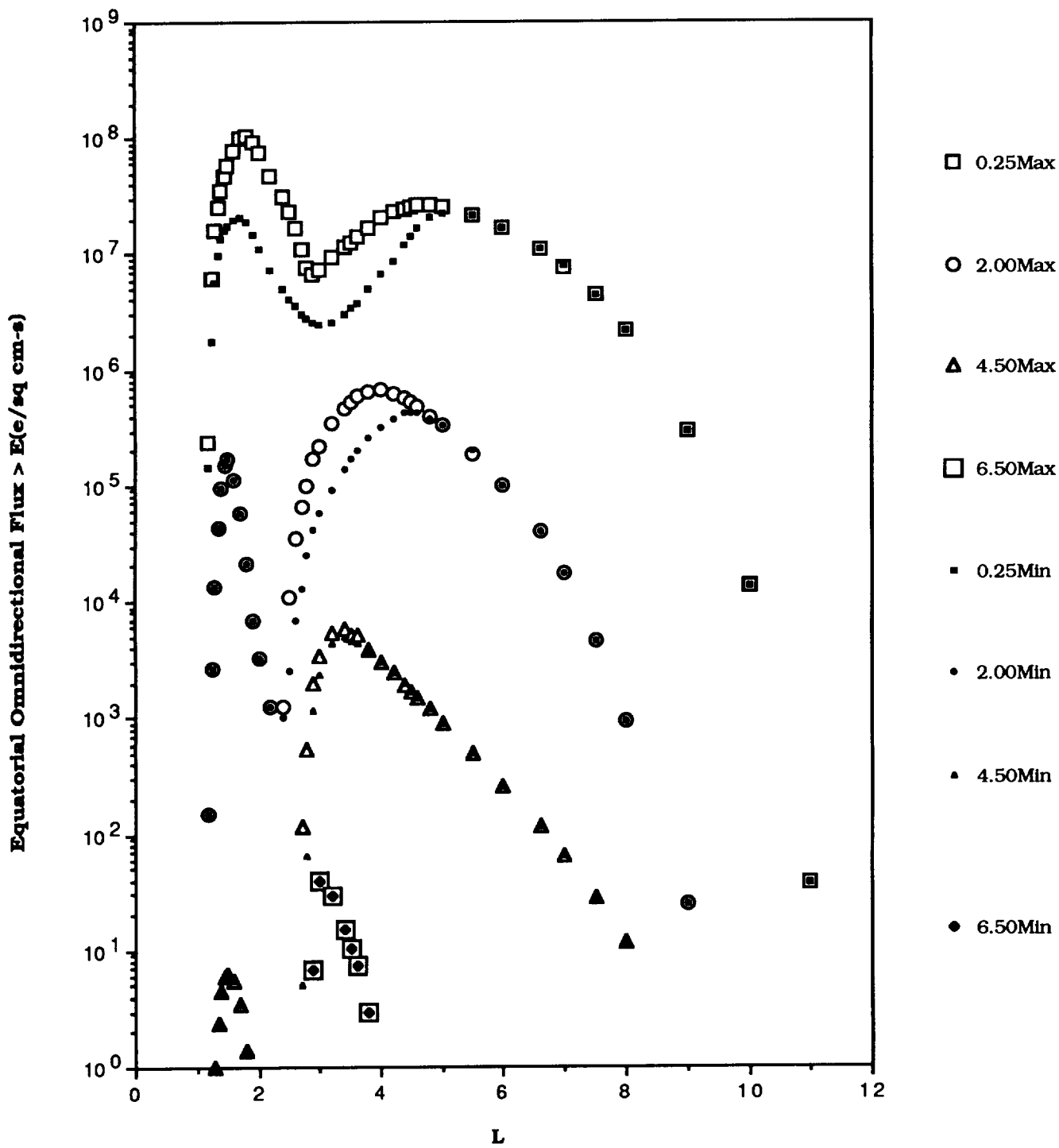
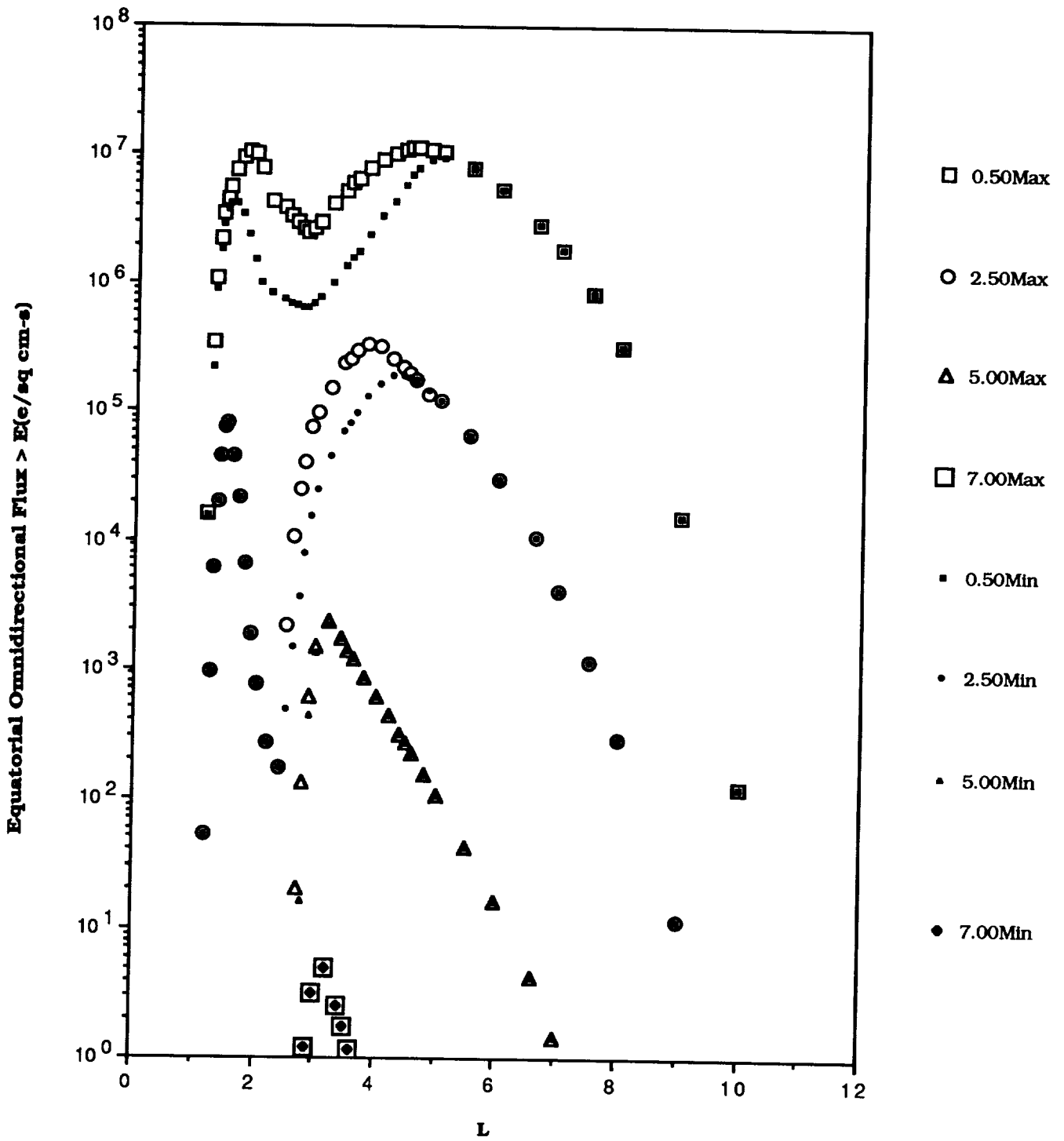Figure 43. AE-8MAX/MIN Comparison at 0.25, 2.00, 4.50, and 6.50 MeV
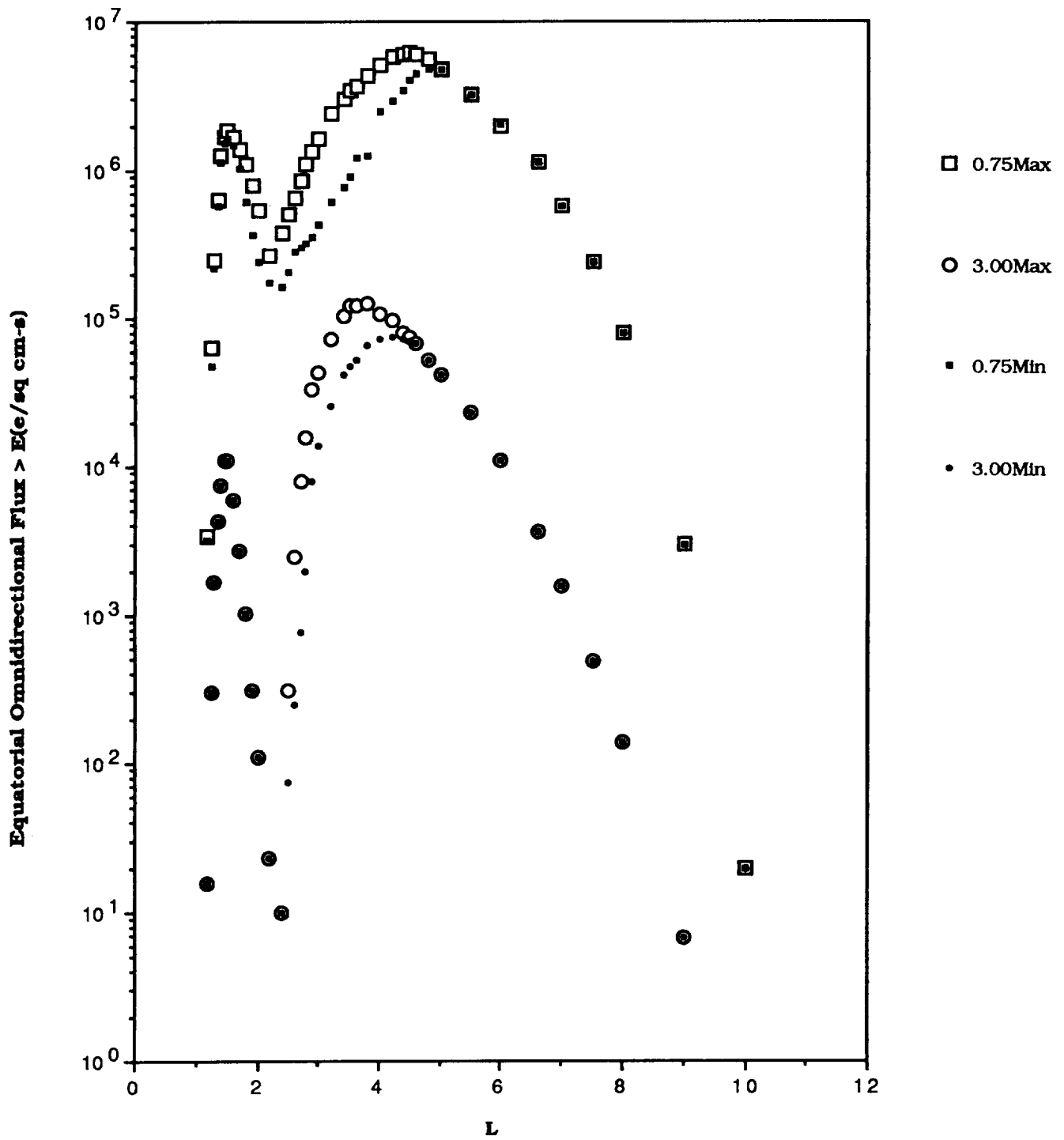
Figure 44. AE-8MAX/MIN Comparison at 0.50, 2.50, 5.00, and 7.00 MeV

Figure 45. AE-8MAX/MIN Comparison at 0.75 and 3.00 MeV